Universitat
de les Illes Balears

DOCTORAL THESIS
2022

CELL WALL COMPOSITION IN RELATION TO PHOTOSYNTHESIS

Margalida Roig Oliver

Universitat
de les Illes Balears

DOCTORAL THESIS
2022

Doctoral Programme in Plant Biology

CELL WALL COMPOSITION IN RELATION TO PHOTOSYNTHESIS

Margalida Roig Oliver

Thesis Supervisor: Jaume Flexas Sans
Thesis Supervisor: Josefina Maria Bota Salort
Thesis tutor: Jaume Flexas Sans

Doctor by the Universitat de les Illes Balears

Universitat de les Illes Balears

Dr. Jaume Flexas Sans, Catedràtic de Fisiologia Vegetal de la Universitat de les Illes Balears i Dra. Josefina Maria Bota Salort, Professora Titular de la Universitat de les Illes Balears

DECLAREM:

Que la tesi doctoral que porta per títol "Cell wall composition in relation to photosynthesis", presentada per Margalida Roig Oliver per a l'obtenció del títol de doctor, ha estat dirigida sota la meva supervisió i que compleix amb els requisits necessaris per optar al títol de Doctor Internacional.

I perquè quedi constància d'això signo aquest document.

Signatura

Dr. Jaume Flexas Sans

Dra. Josefina Maria Bota Salort

Palma de Mallorca, 26 de maig del 2021

Als meus pares

Agraïments

Escriure aquestes paraules suposa finalitzar una etapa que m'ha aportat molt, tant a nivell personal com professional. De totes maneres, però, tenc molt clar que gran part de l'enriquiment personal que m'emporto d'aquesta experiència està estretament lligat a totes aquelles persones que, simplement per ser-hi –ja sigui estant físicament a prop o a mils de quilòmetres de distància–, l'han feta més fàcil. I és que el sentir-me sempre acompanyada i com a casa, inclús estant molt enfora, ha estat gràcies a tots vosaltres.

Si m'aturo a pensar-ho, tot i que són molts els que han seguit des de ben a prop el transcurs d'aquests quatre anys, n'hi ha d'altres que des de sempre han caminat al meu costat, tant en els moments bons com en els dolents. Així doncs, vull donar primerament les gràcies a la meva família i, en especial, als meus pares per recolzar-me en totes les decisions que he pres, per escoltar-me i aconsellar-me, per haver-me fet costat en tot moment i, sobretot, per sempre haver confiat i cregut en mi. Gràcies a vosaltres he arribat on soc i a ser qui soc, sempre us n'estaré agraïda.

Continuant fent la vista enrere, record els horabaixes que passava a l'hort des de ben petita anant d'un lloc a un altre, fent unes quantes coses alhora i fixant-me en més coses encara. En aquest sentit, atribueixo al meu oncle Joan el despertar-me la curiositat i l'interès per conèixer, voler entendre i qüestionar-me el per què del que passava a la natura que m'envoltava. Gràcies per transmetre'm la teva passió.

A en Mateu, per haver-te convertit en un pilar fonamental del meu dia a dia. Gràcies per fer-ho tot més fàcil, per entendre'm, per ensenyar-me a veure la part positiva de cada situació i, sobretot, per ser com ets. Sense cap dubte ets el millor que m'emporto d'aquesta experiència.

Als meus amics, especialment a na Maria i na Bàrbara, qui cada dia s'han encarregat de treure'm una rialla i han estat una importantíssima font de desconnexió després de jornades intensives de treball. Per les nostres converses desbaratades, per les mil i una anècdotes que tenim al darrere després de tants anys i, fonamentalment, per seguir sumant moltes més vivències durant molt de temps. Gràcies per ser-hi sempre.

Malgrat que rere els paràgrafs anteriors apareixen aquelles persones que formen part del meu dia a dia més immediat, com no comentar el que ha suposat aquesta experiència a nivell professional! Haver format part d'un dels grups de recerca més actius dins l'àmbit de la biologia de les plantes m'ha ofert l'oportunitat de treballar amb

científics excepcionals tals com els meus directors de tesi, en Jaume Flexas i na Josefina Bota, a qui agraeixo tots els consells, pautes i directrius donats al llarg de la tesi. Gràcies per donar-me l'oportunitat d'emprendre aquesta aventura i, també, per haver pogut participar en una experiència tan enriquidora, increïble i pràcticament irrepetible tal com és la campanya antàrtica.

A tots els membres del "Greek team", i especialment a na Panagiota Bresta, per haver-me acollit al seu laboratori a la Universitat d'Atenes i no només fer-me sentir un membre més del grup, sinó com a casa. Gràcies per la vostra dedicació i implicació. Agrair també a na Catherine Rayon i als demés membres del BIOPI la seva ajuda i cooperació durant la meva estada a la Universitat d'Amiens.

Per acabar, però no per això menys important, voldria dedicar unes paraules a tots els companys amb qui he coincidit a Ca'n Boom durant aquests anys. Em sento afortunada d'haver compartit moments junts i d'haver pogut treballar amb alguns de vosaltres. M'emporto molts bons moments i anècdotes que segur que d'aquí uns anys recordarem, incloent els moments de "pànic licorer" (Cyril!) i les xerradetes entre centrifugació i centrifugació (Pere!).

A tots vosaltres, moltíssimes gràcies! Aquesta experiència no hagués estat ni de bon tros el mateix si no m'hi haguéssiu acompanyat!

Funding:

This PhD Thesis was supported by the project PGC2018-093824-B-C41 from the Ministerio de Economía y Competitividad (MINECO, Spain). Also, MINECO awarded a pre-doctoral fellowship (FPU16/01544) to Margalida Roig Oliver.

Symbols and abbreviations

Symbols and abbreviations used along this Thesis*:

Symbol	Meaning
AE	Acetylesterase
a_f	Apoplastic water fraction
AIR	Alcohol insoluble residue
A_N	Net CO_2 assimilation
BL	Biochemical *relative* contribution to *d*A/A
(C+H)/P	Cellulose and hemicelluloses to pectins ratio
C_a	Ambient CO_2 concentration
C_c	CO_2 concentration at chloroplasts stroma
C_i	CO_2 concentration at the sub-stomatal cavity
CMA	Canopy mass per area
C^*_{ft}	Leaf area specific capacitance at full turgor
DW	Dry weight
ETR	Electron transport rate
f_{ias}	Fraction of mesophyll intercellular air spaces
F_m’	Maximum chlorophyll fluorescence
F_s	Steady-state chlorophyll fluorescence
FW	Fresh weight
GalA	Galacturonic acid
g_m	Mesophyll conductance
g_s	Stomatal conductance
HG	Homogalacturonan
IRGA	Infrared gas analyser
LA	Leaf area
l_b	Biochemical *absolute* limitation to photosynthesis
L_{betchl}	Distance between chloroplasts
L_{chl}	Chloroplasts length
LD	Leaf density
l_m	Mesophyll conductance *absolute* limitation to photosynthesis

LMA	Leaf mass per area
l_s	Stomatal conductance *absolute* limitation to photosynthesis
LT	Long-term water deficit stress
ML	Mesophyll conductance *relative* contribution to *d*A/A
N_{PAL}	Number of palisade layers
PAE	Pectin acetylesterase
PME	Pectin methylesterase
PPFD	Photosynthetic photon flux density
PRE	Pectin remodelling enzymes
P-V	Pressure-volume curves
RG-I	Rhamnogalacturonan type I
RG-II	Rhamnogalacturonan type II
R_{light}	Light respiration
Rubisco	Ribulose-1,5-bisphosphate carboxylase/oxygenase
RWC	Relative water content
RWC_{tlp}	Relative water content at turgor loss point
S_c/S	Chloroplasts surface area exposed to intercellular air spaces
S_c/S_m	Ratio between chloroplasts and mesophyll surface areas exposed to intercellular air spaces
SL	Stomatal conductance *relative* contribution to *d*A/A
S_m/S	Mesophyll surface area exposed to intercellular air spaces
ST	Short-term water deficit stress
T_{chl}	Chloroplasts thickness
T_{cw}	Cell wall thickness
T_{cyt}	Cytosol thickness
T_{le}	Lower epidermis thickness
T_{leaf}	Leaf thickness
T_{mes}	Mesophyll thickness
T_{ue}	Upper epidermis thickness
TW	Turgid weight
VPD	Vapour pressure deficit
WUE_i	Intrinsic water use efficiency
XGA	Xylogalacturonan

Γ^*	CO_2 compensation point in the absence of respiration
ε	Bulk modulus of elasticity
π_o	Osmotic potential at full turgor
Φ_{PSII}	Real quantum efficiency of photosystem II
Ψ_{md}	Midday water potential
Ψ_{pd}	Pre-dawn water potential
Ψ_{tlp}	Leaf water potential at turgor loss point

* The use of distinct symbols and abbreviations of the list presented above is because of Journal Editorial decisions and guidelines. In all cases, they are specifically defined in each publication.

Publications list

Publications derived from the present Thesis

This PhD Thesis is presented as a compendium of eight manuscripts, either published or submitted to scientific journals:

1. **Roig-Oliver M**, Bresta P, Nadal M, Liakopoulos G, Nikolopoulos D, Karabourniotis G, Bota J, Flexas J. (2020). Cell wall composition and thickness affect mesophyll conductance to CO_2 diffusion in *Helianthus annuus* under water deprivation. *Journal of Experimental Botany* 71, 7198–7209.

2. **Roig-Oliver M**, Bresta P, Nikolopoulos D, Bota J, Flexas J. Mature sunflower leaves show dynamic changes in cell wall composition uncoupled from photosynthesis upon rewatering. Submitted to *Journal of Experimental Botany*.

3. **Roig-Oliver M**[*], Nadal M[*], Bota J, Flexas J. (2020). *Ginkgo biloba* and *Helianthus annuus* show different strategies to adjust photosynthesis, leaf water relations, and cell wall composition under water deficit stress. *Photosynthetica* 58, 1098–1106.

4. **Roig-Oliver M**[*], Nadal M[*], Clemente-Moreno MJ, Bota J, Flexas J. (2020). Cell wall components regulate photosynthesis and leaf water relations of *Vitis vinifera* cv. Grenache acclimated to contrasting environmental conditions. *Journal of Plant Physiology* 244, 153084.

5. **Roig-Oliver M**, Fullana-Pericàs M, Bota J, Flexas J. Adjustments in photosynthesis and leaf water relations are related to changes in cell wall composition in *Hordeum vulgare* and *Triticum aestivum* subjected to water deficit stress. Submitted to *Plant Science*.

6. **Roig-Oliver M**, Fullana-Pericàs M, Bota J, Flexas J. Distinct photosynthetic regulation under water shortage and recovery in tomato genotypes: water relations, leaf anatomy, and cell wall composition. Submitted to *Plant, Cell & Environment*.

7. **Roig-Oliver M**, Rayon C, Roulard R, Fournet F, Bota J, Flexas J. (2020). Reduced photosynthesis in *Arabidopsis thaliana atpme17.2* and *atpae11.1* mutants is associated to altered cell wall composition. *Physiologia Plantarum* 172, 1439–1451.

8. **Roig-Oliver M**, Douthe C, Bota J, Flexas J. Cell wall thickness and composition are related to photosynthesis in Antarctic mosses. Submitted to *Physiologia Plantarum.*

* Both authors contributed equally to this paper.

CONTENT

Summary

Photosynthesis is an essential process for plants. To comprehend how diffusive and biochemical CO_2 processes involved in photosynthesis occur is of great relevance to understand plant physiology. For decades, photosynthesis was thought to be only limited by stomatal conductance (g_s) and biochemistry. However, it is now well-known that mesophyll conductance (g_m) is also a crucial trait determining photosynthetic rates in plants subjected to some stresses as well as along land plants' phylogeny. Although the specific nature of those traits most affecting g_m remains unknown, biochemical and structural facts could be involved. Regarding structural elements, it has been demonstrated that leaf anatomical characteristics –particularly, the chloroplasts surface area exposed to intercellular air spaces (S_c/S) and the cell wall thickness (T_{cw})– are crucial in determining g_m. Additionally, it has been recently described that the bulk modulus of elasticity (ε) also influences g_m probably due to cell wall characteristics, such as T_{cw} and its composition. Mainly compounded by cellulose, hemicelluloses and pectins, recent studies have suggested that cell wall composition could also be of special relevance determining g_m and, thus, photosynthesis. However, this relationship remains almost unexplored.

The present Thesis is compounded by eight publications which have, as a main idea, to explore the relationship between photosynthesis and cell wall composition. Hence, this Thesis is divided in four sections. In the first one, possible correlations between changes in cell wall composition and g_m were explored studying a model plant subjected to water deficit stress. In the second, various crops submitted to contrasting abiotic stresses were studied to determine how modifications in cell wall composition influence g_m. In the third, mutant plants were utilized to examine the effect of specific mutations in pectins remodelling enzymes affecting g_m. Finally, in the last section, a relationship between photosynthesis and cell wall compositional characteristics was analysed in the most basal land plants lineage.

Overall, the obtained results evidence the importance of cell wall composition as a g_m determinant, consequently affecting photosynthesis. Along phylogeny, the specific cell wall composition of each land plant lineage also influences T_{cw}. Under abiotic stress conditions, it has been demonstrated that dynamic and fast modifications occurring in the cell wall composition also promote modifications in other plant functional traits, for instance, leaf water relations, being ε a key parameter. Even though the specific nature of

some of these changes varies in a species-specific way, it has been proposed that pectins could be the most relevant cell wall components determining distinct plant functional traits under abiotic stress conditions. Finally, we focused on the current state of those methodologies used to study the cell wall composition in more detail as well as on which are the future perspectives to continue deepening on how cell wall composition influences g_m and, thus, photosynthesis.

Resum

La fotosíntesi és un procés imprescindible per les plantes. Entendre com esdevenen els processos difusius i bioquímics del CO_2 involucrats en la fotosíntesi té gran rellevància per comprendre la fisiologia vegetal. Tot i que durant dècades es pensava que la fotosíntesi estava únicament limitada per la conductància estomàtica (g_s) i per processos bioquímics, actualment es coneix que la conductància del mesòfil (g_m) és també un tret crucial determinant les taxes fotosintètiques tant en plantes sotmeses a algun estrès així com al llarg de la filogènia de les plantes terrestres. Malgrat que la naturalesa específica d'aquells factors que més afecten la g_m encara no està del tot identificada, elements bioquímics i estructurals poden estar-hi involucrats. Respecte als estructurals, s'ha demostrat que les característiques anatòmiques foliars, particularment la superfície de cloroplasts exposada a espais aeris intercel·lulars (S_c/S) i la gruixa de la paret cel·lular (T_{cw}), són decisives determinant la g_m. A més, recentment s'ha descrit que el mòdul d'elasticitat (ε) també influencia la g_m, probablement a causa de característiques de la paret cel·lular tals com la T_{cw} i la seva composició. Principalment composta per cel·lulosa, hemicel·luloses i pectines, estudis recents han suggerit que la composició de la paret cel·lular també podria tenir especial rellevància determinant la g_m i, per tant, la fotosíntesi. Tot i això, aquesta relació ha estat molt poc explorada.

La present Tesi està composta per un total de vuit articles que tenen, com a idea principal, explorar la relació entre la fotosíntesi i la composició de la paret cel·lular. Així, aquesta Tesi es troba dividida en quatre seccions. A la primera d'elles, s'exploren les possibles correlacions entre canvis en la composició de la paret cel·lular que afectin la g_m estudiant una planta model sotmesa a dèficit hídric. A la segona, se cerquen correlacions entre canvis en la composició de la paret cel·lular que influenciïn la g_m havent aclimatat diversos cultius a diferents estressos abiòtics. A la tercera part, s'estudia l'efecte de mutacions específiques en enzims remodeladors de pectines sobre la g_m a partir de plantes mutants. Finalment, a la darrera secció s'ha cercat una relació entre la fotosíntesi i les característiques de la composició de la paret cel·lular en el llinatge de plantes terrestres més basal.

En conjunt, els resultats obtinguts evidencien la importància de la composició de la paret cel·lular com a factor determinant de la g_m i, en conseqüència, de la fotosíntesi. Al llarg de la filogènia, la composició de la paret cel·lular específica de cada grup també influeix la T_{cw}. Sota condicions d'estrès abiòtic, s'ha demostrat que ocorren

modificacions dinàmiques i ràpides en la composició de la paret cel·lular que també promouen canvis en altres trets funcionals, per exemple, les relacions hídriques, essent-ne ε un paràmetre clau. Tot i que la naturalesa d'alguns d'aquests canvis varia de manera particular segons l'espècie estudiada, es discuteix el potencial de les pectines com a components més rellevants de la paret cel·lular que poden determinar ajustos en distints trets funcionals sota condicions d'estrès abiòtic. Finalment, es comenta quin és l'estat actual de les metodologies emprades per estudiar la composició de la paret cel·lular amb més detall i també quines són les perspectives de futur per tal de continuar aprofundint en l'estudi de com la paret cel·lular influencia la g_m i, per tant, la fotosíntesi.

Resumen

La fotosíntesis es un proceso imprescindible para las plantas. Entender cómo suceden los procesos difusivos y bioquímicos del CO_2 involucrados en la fotosíntesis tiene gran relevancia para comprender la fisiología vegetal. Aunque durante décadas se creía que la fotosíntesis estaba únicamente limitada por la conductancia estomática (g_s) y por procesos bioquímicos, actualmente se conoce que la conductancia del mesófilo (g_m) es también un rasgo crucial que determina las tasas fotosintéticas tanto en plantas sometidas a algún estrés, así como a lo largo de la filogenia de las plantas terrestres. Aunque la naturaleza específica de aquellas características que más afectan la g_m aún no ha sido completamente identificada, elementos bioquímicos y estructurales pueden estar involucrados. En cuanto a los estructurales, se ha demostrado que las características anatómicas foliares, particularmente la superficie de cloroplastos expuesta a espacios aéreos intercelulares (S_c/S) y el grosor de la pared celular (T_{cw}), son decisivas determinando la g_m. Además, recientemente se ha descrito que el módulo de elasticidad (ε) también influye la g_m, probablemente debido a características de la pared celular tales como T_{cw} y su composición. Principalmente compuesta por celulosa, hemicelulosas y pectinas, estudios recientes han sugerido que la composición de la pared celular también podría tener especial relevancia determinando la g_m y, por lo tanto, la fotosíntesis. Aun así, esta relación ha sido muy poco explorada.

La presente Tesis está compuesta por un total de ocho artículos que tienen, como idea principal, explorar la relación entre la fotosíntesis y la composición de la pared celular. Así, dicha Tesis se encuentra dividida en cuatro secciones. En la primera de ellas, se exploran las posibles correlaciones entre cambios en la composición de la pared celular que afecten la g_m estudiando una planta modelo sometida a déficit hídrico. En la segunda, se buscan correlaciones entre cambios de composición de la pared celular que influyan la g_m habiendo aclimatado varios cultivos a diferentes estreses abióticos. En la tercera parte, se estudia el efecto de mutaciones específicas en enzimas remoldeadores de pectinas sobre la g_m a partir de plantas mutantes. Finalmente, en la última sección se ha buscado una relación entre la fotosíntesis y las características de la composición de la pared celular en el linaje de plantas terrestres más primitivo.

En conjunto, los resultados obtenidos evidencian la importancia de la composición de la pared celular como un factor determinante de la g_m y, consecuentemente, de la fotosíntesis. A lo largo de la filogenia, la composición de la pared celular específica de

cada grupo también influye la T_{cw}. Bajo condiciones de estrés abiótico, se ha demostrado que ocurren modificaciones dinámicas y rápidas en la composición de la pared celular que también promueven cambios en otros rasgos funcionales, por ejemplo, las relaciones hídricas, siendo ε un parámetro clave. Aunque la naturaleza de algunos de estos cambios varía de manera particular según la especie estudiada, se discute el potencial de las pectinas como componentes más relevantes de la pared celular que pueden determinar ajustes en distintos rasgos funcionales bajo condiciones de estrés abiótico. Finalmente, se comenta cuál es el estado actual de las metodologías usadas para estudiar la composición de la pared celular con más detalle y también cuáles son las perspectivas de futuro para continuar profundizando en el estudio de cómo la pared celular influye la g_m y, por lo tanto, la fotosíntesis.

Chapter 1

General Introduction

1.- Photosynthesis

Life on Earth depends on energy-rich organic molecules synthetized by photosynthesis. In most plants, this complex process is performed in highly specialized organelles called chloroplasts, which are designed to maximize the use of both CO_2 and light. Thus, understanding how photosynthesis occurs from a molecular to an ecophysiological perspective is crucial to elucidate its importance for plant physiology.

During photosynthesis, light energy is captured and converted into chemical energy in chloroplasts' thylakoid membranes to be used for CO_2 fixation in the Calvin-Benson cycle, which takes place in chloroplasts stroma. In most plant species, these CO_2 molecules are incorporated in three-carbon carbonate compounds (C_3) –particularly, 3-phosophoglycerate– by the action of the Ribulose-1,5-bisphosphate carboxylase/oxygenase (Rubisco) enzyme. The Rubisco double functionality (i.e., carboxylase and oxygenase) strongly constrains photosynthesis since oxygenase reactions provoke photorespiration, resulting in CO_2 losses by the plant. Overall, photosynthesis depends on the CO_2 capacity to diffuse from the atmosphere to its carboxylation sites at chloroplasts stroma as well as on the Rubisco velocity to fix carbon (Gaastra, 1959; Farquhar *et al.*, 1980). Thus, it comprehends both diffusional and biochemical processes (Farquhar *et al*., 1980; Flexas *et al*., 2004, 2012, 2018; von Caemmerer *et al*., 2009).

1.1.- The CO_2 pathway in photosynthetic organs

During photosynthesis, the diffusional process comprises the pathway that CO_2 has to follow from the atmosphere to sub-stomatal cavities to then cross the leaf mesophyll, finally reaching chloroplasts stroma, where biochemical processes occur by the action of Rubisco enzyme (Flexas *et al*., 2004; von Caemmerer *et al*., 2009). As appreciated in Fig. 1, the first resistance that CO_2 has to overcome before entering into a leaf from the surrounding atmosphere is crossing a boundary layer with impaired air turbulence. Because cuticle and epidermal cells are highly impermeable to CO_2 diffusion (Boyer *et al*., 1997), most CO_2 molecules diffuse across stomatal pores –in those leaves presenting stomata– due to a positive gradient of CO_2 concentration until reaching sub-stomatal cavities. Stomata are surface foliar apertures that enable CO_2 entrance in leaves while restricting H_2O losses. They are composed by the guard cells, the subsidiary cells (not found in all species) and the stomatal pore, which is regulated by guard cells' turgor

(Franks and Farquhar, 2007). Both stomata distribution and pore size influence stomatal conductance (g_s), which can be defined for CO_2 and H_2O vapour diffusion (g_{sc} and g_{sw}, respectively). Since CO_2 and H_2O share an inverse pathway through the stomatal pore, g_{sc} and g_{sw} are directly interconnected by the molecular weight of CO_2 and H_2O molecules, i.e., $g_{sw}/1.6 = g_{sc}$ (Farquhar and Sharkey, 1982).

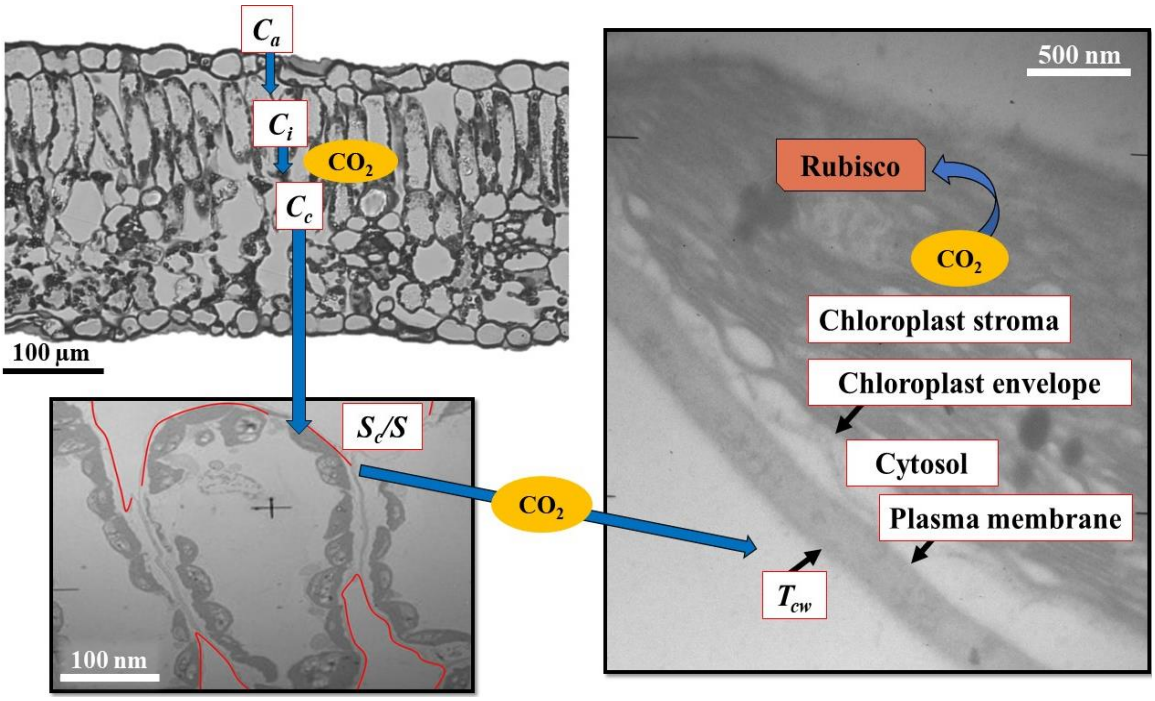

Fig. 1. Transversal sections of *Helianthus annuus* representing the CO_2 pathway from the atmosphere to Rubisco carboxylation sites located in chloroplasts stroma. Main anatomical resistances are shown. For parameters abbreviations, see "Symbols and abbreviations" section in page "iii" of this Thesis.

From sub-stomatal cavities, CO_2 enters the leaf mesophyll and overcomes numerous physical barriers until reaching Rubisco carboxylation sites (Fig. 1). The sum of all these resistances defines the total efficiency of CO_2 diffusion through photosynthetic organs, commonly referred as mesophyll resistance, or its inverse, mesophyll conductance (g_m; Evans *et al.*, 1994; Niinemets and Reichstein, 2003; Terashima *et al.*, 2006; Flexas *et al.*, 2008). CO_2 continues diffusing thanks to a strong positive diffusional gradient through the gaseous phase, which is comprised between the

sub-stomatal cavities and the surface of mesophyll cell walls. The resistance imposed by this gaseous phase was typically believed to be low as air exerts a minimum resistance to CO_2 mobility (Evans *et al*., 2009). However, recent studies have revaluated its importance limiting g_m as changes in leaf thickness (T_{leaf}) and in the fraction of intercellular air spaces (f_{ias}) can influence the tortuosity, the intercellular air spaces connectivity, and the lateral CO_2 conductance (Earles *et al*., 2018, 2019).

After crossing the gaseous phase, CO_2 gets dissolved in the liquid medium of the cell wall water-filled pores in the liquid phase (Fig. 1), representing one of the major limitations for g_m as CO_2 diffuses 10.000 times lower in water than in air (Evans *et al*., 2009). In fact, several studies have recognized that the cell wall thickness (T_{cw}) is a major trait limiting CO_2 diffusion (Terashima *et al.*, 2001; Evans *et al.*, 2009; Flexas *et al.*, 2012, 2018; Tosens *et al.*, 2012*a*, 2015; Tomás *et al.*, 2013; Carriquí *et al*., 2015, 2019*a*, 2020; Peguero-Pina *et al.*, 2017; Veromann-Jürgenson *et al.*, 2017; Gago *et al*., 2019; Flexas and Carriquí, 2020). Nonetheless, protein-facilitated processes such as those mediated by carbonic anhydrases (CAs) may ease CO_2 diffusivity (Cowan, 1986; Price *et al*., 1994; Williams *et al*., 1996; Gillon and Yakir, 2000; Fabre *et al*., 2007; Pérez-Martín *et al*., 2014). From the cell wall, CO_2 crosses the lipidic bilayer of the plasma membrane, process that can be facilitated by the presence of aquaporins (AQPs; Terashima and Ono, 2002; Uehlein *et al*., 2003, 2008; Hanba *et al*., 2004; Flexas *et al*., 2006*a*; Heckwolf *et al*., 2011; Li *et al*., 2014; Sade *et al*., 2014; Groszmann *et al*., 2017). Finally, the third component of the liquid phase constitutes the CO_2 entrance into the cytosol layer, which is located between the plasma membrane and the chloroplasts envelope. In fact, chloroplasts are generally positioned close to cell walls, shortening the diffusion length through the cytosol (Terashima *et al*., 2011). Also, their distribution and coverage of the intercellular air spaces –usually referred as chloroplasts surface area exposed to intercellular air spaces (S_c/S)– represent another key determinant for g_m (Ren *et al*., 2019).

Finally, chloroplasts constitute the last and major resistance for CO_2 diffusion, englobing two components: the chloroplasts double membrane and the stroma (Fig. 1). Due to the similarities between chloroplasts and plasma membranes, both are assumed to have similar relevance for CO_2 diffusivity (Uehlein *et al*., 2008). However, the presence of carbonic anhydrases in the chloroplast stroma could facilitate CO_2 diffusion until reaching the Rubisco enzyme (Momayyezi and Guy, 2017), which mediates carbon fixation (Evans *et al*., 2009; Flexas *et al*., 2012, 2018).

1.2.- Mesophyll conductance

1.2.1.- Mesophyll conductance as an important determinant of photosynthesis

Early studies focusing on photosynthetic diffusional limitations recognised both stomatal and mesophyll diffusions (Gaastra, 1959). With the spread of gas exchange analyses as the most useful techniques for *in vivo* photosynthesis estimations, mathematical models were designed for the identification and quantification of photosynthesis limitations that separated g_s from "other limitations". However, these early models did not distinguish properly between biochemical components and g_m (Sestak *et al*., 1971). Therefore, CO_2 diffusion inside photosynthetic tissues was referred as "internal conductance", which combined both diffusional and biochemical components. Neglecting those potential limitations imposed by the CO_2 diffusion implies the assumption that the CO_2 concentration at the sub-stomatal cavities (C_i) equals that of the chloroplasts stroma (C_c), which in turn assumes that g_m is infinite and, thus, it cannot be a photosynthesis determinant. Hence, during decades, only g_s and biochemical processes were considered as main photosynthesis determinants (Farquhar *et al*., 1980; Flexas *et al*., 2012, 2018; Gago *et al*., 2020). Nonetheless, with the development of new tools to study *in vivo* leaf gas exchange, several studies evidenced that g_m is finite (and likely regulated dynamically), which means that C_c is significantly lower than C_i (see, for instance, Loreto *et al*., 1992; Epron *et al*., 1995; Flexas *et al*., 2002; Ethier and Livingston, 2004). Thus, new models that allowed for g_m estimation were proposed (Evans *et al*., 1986; Harley *et al*., 1992) and, nowadays, they have been widely used to quantify and differentiate the contribution of both g_s and g_m from biochemistry, providing robust evidence on how g_m strongly contributes to determine photosynthesis in different species and even under contrasting environmental conditions (Grassi and Magnani, 2005; Flexas *et al*., 2018). In general, it has been shown that g_m is the most limiting factor for photosynthesis or a factor as much limiting as g_s and biochemistry, depending on the conditions, the species, and the phylogenetic group (Galmés *et al*., 2007; Gago *et al*., 2019).

1.2.2.- Methodologies for g_m estimation

The most widely used techniques for g_m calculation combine gas exchange measurements with carbon isotopic discrimination or chlorophyll fluorescence (Pons *et al*., 2009). On the one hand, the isotopic method assumes that ^{13}C isotopic discrimination occurs during the CO_2 diffusion through the leaf. Hence, the degree of $^{13}CO_2$ discrimination for a given

condition depends on the ratio between the CO_2 concentration at the chloroplasts stroma and at ambient concentration (i.e., C_c/C_a), from which g_m can be calculated (Evans *et al*., 1986; Evans, 1989). Nonetheless, ^{13}C isotopic discrimination has to be addressed by a mass spectrometer or by a tunable-diode laser absorption spectroscopy (TDLAS), leading to different accuracy for g_m determination. In this sense, the use of a mass spectrometer is time-consuming and requires large CO_2 concentration drawdowns in the cuvette, which may difficult measurements in leaves with small areas and/or with low photosynthetic rates (Pons *et al*., 2009). Nonetheless, the use of TDLAS represents a more accessible, but less accurate methodology to estimate g_m through carbon isotopic discrimination (Pons *et al*., 2009).

On the other hand, the variable *J* method, which combines gas exchange and chlorophyll fluorescence measurements, is the most widely used model for g_m determination. This mathematical method, firstly proposed by Di Marco *et al*. (1990) and then modified by Harley *et al*. (1992), allows for the calculation of g_m at a given C_i. Also, it represents the most robust model to calculate low g_m values. However, accurate measurements of the electron transport rate (*ETR*) under low O_2 conditions (Valentini *et al*., 1995) as well as proper estimations of the light respiration (R_{light}) are necessary for reliable g_m estimations, which also depend on the knowledge of the CO_2 compensation point in the absence of respiration (Γ^*; Pons *et al*., 2009).

The curve fitting method represents an alternative model to estimate g_m that is only based on gas exchange measurements (Ethier and Livingston, 2004; Sharkey *et al*., 2007). This method relies on the estimations of net CO_2 assimilation (A_N) and C_i through a wide range of CO_2 concentrations. With previous knowledge of Rubisco catalytic constants and R_{light}, complete A_N/C_i curves are used to obtain the maximum velocity of carboxylation (V_{cmax}), the maximum electron transport rate (J_{max}) and g_m. Thus, this model requires a precise differentiation between the Rubisco and the ribulose-1,5-bisphosphate (RuBP) regeneration limited regions along the A_N/C_i curve for correct g_m estimations. Nonetheless, the degree of accuracy of this model is presumably lower than that of the other two methods explained above and it assumes that g_m is constantly maintained along changes in CO_2 concentrations (Pons *et al*., 2009).

Finally, anatomical models for g_m estimation are completely independent from gas exchange measurements as they are exclusively based on foliar anatomical characteristics (Tosens *et al*., 2012*a*; Tomás *et al*., 2013). See section 2.1 for a detailed description of the assumptions and potential errors of these models.

2.- Structural determinants of mesophyll conductance

2.1.- Leaf anatomical traits

Intercellular air spaces in the liquid phase represent the first resistance to CO_2 diffusion inside photosynthetic tissues, being determined by T_{leaf}, f_{ias}, and both stomatal density and distribution (see section 1.1. for more detail). Even though it is possible that the gaseous phase resistance plays an important role determining g_m (Earles *et al*., 2018, 2019), it has been traditionally ignored because air imposes a minimum resistance to CO_2 movement (Evans *et al*., 2009).

After diffusing through intercellular air spaces, CO_2 dissolves in the apoplastic water of the cell wall surface according to its thickness, porosity, and tortuosity characteristics (Evans *et al*., 2009). Despite that the relevance of cell wall porosity and tortuosity influencing CO_2 diffusion is still under debate, the negative relationship between T_{cw} and g_m has been widely demonstrated (Flexas *et al*., 2012, 2018; Tomás *et al*., 2013; Carriquí *et al*., 2015, 2019*a*, 2020; Tosens *et al*., 2015; Peguero-Pina *et al*., 2017; Veromann-Jürgenson *et al*., 2017; Gago *et al*., 2019; Flexas and Carriquí, 2020). Additionally, because of the low CO_2 diffusion in the liquid phase, the shortest pathway is the most effective and consists in crossing S_c/S (Terashima *et al*., 2011). Thus, many studies reported a positive correlation between g_m and S_c/S (Tholen *et al*., 2008; Galmés *et al*., 2011; Terashima *et al*., 2011; Tosens *et al*., 2015; Xiong *et al*., 2016; Carriquí *et al*., 2019*a*). These changes in both T_{cw} and S_c/S affecting g_m can occur due to modifications in environmental conditions (Tholen *et al*., 2008; Galmés *et al*., 2013), nutrients supply (Xiong *et al*., 2015; Barbour and Kaiser, 2016; Ruiz-Vera *et al*., 2017; Shrestha *et al*., 2018; Singh and Reddy, 2018) or because of species-specific particularities (Tosens *et al*., 2012*a*, 2015; Tomás *et al*., 2013; Carriquí *et al*., 2015, 2019*a*, 2020; Veromann-Jürgenson *et al*., 2017).

Since it was demonstrated that g_m is influenced by leaf anatomical characteristics, mathematic one-dimensional models were designed to estimate g_m from foliar anatomical traits (Tosens *et al*., 2012*a*; Tomás *et al*., 2013). Even though that these models contain several inputs that are calculated from light and transmission electron microscopy pictures, they do not integrate the effect of various foliar CO_2 sinks and sources. For instance, whilst cellular and sub-cellular membranes present bonded proteins with a specific shape and size that may reduce the area for CO_2 diffusion, they can also contain specific structures such as AQPs and CAs that ease CO_2 diffusion (Evans *et al*., 2009;

Groszmann *et al*., 2017; Flexas *et al*., 2018). Furthermore, thylakoid membranes, starch granules, and mitochondria may also influence CO_2 diffusion, but they are not considered in these models (Flexas *et al*., 2018). Additionally, many parameters included in these models such as the effective cell wall porosity, the CO_2 diffusion viscosity, and the effective pathway length of CO_2 diffusion are based on assumptions rather than on empirical measurements as they cannot be estimated precisely yet. Together with the simplification of the complexity of a three-dimensional organ, all these facts induce incertitude to these models (Flexas *et al*., 2018). Nonetheless, some recent studies have proposed preliminary three-dimensional models to estimate g_m in a more accurate way, being especially complex from a mathematic perspective (Ho *et al*., 2016; Xiao and Zhu, 2017; Earles *et al*., 2018; 2019).

2.2.- Leaf elasticity

The bulk modulus of elasticity (ε) –a parameter commonly obtained from pressure-volume (*P*-*V*) curves– represents the elasticity (or rigidity) of foliar tissues (Bartlett *et al*., 2012) and could be associated with the total amount of cell wall (Niinemets, 2001). Although the mechanistic basis of ε regulation and/or acclimation to specific environmental stresses remains unclear, some studies have suggested that it could be affected by cell wall properties such as thickness (Peguero-Pina *et al*., 2017) and composition (Corcuera *et al*., 2002; Moore *et al*., 2008; Álvarez-Arenas *et al*., 2018; Miranda-Apodaca *et al*., 2018), which in turn may influence g_m. In this sense, Nadal *et al*. (2018) demonstrated that ε is an important parameter linking foliar traits with photosynthesis due to a common mechanistic basis. Specifically, they performed a meta-analysis and found a negative correlation between ε and g_m which was fitted from ferns to angiosperms. Particularly, crops presented the highest photosynthesis with the lowest ε (i.e., more elastic leaves), which indicates low drought tolerance. On the other hand, ferns achieved the lowest photosynthetic rates among the tested species, but presented the highest leaves rigidity, being associated to the prevention of leaf damage during dehydration (Bálsamo *et al*., 2003). Nonetheless, this trade-off between ε and g_m is not extended to lycophytes and bryophytes since they present low photosynthesis and low ε (Perera-Castro *et al*., 2020*a*). However, when plotting all the data for vascular and non-vascular plants, it was shown that ε regulated photosynthesis reduction during desiccation in those species presenting an active or passive stomatal regulation as well as in those lacking stomata.

3.- The plant cell wall

3.1.- First evidences

Even though the first reference on the plant cell wall was done by Gardiner (1900), those studies focusing on cell wall carbohydrates chemistry were first performed by Haworth *et al*. (1934), Hirst and Jones (1938, 1939) and Haworth (1946). From the 1960s, the cell wall chemistry has been an active area of research (see, for instance, Wardrop, 1962; Nevins *et al*., 1967; Jones, 1970; Keegstra *et al*., 1973; Harris and Hartley, 1976). Nowadays, several aspects are known regarding the plant cell wall, a complex and dynamic three-dimensional structure composed by several types of polysaccharides, phenolic compounds, structural proteins and other small molecules, which acts as the first physical barrier that faces those biotic and abiotic stresses occurring during plants life (Somerville *et al*., 2004; Cosgrove, 2005, 2018; Sarkar *et al*., 2009; Keegstra, 2010; Tenhaken, 2015; De Lorenzo *et al*., 2019; Anderson and Kieber, 2020; Yokoyama, 2020). As a consequence of distinct turgor pressure-driven processes taking place during cells growth, different degrees of water uptake promote changes in the physiochemical interactions between cell wall components leading to modifications in wall mechanical properties that affect cells' shape and size at each developmental stage, ultimately, defining plants morphology and growth (McCann and Roberts, 1992; Carpita and Gibeaut, 1993; Carpita and McCann, 2002; Somerville *et al*., 2004; Sarkar *et al*., 2009; Tenhaken, 2015; De Lorenzo *et al*., 2019; Anderson and Kieber, 2020; Lundgren and Fleming, 2020; Yokoyama, 2020).

3.2.- General traits of cell wall physicochemical composition

Prevailing models suggest that cell walls are compounded by three types of layers: the middle lamella and the primary and secondary walls. The middle lamella is originated after the cell mitosis by the synthesis of a barrier between the two nuclei. When these cells are independent, the primary cell wall –which is relatively thin and flexible– is deposited and continues being synthetized during cell growth, expansion, and division. Finally, secondary walls are internally deposited in some types of primary walls providing strength and rigidity to those tissues that are no longer growing, presenting a specific composition according to cells' function (Cosgrove, 2005; Popper, 2008; Keegstra, 2010; Tucker *et al*., 2018). Although each land plant lineage presents specific particularities regarding cell wall composition (see section 7 for more detail), most research has been

specifically focused on primary cell walls (see Fig. 2), which are mainly compounded by cellulose, hemicelluloses and pectins, being cellulose the most abundant polysaccharide (Carpita and Gibeaut, 1993; Carpita and McCann, 2002; Somerville *et al*., 2004; Cosgrove, 2005; Sarkar *et al*., 2009; Tenhaken, 2015; De Lorenzo *et al*., 2019; Anderson and Kieber, 2020; Lundgren and Fleming, 2020; Yokoyama, 2020). Cellulose consists in a few hundred to over 10.000 residues of (1,4)-linked-β-D-glucose chains interacting by hydrogen bonds forming long, insoluble, and unbranched crystalline microfibrils (Somerville *et al*., 2004; Cosgrove, 2005, 2018; Keegstra, 2010; Anderson and Kieber, 2020). Between those closely packed microfibrils, hemicelluloses are deposited by the enzymatic action of expansins and xyloglucan endotransglucosylases/hydrolases (XTH) by non-covalent hydrogen bonds, providing strength to the wall (Cosgrove, 2005; Keegstra, 2010; Tenhaken, 2015; Lundgren and Fleming, 2020; Yokoyama, 2020). Particularly, hemicelluloses comprise non-cellulosic neutral sugars such as glucose, galactose, mannose, xylose, arabinose and rhamnose, some of which are decorated with complex side chains (Somerville *et al*., 2004; Cosgrove, 2005; Popper, 2006; Sørensen *et al*., 2010; Anderson and Kieber, 2020). Thus, this enzymatic cross-linking between cellulose and hemicelluloses constitutes a strong but extensible network that prevents cellulose aggregation facilitating cell wall expansion, specially, during growth (Somerville *et al*., 2004).

Due to interactions between pectins and cellulose (Dick-Pérez *et al*., 2011), this cellulose-hemicelluloses network is embedded within a pectin matrix that is thought to regulate several cell wall properties, such as porosity, flexibility, thickness, microfibril spacing, hydrophilic state and ion balance (Carpita and Gibeaut, 1993; Carpita and McCann, 2002; Cosgrove, 2005; Leucci *et al*., 2008; Moore *et al*., 2008, 2013; Solecka *et al*., 2008; Voragen *et al*., 2009; Ochoa-Villarreal *et al*., 2012; Schiraldi *et al*., 2012; Tenhaken, 2015; Houston *et al*., 2016; Rui and Dinneny, 2019; Yokoyama, 2020). Particularly, pectins englobe a complex and heterogeneous group of acidic polysaccharides deposited in early stages of the cell expansion and consist in distinct domains covalently bonded forming a hydrated gel (Cosgrove, 2005; Voragen *et al*., 2009; Tucker *et al*., 2018). These acidic polysaccharides are rich in galacturonic acid (GalA) residues, which can be distinguished in four different main polymers according to their backbone chemical structure: rhamnogalacturonans types 1 and 2 (RG-I and RG-II, respectively), xylogalacturonans (XGA) and homogalacturonans (HG) (Carpita and McCann, 2002; Cosgrove, 2005; Pelloux *et al*., 2007; Caffall and Mohnen, 2009;

Voragen *et al*., 2009; Keegstra, 2010; Sørensen *et al*., 2010; Atmodjo *et al*., 2013; Tucker *et al*., 2018; De Lorenzo *et al*., 2019; Haas *et al*., 2020; Palacio-López *et al*., 2020). Briefly, RG-I consist in altern GalA and rhamnose residues presenting additional side chains; RG-II are complex polysaccharides with extremely diverse side chains linked to HG backbones; XGA are specific types of HG that can be modified by the addition of xylose branches; and HG present linear chains of more than 200 α-(1,4)-linked GalA residues that are secreted to the cell wall in a highly methyl-esterified form (70-80%) (Carpita and McCann, 2002; Cosgrove, 2005; Pelloux *et al*., 2007; Caffall and Mohnen, 2009; Guénin *et al*., 2017; Haas *et al*., 2020; Palacio-López *et al*., 2020). Of the previous, HG are the most abundant pectin components, and are believed to be the responsible of the maintenance of an appropriated hydric status of the pectin matrix (Guénin *et al*., 2017; Cosgrove, 2018; De Lorenzo *et al*., 2019; Anderson and Kieber, 2020; Haas *et al*., 2020).

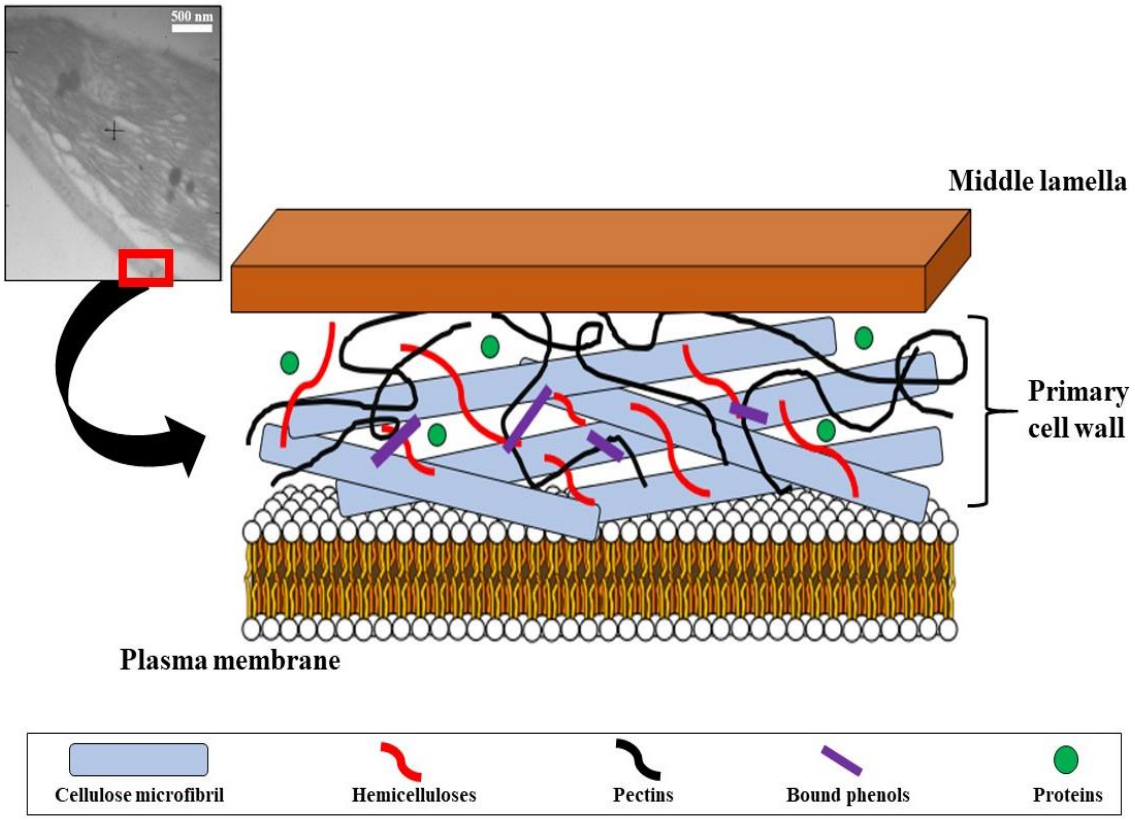

Fig. 2. Schematic representation of a primary plant cell wall architecture and composition.

Besides the cell wall components explained above, lignins represent other major wall compounds placed in secondary walls (Sarkar *et al*., 2009; Terrett and Dupree, 2019;

Anderson and Kieber, 2020). They are complex hydrophobic polyphenolic compounds presenting a specific chemical composition which quantity depends on the cell developmental stage and location, as well as on the presence of environmental stresses (Fry, 1979; Wallace and Fry, 1994; Campbell and Sederoff, 1996; Terrett and Dupree, 2019; Anderson and Kieber, 2020). Interestingly, it has been described that hemicelluloses and lignins are covalently cross-linked in the plant cell wall, influencing its strength, flexibility, and extensibility (Iiyama *et al*., 1994; Wallace and Fry, 1994; Fan *et al*., 2006; Sarkar *et al*., 2009; Terrett and Dupree, 2019).

Additionally, plant cell walls also contain minor compounds which may play a key role defining its characteristics in specific developmental stages and during biotic and/or abiotic stresses (Fry, 1979; Carpita and Gibeaut, 1993; Wallace and Fry, 1994; Carpita and McCann, 2002; Cosgrove, 2005; Sarkar *et al*., 2009; Anderson and Kieber, 2020). For instance, in Fig. 2 it is shown that some cell wall bound phenolics can be covalently linked to main cell wall compounds –specifically, pectins and/or hemicelluloses (Fry, 1979, 2004)–, decreasing wall porosity (Wallace and Fry, 1994) and enhancing its rigidity when high amounts are deposited (Fry, 1979). Moreover, the presence of highly diverse proteins associated to the primary cell wall may determine its properties due to their interaction with polysaccharides (Carpita and McCann, 2002; Novaković *et al*., 2018). For example, it has been proposed that extensins may alter the interactions between cellulose and hemicelluloses by non-enzymatic activity (Anderson and Kieber, 2020), affecting cell wall mechanical properties (Cosgrove, 2005; Popper, 2008). However, the functional characterization of each specific protein remains to be further investigated as they belong to a large gene family (Novaković *et al*., 2018; Anderson and Kieber, 2020).

4.- Photosynthesis under abiotic stress: the role of g_m

During their whole life, plants can be exposed to sub-optimal conditions that limit their growth. Thus, they have developed anatomical, biochemical, morphological, and physiological strategies that enable their adaptation and acclimation to guarantee their survival (Le Gall *et al*., 2015; Novaković *et al*., 2018). Among them, g_m adjustments are recognized as relevant traits determining photosynthetic responses under non-favourable environmental conditions. Whilst g_m has been shown to respond to environmental conditions such as changes in light intensity (Hanba *et al*., 2002; Niinemets *et al*., 2009;

Douthe *et al*., 2011, 2012; Tosens *et al*., 2012*b*; Xiong *et al*., 2015; Carriquí *et al*., 2019*b*) and in CO_2 concentrations (Bernacchi *et al*., 2005; Flexas *et al*., 2007; Vrabl *et al*., 2009; Tazoe *et al*., 2011; Crous *et al*., 2013; Singh *et al*., 2013; Xiong *et al*., 2015; Carriquí *et al*., 2019*b*), among others, we will focus on the two mostly used stresses along the present Thesis given their importance under a climate change scenario, i.e., water deficit stress and changes in leaf temperature (Lipiec *et al*., 2013; Nadal and Flexas, 2019).

4.1.- Mesophyll conductance response to water deficit stress

Together with cell growth, photosynthesis is among the first processes to be affected by water deficit stress. Even though the intensity, duration and progression of the stress determine plant responses to water deprivation (Chaves *et al*., 2003, 2009), photosynthesis is affected during dehydration progression due to the loss of the rehydration capacity in the damaged tissues and the loss of the photochemical apparatus under extreme dehydration.

Stomatal closure in response to leaf turgor reductions because of decreased amounts of water in cells and/or due to drought-induced hormonal regulation is the first event limiting photosynthesis from mild to moderate levels of water deficit stress. In most cases, photosynthesis is almost stopped by stomatal closure before the appearance of metabolic disruptions (Flexas *et al*., 2004). Although both short-term (i.e., from minutes to hours) and long-term (i.e., from weeks to months) water deficit stress application evidenced that g_m decreases concomitantly with g_s in many plant species (Grassi and Magnani, 2005; Flexas *et al*., 2006*b*, 2009; Díaz-Espejo *et al*., 2007; Galmés *et al*., 2007; Gallé *et al*., 2009, 2011), Bunce (2009) reported that g_m was not reduced until g_s declined by up to 90%. These reductions in g_m may be linked to physical alterations in the structure of intercellular spaces due to leaf shrinkage, to biochemical alterations (bicarbonate to CO_2 conversion) and/or to alterations in membrane permeability (aquaporins) (Chaves *et al*., 2009). Additionally, whereas some studies performed under water shortage conditions reported that common anatomical modifications affecting g_m involve reduced f_{ias} and chloroplasts size while increasing T_{cw} (Niinemets *et al*., 2009; Poorter *et al*., 2009; Galmés *et al*., 2013), Tomás *et al*. (2014) could not relate g_m reductions to anatomical alterations in water-stressed vines.

Regardless of those changes occurring in a particular species, water deficit stress promotes a decline in the CO_2 supply to the Rubisco enzyme because of a reduction in both diffusive conductances. Furthermore, g_m recovered slowly after rewatering in some

studies, being probably related to species-specific characteristics as well as to particular environmental conditions, contributing to limited photosynthesis during drought cycles (Flexas *et al*., 2009; Gallé *et al*., 2009, 2011). Additionally, decreased g_m and g_s under water deprivation have important implications since the g_m/g_s ratio is positively correlated with the intrinsic water use efficiency (WUE_i; Flexas *et al*., 2013*a*). Thus, whereas the g_m/g_s ratio has been proposed as a key trait to simultaneously improve photosynthesis and WUE_i in those crops prone to be drought-affected (Flexas *et al*., 2015), the mechanistic basis of g_m/g_s regulation under water deficit stress remains largely unknown (Flexas *et al*., 2018).

4.2.- Mesophyll conductance response to changes in leaf temperature

Photosynthesis is highly affected by temperature variations (Yamori *et al*., 2014). Although different g_s patterns have been recognized as photosynthetic determinants during the acclimation to contrasting temperatures (Sage and Kubien, 2007), the role of g_m has been traditionally neglected. However, some studies evidenced that g_m increases from low to high temperatures, but with different slopes and/or behaviours once a maximum temperature is achieved (Bernacchi *et al*., 2002; Pons and Welschen, 2003; Yamori *et al*., 2006; Flexas *et al*., 2008; Scafaro *et al*., 2011; Evans and von Caemmerer, 2013; von Caemmerer and Evans, 2015; Xiong *et al*., 2015). On the one hand, Yamori *et al*. (2006) proposed a potential role of g_m limiting photosynthesis at warmer temperatures in spinach acclimated to cold. Particularly, they showed that the optimum temperature for g_m depended on the growth temperature, being 25ºC and 20ºC for plants grown at day/night temperatures of 30/25ºC and 15/10ºC, respectively. These results were further corroborated by Flexas *et al*. (2008), who reported that *Brassica oleracea* plants developed at 5ºC presented 300-folds lower g_m than those grown at 20ºC. Similarly, g_m increased exponentially while enhancing the temperature from 10ºC to 35ºC in tobacco, but decreased thereafter (Bernacchi *et al*., 2002). Nonetheless, von Caemmerer and Evans (2015) proposed that g_m responses to temperature seem to be species-specific since they found large g_m variations subjecting some species from 15ºC to 40ºC, whilst it was almost maintained in others over the same temperature ranges. However, only Pons and Welschen (2003) observed that g_m was reduced while increasing the temperature from 28 to 38ºC in *Eperua grandiflora*.

5.- Cell wall composition rearrangements under abiotic stress

Even though several studies have described how changes in cell wall composition occur due to the imposition of distinct environmental stresses testing different species (see, for instance, Sweet *et al*., 1990; Kubacka-Zębalska and Kacperska, 1999; Vicré *et al*., 1999, 2004; Bray, 2004; Moore *et al*., 2006, 2008, 2013; Leucci *et al*., 2008; Solecka *et al*., 2008; Hura *et al*., 2009, 2012; Suwa *et al*., 2010; Carvalho *et al*., 2013; Domon *et al*., 2013; Baldwin *et al*., 2014; Zheng *et al*., 2014; Clemente-Moreno *et al*., 2019; Nadal *et al*., 2020), those specific cell wall alterations promoted by a particular stress are not completely understood (Le Gall *et al*., 2015; Tenhaken, 2015; Rui and Dinneny, 2019). In this section, we will focus on those cell wall modifications attributed to the mostly studied abiotic stresses along this Thesis, i.e., water deficit stress and heat, which coincide with those conditions mainly imposed by the climate change (Lipiec *et al*., 2013; Nadal and Flexas, 2019).

5.1.- Water deficit stress

The effect of water deficit stress modifying cell wall composition has been studied in different angiosperms (Sweet *et al*., 1990; Vicré *et al*., 1999, 2004; Bray, 2004; Moore *et al*., 2006, 2008, 2013; Zheng *et al*., 2014; Clemente-Moreno *et al*., 2019; Nadal *et al*., 2020). From their results, species-specific adjustments in both cellulose and hemicelluloses contents were observed, suggesting that changes in these components may depend on the plant age, the studied tissue, and/or the level of water deprivation. For instance, Bray (2004) found decreased cellulose content submitting *Arabidopsis* to drought, whilst Nadal *et al*. (2020) did not report changes in cellulose amounts in water-stressed *Arbutus unedo*. Nonetheless, Sweet *et al*. (1990) and Clemente-Moreno *et al*. (2019) showed cellulose increasing after acclimating vines and tobacco, respectively, to water deprivation. In cotton, encoding genes for cellulose biosynthesis increased after drought exposition, suggesting potentially higher cellulose biosynthesis (Zheng *et al*., 2014). Similarly, hemicelluloses have been found to either increase (Vicré *et al*., 1999), decrease (Sweet *et al*., 1990) or stay constant (Clemente-Moreno *et al*., 2019; Nadal *et al*., 2020) after water shortage application. Specifically, Vicré *et al*. (2004) reported changes in non-cellulosic neutral sugars in dry leaves of the resurrection plant *Craterostigma wilmsii*, which decreased glucose content and replaced xyloglucan by galactose after desiccation.

Despite of this varying behaviour for both cellulose and hemicelluloses, more agreement is found regarding pectins as their increasing under water-limiting conditions plays a crucial role modulating the cell wall hydric status (Vicré *et al*., 1999, 2004; Moore *et al*., 2006, 2008, 2013; Leucci *et al*., 2008; Tenhaken, 2015; Novaković *et al*., 2018; Clemente-Moreno *et al*., 2019; Rui and Dinneny, 2019), specially due to alterations in the degree of HG methylesterification (Leucci *et al*., 2008). Interestingly, Vicré *et al*. (1999, 2004) and Moore *et al*. (2006, 2008, 2013) evidenced the dynamics of those changes occurring in the cell wall pectin fraction testing resurrection plants subjected to various cycles of water deficit stress followed by rehydration.

5.2.- Heat stress

Despite that the cell wall is not the main structure affected by a heat exposition (Le Gall *et al*., 2015), some studies have demonstrated that it can be altered at distinct levels. Particularly, the cell wall gene expression was modified due to high temperature in *Brassica rapa*, suggesting that specific genes may be related to the acquisition of thermotolerance (Yang *et al*., 2006). In *Agrostis* spp., expansins were up-regulated at 40ºC, evidencing their relevance increasing the cell wall elasticity during a heat exposition in order to maintain the cellular functionality (Xu *et al*., 2008). Additionally, Lima *et al*. (2013) detected a decrease of around 50% and an increase of 40% in pectins and hemicelluloses contents, respectively, testing coffee plants subjected to 37ºC. Furthermore, they demonstrated that lignins synthesis was also altered because of high temperature, which leaded to changes in their chemical structure. However, modifications in the cell wall composition after heat acclimation seem to be species-specific (Le Gall *et al*., 2015).

6.- Photosynthesis through land plants' phylogeny: the role of g_m

During the colonization of terrestrial ecosystems by plants, they developed numerous mechanisms and/or structures that ensured the maintenance of an appropriated degree of hydration and functionality of the photosynthetic structures in the dry atmosphere. Overall, these structures have been related with the development of water conducting tissues and with the water use efficiency regulation by the appearance of cuticles, stomata, and foliar mesophylls (Brodribb *et al*., 2009; Brodribb and McAdam, 2011; Ducket and Pressel, 2018). Due to these evolutionary adaptations, a tendency to increase the

photosynthetic capacity from early non-vascular plants (i.e., bryophytes) to angiosperms (the most modern plant group) appeared. Even though the relevance of g_s determining this enhanced photosynthetic capacity along land plants' phylogeny has been well established thanks to the current knowledge regarding stomata appearance and evolution (Brodribb *et al*., 2009; Brodribb and McAdam, 2011), the importance of g_m has been recently elucidated (Flexas *et al*., 2018; Gago *et al*., 2019; Flexas and Carriquí, 2020).

Thus far, numerous studies have reported g_m values in several spermatophytes, i.e., angiosperms and gymnosperms (see, for instance, Rho *et al*., 2012; Flexas *et al*., 2013*b*; DaMatta *et al*., 2016; Veromann-Jürgenson *et al*., 2017; Carriquí *et al*., 2020). However, less g_m values have been described for ferns (Volkova *et al*., 2009; Gago *et al*., 2013; Carriquí *et al*., 2015; Tosens *et al*., 2015) and even less for bryophytes due to technical difficulties for their measurement (Williams and Flanagan, 1998; Meyer *et al*., 2008; Hanson *et al*., 2014). Nonetheless, by the improvement of gas exchange systems, recent studies have provided g_m values for many moss species (Carriquí *et al*., 2019*a*; Perera-Castro *et al*., 2020*b*). When pooling all this data together, g_m follows a clear phylogenetic trend, from the lowest values in bryophytes to the largest in angiosperms (Gago *et al*., 2019; Flexas and Carriquí, 2020). Within angiosperms, g_m also differs among growth forms and leaf types. Hence, the highest g_m values are found in non-woody angiosperms, particularly, grasses and herbs (around 0.40 and 0.30 mol CO_2 m^{-2} s^{-1}, respectively; Flexas *et al*., 2008). They are followed by semi-deciduous and deciduous shrubs and trees, whereas the lowest g_m values within angiosperms correspond to evergreen shrubs and trees, which present similar g_m values than conifers (0.15 mol CO_2 m^{-2} s^{-1}, approximately; Flexas *et al*., 2008). In ferns, g_m values are two- and seven-folds lower than the averaged g_m for conifers and grasses, respectively. Additionally, even within ferns and ferns allies, significant variability has been detected since horsetails achieve the highest g_m whilst lycophytes present the lowest (Tosens *et al*., 2015; Flexas *et al*., 2018). Finally, the lowest g_m values along land plants' phylogeny are found in bryophytes (i.e., mosses, liverworts, and hornworts), non-vascular plants presenting from 10 to 16-folds lower g_m than grasses (Carriquí *et al*., 2019*a*; Flexas and Carriquí, 2020).

The photosynthetic characterization through land plants' phylogeny has enabled the analysis of those photosynthetic limitations much more affecting each land plant lineage (Gago *et al*., 2019). Thus, another phylogenetic tendency is observed regarding photosynthetic limitations (Gago *et al*., 2019). Mesophyll conductance limitation (l_m) predominantly restrains photosynthesis in bryophytes and in eusporangiate ferns

(lycopodiophytes, equisetophytes and psilophytes), whereas both stomatal conductance limitation (l_s) and l_m co-determine photosynthesis in more modern ferns (i.e., leptosporangiates) and gymnosperms, achieving a balanced co-regulation by l_s, l_m and biochemical limitation (l_b) in angiosperms.

7.- Cell wall composition along land plants' phylogeny

Although the cell wall composition is relatively conserved along land plants' phylogeny (Sarkar *et al*., 2009; Popper and Tuohi, 2010; Sørensen *et al*., 2010; Popper *et al*., 2011), specific changes in its architecture and chemical composition have been described comparing distinct land plants lineages (Popper and Fry, 2003; Niklas, 2004; Popper, 2008; Sarkar *et al*., 2009; Sørensen *et al*., 2010; Popper *et al*., 2011). These main differences and/or particularities are found in Table 1 and have leaded to the establishment of three main types of primary cell walls (Carpita, 1996; Carpita and McCann, 2002; Sarkar *et al*., 2009; Silva *et al*., 2011).

7.1.- Bryophytes

Just a few studies have focused on the cell wall composition of bryophytes (mosses, liverworts, and hornworts), showing that they contain high amounts of cellulose, pectins and hemicelluloses, specifically, mannose (Popper and Fry, 2003; Sarkar *et al*., 2009; Popper *et al*., 2011; Roberts *et al*., 2012). Even though that their hemicelluloses are chemically different to that of angiosperms due to the presence of distinct enzymes, their high amounts could be indicative of cell wall fortification in comparison to algae ancestors (Popper and Fry, 2003; Peña *et al*., 2008; Sarkar *et al*., 2009; Sørensen *et al*., 2010). Similarly, an increasing in pectins content –particularly, in the amounts of GalA– has been linked to desiccation avoidance mechanisms, which could be of crucial importance given the poikilohydry exhibited by most of them (Popper and Fry, 2003; Sarkar *et al*., 2009). Additionally, it has been suggested that RG-I and RG-II were originated during the transition from water to land in order to increase the cell wall strength (Matsunaga *et al*., 2004; Niklas *et al*., 2004; Sørensen *et al*., 2010). Particularly, RG-II cross-linking is believed to play a key role defining bryophytes' pectin matrix properties (Matsunaga *et al*., 2004). Despite bryophytes do not contain lignin, lignin-like polymers have been described in some moss species (Popper and Fry, 2003; Ligrone *et al*., 2008; Sarkar *et al*., 2009; Xu *et al*., 2009).

Table 1. Main distinctive cell wall traits of each land plant lineage.

Plant groups			**Cell wall characteristics**	
Bryophytes			- High amounts of cellulose and hemicelluloses (particularly, mannose). - High pectins proportion (specially, GalA). - Origination of RG-I and RG-II, the later defining pectin matrix properties. - Lignin-like polymers in some species. - Primitive species with lower amounts of mannose, glucuronic acid, and GalA than more modern species.	
Ferns	Eusporangiates		Type III cell walls	- Higher mannans and lower pectins amounts in primary cell walls than leptosporangiates.
	Leptosporangiates			- Presence of lignins in some species. - The highest tannins abundance along terrestrial phylogeny.
Spermatophytes	Gymnosperms		Type I cell walls	- XG cross-linking cellulose. - XG contain more fucose side chains than previous plant groups. - RG-II residues are less methylated than in previous plant groups. - Lignins abundance in secondary cell walls.
	Angiosperms	Dicotyledonous	Type I cell walls	- Cell walls similar to those of gymnosperms, but with less lignins in secondary cell walls.
		Commelinoid monocotyledonous	Type II cell walls	- Larger amounts of cellulose and hemicelluloses than dicotyledonous. - Significant reductions of pectins and structural proteins. - Low XG amounts. - GAX is the main polymer cross-linking cellulose. - Grasses also contain high quantities of mixed-linked (1→3),(1→4)*β*-D-glucans and phenolic polymers.

Even within bryophytes, some differences regarding cell wall composition have been observed analysing primitive and more modern species (Popper and Fry, 2003). For instance, low amounts of mannose and both glucuronic and galacturonic acids were quantified in primitive mosses presenting a simple vegetative structure, which could represent a less complex cell wall architecture as compared with more modern species (Popper and Fry, 2003).

7.2.- Ferns

Within terrestrial plants, ferns (or pteridophytes) –which can be divided in eusporangiates (lycopodiophytes, equisetophytes and psilophytes) and leptosporangiates (more modern ferns) (Popper, 2006; Sarkar *et al*., 2009)– present a specific cell wall composition, commonly referred as Type III cell walls (Popper and Fry, 2003, 2004; Popper, 2006; Silva *et al*., 2011). Even though that ferns may present significant differences in cell wall composition considering primary or secondary walls (Sarkar *et al*., 2009), their cell walls are mainly characterized to contain large quantities of mannans and low pectins amounts (Silva *et al*., 2011). These cell wall particularities are even more pronounced in eusporangiates since they contain more mannan-rich primary cell walls with lower pectins content than leptosporangiates (Popper and Fry, 2003, 2004; Popper, 2006; Silva *et al*., 2011). Nonetheless, lignin has been detected in some leptosporangiates, which may reflect an increasing of the cell wall mechanical strength due to larger complexity of the plant body (Wallace and Fry, 1994; Popper and Fry, 2004; Sarkar *et al*., 2009). Additionally, leptosporangiates present the highest tannins amounts along terrestrial plants groups (Popper and Fry, 2004; Popper, 2006; Sarkar *et al*., 2009).

7.3.- Spermatophytes

7.3.1.- Gymnosperms

Together with dicotyledonous angiosperms, gymnosperms possess Type I cell walls, being characterized by cellulose cross-linked to hemicelluloses –mainly xyloglucans (XG)–, embedded in a pectin matrix (Carpita and Gibeaut, 1993; Carpita, 1996; Carpita and McCann, 2002; Anderson and Kieber, 2020). However, in comparison to the previous phylogenetic groups explained above, XG contain a higher number of fucose side chains and RG-II domains are less methylated (Popper and Fry, 2004; Sarkar *et al*., 2009). Finally, one of the main characteristics of gymnosperms' cell walls is that they present

large amounts of lignins in secondary walls, which are involved in providing mechanical strength to tall trees (Sarkar *et al*., 2009).

7.3.2.- Angiosperms

Within angiosperms, the cell wall composition varies considering dicotyledonous and commelinoid monocotyledonous species (Carpita and Gibeaut, 1993; Carpita, 1996; Carpita and McCann, 2002; Popper, 2006; Vogel, 2009; Sørensen *et al*., 2010). Whereas dicotyledonous possess Type I cell walls, commelinoid monocotyledonous (i.e., grasses, rushes, gingers, and sedges) present Type II cell walls, being characterized by even higher amounts of both hemicelluloses and cellulose with significant reductions of pectins –presenting a similar physicochemical structure of that of dicotyledonous– and structural proteins (Carpita and Gibeaut, 1993; Carpita, 1996; Cosgrove, 1997; Carpita and McCann, 2002; Popper, 2006; Anderson and Kieber, 2020). Even though Type II cell walls contain lower amounts of XG as compared to Type I, the number of XTH genes for xyloglucans modification found in grasses is close to that of dicotyledonous (Popper, 2008). This fact supports the idea that, while grasses apparently have the genetic capacity to form XG-rich cell walls, these genes probably remain inactive (Sarkar *et al*., 2009). Instead, the principal polymer cross-linking cellulose microfibrils in commelinoid monocotyledonous is glucuronoarabinoxylan (GAX; Carpita and Gibeaut, 1993; Carpita, 1996; Carpita and McCann, 2002). In addition to GAX, grasses (i.e., family Poaceae) represent a specific group within commelinoid monocotyledonous as they also accumulate large quantities of mixed-linked (1→3),(1→4)*β*-D-glucans (Carpita and Gibeaut, 1993; Carpita, 1996; Carpita and McCann, 2002). Furthermore, grasses' cell walls are enriched by phenolic substances such as ferulic and coumaric acids (Hartley, 1973; Harris and Hartley, 1976; Hartley and Jones, 1977; Carpita and Gibeaut, 1993; Iiyama *et al*., 1994; Carpita, 1996; Carpita and McCann, 2002).

8.- Evidences of cell wall composition impacting g_m

Despite that the potential implication of cell wall composition determining photosynthesis –specifically, via g_m adjustments– has been proposed (Gago *et al*., 2020; Flexas *et al*., 2021), this field remains largely unexplored. However, Weraduwage *et al*. (2016) showed that pectin methylesterases (PME) suppression –i.e., an alteration of the functionality of a specific pectin remodelling enzyme (PRE)– in double *Arabidopsis* mutants reduced the

CO_2 uptake, thus, diminishing photosynthesis. This result leaded to the suggestion that specific PME activity could modulate mesophyll cell wall properties and, consequently, g_m (Lundgren and Fleming, 2019). Nonetheless, only the study by Ellsworth *et al*. (2018) evidenced significant g_m declines in *Oryza sativa* mutant genotypes exhibiting alterations in mixed-linked glucans. Particularly, mutants presented g_m reductions of around 83% as compared to wild-type genotypes, being 28% of this reduction attributed to anatomical alterations –specifically, in S_c/S–, whilst the rest was influenced by cell wall properties that modified CO_2 diffusivity. More recently, Zhang *et al*. (2020) tested other rice mutants presenting alterations in the conversion of UDP-glucose into UDP-galactose showing that disruptions in cellulose microfibrils orientation as well as in hemicelluloses structure were related to photosynthesis declines. On the other hand, Clemente-Moreno *et al*. (2019) reported that pectins and/or the hemicelluloses to pectins ratio co-variated with g_m in *Nicotiana sylvestris* subjected to short-term salinity and drought followed by a subsequent recovery. Interestingly, they hypothesised that pectins accumulation under both abiotic stresses could increase T_{cw}, hence, enlarging the CO_2 pathway until reaching its carboxylation sites. Moreover, the studies by Hura *et al*. (2009, 2012) revealed that minor cell wall components such as cell wall bound phenolics –particularly, ferulic acid– were related to the photosynthetic capacity in triticale genotypes submitted to drought. Finally, Carriquí *et al*. (2020) tested seven conifer species acclimated to the same non-stressing environmental conditions and demonstrated that the total amount of isolated cell wall content (i.e., the alcohol insoluble residue; AIR) as well as both cellulose and hemicelluloses contents correlated negatively with g_m. However, what was even more interesting is that the pectins to cellulose and hemicelluloses ratio strongly influenced g_m, evidencing that not only a specific cell wall component but the proportion between them –with pectins playing a key role– are likely to strongly regulate g_m. Additionally, first empirical evidence on the specific role of pectins and cellulose influencing T_{cw} at interspecific level was shown.

9.- The cell wall from a biotechnological perspective

As explained in section 3, cell wall biosynthesis and its subsequent modification are determined by complex processes that can be altered from the beginning of monomer building to wall restructuration by the addition of new polymers (Carpita and McCann, 2002). Even though specific biochemical pathways occurring during cell wall synthesis

and/or remodelling have been studied, they are not completely understood due to the complexity of the relationships between cell wall components (Carpita and McCann, 2002; Tucker *et al*., 2018; Lundgren and Fleming, 2019; Anderson and Kieber, 2020; Yokoyama, 2020).

A huge number of enzyme families such as glycosyltransferases, glycosylhydrolases, methyltransferases and acetylesterases –commonly designed as carbohydrate-active enzymes (CAZymes)– determine the appropriate structure and functioning of the cell wall (Tucker *et al*., 2018; Yokoyama, 2020). Hence, the classification of cell wall enzymes according to the family they belong to is important to elucidate the function of a specific enzyme, but it is still a difficult task (Yokoyama, 2020). In this sense, mutant genotypes represent a useful tool to identify which alterations are caused by specific cell wall disruptions (Yokoyama, 2020). Thus, first screenings of cell wall mutants were performed by Reiter *et al*. (1993, 1997) testing *A. thaliana*. Particularly, they studied the function of specific non-cellulosic cell wall polysaccharides and that of the genes involved in their synthesis detecting alterations in hemicelluloses and pectins architecture that affected mutants' growth and development as compared to wild-type lines. From then to now, the publication of *A. thaliana* complete genome sequence (Arabidopsis Genome Initiative, 2000) has converted this species in the most widely used model plant to further investigate the effects of several cell wall mutations testing different genotypes.

Due to the importance of pectins determining several cell wall properties, pectin remodelling enzymes (PRE) have been largely studied since their over/under-expression can alter signalling pathways, thus, promoting modifications in the status, dynamics, and organization of the cell wall (Cosgrove, 2005; Cavalier *et al*., 2008; Park and Cosgrove, 2012; Tucker *et al.*, 2018; Anderson and Kieber, 2020). Specifically, PRE comprehend the action of pectin methylesterases (PME), pectin acetylesterases (PAE) and pectin galacturonases (PG). Particularly, PME remove specific HG methyl groups leading to changes in pectins' physical structure, creating new targets for the action of both PG and PAE (Pelloux *et al*., 2007; Levesque-Tremblay *et al*., 2015; Turbant *et al*., 2016; Palacio-López *et al*., 2020). Whilst PAE control the acetylation degree of HG and RG-I residues, PG catalyse pectins hydrolysis (Pelloux *et al*., 2007; Gou *et al*., 2008, 2012; Turbant *et al*., 2016; Guénin *et al*., 2017; Yang *et al*., 2018; Kong *et al*., 2019). Thus, the action of these enzymes alters pectins physicochemical structure modifying their interaction with other cell wall compounds, ultimately defining wall characteristics (Pelloux *et al*., 2007;

Gou *et al*., 2008, 2012; Turbant *et al*., 2016; Guénin *et al*., 2017; Kong *et al*., 2019). Although several studies have tested different mutant genotypes in order to elucidate the importance of an appropriated functionality of these enzymes (see, for instance, Rhee *et al*., 2003; Bosch and Hepler, 2005; Parre and Geitmann, 2005; Derbyshire *et al*., 2007; Gou *et al*., 2008, 2012; Peaucelle *et al*., 2008, 2011; Zhang *et al*., 2008; Pelletier *et al*., 2010; Müller *et al*., 2013; de Souza *et al*., 2014; Sénéchal *et al*., 2014; de Souza and Pauly, 2015; Leroux *et al*., 2015; Levesque-Tremblay *et al*., 2015; Scheler *et al*., 2015; Turbant *et al*., 2016; Wang *et al*., 2016; Weraduwage *et al*., 2016; Guénin *et al*., 2017; Hocq *et al*., 2017; Yang *et al*., 2018; Kong *et al*., 2019), their biological implications are still poorly understood.

Chapter 2

Objectives and Thesis outline

Objectives

As stated in the General Introduction, cell wall composition has been proposed to be an important photosynthesis determinant as it may affect g_m. Thus, this Thesis was focused on three General Objectives:

1. To explore possible relationships between changes in cell wall composition and g_m during water deficit stress exposition in a model plant.
2. To study the relationships between changes in cell wall composition and g_m in different crops acclimated to contrasting abiotic stresses.
3. To study genetic and phylogenetic conditionings for the relationships between photosynthesis and cell wall composition.

The previous General Objectives were approached by six Specific Objectives:

1. To study short- and long-term water deficit stress responses in cell wall composition, leaf water relations, foliar anatomy, and photosynthesis.
2. To determine the dynamics and the speed of those changes occurring in cell wall composition and photosynthesis after plants exposition to specific levels of water availability.
3. To investigate the effect of temperature and distinct water deficit stress regimes promoting modifications in cell wall composition that influence leaf water relations, leaf anatomy, and photosynthesis performance.
4. To examine the effect of specific cell wall mutations regulating g_m in mutant plants.
5. To analyse the role of cell wall composition in relation to photosynthesis and leaf anatomy in plants belonging to a single phylogenetic group distant from angiosperms.
6. To evaluate the importance of cell wall composition in determining photosynthesis performance and leaf anatomy along land plants' phylogeny.

Thesis outline

The present Thesis is organized as follows:

Chapter 1: General Introduction

This chapter provides the background and the framework of this Thesis. It explains the pathway that CO_2 has to follow during photosynthesis highlighting g_m relevance as a photosynthesis limitation. A description of g_m changes due to abiotic stresses and along land plants' phylogeny is included. The structural traits most affecting g_m are explained, proposing that cell wall composition could be a novel fact regulating g_m. Thus, cell wall compositional properties are described as well as those modifications occurring due to abiotic stresses and along terrestrial plants lineages. Finally, it is discussed that the use of mutants could elucidate how specific cell wall mutations affect plants' functional traits.

Chapter 2: Objectives and Thesis outline

This chapter describes the General and the Specific Objectives of this Thesis as well as the Thesis outline.

Chapter 3: Exploring the role of cell wall composition influencing changes in photosynthesis, leaf water relations and foliar anatomy in *Helianthus annuus* subjected to distinct levels of water availability

In this chapter, the species *H. annuus* was submitted to distinct water availability regimes to detect possible relationships between changes in cell wall composition and adjustments occurring in photosynthesis, leaf water relations and anatomical properties. Also, the speed and the dynamics of these changes were evaluated. Finally, *H. annuus* was compared to a phylogenetically distant species to determine if modifications in cell wall composition after water deficit stress application similarly affected photosynthesis, leaf water relations and anatomy.

- General Objective 1 and Specific Objectives 1 and 2 are addressed in this chapter.

Chapter 4: The importance of cell wall composition regulating species-specific responses to different environmental conditions

This chapter describes the effect of species-specific cell wall composition adjustments in determining photosynthesis performance, leaf water relations and anatomical

characteristics after the acclimation of different crop species to contrasting environmental conditions.

- General Objective 2 and Specific Objective 3 are addressed in this chapter.

Chapter 5: The use of mutant plants to elucidate the effect of specific cell wall disruptions affecting photosynthesis

Using *Arabidopsis thaliana* mutant genotypes, this chapter investigates how specific mutations affecting cell wall composition and pectins enzymatic performance could ultimately influence g_m.

- General Objective 3 and Specific Objective 4 are addressed in this chapter.

Chapter 6: Cell wall composition: an important photosynthesis determinant conserved in the most primitive land plant lineage

This chapter focuses on the role of cell wall composition influencing photosynthesis and anatomical properties in the most basal land plant group, i.e., bryophytes.

- General Objective 3 and Specific Objective 5 are addressed in this chapter.

Chapter 7: General Discussion.

This chapter comprehends a general vision of the most relevant findings of this Thesis, discusses its limitations and proposes areas for further investigation. Here, data from all previous chapters are pooled together to find the most conserved relationships between g_m and cell wall compositional and anatomical traits in plants subjected to abiotic stresses. Additionally, a data compilation of those species in which cell wall composition, photosynthesis and anatomical properties have been studied is used to highlight the relevance of cell wall compositional characteristics regulating g_m along land plants' phylogeny. The merged and discussed data from this section allow for a more detailed deepening in the General Objectives, and specifically adds insights to the Specific Objective 6.

Chapter 8: Conclusions

This chapter presents a list of the main conclusions derived from the present Thesis in relation to the General and Specific Objectives.

Chapter 3

Exploring the role of cell wall composition influencing changes in photosynthesis, leaf water relations and foliar anatomy in *Helianthus annuus* subjected to distinct levels of water availability

Cell wall composition and thickness affect mesophyll conductance to CO_2 diffusion in *Helianthus annuus* under water deprivation

Margalida Roig-Oliver[1*], Panagiota Bresta[2], Miquel Nadal[1], George Liakopoulos[2], Dimosthenis Nikolopoulos[2], George Karabourniotis[2], Josefina Bota[1], Jaume Flexas[1]

[1]Research Group on Plant Biology under Mediterranean Conditions, Departament de Biologia, Universitat de les Illes Balears (UIB) – Agro-Environmental and Water Economics Institute (INAGEA). Carretera de Valldemossa Km 7.5, 07122 Palma, Illes Balears, Spain.
[2]Laboratory of Plant Physiology and Morphology, Department of Crop Science, Agricultural University of Athens (AUA), Iera Odos 75, Botanikos, 11855 Athens, Greece.

[*] Corresponding author.

Published in *Journal of Experimental Botany* in 2020.

Journal of Experimental Botany
doi:10.1093/jxb/eraa413 Advance Access Publication 9 September 2020

RESEARCH PAPER

Cell wall composition and thickness affect mesophyll conductance to CO_2 diffusion in *Helianthus annuus* under water deprivation

Margalida Roig-Oliver[1,*], Panagiota Bresta[2], Miquel Nadal[1], Georgios Liakopoulos[2], Dimosthenis Nikolopoulos[2], George Karabourniotis[2], Josefina Bota[1] and Jaume Flexas[1],

[1] Research Group on Plant Biology under Mediterranean Conditions, Departament de Biologia, Universitat de les Illes Balears (UIB), INAGEA, Carretera de Valldemossa Km 7.5, 07122 Palma de Mallorca, Illes Balears, Spain
[2] Laboratory of Plant Physiology and Morphology, Department of Crop Science, Agricultural University of Athens (AUA), Iera Odos 75, Botanikos, 11855 Athens, Greece

* Correspondence: margaroig93@gmail.com

Received 16 May 2020; Editorial decision 1 September 2020; Accepted 6 September 2020

Editor: Andrea Braeutigam, Bielefeld University, Germany

Abstract

Water deprivation affects photosynthesis, leaf anatomy, and cell wall composition. Although the former effects have been widely studied, little is known regarding those changes in cell wall major (cellulose, hemicelluloses, pectin, and lignin) and minor (cell wall-bound phenolics) compounds in plants acclimated to short- and long-term water deprivation and during recovery. In particular, how these cell wall changes impact anatomy and/or photosynthesis, specifically mesophyll conductance to CO_2 diffusion (g_m), has been scarcely studied. To induce changes in photosynthesis, cell wall composition and anatomy, *Helianthus annuus* plants were studied under five conditions: (i) control (i.e. without stress) (CL); (ii) long-term water deficit stress (LT); (iii) long-term water deficit stress with recovery (LT-Rec); (iv) short-term water deficit stress (ST); and (v) short-term water deficit stress with recovery (ST-Rec), resulting in a wide photosynthetic range (from 3.80 ± 1.05 µmol CO_2 m^{-2} s^{-1} to 24.53 ± 0.42 µmol CO_2 m^{-2} s^{-1}). Short- and long-term water deprivation and recovery induced distinctive responses of the examined traits, evidencing a cell wall dynamic turnover during plants acclimation to each condition. In particular, we demonstrated for the first time how g_m correlated negatively with lignin and cell wall-bound phenolics and how the (cellulose+hemicelloses)/pectin ratio was linked to cell wall thickness (T_{cw}) variations.

Keywords: Cell wall-bound phenolics, cell wall composition, cell wall thickness, *Helianthus annuus*, lignin, mesophyll conductance to CO_2 diffusion, photosynthesis, recovery, water deficit stress, water use efficiency.

Abbreviations: a_f, apoplastic water fraction; *AIR*, alcohol insoluble residue; A_N, leaf net CO_2 assimilation rate; C^*_Γ, leaf area specific capacitance at full turgor; *ETR*, electron transport rate; f_{ias}, fraction of mesophyll intercellular air spaces; g_m, mesophyll conductance to CO_2 diffusion; g_s, stomatal conductance to gas diffusion; L_{betchl}, distance between chloroplasts; L_{chl}, chloroplasts length; N_{PAL}, number of palisade layers; R_{light}, light mitochondrial non-photorespiratory respiration rate; RWC_{tlp}, relative water content at turgor loss point; S_c/S, chloroplast surface area exposed to intercellular air spaces per unit (one side) leaf surface area; S_c/S_m, chloroplast surface area exposed to intercellular air spaces per unit mesophyll surface area exposed to intercellular air spaces; S_m/S, mesophyll surface area exposed to intercellular air spaces per unit (one side) leaf surface area; T_{chl}, chloroplasts thickness; T_{cw}, cell wall thickness; T_{cyt}, cytosol thickness; T_{LE}, lower epidermis thickness; T_{LEAF}, leaf thickness; T_{MES}, mesophyll thickness; T_{PAL}, palisade mesophyll thickness; T_{SPO}, spongy mesophyll thickness; T_{UE}, upper epidermis thickness; *WUE*, water use efficiency; ε, bulk modulus of elasticity; πo, leaf osmotic potential at full turgor; Ψ_{md}, midday leaf water potential;Ψ_{pd}, pre-dawn leaf water potential; Ψ_{tlp}, leaf water potential at turgor loss point.

Introduction

During photosynthesis, a process that involves both diffusional and biochemical processes, CO_2 has to diffuse from the atmosphere to substomatal cavities (stomatal conductance to gas diffusion, g_s) and from these to its carboxylation sites at chloroplast stroma (mesophyll conductance to CO_2 diffusion, g_m) (Flexas *et al.*, 2004, 2008; von Caemmerer *et al.*, 2009). Nowadays, g_m is recognized as a key trait limiting photosynthesis amongst species and in response to different environmental conditions (Flexas *et al.*, 2008, 2012; Warren, 2008; Chaves *et al.*, 2009; Gago *et al.*, 2019; Nadal and Flexas, 2019). Although it is widely assumed that g_m is a complex trait that integrates the CO_2 diffusion through several steps across the mesophyll, the specific nature of those factors determining g_m is still not fully understood (Evans *et al.*, 2009; Flexas *et al.*, 2012). Among these steps, anatomical traits, particularly the chloroplast surface area exposed to intercellular air spaces per unit (one side) of leaf surface area (S_c/S) and the cell wall thickness (T_{cw}), play an important role in modulating g_m (Terashima *et al.*, 2001; Evans *et al.*, 2009; Flexas *et al.*, 2012; Tomás *et al.*, 2013; Carriquí *et al.*, 2015, 2019, 2020; Tosens *et al.*, 2016; Onoda *et al.*, 2017; Peguero-Pina *et al.*, 2017; Veromann-Jürgenson *et al.*, 2017). In particular, thicker cell walls limit g_m and, simultaneously, enhance cell rigidity (higher bulk modulus of elasticity, ε; Zimmermann *et al.*, 1978; Peguero-Pina *et al.*, 2017). Hence, Nadal *et al.* (2018) reported a trade-off between g_m and leaf net CO_2 assimilation rate (A_N), with ε potentially driven by T_{cw}. In addition, some studies have suggested that cell wall composition properties could determine ε as well as photosynthesis (Peltier and Marigo, 1999; Corcuera *et al.*, 2002; Ellsworth *et al.*, 2018; Clemente-Moreno *et al.*, 2019; Carriquí *et al.*, 2020; Roig-Oliver *et al.*, 2020).

A leaf cell wall is a complex structure that acts as a primary barrier to face those biotic and abiotic stresses occurring during a plant's life (Carpita and Gibeaut, 1993; Carpita and McCann, 2002; Fry, 2004; Cosgrove, 2005; Moore *et al.*, 2008; Sarkar *et al.*, 2009; Ochoa-Villarreal *et al.*, 2012; Tenhaken, 2015; Houston *et al.*, 2016; Rui and Dinnery, 2019). Cellulose is the major component of primary cell walls and it is found forming a microfibril matrix that confers mechanical strength to the wall (Carpita and Gibeaut, 1993; Carpita and McCann, 2002; Fry, 2004; Cosgrove, 2005; Sarkar *et al.*, 2009; Rui and Dinnery, 2019). Hemicelluloses are placed within these closely packed microfibrils, conferring stability to the wall (Carpita and Gibeaut, 1993; Carpita and McCann, 2002; Cosgrove, 2005; Tenhaken, 2015; Rui and Dinnery, 2019). This cellulose–hemicelluloses network is embedded in a pectin matrix because of the interaction between pectins and cellulose (Carpita and Gibeaut, 1993; Carpita and McCann, 2002; Moore *et al.*, 2008; Tenhaken, 2015; Rui and Dinnery, 2019). This pectin matrix determines wall porosity, thickness, microfibril spacing, and hydrophilic properties (Carpita and McCann, 2002; Cosgrove, 2005; Moore *et al.*, 2008; Solecka *et al.*, 2008; McKenna *et al.*, 2010; Ochoa-Villarreal *et al.*, 2012; Schiraldi *et al.*, 2012; Tenhaken, 2015; Houston *et al.*, 2016; Rui and Dinnery, 2019). Additionally, lignin is another cell wall main component placed in secondary cell walls (Poorter *et al.*, 2009; Zhang *et al.*, 2019). In particular, lignins belong to the heterogenous group of phenolic compounds, the most abundant type of secondary metabolites in plants (Fry, 1979; Wallace and Fry, 1994; Sánchez-Rodríguez *et al.*, 2011; Karabourniotis *et al.*, 2014). Thus, lignins interact with hemicelluloses, and their accumulation determines cell wall mechanical strength, flexibility, extensibility, and hydrophobicity (Iiyama *et al.*, 1994, Wallace and Fry, 1994; Fan, 2006; Sarkar *et al.*, 2009; Terrett and Dupree, 2019). Hence, the constant reorganization of these cell wall main compounds ensures an appropriate development at each plant growth stage according to environmental conditions, as it determines cell morphology, growth, and organ differentiation, among others (Carpita and Gibeaut, 1993; Carpita and McCann, 2002; Cosgrove, 2005; Sarkar *et al.*, 2009; Ochoa-Villarreal *et al.*, 2012; Tenhaken, 2015; Rui and Dinnery, 2019). However, plant cell walls also contain other minor components which are important for development (Fry, 1979; Carpita and Gibeaut, 1993; Wallace and Fry, 1994; Carpita and McCann, 2002; Cosgrove, 2005; Sarkar *et al.*, 2009; Houston *et al.*, 2016). Specifically, some phenolic polymers can be covalently bound to wall polysaccharides (Fry, 1979), particularly hemicelluloses and/or pectins (Fry, 2004; Vogt, 2010), restricting wall porosity (Wallace and Fry, 1994) and increasing wall rigidity when higher amounts are produced due to environmental stresses (Fry, 1979).

Whilst some studies have demonstrated the potential importance of how environmental stressors promote modifications in the proportion of cellulose, hemicelluloses, and pectins and how they are linked to changes in photosynthesis, specifically via g_m (Clemente-Moreno *et al.*, 2019; Roig-Oliver *et al.*, 2020), no previous studies have analysed the importance of lignin and cell wall-bound phenolics in determining g_m. Considering the relevant role proposed for pectins on g_m (Clemente-Moreno *et al.*, 2019; Carriquí *et al.*, 2020) and the fact that CO_2 diffuses through cell walls in the aqueous phase (Evans *et al.*, 2009), some cell wall-bound phenolic compounds (e.g. ferulic acid or coumaric acid) might be expected to somehow alter g_m as they strongly modify pectin (Lara-Espinoza *et al.*, 2018) and lignin properties due to their extensive hydrophobicity (Sarkar *et al.*, 2009). Furthermore, although some studies have hypothesized that T_{cw} changes could be attributed to modifications of cell wall compounds, particularly due to alterations in the pectin fraction (Carpita and McCann, 2002; Cosgrove, 2005; Moore *et al.*, 2008; Solecka *et al.*, 2008; Tenhaken *et al.*, 2015; Rui and Dinnery, 2019), to our knowledge only Carriquí *et al.* (2020) provided evidence on that issue in non-stressed gymnosperms.

It has been reported that water shortage induces changes in cell wall composition (Leucci *et al.*, 2008; Moore *et al.*, 2008; Clemente-Moreno *et al.*, 2019; Roig-Oliver *et al.*, 2020) as reduces A_N because of decreasing within-leaf CO_2 diffusion (i.e. reduction in g_s and g_m) (Chaves *et al.*, 2002, 2009; Flexas *et al.*, 2012; Nadal and Flexas, 2019), while promoting an increase in water use efficiency (WUE) due to larger reductions in g_s than in g_m (Galmés *et al.*, 2011; Flexas *et al.*, 2013a; Théroux-Rancourt *et al.*, 2015). Thus, the main hypothesis of the present study is that the rearrangement of cell wall components due

to acclimation to water deprivation and re-watering is linked to changes in both photosynthetic and anatomical parameters, in particular WUE, g_m, and T_{cw}. Hence, we tested *Helianthus annuus* plants submitted to short- and long-term water deficit stress as both conditions are expected to promote changes at different levels (Chaves *et al.*, 2002, 2009). Furthermore, recovery treatments were assessed to uncouple the frequently proportional responses between g_s and g_m (Flexas *et al.*, 2013b) in an attempt to associate cell wall and anatomical changes specifically with g_m.

Materials and methods

Plant material and growth conditions

Helianthus annuus seeds were sown individually in water-irrigated 3 litre pots containing a mixture of 3:1 substratum:perlite. They were placed for 44 d in a growing chamber at 22 °C receiving 200–300 μmol m^{-2} s^{-1} photosynthetic photon flux density (PPFD) for 12 h followed by 12 h of darkness. On the day of sowing, six individual replicates were randomly subjected to five different growing conditions: (i) control (CL); (ii) long-term water deficit stress (LT); (iii) long-term water deficit stress with recovery (LT-Rec); (iv) short-term water deficit stress (ST); and (v) short-term water deficit stress with recovery (ST-Rec). Control plants were maintained at 100% field capacity (FC). LT treatment consisted of decreasing FC from 100% to 35% starting from the day of sowing to the end of the treatment. In particular, pots reached 35% FC 3 weeks after sowing. This water status was then maintained for 22 d. The same conditions were applied to LT-Rec for 42 d, followed by 2 d recovery to reach 100% FC. ST treatment consisted of maintaining pots at 100% FC for a month followed by 14 d water deprivation until 35% FC. ST-Rec treatment was identical to ST treatment, but it was followed by 2 d recovery until 100% FC. Plants water status was monitored every 2 d, weighing all the pots to maintain each one at a specific FC by replacing evapotranspired water. Whilst LT and LT-Rec measurements were assessed in fully expanded leaves constantly submitted to water deficit stress, ST and ST-Rec measurements were performed in those fully expanded leaves developed under water irrigation and later acclimated to water deprivation.

Gas exchange and fluorescence measurements

At the end of each treatment, gas exchange and Chl *a* fluorescence were measured simultaneously in one fully developed leaf per plant (third or fourth leaf from the apex) using an infrared gas analyser (IRGA) LI-6400XT equipped with a fluorometer (Li-6400-40; Li-Cor Inc., Lincoln, NE, USA). Each leaf was clamped into the 2 cm^2 cuvette, the block temperature was fixed at 25 °C, and the vapour pressure deficit (VPD) was fixed at ~1.5 kPa. Leaf steady-state conditions were induced at a saturating PPFD (1500 μmol m^{-2} s^{-1}, 90–10% red–blue light) and 400 μmol CO_2 mol^{-1} air. The flow rate was kept at 300 μmol air min^{-1}. Once steady-state conditions were reached, A_N–C_i curves were performed, increasing ambient CO_2 concentrations (C_a) from 50 μmol CO_2 mol^{-1} to 1500 μmol CO_2 mol^{-1} air. Leaf net CO_2 assimilation rate (A_N), stomatal conductance to gas diffusion (g_s), CO_2 concentration at the substomatal cavity (C_i), and steady-state fluorescence (F_s) were recorded after the stabilization of the gas exchange rates at each given C_a (typically occurring in a range between 3 min and 4 min after changing the CO_2 concentration in the cuvette). Then, a saturating light flash was applied, obtaining the maximum fluorescence (F_m'). From these values, the real quantum efficiency of PSII (Φ_{PSII}) was registered. A correction for the CO_2 leakage in and out of the IRGA chamber was applied to correct A_N–C_i data (Flexas *et al.*, 2007). The electron transport rate (ETR) was calculated as in Valentini *et al.* (1995) performing light curves under negligible photorespiratory conditions (1% O_2). The light mitochondrial non-photorespiratory respiration rate (R_{light}) was assumed to be half the dark respiration rate, determined after exposure of plants to darkness for at least 20 min (Niinemets *et al.*, 2005). The CO_2 compensation point in the absence of non-photorespiratory respiration ($\Gamma^\star$) was obtained as the mean from values previously reported for *H. annuus* (Parry *et al.*, 1989; Kent *et al.*, 1992; Kanevski *et al.*, 1999; Sharwood *et al.*, 2008). From all these values, the mesophyll conductance to CO_2 diffusion (g_m) was calculated using the variable *J* method following Harley *et al.* (1992).

Leaf water status

The leaf water potential of each plant was determined by measuring pre-dawn (Ψ_{pd}) and midday (Ψ_{md}) water potentials in fully developed leaves neighbouring those used for gas exchange with a pressure chamber (Model 600D; PMS Instrument Company, Albany, OR, USA).

Pressure–volume curves

A fully developed leaf neighbouring the one used for gas exchange was selected to perform *P*–*V* curves. Leaves were rehydrated in distilled water and kept in the dark overnight. The following day, the water potential of leaves was measured with a pressure chamber (Model 600D; PMS Instrument Company) in a well-ventilated room with controlled temperature. Fresh weight was measured immediately after water potential. From (at least) 10 point *P*–*V* curves, values for leaf water potential at turgor loss point (Ψ_{tlp}), relative water content at turgor loss point (RWC_{tlp}), leaf osmotic potential at full turgor (π_o), apoplastic water fraction (a_f), and leaf area-specific capacitance ($C^\star_{ft}$) were obtained (Sack and Pasquet-Kok, 2011). The bulk modulus of elasticity (ε) was calculated using standardized major axes (SMA), a Model II regression from which one variable can be robustly calculated from another (Sack *et al.*, 2003; Sack and Pasquet-Kok, 2011).

Anatomical measurements

After gas exchange measurements, small portions of the leaf lamina enclosed in the leaf chamber were cut into small pieces avoiding major veins. Samples were fixed rapidly under vacuum pressure with 4% glutaraldehyde and 2% paraformaldehyde in a 0.01 M phosphate buffer (pH 7.4). They were then post-fixed in 2% buffered osmium tetroxide for 2 h and dehydrated by a graded ethanol series. Obtained pieces were embedded in LR white resin (London Resin Company) and were placed in an oven at 60 °C for 48 h (Tomás *et al.*, 2013; Carriquí *et al.*, 2015, 2019).

Semi-fine (0.8 μm) and ultra-fine (90 nm) cross-sections were cut with an ultramicrotome (Leica UC6, Vienna, Austria). Semi-fine sections were dyed with 1% toluidine blue to be observed in bright field with an Olympus BX60 optic microscope. Pictures at ×200 magnifications were taken using a digital camera (U-TVO.5XC; Olympus, Tokyo, Japan) and were used for the estimation of leaf thickness (T_{LEAF}), upper epidermis thickness (T_{UE}), lower epidermis thickness (T_{LE}), mesophyll thickness (T_{MES}), number of palisade layers (N_{PAL}), and fraction of mesophyll intercellular air spaces (f_{ias}). Ultra-fine sections were contrasted with uranyl acetate and lead citrate to take pictures at ×1500 and ×30 000 magnifications using TEM (TEM H600; Hitachi, Tokyo, Japan). Images at ×1500 magnifications were used for the determination of chloroplast thickness (T_{chl}), chloroplast length (L_{chl}), distance between chloroplasts (L_{betchl}), mesophyll and chloroplast surface area exposed to intercellular air spaces per unit (one side) leaf surface area (S_m/S and S_c/S, respectively), and chloroplast surface area exposed to intercellular air spaces per unit mesophyll surface area exposed to intercellular air spaces (S_c/S_m). Cell wall thickness (T_{cw}) and cytoplasm thickness (T_{cyt}) were estimated from images at ×30 000 magnification. Additionally, the cell curvature correction factor was determined following Thain (1983) from a mean of the length/width ratio of five cells according to the mesophyll type (palisade or spongy) in which measurements were done. Values for all parameters were obtained as a mean of 10 measurements from randomly selected cell structures using ImageJ software (Wayne Rasband/NIH, Bethesda, MD, USA).

Cell wall extraction and fractionation

Sampling for cell wall composition was performed in the same leaves used for gas exchange and anatomy. Plants were kept under darkness conditions overnight and, the next morning, 1 g of fresh leaf tissue per plant was cut into small pieces. They were set in screw-capped glass tubes containing absolute ethanol in a ratio of 1:10 (w/v). Samples were boiled and ethanol-cleaned until bleached. Then, they were cleaned twice with >95% acetone, resulting in the alcohol-insoluble residue (AIR), an approximation of the amount of isolated cell wall. The fraction for the evaluation of cellulose, hemicelluloses, and pectin was digested with α-amylase to eliminate starch residues. Once starch remains were no longer detected, three analytical replicates of each AIR weighing 3 mg were taken. They were hydrolysed with 2 M trifluoroacetic acid and heated at 121 °C for 1 h. Then, they were centrifuged at 13 000 *g*, giving an upper aqueous phase (non-cellulosic cell wall fraction) and a pellet (cellulosic cell wall fraction). Whilst the supernatants were stored at –20 °C for quantification of soluble sugars (hemicelluloses) and uronic acids (pectin), the pellets were cleaned twice with distilled water and >95% acetone. They were dried at room temperature before been resuspended in 200 µl of 72% (w/v) sulfuric acid for 1 h, diluted to 6 ml with distilled water, and heated at 121 °C until pellet degradation. Once cooled, the obtained aqueous samples were used for cellulose quantification. The phenol–sulfuric acid method (Dubois *et al.*, 1956) was performed to determine cellulose and hemicelluloses concentration. The absorbance of samples was read at 490 nm using a Multiskan Sky Microplate Spectrophotometer (ThermoFisher Scientific) and the content of both sugars was determined by interpolating samples values from a glucose calibration curve. For pectin quantification, sample absorbance was read at 520 nm with the same spectrophotometer, and pectin content was determined by interpolating samples values from a galacturonic acid calibration curve (Blumenkrantz and Asboe-Hansen, 1973).

The remaining AIR fraction used for the evaluation of lignin and cell wall-bound phenolics was placed in an oven at 70 °C for 72 h to ensure its total dehydration before been ground. Lignin quantification was performed by the acetyl bromide method (Fagerstedt *et al.*, 2015) testing 15 mg of AIR per sample. Samples absorbance was read at 280 nm with the UV-160A Shimadzu spectrophotometer (Shimadzu Corp.) and lignin concentration was obtained by interpolating samples values from a lignin calibration curve. For cell wall-bound phenolics, 150 mg of each AIR per sample were resuspended in 10 ml of distilled water and were subjected to alkaline hydrolysis by adding 7 ml of 2 M sodium hydroxide. They were incubated at 80 °C for 1 h and shaken at 21 °C for 14 h. Then, the hydrolysates were acidified with 85% (w/w) phosphoric acid and filtered through a ceramic filter under vacuum. Samples were extracted three times with ethyl acetate and the combined extracts were subjected to aqueous extraction twice to remove acid remains. The separation of the aqueous phase was facilitated by adding dehydrated calcium chloride, resulting in clear ethyl acetate extracts. Solvent was evaporated in a rotary evaporator at 40 °C, and dry residues were rediluted with 6 ml of 80% methanol before been kept at 4 °C until used. HPLC was performed in a Prominence HPLC system (Shimadzu Co., Tokyo, Japan). An aliquot was filtered through a membrane filter (Teknokroma OlimPeak, Reg. Cellulose 13 mm filter diameter, 0.22 µm pore diameter) and 20 µl were injected into a Zorbax Stablebond C18 column (5 µm, 250×4.6 mm, Agilent Technologies, Palo Alto, CA, USA) thermostatted at 33 °C. Mobile phase components were A, 1% aqueous acetic acid (w/v); B, methanol; and C, acetonitrile. Detection of peaks was performed with a photodiode array detector (SPD-M20A) and chromatograms were recorded in the 200–500 nm region using Shimadzu LC Solutions ver. 1.23 SP1 software. Phenolic compounds were identified based on spectral and mobility data of pure standards, and their quantification was based on pure standard reference curves for ferulic, *p*-coumaric, and caffeic acids. Finally, 200 µl of the same solutions were used to determine the total amount of cell wall-bound phenolics by the Folin–Ciocalteu method (Singleton and Rossi, 1965). Samples absorbance was read at 760 nm with the UV-160A Shimadzu spectrophotometer (Shimadzu Corp.), and the concentration of cell wall-bound phenolics was obtained by interpolating samples values from a tannic acid calibration reference curve.

Statistical analysis

Thompson's test was performed to detect and eliminate outliers for all measured parameters. Afterwards, data passed Shapiro–Wilk and Bartlett tests for normality and equality of variances, respectively. Then, one-way ANOVA and subsequent LSD test were assessed to detect statistically significant differences for the studied parameters among treatments ($P<0.05$). A principal component analysis (PCA) was performed with mean values per parameter and treatment to study the effect of distinct treatments and the interaction between different parameters. Additionally, Pearson's correlation matrices were addressed to find correlations between all parameters, these being significant when $P<0.05$ and highly significant when $P<0.01$. Finally, linear regressions between cell wall compositional characteristics, photosynthetic, and anatomical parameters were fitted using mean values per treatment. All analyses were performed with R software (ver. 3.2.2; R Core Team, Vienna, Austria).

Results

Plant water status and P–V curves

Both Ψ_{pd} and Ψ_{md} were lower in both water deficit stress treatments than in the control, but the reduction was significantly larger in ST than in LT treatment (Table 1). Upon rewatering, both treatments recovered control values for both parameters (Table 1). Regarding *P–V* curves, no statistical differences were found considering Ψ_{tlp}, RWC_{tlp}, ε, and $C^{\star}_{ft}$ (see Supplementary Fig. S1A, B, D, F at *JXB* online, respectively). However, π_o was higher in ST and lower in both CL and LT (Supplementary Fig. S1C). Nonetheless, ST presented increased a_f (0.69 ± 0.03) in comparison with other treatments, with ST-Rec being the treatment with the lowest a_f (0.15 ± 0.01) (Supplementary Fig. S1E).

Photosynthetic characterization

Significant variability was induced with the established treatments in A_N and related parameters (Fig. 1). In particular, A_N was increased by 24% in LT and reduced by almost 65% in ST

Table 1. Leaf water status of *H. annuus* plants grown under different conditions

Parameters	Treatments					
	CL	LT	LT-Rec	ST	ST-Rec	*P*
Ψ_{pd} (MPa)	–0.31 ± 0.01 a	–0.88 ± 0.01 b	–0.30 ± 0.04 a	–2.29 ± 0.29 c	–0.31 ± 0.03 a	<0.001
Ψ_{md} (MPa)	–0.61 ± 0.03 a	–1.62 ± 0.26 b	–0.65 ± 0.09 a	–2.69 ± 0.17 c	–0.58 ± 0.04 a	<0.001

CL, control; LT, long-term water deficit stress; LT-Rec, long-term water deficit stress with recovery; ST, short-term water deficit stress; and ST-Rec, short-term water deficit stress with recovery. Mean values ± SE are shown for pre-dawn leaf water potential (Ψ_{pd}) and midday leaf water potential (Ψ_{md}). *P*-values from one-way ANOVA are shown. Letters indicate a significant difference ($P<0.05$) across all experimental conditions according to LSD test.

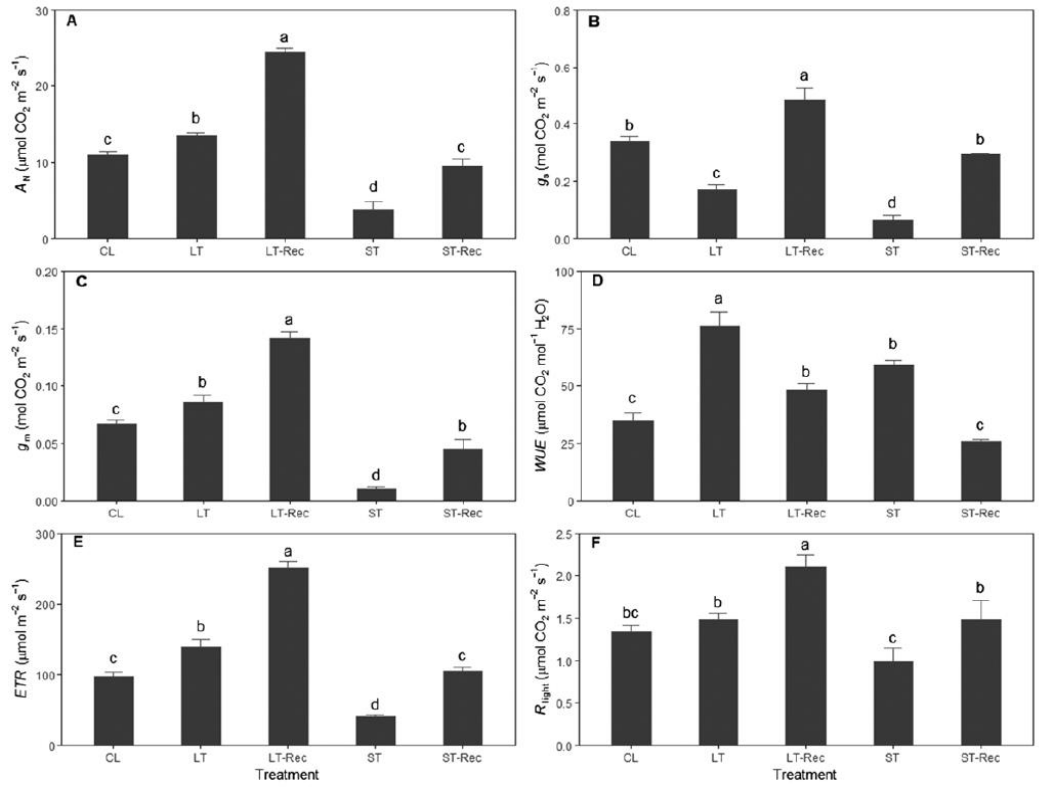

Fig. 1. Photosynthetic characterization of *H. annuus* plants grown under different conditions (CL, control; LT, long-term water deficit stress; LT-Rec, long-term water deficit stress with recovery; ST, short-term water deficit stress; and ST-Rec, short-term water deficit stress with recovery). (A) Leaf net CO_2 assimilation rate (A_N), (B) stomatal conductance to gas diffusion (g_s), (C) mesophyll conductance to CO_2 diffusion (g_m), (D) water use efficiency (WUE), (E) electron transport rate (ETR), and (F) light mitochondrial non-photorespiratory respiration rate (R_{light}). Different letters indicate a significant difference (P<0.05) across all experimental conditions according to LSD test. n=4–6 (means ± SE).

compared with control values (Fig. 1A). Recovery resulted in an even further increase of A_N in LT-Rec and restored control values in ST-Rec (Fig. 1A). Instead, g_s decreased in both LT and ST, although to a much larger extent in the latter (Fig. 1B), resulting in increased WUE, especially in LT (Fig. 1D). However, whilst recovery increased both g_s and WUE in LT-Rec in comparison with control conditions, ST-Rec reached values for both parameters similar to the control (Fig. 1B, D, respectively). The patterns for g_m and ETR closely resembled that of A_N (Fig. 1C, E, respectively). Although R_{light} showed less variability than photosynthetic parameters, differences were significant among treatments (Fig. 1F).

Leaf cell wall composition

The highest proportion of isolated AIR was found in the control, differing from other treatments (Table 2). Regarding cellulose, no significant differences between treatments were detected (Table 2). The control showed the highest proportion of hemicelluloses, and the lowest was found in LT-Rec, which also contained the lowest amount of pectin (Table 2). The control, ST, and ST-Rec contained higher lignin than LT and LT-Rec (Table 2). ST had the highest proportion of cell wall-bound phenolics, whilst LT-Rec presented the lowest. Again, ST presented the highest quantities of both coumaric and ferulic acids, but no coumaric acid was found in LT-Rec and the lowest ferulic acid was quantified in both LT and LT-Rec (Table 2). Finally, caffeic acid was higher in the control, ST, and ST-Rec than in LT and LT-Rec (Table 2).

Anatomical characterization

Regarding the analysis of semi-fine cross-sections, no statistical differences between treatments were found for T_{LEAF}, T_{UE}, T_{LE}, T_{SPO}, T_{MES}, N_{PAL}, and f_{ias} (Table 3). However, LT-Rec and ST presented higher values for T_{PAL} in comparison with other treatments (Table 3). In relation to the analysis of ultra-fine cross-sections, statistical differences were found for chloroplast characterization, revealing that LT-Rec achieved higher L_{chl} than the rest of treatments and also higher T_{chl} than drought treatments (i.e. LT and ST) (Table 4). In contrast, ST had the lowest values for T_{chl} and L_{chl}, even though the latter did not differ statistically from that

Table 2. Leaf cell wall characterization of *H. annuus* plants grown under different conditions

Parameters	Treatments					
	CL	LT	LT-Rec	ST	ST-Rec	*P*
AIR (g g^{-1} dry weight)	1.36 ± 0.34 a	0.42 ± 0.08 b	0.59 ± 0.06 b	0.84 ± 0.12 b	0.60 ± 0.14 b	0.011
Cellulose (mg g^{-1} AIR)	135.23 ± 5.46 a	142.97 ± 6.18 a	127.43 ± 19.44 a	151.94 ± 5.26 a	183.03 ± 29.81 a	0.133
Hemicelluloses (mg g^{-1} AIR)	303.39 ± 30.73 a	231.34 ± 9.64 b	121.00 ± 8.22 c	217.09 ± 16.04 b	249.32 ± 5.41 ab	<0.001
Pectin (mg g^{-1} AIR)	99.35 ± 3.95 bc	145.88 ± 4.97 a	74.63 ± 8.02 d	110.25 ± 2.87 b	82.80 ± 1.02 cd	<0.001
Lignin (mg g^{-1} AIR)	298.88 ± 20.50 a	219.30 ± 11.28 b	220.40 ± 7.87 b	325.08 ± 23.74 a	305.38 ± 26.41 a	<0.001
Cell wall-bound phenolics (mg tannic acid g^{-1} AIR)	2.81 ± 0.25 ab	2.20 ± 0.04 bc	1.75 ± 0.14 c	2.97 ± 0.20 a	2.43 ± 0.33 abc	0.006
Coumaric acid (mg g^{-1} AIR)	1.08 ± 0.05 bc	0.39 ± 0.14 b	0.00 ± 0.00 c	1.81 ± 0.36 a	1.12 ± 0.04 ab	<0.001
Ferulic acid (mg g^{-1} AIR)	0.29 ± 0.02 b	0.06 ± 0.03 d	0.14 ± 0.04 cd	0.46 ± 0.02 a	0.19 ± 0.02 c	<0.001
Caffeic acid (mg g^{-1} AIR)	4.51 ± 0.83 a	1.09 ± 0.25 b	1.69 ± 0.57 b	5.60 ± 0.70 a	4.04 ± 0.20 a	0.004

CL, control; LT, long-term water deficit stress; LT-Rec, long-term water deficit stress with recovery; ST, short-term water deficit stress; and ST-Rec, short-term water deficit stress with recovery. Mean values ± SE are shown for alcohol-insoluble residue (AIR), cellulose, hemicelluloses, pectin, lignin, cell wall-bound phenolics, coumaric acid, ferulic acid, and caffeic acid. *P*-values from one-way ANOVA are shown. Letters indicate significant difference ($P<0.05$) across all experimental conditions according to LSD test. $n=4–6$ in all cases.

Table 3. Anatomical characterization from semi-fine cross-sections of *H. annuus* plants grown under different conditions

Parameters	Treatments					
	CL	LT	LT-Rec	ST	ST-Rec	*P*
T_{LEAF} (μm)	193.21 ± 5.13 a	187.26 ± 5.49 a	207.67 ± 5.44 a	191.63 ± 10.46 a	191.43 ± 6.48 a	0.379
T_{UE} (μm)	14.01 ± 1.94 a	12.00 ± 0.82 a	14.82 ± 1.48 a	12.50 ± 0.31 a	13.88 ± 1.65 a	0.579
T_{LE} (μm)	10.48 ± 0.30 a	12.39 ± 0.36 a	12.49 ± 0.87 a	10.74 ± 1.00 a	12.35 ± 1.82 a	0.322
T_{PAL} (μm)	68.47 ± 3.72 b	72.56 ± 2.31 b	89.28 ± 7.38 a	87.91 ± 2.97 a	70.72 ± 3.85 b	0.009
T_{SPO} (μm)	91.99 ± 4.81 a	78.11 ± 10.93 a	91.04 ± 10.36 a	70.51 ± 8.51 a	74.04 ± 9.60 a	0.344
T_{MES} (μm)	160.45 ± 7.48 a	147.38 ± 11.54 a	169.22 ± 3.09 a	155.03 ± 9.37 a	144.76 ± 6.48 a	0.343
N_{PAL}	1.58 ± 0.23 a	1.10 ± 0.04 a	1.51 ± 0.01 a	1.64 ± 0.11 a	1.50 ± 0.16 a	0.200
f_{ias} (%)	34.77 ± 4.43 a	24.40 ± 4.07 a	33.04 ± 3.37 a	39.31 ± 5.01 a	26.04 ± 6.09 a	0.149

CL, control; LT, long-term water deficit stress; LT-Rec, long-term water deficit stress with recovery; ST, short-term water deficit stress; and ST-Rec, short-term water deficit stress with recovery. Mean values ± SE are shown for leaf thickness (T_{LEAF}), upper epidermis thickness (T_{UE}), lower epidermis thickness (T_{LE}), palisade mesophyll thickness (T_{PAL}), spongy mesophyll thickness (T_{SPO}), mesophyll thickness (T_{MES}), number of palisade layers (N_{PAL}), and fraction of mesophyll intercellular air spaces (f_{ias}). *P*-values from one-way ANOVA are shown. Letters indicate significant difference ($P<0.05$) across all experimental conditions according to LSD test. $n=4–6$ in all cases.

in LT (Table 4). Additionally, ST had the lowest value for S_c/S_m, differing from the rest of treatments (Table 4). No significant differences at $P<0.05$ were found for S_m/S, S_c/S, T_{cyt}, and T_{cw} among tested conditions, but marginally significant differences at $0.05<P<0.10$ were found for T_{cyt} and T_{cw} (Table 4).

Principal component analysis

A PCA was performed, in which two principal components (PCs) accounted for 81.5% of the total variation (Fig. 2). PC1 (53.7% total variation) was mostly represented by gas exchange (A_N, g_m, and ETR) and specific cell wall components (cell wall-bound phenolics and, in particular, coumaric acid) parameters, whereas pectin amount, WUE, g_m/g_s, and (cellulose+hemicelluloses)/pectin ratios were mostly found in PC2 (27.8% total variation). Interestingly, the representation of the measured parameters grouped differently, indicating that each treatment promoted different responses.

Relationships between parameters

Several significant correlations were observed among the studied parameters (Supplementary Table S1). Concerning relationships between cell wall components and photosynthesis, significant negative correlations were found between g_m and cell wall-bound phenolics ($R^2=0.74$, $P=0.038$, Fig. 3A), coumaric acid ($R^2=0.91$, $P=0.008$, Fig. 3B), and lignin ($R^2=0.68$, $P=0.053$, Fig. 3C). A significant positive correlation was detected between WUE and the ratio g_m/g_s ($R^2=0.88$, $P=0.012$, Fig. 4A) and a negative correlation between WUE and (cellulose+hemicelluloses)/pectin ratio ($R^2=0.94$, $P=0.004$, Fig. 4B) was found. Moreover, whilst negative correlations were found between the g_m/g_s ratio and T_{cw} ($R^2=0.88$, $P=0.012$, Fig. 5A) and between WUE and T_{cw} ($R^2=0.73$, $P=0.041$, Fig. 5B), a positive correlation between the (cellulose+hemicelluloses)/pectin ratio and T_{cw} was detected ($R^2=0.81$, $P=0.023$, Fig. 5C).

Discussion

The plant water shortage treatments we applied in the current study on *H. annuus* induced the photosynthetic changes classically reported under the same conditions in different species (e.g. Flexas *et al.*, 2004; Chaves *et al.*, 2009) with the exception of LT, which presented larger A_N (despite low g_s and,

Table 4. Anatomical characterization from ultra-fine cross-sections of *H. annuus* plants grown under different conditions

Parameters	Treatments					
	CL	LT	LT-Rec	ST	ST-Rec	*P*
T_{chl} (μm)	2.66 ± 0.17 ab	2.41 ± 0.21 b	2.93 ± 0.14 a	1.71 ± 0.11 c	2.60 ± 0.24 ab	<0.001
L_{chl} (μm)	5.10 ± 0.28 b	4.34 ± 0.20 bc	6.55 ± 0.34 a	3.91 ± 0.18 c	4.95 ± 0.29 b	<0.001
L_{betchl} (μm)	0.85 ± 0.12 b	0.87 ± 0.11 b	0.70 ± 0.07 b	1.44 ± 0.21 a	1.07 ± 0.15 ab	0.010
S_m/S (m^2 m^{-2})	22.32 ± 1.03 a	20.61 ± 1.43 a	20.72 ± 0.46 a	20.90 ± 1.91 a	20.88 ± 3.13 a	0.945
S_c/S (m^2 m^{-2})	19.57 ± 1.36 a	17.19 ± 1.38 a	18.99 ± 0.34 a	13.30 ± 2.62 a	16.58 ± 1.73 a	0.125
S_c/S_m	0.87 ± 0.03 a	0.83 ± 0.03 a	0.91 ± 0.01 a	0.61 ± 0.07 b	0.81 ± 0.04 a	<0.001
T_{cyt} (μm)	0.45 ± 0.07 ab	0.45 ± 0.06 ab	0.34 ± 0.02 b	0.56 ± 0.02 a	0.48 ± 0.07 ab	0.054
T_{cw} (μm)	0.16 ± 0.01 ab	0.13 ± 0.01 b	0.15 ± 0.01 ab	0.16 ± 0.01 ab	0.17 ± 0.01 a	0.070

CL, control; LT, long-term water deficit stress; LT-Rec, long-term water deficit stress with recovery; ST, short-term water deficit stress; and ST-Rec, short-term water deficit stress with recovery. Mean values ± SE are shown for chloroplasts thickness (T_{chl}), chloroplast length (L_{chl}), distance between chloroplasts (L_{betchl}), mesophyll surface area exposed to intercellular air spaces per unit (one side) leaf surface area (S_m/S), chloroplast surface area exposed to intercellular air spaces per unit (one side) leaf surface area (S_c/S), chloroplast surface area exposed to intercellular air spaces per unit mesophyll surface area exposed to intercellular air spaces (S_c/S_m), cytosol thickness (T_{cyt}), and cell wall thickness (T_{cw}). *P*-values from one-way ANOVA are shown. Letters indicate a significant difference (0.05<*P*<0.1) across all experimental conditions according to LSD test. *n*=4–6 in all cases.

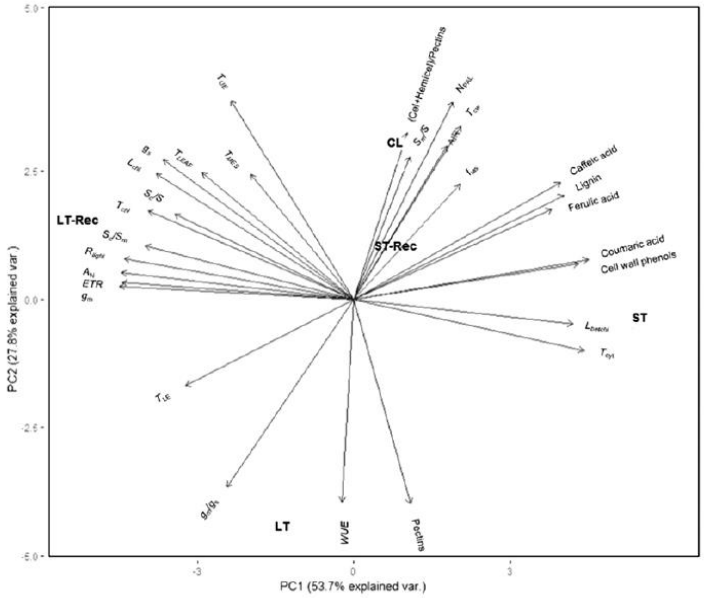

Fig. 2. Principal component analysis (PCA) of gas exchange, cell wall, and anatomical parameters for all treatments. The same abbreviations as in Fig. 1 and Tables 1–4 are used except for the (cellulose+hemicelluloses)/pectins ratio, which is shown as '(Cel+Hemicel)/Pectins'. Axes represent the two principal components (PCs), which explain 81.5% of the total variance.

hence, larger WUE) and other photosynthetic traits than the control (Fig. 1). Although it might appear surprising, other studies demonstrated an increase of photosynthetic capacity in plants acclimated to long-term water deficit stress. For instance, Huck *et al.* (1983) reported that prolonged water deficit stress restricted shoot growth while enhancing root growth in soybean. This imbalanced growth resulted in larger photosynthesis rates at the leaf level in water-limited than in irrigated plants, although it depended on leaf age, hour of the day, and time after imposition of the stress. Additionally, Panković *et al.* (1999) observed the same pattern in some specific sunflower genotypes, but not in others, due to increased amounts and activity of Rubisco. Regardless of the exact mechanism behind it, this particular behaviour of our LT plants allowed us to establish five treatments that led to a wide range of photosynthetic rates. We then analysed how these treatments also promoted modifications in cell wall major and minor compounds (Table 2).

Although water deficit stress has been linked to alterations in cell wall sugars (i.e. cellulose and hemicelluloses) and pectin metabolism (Moore *et al.*, 2008; Leucci *et al.*, 2008; Tenhaken, 2015; Clemente-Moreno *et al.*, 2019; Roig-Oliver *et al.*, 2020), we found no significant differences in cell wall cellulose content among treatments and, in contrast to Cho

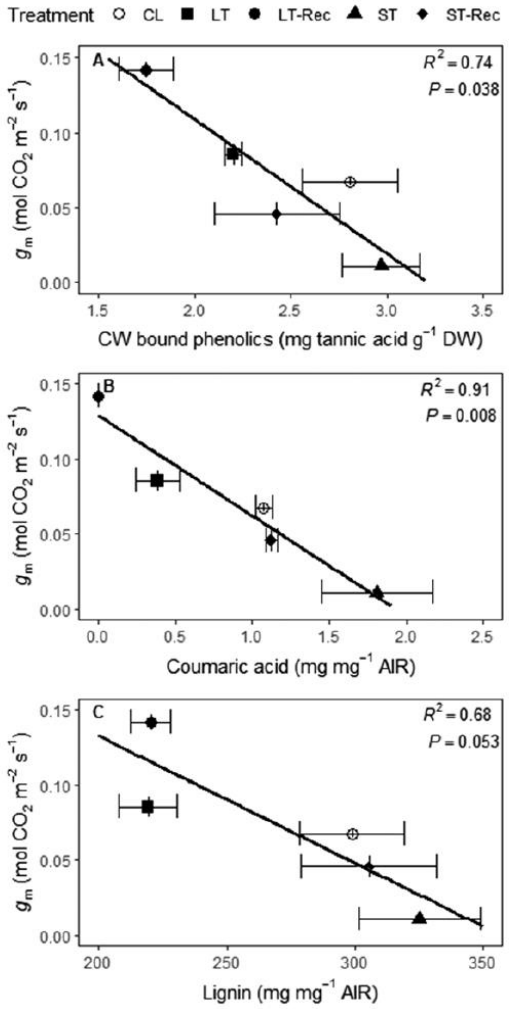

Fig. 3. Mesophyll conductance to CO_2 diffusion (g_m) in relation to cell wall composition. (A) Cell wall-bound phenolics, (B) coumaric acid, and (C) lignin in *H. annuus* across all experimental conditions. *n*=4–6 (means ± SE).

et al. (2006) and Choi *et al.* (2011), we observed a decrease in hemicelluloses in both LT and ST (Table 2). In fact, increases in hemicelluloses have been interpreted as cell wall mechanical adjustments which offer increased cell wall rigidity and protection of mesophyll cells to face water deprivation (Cho *et al.*, 2006; Choi *et al.*, 2011). However, whilst Lo Gullo and Salleo (1988) observed higher leaf rigidity in *Ceratonia siliqua* and *Laurus nobilis* leaves exposed to water deficit stress, Roig-Oliver *et al.* (2020) showed that water deprivation enhanced leaf elasticity in grapevines. Nonetheless, Barlett *et al.* (2012) reported that elastic adjustments are usually mild to none under water deficit stress conditions, which is in agreement with our results as well as with those reported by Sobrado and Turner (1983) testing *Helianthus* as no significant differences were found for ε (Supplementary Fig. S1D). In contrast to hemicelluloses, pectins increased in response to water deficit stress, as already shown by Leucci *et al.* (2008), Moore *et al.* (2008), Clemente-Moreno *et al.* (2019), and Roig-Oliver *et al.* (2020), which has been interpreted as a reflection of their crucial role in controlling the cell wall hydration status during water deficit stress. In this sense, it is remarkable that the increase in pectins was larger in LT than in ST (Table 2). Interestingly, only a 2 d recovery (LT-Rec and ST-Rec) was enough to significantly decrease pectin concentration as compared with LT and ST (Table 2), illustrating how dynamic cell wall polysaccharide rearrangement is in mature non-reproductive plant tissues after rewatering (Vicré *et al.*, 1999; Hoch, 2007).

Regarding to the phenolic polymers tested in this study, an increase of lignin genetic promotors was documented in *Ctenanthe setosa* once submitted to long-term water deficit stress to prevent cell wall damage (Terzi *et al.*, 2013) due to its importance in regulating wall properties such as mechanical strength, flexibility, and extensibility (Wallace and Fry, 1994; Fan, 2006; Sarkar *et al.*, 2009; Terrett and Dupree, 2019). However, our results are in agreement with those reported in Shafi *et al.* (2019) testing *Arabidopsis thaliana* leaves as long-term drought promoted less lignin accumulation, which was also detected in LT-Rec (Table 2), suggesting that lignin deposition may be species-specific. Furthermore, cell wall-bound phenolics tend to increase during environmental stresses (Fry, 1979). However, in our case, these compounds only increased in ST, while instead they decreased in LT (Table 2). Additionally, the same pattern was found for both coumaric and ferulic acids (Table 2). Thus, we suggest that lignin and cell wall-bound phenolic accumulation (including specific phenols) followed different patterns in LT and ST leaves probably because of different exposure to water deficit stress. Whilst LT leaves were fully expanded under continuous water deprivation, ST leaves experienced different foliar changes because water deprivation was applied in already developed leaves, thus leading to different mechanisms to regulate the accumulation of these compounds.

Whilst previous studies demonstrated the relationship of cellulose, hemicelluloses, and pectins with g_m (Ellsworth *et al.*, 2018; Clemente-Moreno *et al.*, 2019; Carriquí *et al.*, 2020; Roig-Oliver *et al.*, 2020), our study provides the first evidence on how g_m also correlated with other additionally tested cell wall compounds (Fig. 3A–C). Karabourniotis *et al.* (2014) reported a negative correlation between the photosynthetic capacity and soluble phenolic compounds at interspecific level. Additionally, they speculated a probable association between the leaf phenolic pool and g_m even at the intraspecific level. From our results, we evidenced a direct relationship between cell wall phenolic compounds and photosynthesis (Fig. 3A, B). Cell wall-bound phenolics and, specifically, coumaric acid negatively correlated with g_m (Fig. 3A, B, respectively), which was opposite to the results reported by Hura *et al.* (2009, 2012) testing triticale under water deficit

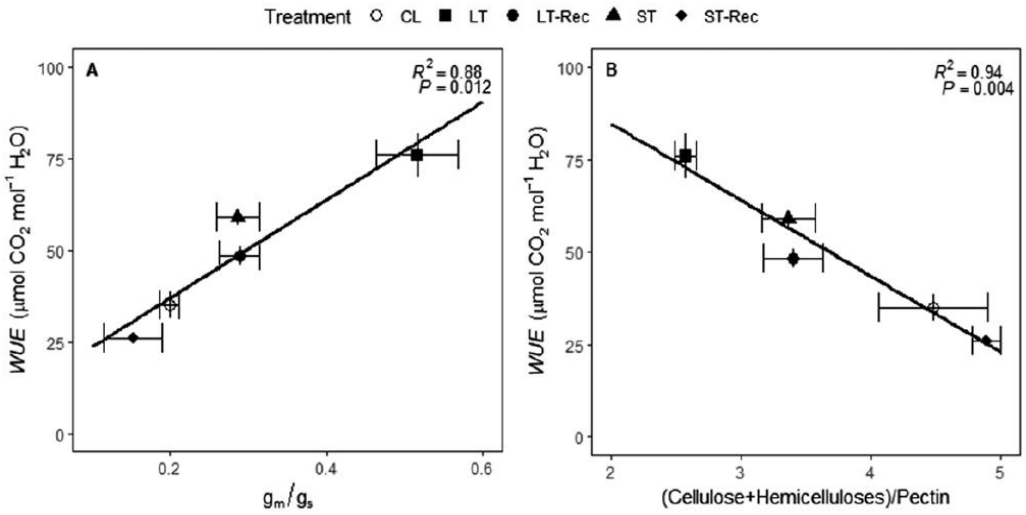

Fig. 4. Water use efficiency (WUE) in relation to (A) g_m/g_s ratio and (B) (cellulose+hemicelluloses)/pectin ratio in *H. annuus* across all experimental conditions. n=4–6 (means ± SE).

stress conditions, as they found a positive correlation of cell wall-bound phenolics and ferulic acid with photosynthesis. Nonetheless, we speculate that our results differed from those of Hura *et al.* (2009, 2012) because monocots present specific cell wall compositional traits different from the rest of the angiosperms (Carpita and McCann, 2002; Sørensen *et al.*, 2010) which may involve different response patterns once submitted to water deficit stress. Together with phenolics, lignin is related to protection against abiotic and biotic stresses (Fry, 1979; Wallace and Fry, 1994; Grabber, 2005; Fan, 2006; Sarkar *et al.*, 2009; Terrett and Dupree, 2019). When lignin deposition takes place, molecules are tightly packed (Grabber, 2005; Sarkar *et al.*, 2009), thus cell wall porosity could diminish, making CO_2 supply more difficult, obtaining lower g_m. Hence, we provided an almost significant negative correlation between lignin and g_m (Fig. 3C), which is in contrast to Kuusk *et al.* (2018), who concluded that lignins were not directly involved in photosynthesis. Furthermore, Fig. 4A illustrates the well-known positive correlation between WUE and the g_m/g_s ratio (Flexas *et al.*, 2013a) concomitant with a previously non-reported negative correlation between WUE and the (cellulose+hemicelluloses)/pectin ratio (Fig. 4B). Simultaneously, the g_m/g_s ratio and WUE correlated negatively with T_{cw} (Fig. 5A, B, respectively), the unique anatomical parameter more affecting g_m in which marginally significant differences were found (Table 4). In contrast, the (cellulose+hemicelluloses)/pectin ratio correlated positively with T_{cw} (Fig. 5C). Although it has already been suggested that modifications in cell wall composition, specifically in the proportion of pectin, could involve changes in T_{cw} (Carpita and McCann, 2002; Cosgrove, 2005; Moore *et al.*, 2008; Solecka *et al.*, 2008; Tenhaken *et al.*, 2015; Rui and Dinnery, 2019), only Carriquí *et al.* (2020) evidenced that issue in non-stressed gymnosperms. Thus, to the best of our knowledge, this study provides the first empirical evidence on how not only pectins, but also the (cellulose+hemicelluloses)/pectin ratio is linked to T_{cw} modifications in response to short- and long-term water deficit stress followed by a recovery (Fig. 5C) at intraspecific level.

To our knowledge, the present study provides strong indications of a cell wall active and dynamic turnover during plant acclimation to short- and long-term water deficit stress as well as under subsequent recovery, with significant consequences on leaf physiology. In fact, understanding the role of the cell wall composition in determining g_m is a prerequisite to advance in the biotechnological improvement of photosynthesis. Hence, the current study sheds some light on this aspect as we show for the first time how cell wall minor components (i.e. cell wall-bound phenolics) and lignin could play a significant role in determining photosynthesis because of g_m adjustments. Additionally, we also provide the first empirical evidence of a correlation between the (cellulose+hemicelluloses)/pectin ratio and T_{cw} at intraspecific level in response to stress. Our findings further support the notion that the degree of hydrophilicity and elasticity of the cell wall may affect g_m (Carriquí *et al.*, 2020) and, additionally, provide evidence on decreased g_m when the deposition of cell wall-stiffening hydrophobic components increases. However, the observed responses for most of the studied parameters largely differed between short- and long-term water deficit stress, which makes our results difficult to compare with previous studies as most of them have only addressed short-term responses. Thus, more studies are required for a better understanding of which processes take place during short- and long-term water deprivation as well as under recovery conditions in a wider range of species to

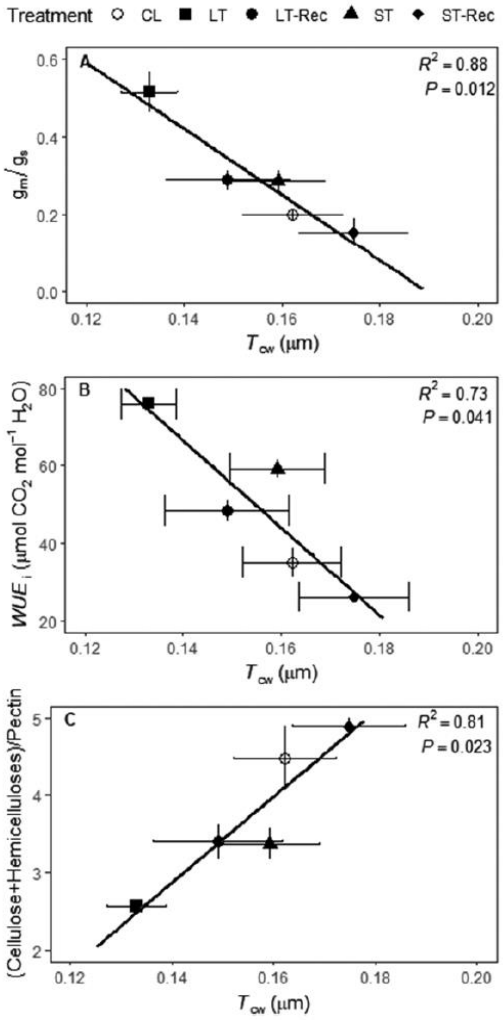

Fig. 5. Relationships of (A) g_m/g_s ratio, (B) water use efficiency (WUE), and (C) (cellulose+hemicelluloses)/pectin ratio with cell wall thickness (T_{cw}) in *H. annuus* across all experimental conditions. *n*=4–6 (means ± SE).

analyse how photosynthetic, biochemical, and anatomical modifications are related to cell wall modifications.

Supplementary data

The following supplementary data are available at *JXB* online.

Table S1. Pearson correlation matrix of physiological, leaf water relations, cell wall, and anatomical parameters measured in *H. annuus* plants across all experimental conditions.

Fig. S1. Characterization of leaf water relations in *H. annuus* plants grown under different conditions.

Acknowledgements

This work was supported by the project PGC2018-093824-B-C41 from the Ministerio de Economía y Competitividad (MINECO, Spain). MR-O and MN were supported by a pre-doctoral fellowship, FPU16/01544 and BES-2015-072578, respectively, from MINECO. Additionally, MN was co-supported by the European Social Found. We thank Dr Cyril Douthe for his advice during gas exchange measurements, and María Teresa Mínguez (Universitat de València, Secció de Microscòpia Electrònica—SCSIE) and Dr Ferran Hierro (Universitat de les Illes Balears, Serveis Cientificotècnics) for technical support during microscopic analyses.

Conflicts of interest

The authors declare no conflicts of interest.

Author contributions

MR-O, PB, MN, JB, and JF designed the study; MR-O, PB, GL, DN, and GK conducted the experiments; MR-O and PB performed the data analysis; and MR-O, JB, and JF wrote the first manuscript version. All authors contributed to its subsequent versions.

Data availability

The data supporting the findings of this study are available from the corresponding author (Margalida Roig-Oliver) upon request.

References

Bartlett MK, Scoffoni C, Sack L. 2012. The determinants of leaf turgor loss point and prediction of drought tolerance of species and biomes: a global meta-analysis. Ecology Letters **15**, 393–405.

Blumenkrantz N, Asboe-Hansen G. 1973. New method for quantitative determination of uronic acids. Analytical Biochemistry **54**, 484–489.

Carpita NC, Gibeaut DM. 1993. Structural models of primary cell walls in flowering plants: consistency of molecular structure with the physical properties of the walls during growth. The Plant Journal **3**, 1–30.

Carpita NC, McCann MC. 2002. The functions of cell wall polysaccharides in composition and architecture revealed through mutations. Plant and Soil **247**, 71–80.

Carriquí M, Cabrera HM, Conesa MÀ, *et al.* 2015. Diffusional limitations explain the lower photosynthetic capacity of ferns as compared with angiosperms in a common garden study. Plant, Cell & Environment **38**, 448–460.

Carriquí M, Nadal M, Clemente-Moreno MJ, Gago J, Miedes E, Flexas J. 2020. Cell wall composition strongly influences mesophyll conductance in gymnosperms. The Plant Journal **103**, 1372–1385.

Carriquí M, Roig-Oliver M, Brodribb TJ, *et al.* 2019. Anatomical constraints to nonstomatal diffusion conductance and photosynthesis in lycophytes and bryophytes. New Phytologist **222**, 1256–1270.

Chaves MM, Flexas J, Pinheiro C. 2009. Photosynthesis under drought and salt stress: regulation mechanisms from whole plant to cell. Annals of Botany **103**, 551–560.

Chaves MM, Pereira JS, Maroco J, Rodrigues ML, Ricardo CP, Osório ML, Carvalho I, Faria T, Pinheiro C. 2002. How plants cope with water stress in the field. Photosynthesis and growth. Annals of Botany **89**, 907–916.

Cho SK, Kim JE, Park JA, Eom TJ, Kim WT. 2006. Constitutive expression of abiotic stress-inducible hot pepper CaXTH3, which encodes a xyloglucan endotransglucosylase/hydrolase homolog, improves drought

and salt tolerance in transgenic *Arabidopsis* plants. FEBS Letters **580**, 3136–3144.

Choi JY, Seo YS, Kim SJ, Kim WT, Shin JS. 2011. Constitutive expression of CaXTH3, a hot pepper xyloglucan endotransglucosylase/hydrolase, enhanced tolerance to salt and drought stresses without phenotypic defects in tomato plants (*Solanum lycopersicum* cv. Dotaerang). Plant Cell Reports **30**, 867–877.

Clemente-Moreno MJ, Gago J, Díaz-Vivancos P, Bernal A, Miedes E, Bresta P, Liakopoulos G, Fernie AR, Hernández JA, Flexas J. 2019. The apoplastic antioxidant system and altered cell wall dynamics influence mesophyll conductance and the rate of photosynthesis. The Plant Journal **99**, 1031–1046.

Corcuera L, Camarero JJ, Gil-Pelegrín E. 2002. Functional groups in *Quercus* species derived from the analysis of pressure–volume curves. Trees **16**, 465–472

Cosgrove DJ. 2005. Growth of the plant cell wall. Nature Reviews. Molecular Cell Biology **6**, 850–861.

Dubois M, Gilles KA, Hamilton JK, Rebers PA, Smith F. 1956. Colorimetric method for determination of sugars and related substances. Analytical Chemistry **28**, 350–356.

Ellsworth PV, Ellsworth PZ, Koteyeva NK, Cousins AB. 2018. Cell wall properties in *Oryza sativa* influence mesophyll CO_2 conductance. New Phytologist **219**, 66–76.

Evans JR, Kaldenhoff R, Genty B, Terashima I. 2009. Resistances along the CO_2 diffusion pathway inside leaves. Journal of Experimental Botany **60**, 2235–2248.

Fagerstedt KV, Saranpää P, Tapanila T, Immanen J, Serra JA, Nieminen K. 2015. Determining the composition of lignins in different tissues of silver birch. Plants **4**, 183–195.

Fan L, Linker R, Gepstein S, Tanimoto E, Yamamoto R, Neumann PM. 2006. Progressive inhibition by water deficit of cell wall extensibility and growth along the elongation zone of maize roots is related to increased lignin metabolism and progressive stelar accumulation of wall phenolics. Plant Physiology **140**, 603–612.

Flexas J, Barbour MM, Brendel O, *et al.* 2012. Mesophyll diffusion conductance to CO_2: an unappreciated central player in photosynthesis. Plant Science **193-194**, 70–84.

Flexas J, Bota J, Loreto F, Cornic G, Sharkey TD. 2004. Diffusive and metabolic limitations to photosynthesis under drought and salinity in C_3 plants. Plant Biology **6**, 269–279.

Flexas J, Díaz-Espejo A, Berry JA, Cifre J, Galmés J, Kaldenhoff R, Medrano H, Ribas-Carbó M. 2007. Analysis of leakage in IRGA's leaf chambers of open gas exchange systems: quantification and its effects in photosynthesis parameterization. Journal of Experimental Botany **58**, 1533–1543.

Flexas J, Niinemets U, Gallé A, *et al.* 2013a. Diffusional conductances to CO_2 as a target for increasing photosynthesis and photosynthetic water-use efficiency. Photosynthesis Research **117**, 45–59.

Flexas J, Ribas-Carbó M, Diaz-Espejo A, Galmés J, Medrano H. 2008. Mesophyll conductance to CO_2: current knowledge and future prospects. Plant, Cell & Environment **31**, 602–621.

Flexas J, Scoffoni C, Gago J, Sack L. 2013*b*. Leaf mesophyll conductance and leaf hydraulic conductance: an introduction to their measurement and coordination. Journal of Experimental Botany **64**, 3965–3981.

Fry SC. 1979. Phonolic components of the primary cell wall and their possible rôle in the hormonal regulation of growth. Planta **146**, 343–351.

Fry SC. 2004. Primary cell wall metabolism: tracking the careers of wall polymers in living plant cells. New Phytologist **161**, 641–675.

Gago J, Carriquí M, Nadal M, Clemente-Moreno MJ, Coopman RE, Fernie AR, Flexas J. 2019. Photosynthesis optimized across land plant phylogeny. Trends in Plant Science **24**, 947–958.

Galmés J, Conesa MÀ, Ochogavía JM, Perdomo JA, Francis DM, Ribas-Carbó M, Savé R, Flexas J, Medrano H, Cifre J. 2011. Physiological and morphological adaptations in relation to water use efficiency in Mediterranean accessions of *Solanum lycopersicum*. Plant, Cell & Environment **34**, 245–260.

Grabber JH. 2005. How do lignin composition, structure, and cross-linking affect degradability? A review of cell wall model studies. Crop Science **45**, 820–831.

Harley PC, Loreto F, Di Marco G, Sharkey TD. 1992. Theoretical considerations when estimating the mesophyll conductance to CO_2 flux by analysis of the response of photosynthesis to CO_2. Plant Physiology **98**, 1429–1436.

Hoch G. 2007. Cell wall hemicelluloses as mobile carbon stores in non-reproductive plant tissues. Functional Ecology **21**, 823–834.

Houston K, Tucker MR, Chowdhury J, Shirley N, Little A. 2016. The plant cell wall: a complex and dynamic structure as revealed by the responses of genes under stress conditions. Frontiers in Plant Science **7**, 984.

Huck MG, Ishihara K, Peterson CM, Ushijima T. 1983. Soybean adaptation to water stress at selected stages of growth. Plant Physiology **73**, 422–427.

Hura T, Hura K, Dziurka K, Ostrowska A, B[illegible]czek-Kwinta R, Grzesiak M. 2012. An increase in the content of cell wall-bound phenolics correlates with the productivity of triticale under soil drought. Journal of Plant Physiology **169**, 1728–1736.

Hura T, Hura K, Grzesiak S. 2009. Possible contribution of cell-wall-bound ferulic acid in drought resistance and recovery in triticale seedlings. Journal of Plant Physiology **166**, 1720–1733.

Iiyama K, Lam T, Stone BA. 1994. Covalent cross-links in the cell wall. Plant Physiology **104**, 315–320.

Kanevski I, Maliga P, Rhoades DF, Gutteridge S. 1999. Plastome engineering of ribulose-1,5-bisphosphate carboxylase/oxygenase in tobacco to form a sunflower large subunit and tobacco small subunit hybrid. Plant Physiology **119**, 133–142.

Karabourniotis G, Liakopoulos G, Nikolopoulos D, Bresta P, Stavroulaki V, Sumbele S. 2014. 'Carbon gain vs. water saving, growth vs. defence': two dilemmas with soluble phenolics as a joker. Plant Science **227**, 21–27.

Kent SS, Andre M, Cournac L, Farineau J. 1992. An integrated model for the determination of the Rubisco specificity factor, respiration in the light and other photosynthetic parameters of C_3 plants in situ. Plant Physiology and Biochemistry **30**, 625–637.

Kuusk V, Niinemets Ü, Valladares F. 2018. A major trade-off between structural and photosynthetic investments operative across plant and needle ages in three Mediterranean pines. Tree Physiology **38**, 543–557.

Lara-Espinoza C, Carvajal-Millán E, Balandrán-Quintana R, López-Franco Y, Rascón-Chu A. 2018. Pectin and pectin-based composite materials: beyond food texture. Molecules **23**, 942.

Leucci MR, Lenucci MS, Piro G, Dalessandro G. 2008. Water stress and cell wall polysaccharides in the apical root zone of wheat cultivars varying in drought tolerance. Journal of Plant Physiology **165**, 1168–1180.

Lo Gullo MA, Salleo S. 1988. Different strategies of drought resistance in three Mediterranean sclerophyllous trees growing in the same environmental conditions. New Phytologist **108**, 267–276.

McKenna BA, Kopittke PM, Wehr JB, Blamey FP, Menzies NW. 2010. Metal ion effects on hydraulic conductivity of bacterial cellulose–pectin composites used as plant cell wall analogs. Physiologia Plantarum **138**, 205–214.

Moore JP, Farrant JM, Driouich A. 2008. A role for pectin-associated arabinans in maintaining the flexibility of the plant cell wall during water deficit stress. Plant Signaling & Behavior **3**, 102–104.

Nadal M, Flexas J. 2019. Variation in photosynthetic characteristics with growth form in a water-limited scenario: implications for assimilation rated and water use efficiency in crops. Agricultural Water Management **216**, 457–472.

Nadal M, Flexas J, Gulías J. 2018. Possible link between photosynthesis and leaf modulus of elasticity among vascular plants: a new player in leaf traits relationships? Ecology Letters **21**, 1372–1379.

Niinemets Ü, Cescatti A, Rodeghiero M, Tosens T. 2005. Leaf internal diffusion conductance limits photosynthesis more strongly in older leaves of Mediterranean evergreen broadleaved species. Plant, Cell & Environment **28**, 1552–1566.

Ochoa-Villarreal M, Aispuro-Hernández E, Vargas-Arispuro I, Martínez-Téllez MÁ. 2012. Plant cell wall polymers: function, structure and biological activity of their derivatives. In: De Souza Gomes A, ed. Polymerization. InTechOpen. doi: 10.5772/2750.

Onoda Y, Wright IJ, Evans JR, Hikosaka K, Kitajima K, Niinemets Ü, Poorter H, Tosens T, Westoby M. 2017. Physiological and structural

tradeoffs underlying the leaf economics spectrum. New Phytologist **214**, 1447–1463.

Panković D, Sakač Z, Kevrešan S, Plesničar M. 1999. Acclimation to long-term water deficit in the leaves of two sunflower hybrids: photosynthesis, electron transport and carbon metabolism. Journal of Experimental Botany **50**, 127–138.

Parry MAJ, Keys AJ, Gutteridge S. 1989. Variation in the specificity factor of C-3 higher-plant Rubisco determined by the total consumption of ribulose-P-2. Journal of Experimental Botany **40**, 317–320.

Peguero-Pina JJ, Sancho-Knapik D, Gil-Pelegrín E. 2017. Ancient cell structural traits and photosynthesis in today's environment. Journal of Experimental Botany **68**, 1389–1392.

Peltier JP, Marigo G. 1999. Drought adaptation in *Fraxinus excelsior* L.: physiological basis of the elastic adjustment. Journal of Plant Physiology **154**, 529–535.

Poorter H, Niinemets U, Poorter L, Wright IJ, Villar R. 2009. Causes and consequences of variation in leaf mass per area (LMA): a meta-analysis. New Phytologist **182**, 565–588.

Roig-Oliver M, Nadal M, Clemente-Moreno MJ, Bota J, Flexas J. 2020. Cell wall components regulate photosynthesis and leaf water relations of *Vitis vinifera* cv. Grenache acclimated to contrasting environmental conditions. Journal of Plant Physiology **244**, 153084.

Rui Y, Dinneny JR. 2019. A wall with integrity: surveillance and maintenance of the plant cell wall under stress. New Phytologist **225**, 1428–1439.

Sack L, Cowan PD, Jaikumar N, Holbrook NM. 2003. The 'hydrology' of leaves: coordination of structure and function intemperate woody species. Plant, Cell & Environment **26**, 1343–1356.

Sack L, Pasquet-Kok J, PrometheusWiki contributors. 2011. Leaf pressure–volume curve parameters. PrometheusWiki. http://prometheuswiki.org/tiki-pagehistory.php?page=Leaf%20pressure-volume%20curve%20parameters&preview=16.

Sánchez-Rodríguez E, Moreno DA, Ferreres F, Rubio-Wilhelmi Mdel M, Ruiz JM. 2011. Differential responses of five cherry tomato varieties to water stress: changes on phenolic metabolites and related enzymes. Phytochemistry **72**, 723–729.

Sarkar P, Bosneaga E, Auer M. 2009. Plant cell walls throughout evolution: towards a molecular understanding of their design principles. Journal of Experimental Botany **60**, 3615–3635.

Schiraldi A, Fessas D, Signorelli M. 2012. Water activity in biological systems—a review. Polish Journal of Food and Nutrition Sciences **62**, 5–13.

Shafi A, Zahoor I, Mir MA. 2019. Structural and functional changes in *Arabidopsis thaliana* cell wall under drought stress. International Journal for Research & Development in Technology **8**, 2349–3585.

Sharwood RE, von Caemmerer S, Maliga P, Whitney SM. 2008. The catalytic properties of hybrid Rubisco comprising tobacco small and sunflower large subunits mirror the kinetically equivalent source Rubiscos and can support tobacco growth. Plant Physiology **146**, 83–96.

Singleton VS, Rossi JA. 1965. Colorimetry of total phenolics with phosphomolybdic–phosphotungstic acid reagent. American Journal of Enology and Viticulture **16**, 144–157.

Sobrado MA, Turner NC. 1983. A comparison of the water relations characteristics of *Helianthus annuus* and *Helianthus petiolaris* when subjected to water deficits. Oecologia **58**, 309–313.

Solecka D, Zebrowski J, Kacperska A. 2008. Are pectins involved in cold acclimation and de-acclimation of winter oil-seed rape plants? Annals of Botany **101**, 521–530.

Sørensen I, Domozych D, Willats WG. 2010. How have plant cell walls evolved? Plant Physiology **153**, 366–372.

Tenhaken R. 2015. Cell wall remodeling under abiotic stress. Frontiers in Plant Science **5**, 771.

Terashima I, Miyazawa SI, Hanba YT. 2001. Why are sun leaves thicker than shade leaves? Consideration based on analyses of CO_2 diffusion in the leaf. Journal of Plant Research **114**, 93–105.

Terrett OM, Dupree P. 2019. Covalent interactions between lignin and hemicelluloses in plant secondary cell walls. Current Opinion in Biotechnology **56**, 97–104.

Terzi R, Güler NS, Çalişkan N, Kadioğlu A. 2013. Lignification response for rolled leaves of *Ctenanthe setosa* under long-term drought stress. Turkish Journal of Biology **37**, 614–619.

Thain JF. 1983. Curvature correlation factors in the measurements of cell surface areas in plant tissues. Journal of Experimental Botany **34**, 87–94.

Théroux-Rancourt G, Éthier G, Pepin S. 2015. Greater efficiency of water use in poplar clones having a delayed response of mesophyll conductance to drought. Tree Physiology **35**, 172–184.

Tomás M, Flexas J, Copolovici L, Galmés J, Hallik L, Medrano H, Ribas-Carbó M, Tosens T, Vislap V, Niinemets Ü. 2013. Importance of leaf anatomy in determining mesophyll diffusion conductance to CO_2 across species: quantitative limitations and scaling up by models. Journal of Experimental Botany **64**, 2269–2281.

Tosens T, Nishida K, Gago J, *et al.* 2016. The photosynthetic capacity in 35 ferns and fern allies: mesophyll CO_2 diffusion as a key trait. New Phytologist **209**, 1576–1590.

Valentini R, Epron D, Angelis PD, Matteucci G, Dreyer E. 1995. In situ estimation of net CO_2 assimilation, photosynthetic electron flow and photorespiration of Turkey oak (*Q. cerris* L.) leaves: diurnal cycles under different water supply. Plant, Cell & Environment **18**, 631–64.

Veromann-Jürgenson LL, Tosens T, Laanisto L, Niinemets Ü. 2017. Extremely thick cell walls and low mesophyll conductance: welcome to the world of ancient living! Journal of Experimental Botany **68**, 1639–1653.

Vicré M, Sherwin HW, Driouich A, Jaffer MA, Farrant JM. 1999. Cell wall characteristics and structure of hydrated and dry leaves of the resurrection plant *Craterostigma wilsmii*, a microscopical study. Journal of Plant Physiology **155**, 719–726.

Vogt T. 2010. Phenylpropanoid biosynthesis. Molecular Plant **3**, 2–20.

von Caemmerer S, Farquhar G, Berry J. 2009. Biochemical model of C3 photosynthesis. In: A Laisk, L Nedbal, Govindjee, eds. Photosynthesis in silico: understanding complexity from molecules to ecosystems. Springer Science + Business Media B.V. 209–230.

Wallace G, Fry SC. 1994. Phenolic components of the plant cell wall. International Review of Cytology **151**, 229–267.

Warren CR. 2008. Stand aside stomata, another actor deserves centre stage: the forgotten role of the internal conductance to CO_2 transfer. Journal of Experimental Botany **59**, 1475–1487.

Zhang T, Tang H, Vavylonis D, Cosgrove DJ. 2019. Disentangling loosening from softening: insights into primary cell wall structure. The Plant Journal **100**, 1101–1017.

Zimmermann, U. 1978. Physics of turgor- and osmoregulation. Annual Review of Plant Physiology **29**, 121–148.

Table S1. Pearson correlation matrix of physiological, leaf water relations, cell wall and anatomical parameters measured in *H. annuus* plants across all experimental conditions. Values in italics and bold indicate significant ($P < 0.05$) and highly significant ($P < 0.01$) correlation coefficients, respectively.

	A_N	g_s	WUE_i	g_m	ETR	R_{light}	g_s/g_m	Ψ_{pd}	Ψ_{md}	Ψ_{tlp}	π_o	RWC_{tlp}	ε	a_f	C^*_{ft}	AIR	Cel	Hemicel	Pectin	(Cel+Hemicel)/ Pectin	CW bound phenolics	Coumaric acid	Ferulic acid	Caffeic acid	Lignin	T_{LEAF}	T_{UE}	T_{LE}	T_{PAL}	T_{SPO}	T_{MES}	N_{PAL}	F_{ias}	T_{chl}	L_{chl}	L_{betchl}	S_m/S	S_c/S	S_c/S_m	T_{cyt}	T_{cw}
A_N		0.83	0.04	***0.99***	***0.99***	***0.97***	0.19	0.63	0.58	*-0.89*	-0.52	-0.5	-0.45	-0.12	-0.18	-0.32	-0.56	-0.68	-0.35	-0.23	*-0.92*	*-0.94*	-0.7	-0.78	-0.83	0.78	0.6	0.61	0.27	0.71	-0.23	-0.25	-0.39	0.81	*0.9*	-0.87	-0.22	0.71	0.81	***-0.98***	-0.42
g_s			-0.51	0.8	0.8	0.86	-0.35	0.85	*0.88*	-0.68	-0.39	-0.54	-0.24	-0.18	0.15	0.08	-0.34	-0.35	-0.7	0.34	-0.66	-0.69	-0.49	-0.4	-0.43	0.78	*0.91*	0.36	0	0.82	-0.45	0.14	-0.33	*0.94*	***0.97***	-0.82	0.2	0.85	0.87	*-0.9*	0.1
WUE_i				0.1	0.05	-0.11	*0.95*	-0.53	-0.68	-0.17	-0.24	0.38	-0.02	0.23	-0.35	-0.45	-0.42	-0.29	0.8	***-0.98***	-0.14	-0.21	-0.16	-0.46	-0.51	-0.23	-0.74	0.14	0.31	-0.24	0.65	-0.63	0.06	-0.42	-0.38	0.06	-0.49	-0.31	-0.25	0.09	*-0.89*
g_m					***0.97***	*0.94*	0.26	0.65	0.58	*-0.93*	-0.64	-0.43	-0.34	-0.14	-0.07	-0.28	-0.62	-0.59	-0.24	-0.27	*-0.9*	***-0.96***	-0.74	-0.82	-0.87	0.71	0.53	0.58	0.18	0.75	-0.13	-0.33	-0.43	0.82	0.85	*-0.91*	-0.15	0.76	0.85	***-0.98***	-0.5
ETR						***0.98***	0.2	0.61	0.55	-0.88	-0.47	-0.56	-0.53	-0.17	-0.25	-0.41	-0.5	-0.72	-0.35	-0.25	*-0.95*	*-0.94*	-0.71	-0.8	-0.84	0.78	0.57	0.68	0.3	0.63	-0.29	-0.27	-0.41	0.79	*0.88*	-0.83	-0.31	0.65	0.77	***-0.96***	-0.42
R_{light}							0.06	0.7	0.66	-0.85	-0.43	-0.67	-0.57	-0.27	-0.21	-0.39	-0.37	-0.68	-0.47	-0.08	*-0.95*	*-0.91*	-0.72	-0.74	-0.76	0.78	0.67	0.71	0.22	0.62	-0.44	-0.21	-0.48	0.85	*0.92*	-0.83	-0.28	0.67	0.8	*-0.96*	-0.27
g_s/g_m								-0.27	-0.45	-0.41	-0.48	0.19	-0.04	-0.03	-0.21	-0.54	-0.4	-0.24	0.82	*-0.93*	-0.32	-0.42	-0.44	-0.67	-0.68	-0.25	-0.67	0.33	0.11	-0.12	0.54	-0.83	-0.24	-0.18	-0.27	-0.17	-0.49	-0.09	0	-0.08	*-0.95*
Ψ_{pd}									***0.98***	-0.72	-0.62	-0.63	-0.06	-0.6	0.48	0.03	-0.06	0.04	-0.42	0.44	-0.56	-0.65	-0.7	-0.47	-0.41	0.35	0.68	0.44	-0.49	0.67	-0.5	-0.18	-0.71	***0.96***	0.72	-0.85	0.26	*0.89*	*0.94*	-0.75	0.11
Ψ_{md}										-0.6	-0.47	-0.62	-0.06	-0.52	0.46	0.14	-0.01	0.05	-0.57	0.58	-0.48	-0.53	-0.56	-0.31	-0.26	0.41	0.79	0.34	-0.45	0.67	-0.57	0.02	-0.59	*0.94*	0.75	-0.76	0.34	0.85	*0.88*	-0.7	0.28
Ψ_{tlp}											0.82	0.49	0.25	0.42	-0.1	0.38	0.47	0.38	-0.01	0.29	0.87	***0.98***	*0.92*	*0.93*	*0.92*	-0.41	-0.32	-0.67	0.12	-0.63	0.13	0.61	0.69	-0.82	-0.67	*0.95*	0.17	-0.78	*-0.89*	*0.89*	0.58
π_o												0.07	-0.33	0.36	-0.57	0.01	0.51	-0.15	-0.37	0.26	0.44	0.71	0.75	0.72	0.71	0.03	-0.02	-0.26	0.51	-0.63	-0.27	0.68	0.62	-0.62	-0.29	0.83	-0.23	-0.78	-0.78	0.6	0.6
RWC_{tlp}													0.74	0.76	0.23	0.61	-0.43	0.37	0.47	-0.29	0.7	0.51	0.66	0.47	0.35	-0.31	-0.46	-0.86	0.1	-0.01	0.91	0.23	0.73	-0.62	-0.53	0.4	0.48	-0.27	-0.5	0.48	-0.18
ε														0.27	0.82	0.81	-0.25	0.81	0.39	0.15	0.68	0.38	0.34	0.39	0.36	-0.48	-0.24	-0.79	-0.55	0.25	0.67	0.09	0.25	-0.18	-0.4	0.05	0.85	0.2	-0.05	0.31	0.03
a_f															-0.24	0.48	-0.57	-0.21	-0.06	-0.26	0.37	0.33	0.72	0.43	0.25	0.31	0	-0.68	0.66	0.15	0.62	0.57	*0.94*	-0.45	-0.05	0.33	0.25	-0.25	-0.44	0.16	-0.07
C^*_{ft}																0.67	-0.06	0.84	0.15	0.45	0.35	0.08	-0.09	0.14	0.18	-0.38	0.08	-0.42	-0.86	0.43	0.22	-0.06	-0.26	0.3	-0.08	-0.32	0.84	0.56	0.4	-0.01	0.17
AIR																	-0.24	0.6	-0.2	0.5	0.65	0.46	0.58	0.65	0.57	-0.03	0.27	*-0.88*	-0.26	0.42	0.38	0.63	0.51	-0.03	-0.04	0.08	***0.96***	0.25	-0.02	0.17	0.44
Cel																		0.34	-0.11	0.52	0.3	0.5	0.11	0.38	0.55	-0.5	-0.17	0.17	-0.35	-0.73	-0.64	0.07	-0.27	-0.26	-0.42	0.53	-0.23	-0.59	-0.37	0.57	0.63
Hemicel																			0.32	0.47	0.73	0.55	0.25	0.49	0.56	-0.75	-0.29	-0.57	-0.83	-0.11	0.23	0.02	-0.07	-0.2	-0.56	0.23	0.69	0.02	-0.12	0.53	0.36
Pectin																				-0.66	0.22	0.06	-0.13	-0.24	-0.21	-0.73	*-0.92*	-0.07	-0.27	-0.35	0.68	-0.71	-0.13	-0.47	-0.71	0.16	-0.15	-0.27	-0.27	0.39	-0.67
(Cel+Hemicel)/ Pectin																					0.31	0.36	0.23	0.56	0.63	0.02	0.58	-0.24	-0.44	0.11	-0.58	0.59	-0.06	0.28	0.18	0.06	0.55	0.21	0.14	0.09	*0.93*
CW bound																						*0.94*	0.82	*0.88*	*0.88*	-0.61	-0.4	-0.87	-0.24	-0.4	0.39	0.45	0.58	-0.71	-0.75	0.75	0.53	-0.51	-0.7	0.86	0.46
Coumaric acid																							0.88	*0.94*	*0.95*	-0.53	-0.35	-0.72	-0.06	-0.6	0.15	0.55	0.61	-0.78	-0.72	*0.9*	0.29	-0.7	-0.83	*0.92*	0.6
Ferulic acid																								*0.92*	0.84	-0.13	-0.13	-0.83	0.31	-0.33	0.31	0.78	*0.91*	-0.72	-0.45	0.8	0.34	-0.6	-0.78	0.69	0.5
Caffeic acid																									***0.98***	-0.26	-0.02	-0.79	0	-0.34	0.06	0.79	0.69	-0.58	-0.45	0.76	0.48	-0.5	-0.66	0.73	0.76
Lignin																										-0.37	-0.07	-0.7	-0.13	-0.44	-0.05	0.71	0.54	-0.56	-0.5	0.77	0.43	-0.52	-0.65	0.77	0.81
T_{LEAF}																											0.8	0.25	0.62	0.62	-0.28	0.38	0.16	0.56	*0.9*	-0.48	-0.08	0.43	0.45	-0.76	0
T_{UE}																												0.13	0.12	0.68	-0.54	0.52	-0.05	0.75	*0.89*	-0.52	0.3	0.63	0.61	-0.67	0.44
T_{LE}																													0.06	-0.05	-0.6	-0.6	-0.76	0.49	0.42	-0.46	-0.75	0.19	0.46	-0.53	-0.32
T_{PAL}																														-0.07	0.07	0.34	0.6	-0.26	0.24	0.22	-0.49	-0.37	-0.34	-0.12	-0.19
T_{SPO}																															0.12	0.09	-0.1	0.77	0.77	-0.83	0.53	*0.92*	0.81	-0.81	-0.16
T_{MES}																																-0.15	0.47	-0.45	-0.43	0.11	0.31	-0.09	-0.26	0.23	-0.56
N_{PAL}																																	0.73	-0.16	0.16	0.39	0.44	-0.16	-0.31	0.2	0.75
F_{ias}																																		-0.62	-0.23	0.6	0.25	-0.47	-0.65	0.42	0.2
T_{chl}																																			0.86	*-0.92*	0.16	*0.92*	***0.97***	*-0.9*	-0.03
L_{chl}																																				-0.76	0.03	0.73	0.78	*-0.92*	0
L_{betchl}																																					-0.13	*-0.94*	***-0.98***	*0.93*	0.39
S_m/S																																						0.45	0.2	0.04	0.38
S_c/S																																							***0.96***	-0.83	-0.14
S_c/S_m																																								*-0.89*	-0.21
T_{cyt}																																									0.34
T_{cw}																																									

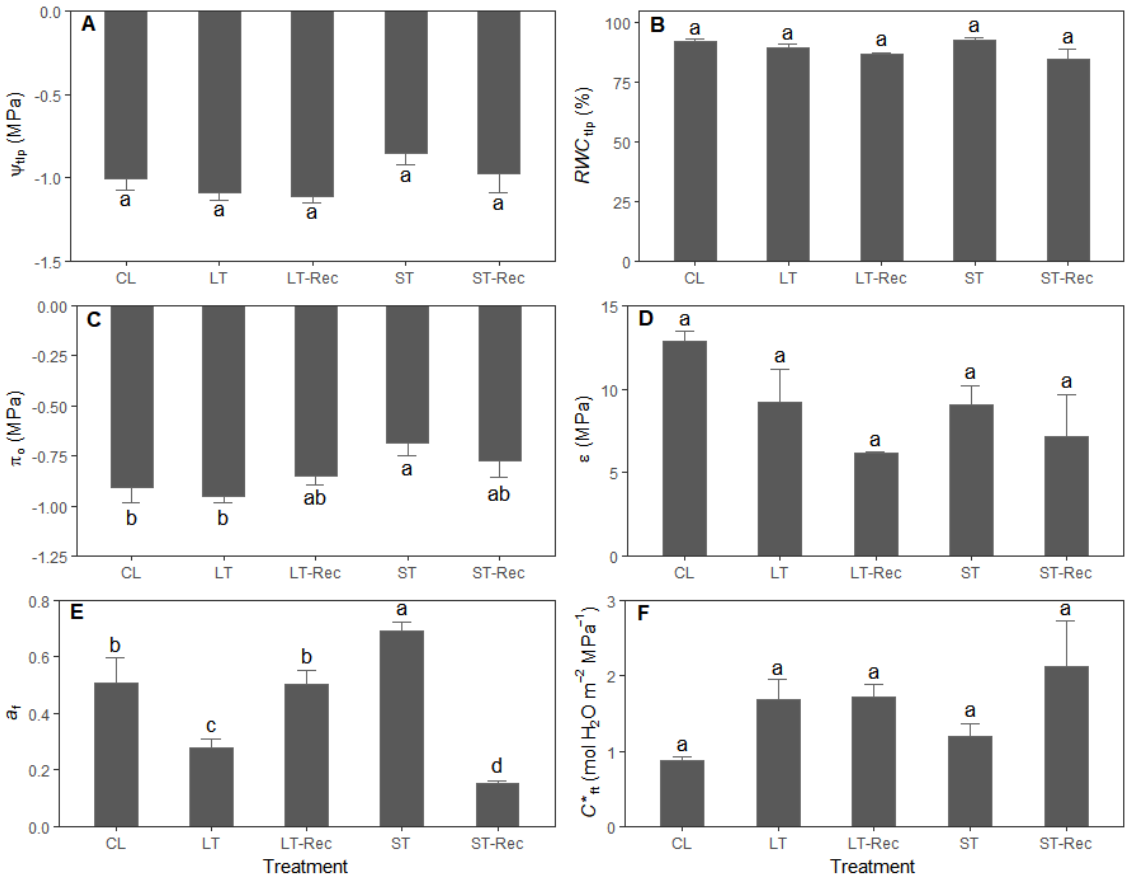

Fig. S1. Leaf water relations characterization in *H. annuus* plants grown under different conditions ("CL": control, "LT": long-term water deficit stress, "LT-Rec": long-term water deficit stress with recovery, "ST": short-term water deficit stress and "ST-Rec": short-term water deficit stress with recovery). (A) Leaf water potential at turgor loss point (Ψ_{tlp}), (B) relative water content at turgor loss point (RWC_{tlp}), (C) leaf osmotic potential at full turgor (π_o), (D) bulk modulus of elasticity (ε), (E) apoplastic water fraction (a_f) and (F) leaf area specific capacitance at full turgor (C^*_{ft}). Different superscript letters indicate significant difference ($P < 0.05$) across all experimental conditions according to LSD test. n = 4–6 (means ± SE).

Mature sunflower leaves show dynamic changes in cell wall composition uncoupled from photosynthesis upon rewatering

Margalida Roig-Oliver[1*], Panagiota Bresta[2], Dimosthenis Nikolopoulos[3], Josefina Bota[1], Jaume Flexas[1,4]

[1]Research Group on Plant Biology under Mediterranean Conditions, Departament de Biologia, Universitat de les Illes Balears (UIB) – Agro-Environmental and Water Economics Institute (INAGEA). Carretera de Valldemossa Km 7.5, 07122 Palma, Illes Balears, Spain.
[2]Laboratory of Electron Microscopy, Department of Crop Science, Agricultural University of Athens (AUA), Iera Odos 75, Botanikos, 11855 Athens, Greece.
[3]Laboratory of Plant Physiology and Morphology, Department of Crop Science, Agricultural University of Athens (AUA), Iera Odos 75, Botanikos, 11855 Athens, Greece.
[4]King Abdulaziz University, Jeddah, Saudi Arabia.

[*] Corresponding author.

Submitted to *Journal of Experimental Botany* on 6th May 2021.

Mature sunflower leaves show dynamic changes in cell wall composition uncoupled from photosynthesis upon rewatering

Running tittle: Recovery uncouples cell wall composition and CO_2 diffusion.

Margalida Roig-Oliver[1], Panagiota Bresta[2], Dimosthenis Nikolopoulos[3], Josefina Bota[1], Jaume Flexas[1,4]

[1]Research Group on Plant Biology under Mediterranean Conditions, Departament de Biologia, Universitat de les Illes Balears (UIB) – Agro-Environmental and Water Economics Institute (INAGEA). Carretera de Valldemossa Km 7.5, 07122 Palma, Illes Balears, Spain.
[2]Laboratory of Electron Microscopy, Department of Crop Science, Agricultural University of Athens (AUA), Iera Odos 75, Botanikos, 11855 Athens, Greece.
[3]Laboratory of Plant Physiology and Morphology, Department of Crop Science, Agricultural University of Athens (AUA), Iera Odos 75, Botanikos, 11855 Athens, Greece.
[4]King Abdulaziz University, Jeddah, Saudi Arabia.

Corresponding author: margaroig93@gmail.com, (+34) 971259556.

Highlight

Changes in cell wall main composition of mature *H. annuus* leaves differentially affect photosynthesis during gradual short-term water deficit stress and during dynamic recovery after long-term water deficit stress.

Abstract

In a previous study, we showed that different water availability conditions induced changes in cell wall composition of mature *Helianthus annuus* L. leaves that correlated with mesophyll conductance to CO_2 diffusion (g_m). Since that study did not determine the velocity of these changes, this issue remains unresolved. To evaluate the dynamism of modifications in cell wall main composition (cellulose, hemicelluloses, pectins and lignins) affecting photosynthesis under different water availability regimes, we tested *H. annuus* subjected to control conditions (i.e., water availability), different levels of short-term water deficit stress (ST), long-term water deficit stress (LT) and long-term water deficit stress followed by gradual recoveries addressed at different times (LT-Rec). The imposition of these conditions promoted modifications in cell

wall composition that were accompanied by distinct photosynthetic adjustments. During the application of gradual ST treatments, pectins enhancements were associated with g_m declines. However, during LT-Rec, pectins content decreased significantly after only 5 h, while the concentration of other cell wall components such as hemicelluloses and lignins changed after 24 h, all of them being uncoupled from g_m. Surprisingly, lignins increased by around 200% as compared to control and were related to stomatal conductance to gas diffusion (g_s) during gradual recovery.

Key words

Cell wall composition, *Helianthus annuus*, lignins, mesophyll conductance to CO_2 diffusion, pectins, photosynthesis, recovery, stomatal conductance to gas diffusion, water deficit stress.

Abbreviations

Alcohol insoluble residue (AIR), net CO_2 assimilation (A_N), electron transport rate (*ETR*), mesophyll conductance to CO_2 diffusion (g_m), stomatal conductance to gas diffusion (g_s), light mitochondrial non-photorespiratory respiration rate (R_{light}), leaf relative water content (RWC), water use efficiency (*WUE*), leaf water potential (Ψ), midday leaf water potential (Ψ_{md}), pre-dawn leaf water potential (Ψ_{pd}).

Introduction

The plant cell wall is a complex structure surrounding plant cells that is composed by distinct types of polysaccharides, phenolic compounds, structural proteins, and other small molecules (Carpita and Gibeaut, 1993; Cosgrove, 2005, 2018; Keegstra, 2010; Tenhaken, 2015; De Lorenzo *et al*., 2019; Anderson and Kieber, 2020). Most studies have focused on primary cell walls, which are mainly formed by cellulose, hemicelluloses and pectins (Carpita and Gibeaut, 1993; Cosgrove, 2005, 2018; Tenhaken, 2015; Novaković *et al*., 2018; De Lorenzo *et al*., 2019; Anderson and Kieber, 2020). Of the previous, cellulose is the most abundant polysaccharide, consisting in a few hundred to over 10.000 residues of (1,4)-linked-β-D-glucose chains forming long, insoluble, and unbranched crystalline microfibrils due to hydrogen bounds (Cosgrove, 2005, 2018; Keegstra, 2010; Anderson and Kieber, 2020). Among those closely packed cellulose microfibrils, non-cellulosic polysaccharides (hereafter "hemicelluloses") are deposited (Carpita and Gibeaut, 1993; Tenhaken, 2015; Novaković *et al*., 2018). This cellulose-hemicelluloses network is entrenched in a pectin matrix, which is thought to be a crucial structure determining cell wall hydrophilic properties as well as its porosity, viscosity, rigidity

and thickness (Baron-Epel *et al*., 1988; Vicré *et al*., 1999; Cosgrove, 2005; Moore *et al*., 2008; Ochoa-Villareal *et al*., 2012; Houston *et al*., 2016; Carriquí *et al*., 2020; Roig-Oliver *et al*., 2020*a*,*b*). In some types of primary cell walls, secondary walls are internally deposited to provide strength and rigidity to no longer growing tissues (Cosgrove, 2005; Keegstra, 2010; Tucker *et al*., 2018). Particularly, lignin is a specific phenolic polymer consisting of highly condensed polymeric matrices (core lignin) and low molecular weight phenolic monomers and oligomers (non-core lignin) relatively abundant in secondary walls (Iiyama *et al.*, 1994; Wallace and Fry, 1994; Moreira-Vilar *et al*., 2014). Lignin accumulation during plant exposition to environmental stresses has been related to alterations in cell wall characteristics, such as extensibility, hydrophobicity, flexibility, and mechanical strength (Iiyama *et al.*, 1994; Wallace and Fry, 1994; Lampugnani *et al*., 2018; Terrett and Dupree, 2019).

The cell wall was traditionally considered to be robust and static from a compositional perspective, but it is now recognized as a highly dynamic structure that is required to define an appropriated leaf architecture (Baskin, 2005; Cosgrove, 2005, 2018; Caffall and Mohnen, 2009; Ochoa-Villarreal *et al*., 2012; Tenhaken, 2015; Weraduwage *et al*., 2018; Lampugnani *et al*., 2018; De Lorenzo *et al*., 2019; Rui and Dinnery, 2019; Anderson and Kieber, 2020). Particularly, cell wall modifications occur during its synthesis and assembly, promoting changes in the orientation of cytoskeleton structures with subsequent alterations in the cross-linking interactions between cell wall components (Weraduwage *et al*., 2018). However, there is still controversy when referring to the dynamism of those modifications occurring in the cell wall of expanded and mature leaves (Houston *et al*., 2016; Cosgrove, 2018). On the one hand, it is assumed that changes in cell wall composition and architecture control different stages of plant cells differentiation during embryogenesis and subsequent growth (Cosgrove, 2018), leading to the establishment of a specific leaf architecture (Weraduwage *et al*., 2018). Thus, during cell growth, the cell wall has to be enough flexible to allow for the cellular expansion and it has to synthesize new wall material to properly encapsulate and reinforce the growing cell while providing structural support (Baskin, 2005; Houston *et al*., 2016; Lampugnani *et al*., 2018; Weraduwage *et al*., 2018). Hence, the genetic regulation of the constant synthesis and modification of the cell wall material promotes disruptions and cross-linkages reassembling (Cosgrove, 2005, 2018; Weraduwage *et al*., 2018). However, when the cell has ceased growing and dividing and mature leaves are constituted, thicker and robust secondary walls are internally deposited in some types of primary walls (Cosgrove, 2005; Keegstra, 2010; Houston *et al*., 2016; Lampugnani et al., 2018; Tucker *et al*., 2018). In these mature leaves, cell wall composition modifications were thought to be of lesser importance in comparison to those

taking place during leaf growth and expansion (Houston *et al*., 2016; Cosgrove, 2018), inhibiting wall ability to rearrange in response to external stressors (Sahaf and Sharon, 2016).

Some studies have recently demonstrated that mature leaves of plants subjected to different abiotic stressors display significant changes in their cell wall composition that are strongly related to photosynthesis –particularly, to mesophyll conductance to CO_2 diffusion (g_m)–, suggesting that these modifications may dynamically affect cell wall porosity in response to stress (Clemente-Moreno *et al*., 2019; Roig-Oliver *et al*., 2020*a*,*b*). Although specific differences were found depending on the tested species and stress conditions, in most of these studies the pectin content or the pectin fraction was somehow related to g_m. Regardless of the specific relationship between g_m and cell wall composition found in these previous studies, all of them analysed photosynthesis and cell wall composition responses after plants acclimation to a particular condition from days to weeks. Therefore, the dynamism of those modifications occurring in cell wall composition of mature leaves determining photosynthesis in small temporal scales remains unexplored. Since the application of distinct water availability regimes induces changes in both photosynthesis and cell wall composition (Chaves *et al*., 2002, 2009; Flexas *et al*., 2004; Vicré *et al*., 1999; Tenhaken, 2015; Novaković *et al*., 2018; Rui and Dinnery, 2019; Roig-Oliver *et al*., 2020*a*,*b*), we tested *Helianthus annuus* L. subjected to different water conditions with two aims: (1) to confirm the relevance of these cell wall modifications affecting photosynthesis in an extended range of short-term water deficit stress conditions; and (2) to evaluate the dynamism of those changes occurring in the cell wall composition of mature leaves immediately after rewatering plants subjected to long-term water deficit stress. Thus, we extended the experimental design of our previous study testing the same species (Roig-Oliver *et al*., 2020*a*) applying gradual short-term water deficit stress treatments and a long-term water deficit stress treatment followed by gradual recoveries to monitor in detail how modifications in cell wall main composition (i.e., cellulose, hemicelluloses, pectins and lignins) and photosynthesis occurred.

Material and Methods

Plant material, experimental design, and growth conditions

H. annuus seeds were sown individually in water-irrigated 3 litre pots containing a substrate mixture of peat:perlite (3:1, v/v). They were placed in a growing chamber at 25 ºC receiving 200–300 µmol m^{-2} s^{-1} of photosynthetic photon flux density (PPFD) for 12 h followed by 12 h of darkness. At the sowing day, pots were randomly subjected to different growing conditions: control (CL, without stress), short-term water deficit stress (ST), long-term water deficit stress

(LT) and long-term water deficit stress followed by a recovery (LT-Rec). Within the plants belonging to ST and LT-Rec treatments, randomly selected individual replicates were kept under distinct water availability conditions for a detailed monitoring of those changes associated to specific levels of ST and LT-Rec (see Fig. 1 for more detail).

Control plants were maintained at 100% field capacity (FC) for 44 days. The same conditions were applied to all plants belonging to ST treatments, being followed by the imposition of water deprivation. In order to monitor those changes occurring immediately after achieving a specific level of water shortage, individual ST replicates were randomly selected to be measured when reaching 80, 65, 50 and 40% FC (ST-80% FC, ST-65% FC, ST-50% FC and ST-40% FC, respectively; Fig. 1). As it took 4 days to descend from a specific % of FC to the following, additional control plants were maintained at 100% FC during the gradual performance of ST. Thus, they were measured at the same ages of ST-65% FC and ST-40% FC treatments (i.e., 52 and 60 days-old, respectively; Fig. 1) to remove the "age effect" from all ST measurements, ensuring that photosynthetic and cell wall compositional changes were exclusively attributed to each specific level of water deficit stress. LT treatment was achieved by decreasing the pots FC from 100% to 40%, starting at the sowing day. Hence, when 40% FC was reached –usually after 18 days from the sowing–, this water status was maintained for 26 days. Plants belonging to LT-Rec treatments were kept under the same conditions that those of LT, but a rewatering to 100% FC was applied at different time points to ensure that all of them were 44 days-old when measured. Particularly, plants were recovered and subsequently maintained at 100% FC for 5, 24, 48, 72 and 96 h (LT-Rec 5h, LT-Rec 24h, LT-Rec 48h, LT-Rec 72h and LT-Rec 96h, respectively; Fig. 1). Considering that no leaves were unfolded during ST treatments, measurements were performed on fully expanded leaves previously developed under well-watering conditions. Instead, LT treatment allowed for leaves expansion under stress conditions. Thus, LT and LT-Rec measurements were performed in leaves completely developed under water shortage.

In all cases, five randomly selected individual replicates were subjected to those specific conditions imposed by each treatment (Fig. 1). All plants were daily monitored to maintain each pot FC at a specific level by replacing evapo-transpired water.

Plants water status

For each plant belonging to CL, LT and ST treatments, a fully expanded leaf was employed to determine the pre-dawn (Ψ_{pd}) and the midday (Ψ_{md}) leaf water potentials with a pressure chamber (Model 600D; PMS Instrument Company, Albany, USA). Instead, the leaf water

potential (Ψ) was determined before starting gas exchange performance in all LT-Rec treatments. Additionally, the leaf relative water content (RWC) was calculated in the same leaves in which Ψ_{md} and Ψ were estimated using the following equation:

$$\mathrm{RWC} = \frac{\mathrm{FW} - \mathrm{DW}}{\mathrm{TW} - \mathrm{DW}} \text{ x } 100$$

Thus, leaves fresh weight (FW) was obtained immediately after measuring Ψ_{md} or Ψ. Then, leaves turgid weight (TW) was obtained after their rehydration in distilled water for 24 h in darkness at 4 ºC. Finally, leaves were transferred to an oven kept at 70 ºC for, at least, 72 h to obtain their dry weight (DW).

Gas exchange and chlorophyll fluorescence measurements

A gas exchange system equipped with a 2 cm^2 fluorescence chamber (Li-6400-40; Li-Cor Inc., Lincoln, NE, USA) was used to perform simultaneous measurements of gas exchange and chlorophyll *a* fluorescence. Per each plant, the third fully-expanded leaf from the apex was employed to determine the net CO_2 assimilation (A_N), the stomatal conductance to gas diffusion (g_s), the CO_2 concentration at the sub-stomatal cavity (C_i) and the steady-state fluorescence (F_s) at 25 ºC, 400 μmol CO_2 mol^{-1} air and saturating light (1500 μmol m^{-2} s^{-1}, 90–10% red-blue light) after reaching steady-state conditions (usually after 15–20 min). Afterward, a saturating light flash of around 8000 μmol m^{-2} s^{-1} was applied to determine the maximum fluorescence (F_m'). From these values, the real quantum efficiency of photosystem II (Φ_{PSII}) was recorded in the equipment. The electron transport rate (*ETR*) was calculated as described in Valentini *et al.* (1995) by the performance of light curves under negligible photorespiratory conditions (≃ 1% O_2). The dark respiration rate was estimated after plants acclimation to darkness for 30 min (Niinemets *et al*., 2005). From this value, the light mitochondrial non-photorespiratory respiration rate (R_{light}) was calculated. The mesophyll conductance to CO_2 diffusion (g_m) was estimated from previous values (Harley *et al.*, 1992) assuming that the CO_2 compensation point in the absence of respiration (Γ^*) was averaged from previously reported values for *H. annuus* (Parry *et al.*, 1989; Kent *et al*., 1992; Kanevski *et al.*, 1999; Sharwood *et al*., 2008).

Cell wall extraction and fractionation

Sampling for cell wall composition analyses was done in the same leaves used for gas exchange measurements. Whereas in CL, LT, and all ST treatments the sampling was performed after

keeping plants under darkness overnight to minimize foliar starch content, LT-Rec sampling was addressed immediately after completing gas exchange measurements. In all cases, around 1 g of fresh foliar tissue per plant was cut avoiding main veins. These portions were placed in screw-capped glass tubes filled with absolute ethanol to be boiled until bleached. In order to eliminate any alcohol-soluble residue, samples were cleaned twice with acetone >95% for 30 min, obtaining the alcohol insoluble residue (AIR), an approximation of the crude isolated cell wall material. Each AIR was split in two for the evaluation of distinct cell wall compounds. The AIR fraction destined to cellulose, hemicelluloses and pectins quantification was subjected to α-amylase digestion to remove starch residues, which were especially abundant in LT-Rec treatments due to sampling conditions. When no starch residues were further observed, 3 technical replicates per AIR weighting around 3 mg were hydrolysed with 2 M trifluoroacetic at 121 ºC for 1 h. They were subsequently centrifuged at 13000 *g*, differentiating an aqueous supernatant (non-cellulosic cell wall material, i.e., hemicelluloses and pectins) and a pellet (cellulosic cell wall material). Although supernatants were kept at –20 ºC until used, cellulosic pellets were cleaned twice with distilled water and twice more with acetone >95%. They were air-dried at room temperature to be hydrolysed with 200 µl sulphuric acid 72% (w/v) for 1 h, diluted to 6 ml with distilled water and heated at 121 ºC until pellet degradation. Once cooled, the obtained aqueous samples were used for cellulose quantification following the phenol sulphuric acid method (Dubois *et al.*, 1956). The same procedure was employed to calculate hemicelluloses concentration. Thus, both sugars contents were estimated interpolating samples absorbances at 490 nm from a glucose calibration curve. To quantify pectins, samples absorbances were read at 520 nm to be calculated from a galacturonic acid calibration curve (Blumenkrantz and Asboe-Hansen, 1973). In all cases, a Multiskan Sky Microplate Spectrophotometer (ThermoFisher Scientific) was employed. The left AIR fraction used for lignins quantification was dehydrated in an oven at 70 ºC for, at least, 72 h. AIRs were grounded to fine powder and around 15 mg of each one were used to quantify lignins content using the acetyl bromide method (Fagerstedt *et al.*, 2015), which quantifies both core and non-core lignin (Moreira-Vilar *et al.*, 2014). Hence, lignins concentration was obtained interpolating samples absorbances at 280 nm from a lignin calibration curve. In this case, a spectrophotometer UV-160A Shimadzu (Shimadzu, corp.) was employed.

Statistical analysis

Before any other statistical analysis, Thompson test was applied to find and subtract outliers for all studied parameters. Afterwards, the R software (ver. 3.2.2; R Core Team, Vienna,

Austria) was used to perform further statistical tests. First, data passed Shapiro–Wilk and Bartlett tests for normality and equality of variances, respectively. Then, one-way ANOVA and subsequent LSD test were addressed to detect statistically significant differences (P<0.05) among treatments during gradual ST and during LT with gradual recoveries for all tested parameters. Afterward, Pearson's correlation matrices were created to find pair-wise correlations among all analysed parameters, being significant and highly significant at P<0.05 and P<0.01, respectively. Finally, linear regressions between photosynthetic features and cell wall compositional traits were fitted utilizing mean values per treatment.

Results

Physiological and cell wall composition changes in response to gradual levels of short-term water deficit stress

The imposition of ST treatments resulted in statistically significant lower values for Ψ_{pd}, Ψ_{md} and RWC than under CL (Table 1). Particularly, Ψ_{pd} decreased gradually when intensifying the level of water shortage until reaching the lowest value in ST-40% FC (-1.69 ± 0.07 MPa; Table 1). Although Ψ_{md} was similarly maintained to CL in ST-80% FC and ST-65% FC, significant reductions were found under ST-50% FC (Table 1). Again, ST-40% FC presented the lowest value (-1.89 ± 0.11 MPa; Table 1). Whilst CL and ST-80% FC exhibited the highest RWC, ST-40% FC reached the lowest (44.59 ± 2.51 %; Table 1).

ST application did not result in statistically significant decrease in A_N compared to CL until reaching ST-40% FC (3.54 ± 0.51 µmol CO_2 m^{-2} s^{-1}; Table 2). CL presented the highest g_s (0.33 ± 0.06 mol CO_2 m^{-2} s^{-1}), which was reduced up to 80% after ST-40% FC imposition (Table 2). Concerning g_m, slight reductions were promoted during gradual ST, achieving the lowest value in ST-40% FC (0.09 ± 0.00 mol CO_2 m^{-2} s^{-1}; Table 2). Similarly, only ST-40% FC displayed significantly increased *WUE* as compared to CL (Table 2). No statistically significant differences were found among treatments regarding *ETR* and R_{light} (Table 2).

Based on absolute values for each cell wall component (Supplementary Table S1), the temporal variation in their relative abundance during gradual ST imposition is shown (Fig. 2). Whilst cellulose relative abundance was gradually reduced from CL to ST-65% (i.e., from 100.00 ± 11.42 to 45.43 ± 3.29 % CL), significant enhancements were subsequently detected (Fig. 2). Although hemicelluloses relative content was maintained to values close to CL in ST-80% FC, it dropped thereafter presenting similarly lower values across ST-65%, 50% and 40% FC (Fig. 2). Pectins relative concentration gradually increased during gradual ST, reaching the

highest value in ST-40% FC (165.87 ± 9.76 % CL; Fig. 2). Even though lignins relative abundance was almost maintained to CL in ST-80% FC and ST-65% FC (116.31 ± 5.94 and 110.74 ± 9.66 % CL, respectively), reductions of around 37% were detected in ST-50% FC as compared to CL (Fig. 2). Nonetheless, ST-40% FC presented almost 1.3 times higher lignins relative concentration compared to CL (Fig. 2).

While all the results described above were obtained after subtracting the age effect in all ST treatments, trends were similar for all parameters even without correcting the data (Supplementary Fig. S1 and Supplementary Tables S2 and S3). Significant correlations between cell wall composition and photosynthetic parameters were detected during gradual ST imposition (Supplementary Table S4). Particularly, whilst g_m and pectins correlated negatively (R^2=0.7, P=0.05, Fig. 3A), a positive relationship between the g_m/g_s ratio and pectins was found (R^2=0.91, P<0.01, Fig. 3B).

Physiological and cell wall composition changes upon long-term water deficit stress and subsequent recoveries

Although LT presented the lowest Ψ among treatments (-1.68 ± 0.30 MPa), it was immediately restored to CL upon recovery (Fig. 4A). Similarly, LT presented the lowest RWC (55.68 ± 0.96 %), which increased gradually during LT-Rec application until reaching a slightly higher value than CL in LT-Rec 96h (85.07 ± 1.25 %; Fig. 4B).

The application of LT-Rec treatments resulted in gradual photosynthesis enhancement since LT-Rec 96h presented almost 2.5 times larger A_N than CL (31.40 ± 1.57 µmol CO_2 m^{-2} s^{-1}; Fig. 5A). Regarding g_s, CL value was achieved in LT-Rec 24h (0.33 ± 0.05 mol CO_2 m^{-2} s^{-1}) and increased thereafter until reaching the highest value in both LT-Rec 72h and LT-Rec 96h (Fig. 5B). Nonetheless, LT and LT-Rec treatments did not promote any statistically significant modification for g_m as compared to CL (Fig. 5C). However, LT-Rec 5h application declined *WUE* around 23% in comparison to LT (Fig. 5D). Further reductions were detected in LT-Rec 24h and thereafter, representing the achievement of CL value (Fig. 5D). The higher *ETR* was exhibited in both LT-Rec 72h and LT-Rec 96h treatments (243.10 ± 13.14 and 274.55 ± 20.93 µmol m^{-2} s^{-1}, respectively), representing more than 2-fold higher *ETR* than CL (Fig. 5E). Finally, R_{light} gradually increased during LT-Rec application, reaching the highest value in LT-Rec 72h (1.81 ± 0.16 µmol CO_2 m^{-2} s^{-1}; Fig. 5F).

Absolute values for each cell wall component are found in Supplementary Table S1. Concerning temporal variation in cell wall composition during LT and gradual LT-Rec application, cellulose relative concentration was equally maintained to CL value across all

tested conditions (Fig. 6). Nonetheless, LT and subsequent LT-Rec treatments resulted in significantly lower hemicelluloses relative abundance as compared to CL (Fig. 6). Although LT exhibited higher pectins relative concentration than CL (123.70 ± 3.64 and 100.00 ± 4.82 % CL, respectively), it was significantly reduced upon recovery, finally reaching an almost similar CL value in LT-Rec 96h (87.82 ± 1.54 % CL; Fig. 6). Lignins relative abundance was around 3.5-fold lower in both LT and LT-Rec 5h in comparison to CL (Fig. 6). However, lignins relative abundance increased up to 200% in LT-Rec 24h, 48h, 72h and 96h (Fig. 6).

Significant relationships between cell wall composition and photosynthetic parameters were found during LT and gradual LT-Rec treatments (Supplementary Table S5). Specifically, a positive correlation between g_s and lignins was detected (R^2=0.69, P=0.01, Fig. 7).

Discussion

Water availability is crucial for plants development, growth, and survival (Chaves *et al*., 2002, 2009; Flexas *et al*., 2004). Since the intensity, the progression and the duration of distinct water shortage conditions promote different photosynthetic adjustments (Chaves *et al*., 2009), we reported contrasting responses due to ST and LT imposition. Although A_N reduction during gradual ST mainly resulted from a g_s decline (Table 2), LT reached higher A_N rates than control because of an enhancement in *ETR* (Fig. 5). These results show a clear acclimation response in those sunflower leaves that emerged after the imposition of long-term water deficit stress and agree with the observed results from previous studies evaluating the same species (Panković *et al*., 1999; Roig-Oliver *et al*., 2020*a*). Nonetheless, gradual photosynthesis enhancements during LT-Rec treatments were attributed to stomatal opening as well as to increments in biochemical capacity (Fig. 5).

By the application of gradual ST and LT-Rec treatments, we could examine in detail how changes in cell wall composition occurred, evidencing their high dynamism in mature leaves (Figs. 2 and 6). On one hand, gradual ST imposition resulted in enhanced pectins relative content, reaching the highest value under ST-40% FC (Fig. 2). The fact that water deficit stress increases the amount of pectins has been widely described (see, for instance, Sweet *et al*., 1990; Vicré *et al*., 1999, 2004; Leucci *et al*., 2008; Moore *et al*., 2008; Clemente-Moreno *et al*., 2019; Nadal *et al*., 2020; Roig-Oliver *et al*., 2020*a*,*b*,*c*) and could reflect the importance of pectins in maintaining an appropriate degree of cell wall hydration during water deprivation, which may also imply alterations in wall flexibility and extensibility (Leucci *et al*., 2008; Moore *et al*., 2008; Tenhaken, 2015). Actually, this role for pectins function has been proposed even in resurrection plants, which are capable to withstand many cycles of several water losses thanks

to modifications in pectins physicochemical properties as well as in their interactions with other cell wall components (Vicré *et al*., 1999, 2004; Moore *et al*., 2008). Similarly to ST application and to those results that we previously reported (Roig-Oliver *et al*., 2020*a*), higher pectins content was also detected under LT as compared to control conditions (Fig. 6), decreasing significantly after only 5 h upon recovery (Fig. 6). These results are of high relevance since most studies exploring the dynamism of cell wall modifications due to abiotic stresses focused on genetic and/or proteomic responses instead of on compositional analyses and did not address potential changes in time scales as short as those evaluated here (reviewed in Tenhaken, 2015). On the other hand, lignins –representing that cell wall component which is mainly found in secondary cell walls– also displayed important variations in their relative abundance (Figs. 2 and 6) which could be potentially associated to alterations in cell wall strength, flexibility, and extensibility (Wallace and Fry, 1994; Terrett and Dupree, 2019). Vincent *et al*. (2005) and Terzi *et al*. (2013) have previously reported that lignins content varied after days of water deficit stress imposition. However, as shown here, these modifications occurred more rapidly than expected and/or previously reported and were of especially large magnitude during gradual LT-Rec application –particularly, after 24 h of rewatering–, evidencing high responsiveness of lignins biosynthesis to different water availability treatments.

Some studies have recently demonstrated that changes in cell wall composition regulate photosynthesis –particularly, via g_m– testing mature leaves developed under well-watering conditions with subsequent acclimation to contrasting abiotic stresses (Clemente-Moreno *et al*., 2019; Roig-Oliver *et al*., 2020*b*,*c*). Although Roig-Oliver *et al*. (2020*b*) detected that changes in cellulose amounts were the main determinant of g_m responses in grapevines subjected to distinct environmental conditions for a month, species-specific adjustments emerged comparing *G. biloba* and *H. annuus* submitted to water deprivation for 40 days (Roig-Oliver *et al*., 2020*c*). However, in the present study we found that modifications in pectins absolute concentration was related to g_m modifications occurring during gradual ST (Fig. 3A), which agrees with the results reported by Clemente-Moreno *et al*. (2019) testing salt- and water-stressed tobacco for six days. Additionally, we observed for the first time that pectins were responsible of enhancements in the g_m/g_s ratio during gradual ST (Fig. 3B). Overall, we suggest that the application of ST treatments differing in their degree of water deprivation promoted pectins accumulation which could be accompanied by modifications in their physicochemical properties as well as in their interactions with other wall components, ultimately altering cell wall characteristics that affect the CO_2 diffusion such as porosity and thickness (Carpita *et al*.,

1979; Baron-Epel *et al*., 1988; Franková and Fry, 2013; Lundgren and Fleming, 2020; Flexas *et al*., 2021).

To the best of our knowledge, only the study by Roig-Oliver *et al*. (2020*a*) examined the effect of LT and LT-Rec testing mature leaves developed under water shortage conditions. However, since in that study the number of different treatments was small, correlations among parameters were tested pooling ST and LT data together. Nonetheless, the more accurate study presented here suggests that LT plants may behave differently than ST ones. Surprisingly, the detailed LT-Rec monitoring that we performed showed that larger g_s achieved upon recoveries were associated to enhancements in lignins amounts (Fig. 7). Whilst Kuusk *et al*. (2018) reported that lignins did not directly affect photosynthesis, Roig-Oliver *et al*. (2020*a*) found that they were almost significantly correlated with g_m combining data for sunflowers subjected to short- and long-term water deficit stresses followed by recoveries. Additionally, Coleman *et al*. (2008) observed that severe reductions of cell wall lignification in transgenic poplar trees were accompanied by significant g_s declines, leading to the suggestion that changes in guard cells' cell wall composition as well as in the functioning of specific wall enzymes could potentially affect stomatal movements (Gago *et al*., 2016) even under water deficit stress (Choi *et al*., 2011). Although more detailed studies are necessary to elucidate how specific changes in guard cells' cell wall composition promote g_s adjustments, our results indicate that even modifications in leaf cell wall composition have the potential to influence g_s.

In conclusion, this study shows photosynthesis responses and a highly dynamic cell wall main composition turnover in mature leaves of *H. annuus* subjected to different levels of water availability. During gradual ST, enhanced pectins content correlated with down-regulated g_m. In contrast, LT leaves did not show impaired g_m, and the detailed monitoring of LT-Rec reflected that photosynthesis was gradually increased from LT because of g_s and *ETR* enhancements. These photosynthetic changes occurring upon recovery were accompanied by fast modifications in cell wall main composition, with pectins and lignins being the fastest and most widely changing compounds, respectively. Particularly, after only 5 h of rewatering, pectins presented an even lower concentration than control, while lignins drastically increased (>200%) after 24 h, being associated with g_s increments. Consequently, given that the observed responses for most of the traits differed between gradual ST as well as during LT and LT-Rec, further studies testing other species subjected to more conditions are required to elucidate the relevance of modifications in cell wall composition distinctly affecting photosynthesis.

Acknowledgements

This work was supported by the project PGC2018-093824-B-C41 from Ministerio de Economía y Competitividad (MINECO, Spain) and the ERDF (FEDER). MR-O was supported by a predoctoral fellowship FPU16/01544 from MINECO. We thank Dr Mateu Fullana-Pericàs for his help with plants maintenance and Dr Cyril Douthe for technical support during gas exchange measurements.

Conflicts of interest

The authors declare no conflicts of interest.

Author contributions

MR-O, JB and JF designed the study; MR-O, PB and DN conducted the experiment; MR-O and JF performed the data analysis and MR-O wrote the first version of the manuscript with the contributions of all co-authors.

Data availability

The data supporting the findings of this study are available from the corresponding author, (Margalida Roig-Oliver) upon request.

References

Anderson CT, Kieber JJ. 2020. Dynamic construction, perception, and remodelling of plant cell walls. Annual Review of Plant Biology **71**, 39–69.

Baron-Epel O, Gharyal PK, Schindler M. 1988. Pectins as mediators of wall porosity in soybean cell. Planta **175**, 389–395.

Baskin TI. 2005. Anisotropic expansion of the plant cell wall. Annual Review of Cell and Developmental Biology **21**, 203–222.

Blumenkrantz N, Asboe-Hansen G. 1973. New method for quantitative determination of uronic acids. Analytical Biochemistry **54**, 484–489.

Caffall KH, Mohnen D. 2009. The structure, function, and biosynthesis of plant cell wall pectic polysaccharides. Carbohydrates Research **344**, 1879–1900.

Carpita NC, Sabularse D, Montezinos D, Delmer DP. 1979. Determination of the pore size of cell walls of living plant cells. Science **205**, 1144–1147.

Carpita NC, Gibeaut DM. 1993. Structural models of primary cell walls in flowering plants: consistency of molecular structure with the physical properties of the walls during growth. The Plant Journal **3**, 1–30.

Carriquí M, Nadal M, Clemente-Moreno MJ, Gago J, Miedes E, Flexas J. 2020. Cell wall composition strongly influences mesophyll conductance in gymnosperms. The Plant Journal **103**, 1372–1385.

Chaves MM, Pereira JS, Maroco J, Rodrigues ML, Ricardo CP, Osorio ML, Carvalho I, Faria T, Pinheiro C. 2002. How plants cope with water stress in the field. Photosynthesis and growth. Annals of Botany **89**, 907–916.

Chaves MM, Flexas J, Pinheiro C. 2009. Photosynthesis under drought and salt stress: regulation mechanisms from whole plant to cell. Annals of Botany **103**, 551–560.

Choi JY, Seo YS, Kim SJ, Kim WT, Shin JS. 2011. Constitutive expression of CaXTH3, a hot pepper xyloglucan endotransglucosylase/hydrolase, enhanced tolerance to salt and drought stresses without phenotypic defects in tomato plants (*Solanum lycopersicum* cv. Dotaerang). Plant Cell Reports **30**, 867–877.

Clemente-Moreno MJ, Gago J, Díaz-Vivancos P, Bernal A, Miedes E, Bresta P, Liakopoulos G, Fernie AR, Hernández JA, Flexas J. 2019. The apoplastic antioxidant system and altered cell wall dynamics influence mesophyll conductance and the rate of photosynthesis. The Plant Journal **99**, 1031–1046.

Coleman HD, Samuels AL, Guy RD, Mansfield S. 2008. Perturbed lignification impacts tree growth in hybrid poplar – A function of sink strength, vascular integrity, and photosynthetic assimilation. Plant Physiology **148**, 1229–1237.

Cosgrove DJ. 2005. Growth of the plant cell wall. Nature Reviews. Molecular Cell Biology **6**, 850–861.

Cosgrove DJ. 2018. Diffusive growth of plant cell walls. Plant Physiology **176**, 16–27.

De Lorenzo G, Ferrari S, Giovannoni M, Mattei B, Cervone F. 2019. Cell wall traits that influence plant development, immunity, and bioconversion. The Plant Journal **97**, 134–147.

Dubois M, Gilles KA, Hamilton JK, Rebers PA, Smith F. 1956. Colorimetric method for determination of sugars and related substances. Analytical Chemistry **28**, 350–356.

Fagerstedt KV, Saranpää P, Tapanila T, Immanen J, Alonso-Serra JA, Nieminen K. 2015. Determining the composition of lignins in different tissues of silver birch. Plants **4**, 183–195.

Flexas J, Bota J, Loreto F, Cornic G, Sharkey TD. 2004. Diffusive and metabolic limitations to photosynthesis under drought and salinity in C_3 plants. Plant Biology **6**, 269–279.

Flexas J, Clemente-Moreno MJ, Bota J, *et al*. 2021. Cell wall thickness and composition are involved in photosynthetic limitation. Journal of Experimental Botany, erab144.

Franková L, Fry SC. 2013. Biochemistry and physiological roles of enzymes that "cut and paste" plant cell-wall polysaccharides. Journal of Experimental Botany **64**, 3519–3550.

Gago J, Daloso DM, Figueroa CM, Flexas J, Fernie AR, Nikoloski Z. 2016. Relationships of leaf net photosynthesis, stomatal conductance, and mesophyll conductance to primary metabolism: a multispecies meta-analysis approach. Plant Physiology **171**, 265–279

Harley PC, Loreto F, Di Marco G, Sharkey TD. 1992. Theoretical considerations when estimating the mesophyll conductance to CO_2 flux by the analysis of the response of photosynthesis to CO_2. Plant Physiology **98**, 1429–1436.

Houston K, Tucker MR, Chowdhury J, Shirley N, Little A. 2016. The plant cell wall: a complex and dynamic structure as revealed by the responses of genes under stress conditions. Frontiers in Plant Science **7**, 984.

Iiyama K, Lam T, Stone BA. 1994. Covalent cross-links in the cell wall. Plant Physiology **104**, 315–320.

Kanevski I, Maliga P, Rhoades DF, Gutteridge S. 1999. Plastome engineering of ribulose-1,5-bisphosphatecarboxylase/oxygenase in tobacco to form a sunflower large subunit and tobacco small subunit hybrid. Plant Physiology **119**, 133–141.

Keegstra K. 2010. Plant Cell Walls. Future Perspective in Plant Biology **154**, 483–486.

Kent SS, Andre M, Cournac L, Farineau J. 1992. An integrated model for the determination of the Rubisco specificity factor, respiration in the light and other photosynthetic parameters of C_3 plants in situ. Plant Physiology and Biochemistry **30**, 625–637.

Kuusk V, Niinemets U, Valladares F. 2018. A major trade-off between structural and photosynthetic investments operative across plant and needle ages in three Mediterranean pines. Tree Physiology **38**, 543–557.

Lampugnani ER, Khan GA, Somssich M, Persson S. 2018. Building a plant cell wall at a glance. Journal of Cell Science **131(2)**: jcs207373.

Leucci MR, Lenucci MS, Piro G, Dalessandro G. 2008. Water stress and cell wall polysaccharides in the apical root zone of wheat cultivars varying in drought tolerance. Journal of Plant Physiology **165**, 1168–1180.

Lundgren MR, Fleming AJ. 2020. Cellular perspectives for improving mesophyll conductance. The Plant Journal **101**, 845–847.

Moore JP, Farrant JM, Driouich A. 2008. A role for pectin-associated arabinans in maintaining the flexibility of the plant cell wall during water deficit stress. Plant Signaling & Behavior **3**, 102–104.

Moreira-Vilar FC, Siqueira-Soares R, Finger-Teixeira A, de Oliveira DM, Ferro AP, da Rocha GJ, Ferrarese M, dos Santos WD, Ferrarese-Filho O. 2014. The acetyl bromide method is faster, simpler and presents best recovery of lignin in different herbaceous tissues than Klason and thioglycolic acid methods. PloS one **9**(10), e110000.

Nadal M, Roig-Oliver M, Bota J, Flexas J. 2020. Leaf age-dependent elastic adjustment and photosynthetic performance under drought stress in *Arbutus unedo* seedlings. Flora **271**, 151662.

Niinemets Ü, Cescatti A, Rodeghiero M, Tosens T. 2005. Leaf internal diffusion conductance limits photosynthesis more strongly in older leaves of Mediterranean evergreen broadleaved species. Plant, Cell & Environment **28**, 1552–1566.

Novaković L, Guo T, Bacic A, Sampathkumar A, Johnson K. 2018. Hitting the wall – Sensing and signaling pathways involved in plant cell wall remodeling in response to abiotic stress. Plants **7**(4):89.

Ochoa-Villarreal M, Aispuro-Hernández E, Vargas-Arispuro I, Martínez-Téllez MA. 2012. Plant cell wall polymers: function, structure and biological activity of their derivatives. In: De Souza Gomes A, ed. Polymerization. InTechOpen. doi: 10.5772/2750.

Panković D, Sakač Z, Kevrešan S, Plesničar M. 1999. Acclimation to long-term water deficit in the leaves of two sunflower hybrids: photosynthesis, electron transport and carbon metabolism. Journal of Experimental Botany **50**, 127–138.

Parry MAJ, Keys AJ, Gutteridge S. 1989. Variation in the specificity factor of C-3 higher plant Rubisco determined by the total consumption of ribulose-P-2. Journal of Experimental Botany **40**, 317–320.

Roig-Oliver M, Bresta P, Nadal M, Liakopoulos G, Nikolopoulos D, Karabourniotis G, Bota J, Flexas J. 2020*a*. Cell wall composition and thickness affect mesophyll conductance to CO_2 diffusion in *Helianthus annuus* under water deprivation. Journal of Experimental Botany **71**, 7198–7209.

Roig-Oliver M, Nadal M, Clemente-Moreno MJ, Bota J, Flexas J. 2020*b*. Cell wall components regulate photosynthesis and leaf water relations of *Vitis vinifera* cv. Grenache acclimated to contrasting environmental conditions. Journal of Plant Physiology **244**, 153084.

Roig-Oliver M, Nadal M, Bota J, Flexas J. 2020*c*. *Ginkgo Biloba* and *Helianthus annuus* show different strategies to adjust photosynthesis, leaf water relations, and cell wall composition under water deficit stress. Photosynthetica **58**, 1098–1106.

Rui Y, Dinneny JR. 2019. A wall with integrity: surveillance and maintenance of the plant cell wall under stress. New Phytologist **225**, 1428–1439.

Sahaf M, Sharon E. 2016. The rheology of a growing leaf: stress-induced changes in the mechanical properties of leaves. Journal of Experimental Botany **67**, 5509–5515.

Sharwood RE, von Caemmerer S, Maliga P, Whitney SM. 2008. The catalytic properties of hybrid rubisco comprising tobacco small and sunflower large subunits mirror the kinetically equivalent source rubiscos and can support tobacco growth. Plant Physiology **146**, 83–96.

Sweet WJ, Morrison JC, Labavitch J, Matthews MA. 1990. Altered synthesis and composition of cell wall of grape (*Vitis vinifera* L.) leaves during expansion and growth-inhibiting water deficits. Plant and Cell Physiology **31**, 407–414.

Tenhaken R. 2015. Cell wall remodeling under abiotic stress. Frontiers in Plant Science **5**, 771.

Terrett OM, Dupree P. 2019. Covalent interactions between lignin and hemicelluloses in plant secondary cell walls. Current Opinion in Biotechnology **56**, 97–104.

Terzi R, Guler NS, Calişkan N, Kadioğlu A. 2013. Lignification response for rolled leaves of *Ctenanthe setosa* under long-term drought stress. Turkish Journal of Biology **37**, 614–619.

Tucker MR, Lou H, Aubert MK, Wilkinson LG, Little A, Houston K, Pinto SC, Shirley NJ. 2018. Exploring the role of cell wall-related genes and polysaccharides during plant development. Plants **7**(2):42.

Valentini R, Epron D, Angelis PD, Matteucci G, Dreyer E. 1995. In situ estimation of net CO_2 assimilation, photosynthetic electron flow and photorespiration of Turkey oak (*Q. cerris* L.) leaves: diurnal cycles under different water supply. Plant, Cell & Environment **18**, 631–64.

Vicré M, Sherwin HW, Driouich A, Jaffer MA, Farrant JM. 1999. Cell wall characteristics and structure of hydrated and dry leaves of the resurrection plant *Craterostigma wilsmii*, a microscopical study. Journal of Plant Physiology **155**, 719–726.

Vicré M, Lerouxel O, Farrant J, Lerouge P, Driouich. 2004. Composition and desiccation-induced alterations of the cell wall in the resurrection plant *Craterostigma wilmsii*. Physiologia Plantarum **120**, 229–239.

Vincent D, Lapierre C, Pollet B, Cornic G, Negroni L, Zivy M. 2005. Water deficits affect caffeate *O*-methyltransferase, lignification, and related enzyme in maize leaves. A proteomic investigation. Plant Physiology **137**, 949–960.

Wallace G, Fry SC. 1994. Phenolic components of the plant cell wall. International Review of Cytology **151**, 229–267.

Weraduwage SM, Campos ML, Yoshida Y, *et al*. 2018. Molecular mechanisms affecting cell wall properties and leaf architecture. In: Adams III W, Terashima I, eds. The leaf: a platform for performing photosynthesis. Advances in Photosynthesis and Respiration (Including Bioenergy and Related Processes), vol 44. Springer, Cham.

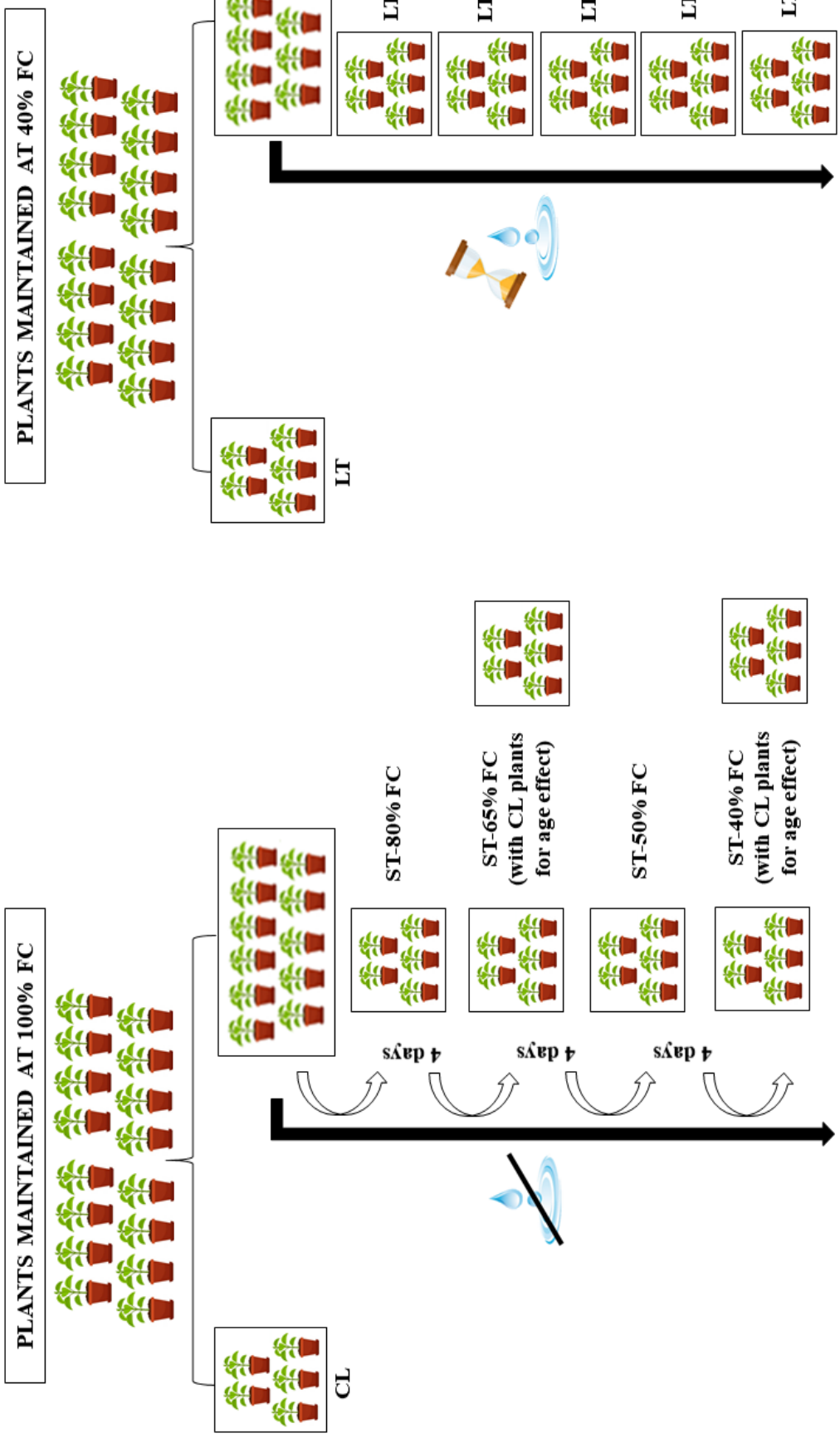

Fig. 1. Diagram representing the experimental design of the study. Specific growing conditions for all treatments are shown. *n*=5 in all treatments.

Table 1. Leaf water status of *H. annuus* plants gradually subjected to different conditions (CL: control; ST-80%, ST-65% FC, ST-50% FC and ST-40% FC: short-term water deficit stress at 80%, 65%, 50% and 40% FC, respectively). Mean values ± SE are shown for pre-dawn leaf water potential (Ψ_{pd}), midday leaf water potential (Ψ_{md}), leaf water potential (Ψ) and leaf relative water content (RWC). Different letters indicate significant difference (P<0.05) across all experimental conditions according to LSD test. n=5 in all cases.

Treatments	**Ψ_{pd}** (MPa)	**Ψ_{md}** (MPa)	**RWC** (%)
CL	-0.12 ± 0.01^{a}	-0.27 ± 0.06^{a}	84.54 ± 0.57^{a}
ST-80% FC	-0.20 ± 0.02^{ab}	-0.35 ± 0.05^{a}	81.17 ± 0.62^{a}
ST-65% FC	-0.29 ± 0.05^{b}	-0.36 ± 0.05^{a}	79.86 ± 0.68^{b}
ST-50% FC	-0.54 ± 0.07^{c}	-0.95 ± 0.08^{b}	81.99 ± 0.82^{ab}
ST-40% FC	-1.69 ± 0.07^{d}	-1.89 ± 0.11^{c}	44.59 ± 2.51^{c}

Table 2. Photosynthetic characterization of *H. annuus* plants gradually subjected to different conditions (CL: control; ST-80%, ST-65% FC, ST-50% FC and ST-40% FC: short-term water deficit stress at 80%, 65%, 50% and 40% FC, respectively). Mean values ± SE are shown for net CO_2 assimilation (A_N), stomatal conductance to gas diffusion (g_s), mesophyll conductance to CO_2 diffusion (g_m), water use efficiency (*WUE*), electron transport rate (*ETR*), and light mitochondrial non-photorespiratory respiration rate (R_{light}). Different letters indicate significant difference (P<0.05) across all experimental conditions according to LSD test. n=5 in all cases.

Treatments	A_N (μmol CO_2 m^{-2} s^{-1})	g_s (mol CO_2 m^{-2} s^{-1})	g_m (mol CO_2 m^{-2} s^{-1})	*WUE* (μmol CO_2 mol^{-1} H_2O)	*ETR* (μmol m^{-2} s^{-1})	R_{light} (μmol CO_2 m^{-2} s^{-1})
CL	13.92 ± 0.37^{a}	0.33 ± 0.06^{a}	0.18 ± 0.03^{a}	52.08 ± 1.82^{b}	101.74 ± 4.71^{a}	0.93 ± 0.15^{a}
ST-80% FC	10.61 ± 2.36^{a}	0.14 ± 0.03^{bc}	0.12 ± 0.02^{bc}	66.65 ± 5.13^{b}	103.61 ± 18.48^{a}	1.10 ± 0.18^{a}
ST-65% FC	9.69 ± 1.26^{a}	0.19 ± 0.04^{bc}	0.14 ± 0.01^{ab}	69.46 ± 6.90^{b}	90.57 ± 0.84^{a}	1.09 ± 0.09^{a}
ST-50% FC	11.37 ± 1.03^{a}	0.21 ± 0.04^{b}	0.13 ± 0.01^{abc}	69.11 ± 5.86^{b}	102.11 ± 2.29^{a}	0.78 ± 0.11^{a}
ST-40% FC	3.54 ± 0.51^{b}	0.06 ± 0.00^{c}	0.09 ± 0.00^{c}	110.28 ± 12.07^{a}	92.26 ± 18.96^{a}	0.88 ± 0.14^{a}

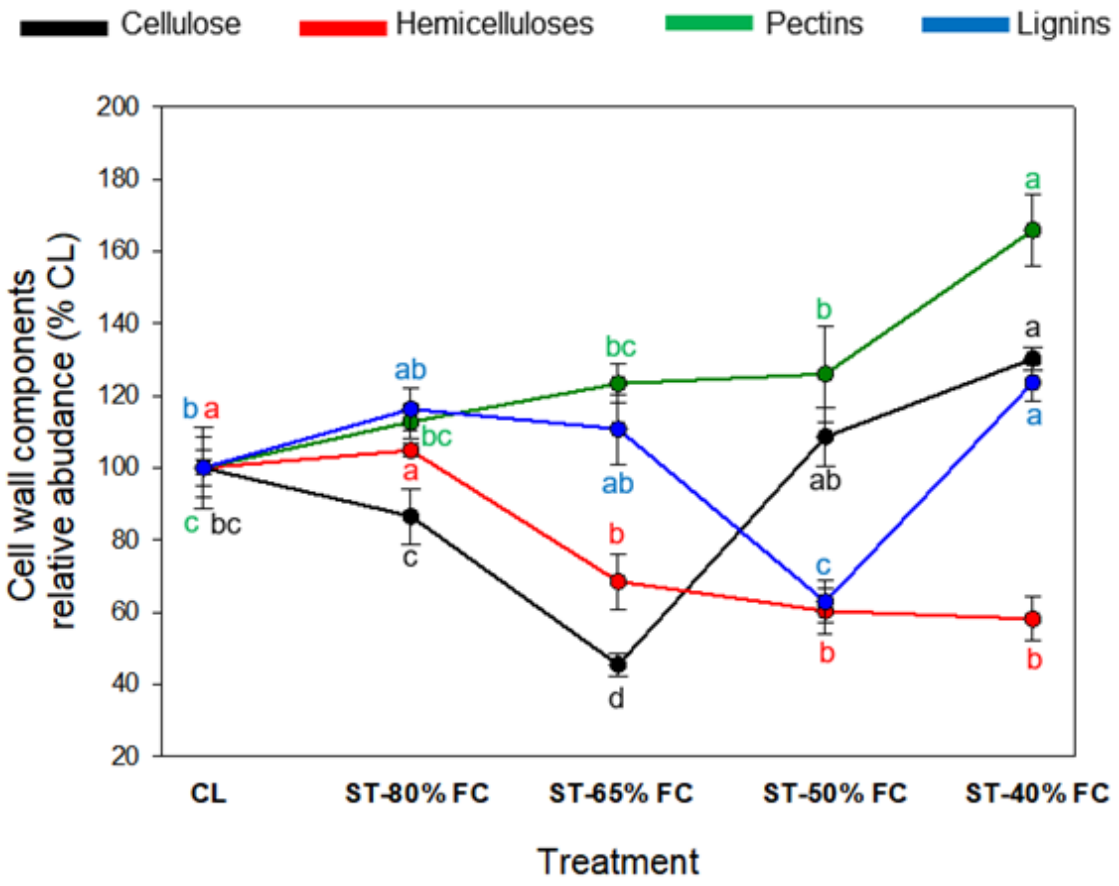

Fig. 2. Relative abundance of main cell wall components during gradual ST imposition. Different letters indicate significant difference (P<0.05) across all experimental conditions according to LSD test. n=5 (means ± SE).

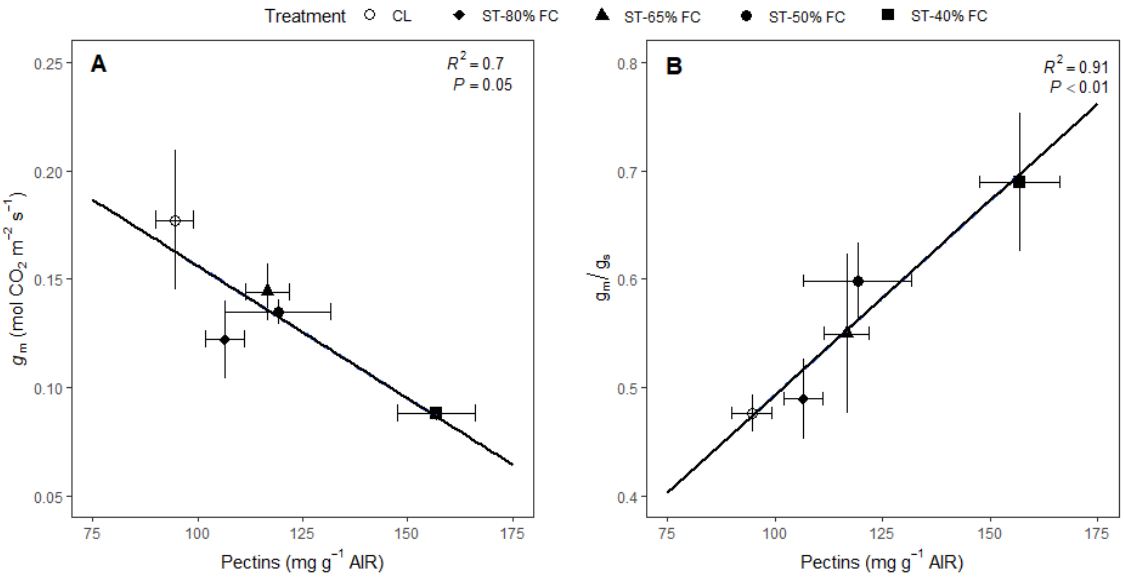

Fig. 3. Relationship between mesophyll conductance to CO_2 diffusion (g_m) and pectins content (A) and relationship between g_m/g_s ratio and pectins content (B) during gradual short-term water deficit stress imposition. n=5 (means ± SE).

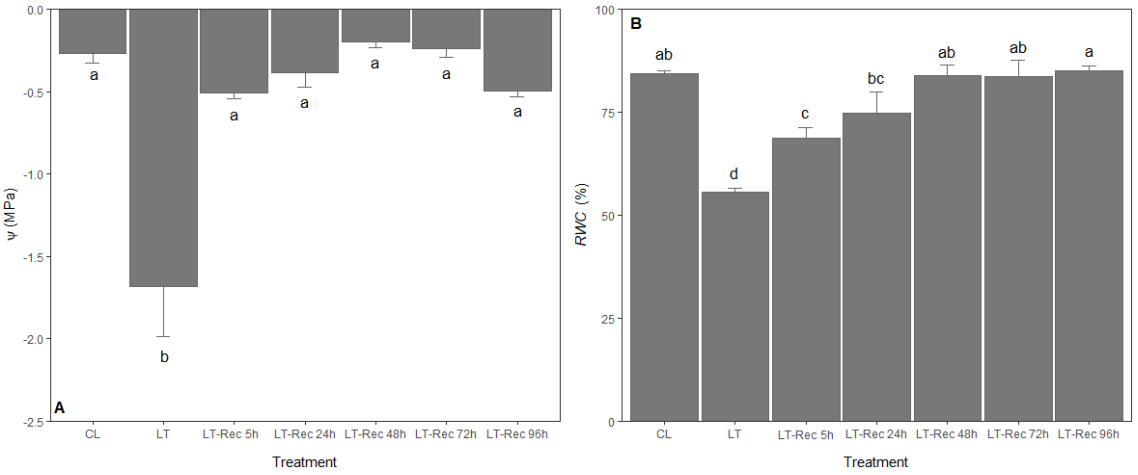

Fig. 4. Recovery of leaf water status of *H. annuus* plants (CL: control; LT: long-term water deficit stress; LT-Rec 5h, LT-Rec 24h, LT-Rec 48h, LT-Rec 72h and LT-Rec 96h: long-term water deficit stress followed by 5, 24, 48, 72 and 96 h of recovery, respectively). Mean values ± SE are shown for leaf water potential (Ψ) and leaf relative water content (RWC). Different letters indicate significant difference (P<0.05) across all experimental conditions according to LSD test. n=5 in all cases.

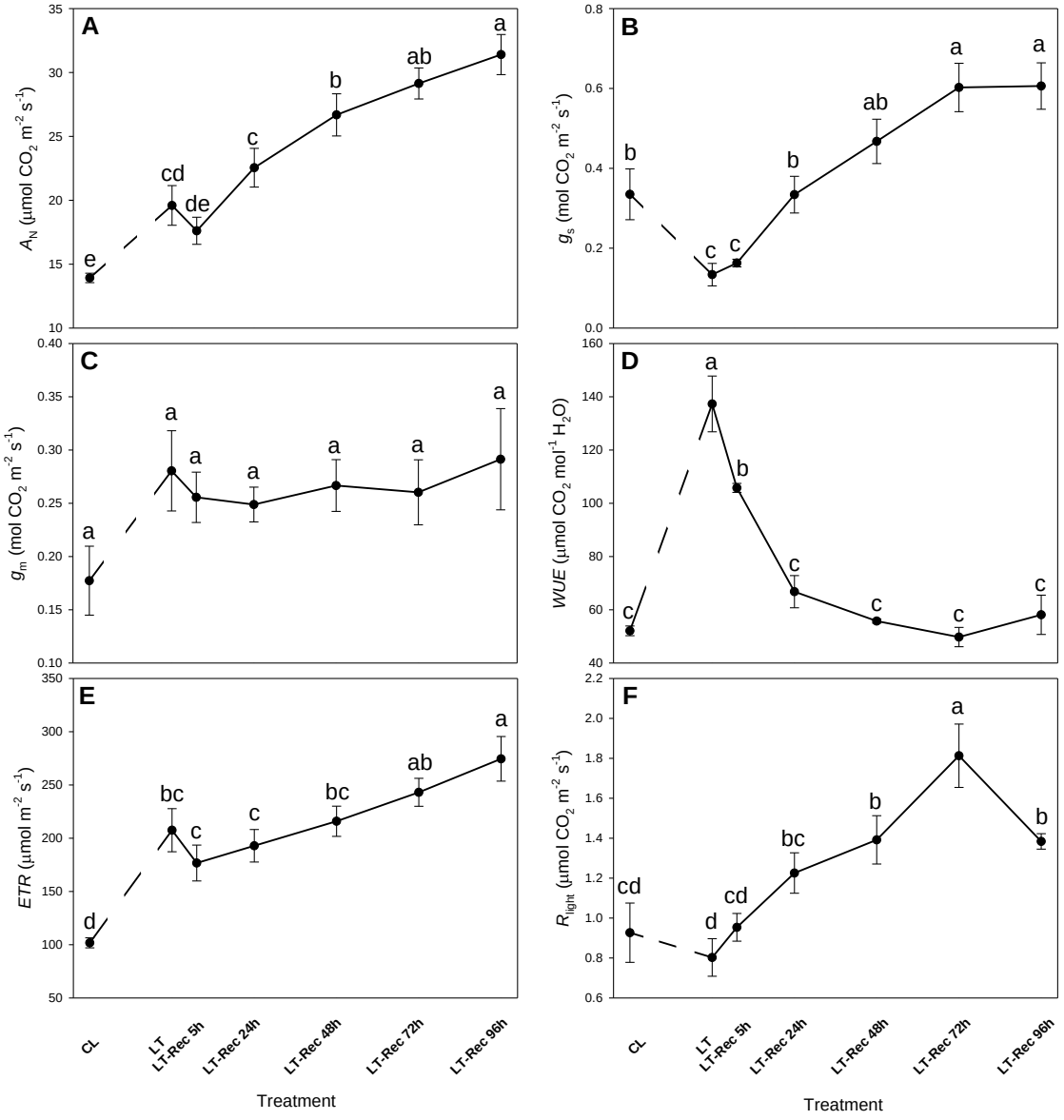

Fig. 5. Recovery of photosynthetic parameters in *H. annuus* plants (LT: long-term water deficit stress; LT-Rec 5h, LT-Rec 24h, LT-Rec 48h, LT-Rec 72h and LT-Rec 96h: long-term water deficit stress followed by 5, 24, 48, 72 and 96 h of recovery, respectively). Mean values ± SE are shown for (A) net CO_2 assimilation (A_N), (B) stomatal conductance to gas diffusion (g_s), (C) mesophyll conductance to CO_2 diffusion (g_m), (D) water use efficiency (*WUE*), (E) electron transport rate (*ETR*), and (F) light mitochondrial non-photorespiratory respiration rate (R_{light}). Different letters indicate significant difference (P<0.05) across all experimental conditions according to LSD test. n=5 in all cases.

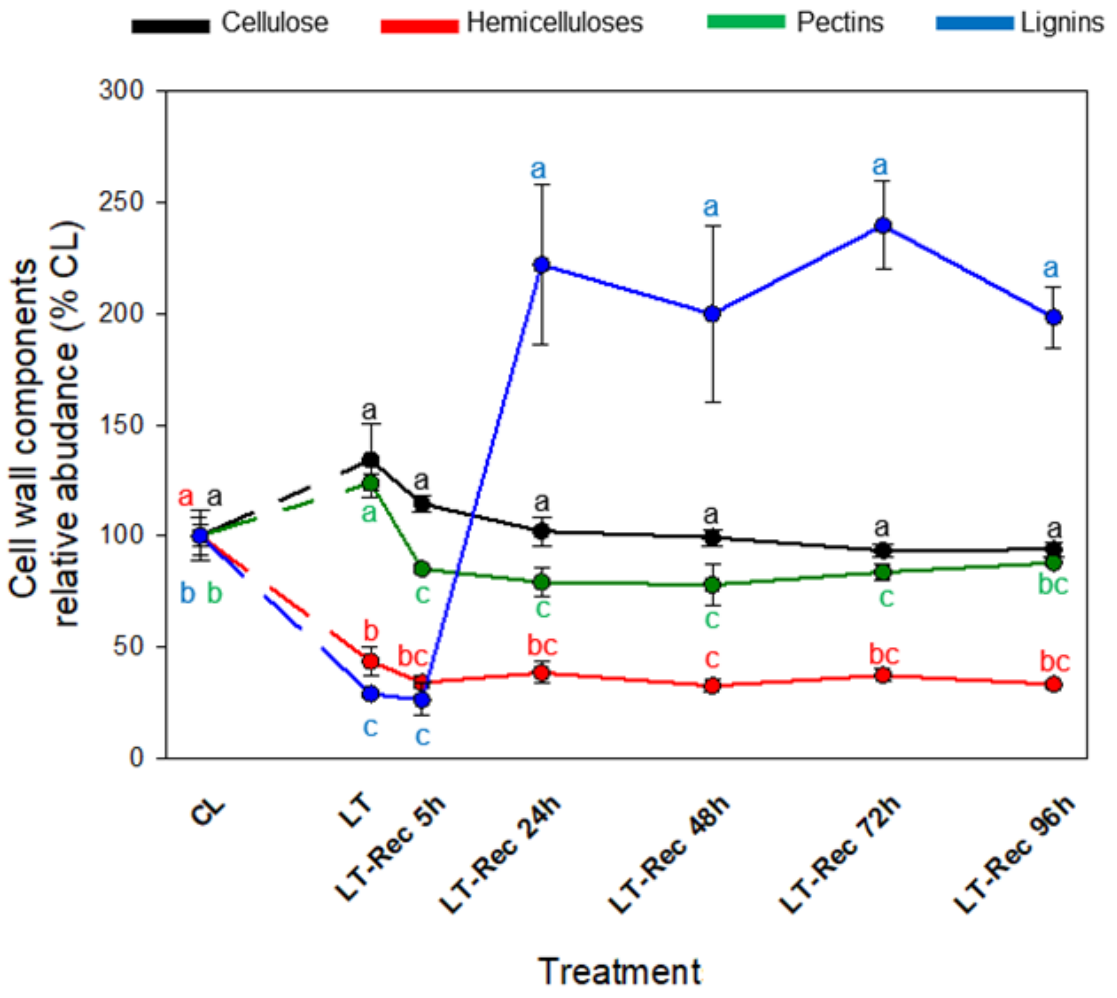

Fig. 6. Relative abundance of main cell wall components during LT and gradual LT-Rec imposition. Different letters indicate significant difference (P<0.05) across all experimental conditions according to LSD test. n=5 (means ± SE).

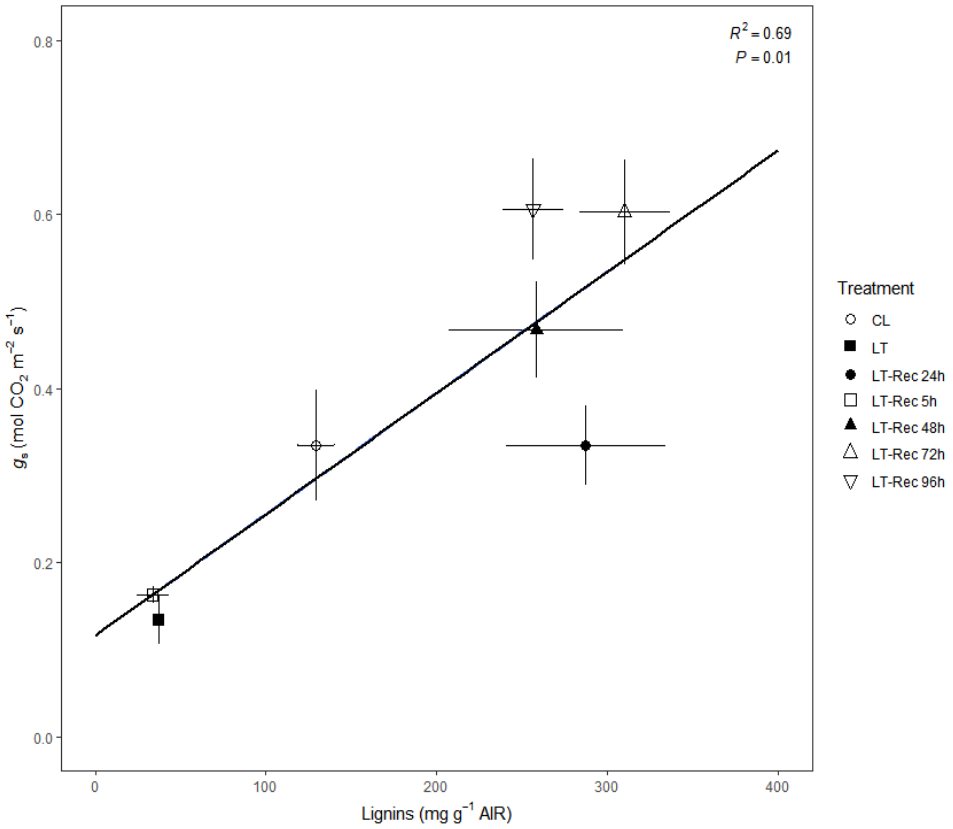

Fig. 7. Relationship between stomatal conductance to gas diffusion (g_s) and lignins content during the imposition of long-term water deficit stress and gradual long-term water deficit stress followed by recovery. n=5 (means ± SE).

Table S1. Leaf cell wall composition of *H. annuus* plants acclimated to different conditions (CL: control; ST-80%, ST-65% FC, ST-50% FC and ST-40% FC: short-term water deficit stress at 80%, 65%, 50% and 40% FC, respectively; LT: long-term water deficit stress; LT-Rec 5h, LT-Rec 24h, LT-Rec 48h, LT-Rec 72h and LT-Rec 96h: long-term water deficit stress followed by 5, 24, 48, 72 and 96 h of recovery, respectively). Mean values ± SE are shown for alcohol insoluble residue (AIR), cellulose, hemicelluloses, pectins and lignins contents.

Treatments	**AIR** ($g\ g^{-1}$ dry weight)	**Cellulose** ($mg\ g^{-1}$ AIR)	**Hemicelluloses** ($mg\ g^{-1}$ AIR)	**Pectins** ($mg\ g^{-1}$ AIR)	**Lignins** ($mg\ g^{-1}$ AIR)
CL	0.30 ± 0.07	127.94 ± 14.62	396.99 ± 8.02	94.52 ± 4.56	129.33 ± 10.76
ST-80% FC	0.28 ± 0.05	110.75 ± 9.86	416.19 ± 7.33	106.56 ± 4.55	150.42 ± 7.68
ST-65% FC	0.35 ± 0.01	58.13 ± 4.20	271.91 ± 30.57	116.59 ± 5.18	143.22 ± 12.50
ST-50% FC	0.28 ± 0.02	138.93 ± 10.18	239.49 ± 25.46	119.13 ± 12.59	81.27 ± 7.48
ST-40% FC	0.34 ± 0.03	166.62 ± 4.07	230.54 ± 24.54	156.78 ± 9.22	159.89 ± 6.88
LT	0.10 ± 0.01	171.60 ± 21.17	172.06 ± 25.90	116.92 ± 3.44	37.16 ± 2.06
LT-Rec 5h	0.14 ± 0.01	146.34 ± 4.28	134.29 ± 11.18	80.37 ± 1.94	33.73 ± 9.48
LT-Rec 24h	0.12 ± 0.00	130.56 ± 8.26	151.98 ± 18.90	74.74 ± 5.90	287.16 ± 46.58
LT-Rec 48h	0.21 ± 0.02	126.99 ± 4.81	128.52 ± 10.79	73.62 ± 9.10	258.50 ± 50.95
LT-Rec 72h	0.22 ± 0.03	119.40 ± 3.63	147.27 ± 11.31	79.04 ± 3.21	310.06 ± 25.90
LT-Rec 96h	0.27 ± 0.00	120.14 ± 4.36	131.23 ± 7.09	83.01 ± 1.45	256.52 ± 17.80

Table S2. Leaf water status of *H. annuus* plants gradually acclimated to different conditions (CL: control; ST-80%, ST-65% FC, ST-50% FC and ST-40% FC: short-term water deficit stress at 80%, 65%, 50% and 40% FC, respectively). Mean values ± SE are shown for direct values (i.e., the combined effect of age and water deficit stress) of pre-dawn leaf water potential (Ψ_{pd}), midday leaf water potential (Ψ_{md}), and leaf relative water content (RWC). Different letters indicate significant difference (P<0.05) across all experimental conditions according to LSD test. n=5 in all cases.

Treatments	**Ψ_{pd}** (MPa)	**Ψ_{md}** (MPa)	**RWC** (%)
CL	-0.12 ± 0.01[a]	-0.27 ± 0.06[a]	84.54 ± 0.57[a]
ST-80% FC	-0.15 ± 0.02[a]	-0.30 ± 0.05[a]	85.40 ± 1.13[a]
ST-65% FC	-0.26 ± 0.07[a]	-0.32 ± 0.07[a]	85.15 ± 0.62[a]
ST-50% FC	-0.45 ± 0.07[a]	-0.80 ± 0.08[b]	85.10 ± 0.51[a]
ST-40% FC	-1.58 ± 0.07[b]	-1.71 ± 0.11[c]	47.74 ± 1.49[b]

Table S3. Leaf cell wall composition of *H. annuus* plants gradually acclimated to different conditions (CL: control; ST-80%, ST-65% FC, ST-50% FC and ST-40% FC: short-term water deficit stress at 80%, 65%, 50% and 40% FC, respectively). Mean values ± SE are shown for direct values (i.e., the combined effect of age and water deficit stress) of alcohol insoluble residue (AIR), cellulose, hemicelluloses, pectins and lignins contents. Different letters indicate significant difference (P<0.05) across all experimental conditions according to LSD test. n=5 in all cases.

Treatments	AIR (g g^{-1} dry weight)	Cellulose (mg g^{-1} AIR)	Hemicelluloses (mg g^{-1} AIR)	Pectins (mg g^{-1} AIR)	Lignins (mg g^{-1} AIR)
CL	0.30 ± 0.07^{a}	127.94 ± 14.62^{bc}	396.99 ± 8.02^{a}	94.52 ± 4.56^{ab}	129.33 ± 10.76^{bc}
ST-80% FC	0.18 ± 0.05^{a}	137.34 ± 9.86^{b}	403.36 ± 7.33^{a}	88.17 ± 4.55^{b}	158.36 ± 7.68^{a}
ST-65% FC	0.17 ± 0.01^{a}	104.65 ± 4.20^{c}	249.46 ± 30.57^{b}	84.41 ± 5.18^{b}	126.93 ± 12.50^{bc}
ST-50% FC	0.16 ± 0.02^{a}	144.61 ± 10.18^{b}	265.40 ± 25.46^{b}	85.50 ± 12.59^{b}	106.75 ± 7.48^{c}
ST-40% FC	0.20 ± 0.03^{a}	173.44 ± 4.07^{a}	261.64 ± 24.38^{b}	116.43 ± 9.22^{a}	144.08 ± 6.88^{ab}

Table S4. Pearson correlation matrix of photosynthetic, leaf water status and cell wall parameters measured in *H. annuus* plants across ST experimental conditions. Values in italics and bold represent significant (P<0.05) and highly significant (P<0.01) correlations, respectively, between parameters. Same abbreviations as those used along the main text are employed except for (C+H)/P, which represents the (Cellulose+Hemicelluloses)/Pectins ratio.

	A_N	g_s	g_m	*WUE*	*ETR*	R_{light}	g_m/g_s	AIR	Cel.	Hemicel.	Pectins	(C+H)/P	Lignins	Ψ_{pd}	Ψ_{md}	RWC
A_N		*0.91*	*-0.91*	*0.91*	0.67	0.09	-0.86	-0.64	-0.37	0.61	***-0.96***	0.75	-0.53	*0.93*	0.87	*0.95*
g_s			***0.98***	-0.87	0.46	-0.08	-0.71	-0.42	-0.24	0.47	-0.84	0.67	-0.46	0.75	0.72	0.75
g_m				-0.91	0.36	0.10	-0.78	-0.32	-0.44	0.49	*-0.88*	0.64	-0.39	0.83	0.81	0.81
WUE					-0.60	-0.24	*0.91*	0.56	0.51	-0.65	***0.99***	-0.74	0.42	***-0.98***	*-0.94*	***-0.97***
ETR						-0.17	-0.57	***-0.99***	0.25	0.63	-0.63	0.76	-0.47	0.55	0.44	0.59
R_{light}							-0.54	0.27	-0.75	0.54	-0.33	0.25	0.65	0.42	0.56	0.26
g_m/g_s								0.48	0.53	***-0.88***	***0.96***	-0.87	0.04	*-0.94*	*-0.96*	-0.85
AIR									-0.27	-0.50	0.57	-0.65	0.59	-0.51	-0.38	-0.59
Cel.										-0.21	0.49	-0.04	-0.11	-0.63	-0.71	-0.57
Hemicel.											-0.77	*0.94*	0.24	0.69	0.73	0.56
Pectins												-0.82	0.30	***-0.98***	*-0.96*	*-0.94*
(C+H)/P													-0.01	0.71	0.70	0.61
Lignins														-0.31	-0.14	-0.50
Ψ_{pred}															***0.98***	***0.98***
Ψ_{mid}																*0.92*
RWC																

Table S5. Pearson correlation matrix of photosynthetic, leaf water status and cell wall parameters measured in *H. annuus* plants across LT and LT-Rec experimental conditions. Values in italics and bold represent significant (P<0.05) and highly significant (P<0.01) correlations, respectively, between parameters. Same abbreviations as those used along the main text are employed except for (C+H)/P, which represents the (Cellulose+Hemicelluloses)/Pectins ratio.

	A_N	g_s	g_m	*WUE*	*ETR*	R_{light}	g_m/g_s	AIR	Cel.	Hemicel.	Pectins	(C+H)/P	Lignins	Ψ	RWC
A_N		*0.82*	0.70	-0.42	***0.93***	*0.83*	-0.44	0.21	-0.52	-0.67	-0.45	-0.65	0.75	0.50	0.43
g_s			0.18	*-0.83*	0.57	***0.89***	*-0.84*	0.68	*-0.87*	-0.17	-0.55	-0.20	*0.86*	-0.65	*0.84*
g_m				0.33	***0.91***	0.30	0.30	-0.41	0.19	***-0.91***	-0.03	*-0.86*	0.15	-0.44	-0.29
WUE					-0.05	-0.69	***1***	*-0.78*	***0.97***	-0.21	0.69	-0.18	*-0.81*	*-0.88*	***-0.98***
ETR						0.63	-0.09	-0.08	-0.19	*-0.82*	-0.22	*-0.76*	0.49	0.16	0.09
R_{light}							-0.69	0.36	-0.75	-0.42	-0.64	-0.39	*0.87*	0.73	0.66
g_m/g_s								*-0.79*	***0.98***	-0.18	0.71	-0.16	*-0.80*	*-0.89*	***-0.99***
AIR									-0.74	0.50	-0.23	0.36	0.37	0.60	*0.86*
Cel.										-0.05	*0.77*	-0.10	*-0.82*	*-0.90*	***-0.97***
Hemicel.											0.36	***0.89***	-0.26	-0.79	0.20
Pectins												0.23	-0.68	***-0.98***	-0.67
(C+H)/P													-0.22	-0.10	0.14
Lignins														0.71	0.72
Ψ															*0.88*
RWC															

Ginkgo biloba and *Helianthus annuus* show different strategies to adjust photosynthesis, leaf water relations, and cell wall composition under water deficit stress

Margalida Roig-Oliver[1*+], Miquel Nadal[1*], Josefina Bota[1], Jaume Flexas[1]

[1]Research Group on Plant Biology under Mediterranean Conditions, Departament de Biologia, Universitat de les Illes Balears (UIB) – Agro-Environmental and Water Economics Institute (INAGEA). Carretera de Valldemossa Km 7.5, 07122 Palma, Illes Balears, Spain.

[*] Both authors contributed equally to this paper.

[+] Corresponding author.

Published in *Photosynthetica* in 2020.

DOI: 10.32615/ps.2020.063 PHOTOSYNTHETICA 58 (5): 1098-1106, 2020

Ginkgo biloba and *Helianthus annuus* show different strategies to adjust photosynthesis, leaf water relations, and cell wall composition under water deficit stress

M. ROIG-OLIVER[+,†], M. NADAL[†], J. BOTA, and J. FLEXAS

Research Group on Plant Biology under Mediterranean Conditions, Department of Biology, Universitat de les Illes Balears (UIB), INAGEA, Carretera de Valldemossa Km 7.5, 07122 Palma, Illes Balears, Spain

Abstract

Cell wall thickness (T_{cw}) determines photosynthesis and leaf elasticity. However, only a few studies in angiosperms addressed cell wall composition implication in regulating photosynthesis and leaf water relations through mesophyll conductance (g_m) and bulk modulus of elasticity (ε) adjustments, respectively. Thus, we compared the phylogenetically distant *Ginkgo biloba* L. and *Helianthus annuus* L. under control and water deprivation to study the relationship between changes in cell wall composition (cellulose, hemicelluloses, and pectins) with g_m and ε. Although no changes were found for T_{cw}, both species differently modified cell wall composition, resulting in different physiological consequences. *H. annuus* increased cellulose, hemicelluloses, and pectins in a similar proportion, maintaining ε. Additionally, it reduced photosynthesis due to stomatal closure. *G. biloba* did not decrease photosynthesis and largely increased hemicelluloses, leaf mass area, and leaf density, enhancing ε. Nonetheless, no association between cell wall composition and g_m was found in either of the two species.

Keywords: angiosperm; gymnosperm; leaf structure.

Introduction

Photosynthesis is a complex phenomenon that involves both diffusional and biochemical processes (Flexas *et al*. 2004, von Caemmerer *et al*. 2009). The diffusional process consists of the CO_2 pathway from the atmosphere to the substomatal cavity (stomatal conductance, g_s) across the mesophyll tissue (mesophyll conductance, g_m) until reaching its carboxylation sites at chloroplasts stroma, where biochemical processes occur (Flexas *et al*. 2004, Evans *et al*. 2009, von Caemmerer *et al*. 2009). Even though the mechanistic nature of g_m is not yet fully understood (Evans *et al*. 2009, Flexas *et al*. 2012), some studies have evidenced that leaf anatomical traits, particularly cell wall thickness (T_{cw}) and chloroplasts surface area exposed to intercellular air spaces per leaf area (S_c/S), are crucial to determine g_m across plants' phylogeny and in response to different environmental conditions (Terashima *et al*. 2001, Evans *et al*. 2009, Flexas *et al*. 2012, Tomás *et al*. 2013, Carriquí *et al*. 2015, 2019, 2020; Tosens *et al*. 2016, Onoda *et al*. 2017, Peguero-Pina *et al*. 2017, Veromann-Jürgenson *et al*. 2017). Hence, as thick cell walls limit g_m and, simultaneously, potentially increase cells rigidity (enhanced bulk modulus of elasticity, ε) (Tyree and Jarvis 1982, Peguero-Pina *et al*. 2017), a trade-off between g_m and net photosynthetic rate (P_N) with ε was demonstrated in a wide range of species under nonstress conditions (Nadal *et al*. 2018). Nonetheless, the mechanistic basis of ε and its intraspecific dynamics during plant's acclimation to changing environmental conditions are still poorly understood. Although Niinemets (2001) and Sack *et al*. (2003) proposed that leaf structure, particularly leaf mass

Received 29 June 2020, *accepted* 27 August 2020.
[+]Corresponding author; e-mail: margaroig93@gmail.com
Abbreviations: a_f – apoplastic water fraction; AIR – alcohol insoluble residue; C^*_{ft} – leaf area specific capacitance at full turgor; ETR – electron transport rate; f_{ias} – fraction of mesophyll intercellular air spaces; g_m – mesophyll conductance; g_s – stomatal conductance; LA – leaf area; LD – leaf density; LMA – leaf mass area; P_N – net photosynthetic rate; R_{light} – light respiration; RWC_{tlp} – relative water content at turgor loss point; S_c/S – chloroplasts surface area exposed to intercellular air spaces per leaf area; T_{cw} – cell wall thickness; WUE_i – intrinsic water-use efficiency; ε – bulk modulus of elasticity; π_o – osmotic potential at full turgor; Ψ_{tlp} – water potential at turgor loss point.
Acknowledgments: This work was supported by the project PGC2018-093824-B-C41 from the Ministerio de Ciencia, Innovación y Universidades (Spain), the ERDF, the UE and the AEI. M. Roig-Oliver and M. Nadal were supported by predoctoral fellowships FPU16/01544 and BES-2015-072578, respectively, from Ministerio de Economía y Competitividad (MINECO, Spain). Additionally, M. Nadal was co-supported by the European Social Fund. We thank Dr. María José Clemente-Moreno for her advice in results analyses and María Teresa Mínguez (Universitat de València, Secció de Microscòpia Electrònica – SCSIE) and Dr. Ferran Hierro (Universitat de les Illes Balears, Serveis Cientificotècnics) for technical support during microscopic analyses. We also thank Mr. Miquel Truyols and collaborators of the UIB Experimental Field and Glasshouses that are supported by the UIB Grant 15/2015.
[†]Both authors contributed equally to this paper.

area (LMA) and leaf density (LD), was the main driver of ε, more recent studies suggested that cell wall composition and properties could be also relevant for determining ε (Moore *et al*. 2008, Solecka *et al*. 2008, Álvarez-Arenas *et al*. 2018, Roig-Oliver *et al*. 2020).

The plant cell wall, a complex structure considered as a protective barrier to face those biotic and abiotic stresses occurring during plants' life, is mainly compounded by cellulose microfibrils (Carpita and Gibeaut 1993, Cosgrove 1997, 2005; Somerville *et al*. 2004, Sarkar *et al*. 2009, Tenhaken 2015, Houston *et al*. 2016, Rui and Dinnery 2019). Between those closely packed microfibrils, noncellulosic neutral sugars (hereafter 'hemicelluloses') are placed, conferring stability to the wall (Carpita and Gibeaut 1993, Cosgrove 1997, 2005; Somerville *et al*. 2004, Sarkar *et al*. 2009, Tenhaken 2015, Rui and Dinnery 2019). This cellulose–hemicelluloses network is embedded in a pectin matrix which has been proposed as a crucial structure to maintain an appropriate cell wall hydric status, especially during water deficit stress (Vicré *et al*. 2004, Cosgrove 2005, Leucci *et al*. 2008, Moore *et al*. 2008, 2013; Schiraldi *et al*. 2012, Le Gall *et al*. 2015, Houston *et al*. 2016). Additionally, the pectin matrix seems to be a key structure determining wall porosity and thickness (Somerville *et al*. 2004, Cosgrove 2005, Tenhaken 2015, Houston *et al*. 2016, Rui and Dinnery 2019), leading to the suggestion that it could influence CO_2 diffusion and, thus, photosynthesis. However, only a few studies directly focused on the relationship between modifications in cell wall components and g_m (Ellsworth *et al*. 2018, Clemente-Moreno *et al*. 2019, Carriquí *et al*. 2020, Roig-Oliver *et al*. 2020). Particularly, Ellsworth *et al*. (2018) provided first evidence on how g_m reductions could be attributed to anatomical alterations due to cell wall changes testing *cslf6* rice mutants. Then, Clemente-Moreno *et al*. (2019) specifically identified pectins and/or the ratio of hemicelluloses to pectins as main drivers of g_m changes in *Nicotiana sylvestris* subjected to different environmental conditions. The relationship between modified cell wall composition and g_m changes could not be exclusively attributed to pectins as Roig-Oliver *et al*. (2020) showed that only cellulose correlated with g_m in *Vitis vinifera* cv. Grenache acclimated to contrasting conditions. Nonetheless, at an interspecific level and under nonstress conditions, the ratio of pectins to cellulose and hemicelluloses determined g_m in conifers (Carriquí *et al*. 2020). Thus, it appears that the relationship between cell wall main composition and g_m could be species-dependent (Roig-Oliver *et al*. 2020) and could be attributed to specific growing conditions.

Some studies have determined that cell wall composition differs among plants belonging to different phylogenetic groups (Popper and Fry 2004, Sørensen *et al*. 2010, Popper *et al*. 2011, Bartels and Classen 2017). Additionally, several studies have characterized cell wall composition changes in different monocot and dicot species under stressing conditions (*see*, for instance, Sweet *et al*. 1990, Vicré *et al*. 1999, 2004; Leucci *et al*. 2008, Moore *et al*. 2008, Solecka *et al*. 2008, Suwa *et al*. 2010, Carvalho *et al*. 2013, Baldwin *et al*. 2014, Zheng *et al*. 2014, Clemente-Moreno *et al*. 2019, Roig-Oliver *et al*. 2020). However, to our knowledge, no information is known regarding stress-induced changes in cell wall properties in other plant groups. Moreover, how these differences in cell wall composition in response to stress could be linked to differed strategies to regulate photosynthesis, leaf water relations and anatomical adjustments remain to be elucidated. In the current study, we compared the gymnosperm living fossil *Ginkgo biloba* L. (Ginkgoaceae) and the herbaceous angiosperm *Helianthus annuus* L. (Asteraceae) acclimated to two different experimental conditions (well-watered, *i.e*., control, and water deficit stress) to induce changes in cell wall composition that could influence photosynthesis, anatomical and/or leaf water relations responses.

Materials and methods

Plant material and growth conditions: One-year-old *G. biloba* plants were acquired from a garden center in horticultural alveolus. *H. annuus* seeds were individually sewed in horticultural alveolus using a mixture of 3:1 substrate:perlite. All plants were placed in a growth chamber at 22°C with 12/12-h light/darkness daily fluctuation receiving PPDF of 200–300 µmol m^{-2} s^{-1}. Water irrigation was assessed every two days to ensure plant growth. Three weeks later, when all plants had fully-developed leaves, they were transplanted to 3-L pots containing a mixture of 2:2 and 3:1 substrate:perlite for *G. biloba* and *H. annuus*, respectively. At this moment, six individual replicates per species were randomly subjected to two treatments: control (*i.e.*, well-watered) and water deficit stress. Water-stressed plants were monitored every two days to maintain pots field capacity at 50% by replacing evapotranspired water and control plants were daily irrigated to keep field capacity at 100%. To identify the onset of new leaves during plants' acclimation to experimental conditions, already emerged ones were labeled. In both cases, treatments lasted 40 d. All measurements were performed in new fully developed leaves developed under control or water-stressed conditions.

Gas-exchange and fluorescence measurements: At the end of the treatments, simultaneous measurements of gas exchange and chlorophyll *a* fluorescence with an open infrared gas-exchange system coupled with a 2-cm^2 fluorescence chamber (*Li-6400-40XT*, *Li-Cor Inc*., Lincoln, NE, USA) were performed in one leaf per plant in each species and treatment. Measurements were performed at saturating PPFD (1,500 µmol m^{-2} s^{-1} for *H. annuus*; 1,250 µmol m^{-2} s^{-1} for *G. biloba*; 90/10% of red/blue light, respectively, in both cases), 25°C block temperature, and 300 µmol min^{-1} flow rate. All gas-exchange measurements were corrected for CO_2 leakage in the leaf-gasket interface (Flexas *et al*. 2007). P_N, g_s, substomatal CO_2 concentration (C_i), and photochemical yield of PSII (Φ_{PSII}) were recorded after steady-state conditions were reached (15–30 min) at ambient CO_2 concentration (C_a) of 400 µmol mol^{-1}. P_N–C_i response curves were then performed by changing C_a in 14 steps (3–4 min), from 50 to 1,500 µmol(CO_2) mol^{-1}(air). Light curves under nonphotorespiratory conditions (1%

O_2) were performed to determine light respiration (R_{light}) and the PPFD fraction harvested by PSII (s) (Yin *et al.* 2009, 2011; Bellasio *et al.* 2016). From previous parameters, the electron transport rate (ETR) was calculated as described in Bellasio *et al.* (2016). The CO_2-compensation point in the absence of respiration (Γ^*) for *G. biloba* and *H. annuus* were obtained from comparing P_N–C_i curves under ambient (21%) and low O_2 (1%) conditions as described in Bellasio *et al.* (2016). Finally, mesophyll conductance (g_m) was determined by the curve-fitting method (Sharkey 2016) using R_{light} as an input and the Rubisco kinetics (K_c, K_o) from tobacco (Bernacchi *et al.* 2002). The mean Γ^* value obtained for each species under well-watered conditions was used for water-stressed plants as *in vivo* methods are not reliable under stress (Galmés *et al.* 2006).

Anatomical measurements: A portion of the leaves used for gas-exchange measurements were cut in small pieces avoiding main foliar structures to be fixed under vacuum pressure using glutaraldehyde 4% and paraformaldehyde 2% prepared in 0.01 M phosphate buffer (pH 7.4). Samples were post-fixed in 2% buffered osmium tetroxide for two hours and dehydrated by a graded ethanol series. The obtained pieces were embedded in *LR White* resin (*London Resin Company*) and placed in an oven at 60°C for 48 h (Tomás *et al.* 2013).

Semi-fine (0.8 µm) and ultra-fine (90 nm) cross-sections were cut using an ultramicrotome (*Leica UC6*, Vienna, Austria). Semi-fine sections were dyed with 1% toluidine blue to be viewed in a bright field with an *Olympus BX60* optic microscope. Pictures at 200× magnifications were taken with a digital camera (*U-TVO.5XC*, *Olympus*, Tokyo, Japan) to determine the fraction of mesophyll intercellular air spaces (f_{ias}). Ultra-fine sections for transmission electron microscopy (*TEM H600*, *Hitachi*, Tokyo, Japan) were contrasted with uranyl acetate and lead citrate to obtain pictures at 1,500× and 30,000× magnifications. The chloroplasts surface area exposed to intercellular air spaces per leaf area (S_c/S) and the cell wall thickness (T_{cw}) were measured from ultra-fine images at 1,500× and 30,000× magnifications, respectively. A cell curvature correction factor was determined according to Thain (1983) making an average length/width ratio of five randomly selected cells from both palisade and spongy mesophyll types for S_c/S estimation. Final values for measured parameters were obtained as an average of ten measurements from randomly selected cell structures using the *ImageJ* software (Wayne Rasband/NIH, Bethesda, MD, USA).

Cell wall extraction and fractionation: The same leaves used for gas exchange and anatomy sampling were kept under dark conditions overnight to minimize starch content. The following morning, around 1 g of fresh leaf tissue per plant was cut in small pieces and they were placed in glass tubes containing absolute ethanol (1:10, w/v). They were boiled until bleached and cleaned twice with acetone > 95% obtaining the alcohol insoluble residue (AIR), an approximation of the total isolated cell wall content. After dried, samples were grounded and starch remains were removed with α-amylase digestion. Then, three analytical replicates of each AIR weighting 3 mg were taken to be hydrolyzed with 2 M trifluoroacetic acid for an hour at 121°C. They were centrifuged at 13,000 × g for the obtention of two phases: the supernatant (noncellulosic cell wall components) and the pellet (cellulosic cell wall components). Whilst the supernatant was kept at –20°C to quantify hemicelluloses and uronic acids (*i.e.*, pectins), the pellet was cleaned twice with distilled water and acetone > 95%. Once dried, pellets were hydrolyzed in 200 µl sulphuric acid 72% (w/v) for an hour, diluted to 6 ml with distilled water, and heated until degradation. Once cooled, the obtained aqueous samples were used for cellulose quantification. Cellulose and hemicellulose quantifications were determined following Dubois *et al.* (1956). Thus, samples absorbance was read at 490 nm and both sugars concentrations were estimated by interpolating sample values from a glucose calibration curve. Finally, pectin quantification was performed following Blumenkrantz and Asboe-Hansen (1973). Hence, samples absorbance was read at 520 nm and pectin content was calculated by interpolating sample values from a galacturonic acid calibration curve. In all cases, a *Multiskan Sky Microplate* spectrophotometer (*ThermoFisher Scientific*) was used.

Pressure-volume curves: A fully developed leaf neighboring the one used for the gas exchange was rehydrated with distilled water and kept under dark conditions overnight. The next morning, leaf water potential and mass were measured simultaneously to obtain pressure–volume (P–V) curves of, at least, ten points. Leaf water potential was determined using a pressure chamber (*Model 600D*, *PMS Instrument Company*, Albany, USA). From P–V curves analysis, leaf water potential at turgor loss point (Ψ_{tlp}), osmotic potential at full turgor (π_o), relative water content at turgor loss point (RWC_{tlp}), apoplastic water fraction (a_f), and leaf area specific capacitance at full turgor (C^*_{ft}) were obtained (Sack and Pasquet-Kok 2011). The bulk modulus of elasticity (ε) was determined using standardized major axes (SMA; Sack *et al.* 2003).

Leaf structure: The same leaves used for P–V curves were utilized to calculate the leaf mass area (LMA), the leaf density (LD), and the leaf area (LA) (Pérez-Harguindeguy *et al.* 2013). Leaves were rehydrated overnight and pictures of the LA including the petiole were analyzed with the *ImageJ* software (Wayne Rasband/NIH). Then, leaves were placed in an oven at 70°C for 72 h to obtain their dry mass. Leaf thickness was determined from six measurements per leaf avoiding main veins with a digital caliper. Thickness per area was used as a proxy to calculate LD.

Statistical analysis: Thompson test was performed to detect and eliminate outliers for all studied parameters. Two-way analysis of variance (*ANOVA*) and subsequent LSD test was assessed to determine significant (P<0.05) 'species' and 'treatments' effects and differences between groups, respectively. All analyses were performed using the *R* statistical software (*ver. 3.2.2*, *R Core Team*, Vienna, Austria).

Results

Physiological characterization: Under control conditions, *H. annuus* achieved the highest P_N and g_s [26.30 ± 2.27 µmol(CO_2) m^{-2} s^{-1} and 0.40 ± 0.06 mol(CO_2) m^{-2} s^{-1}, respectively], which were largely reduced under water deficit stress (Fig. 1*A*,*B*). Contrarily, *G. biloba* showed much lower assimilation under control conditions [7.91 ± 0.43 µmol(CO_2) m^{-2} s^{-1}], but neither P_N nor g_s experienced significant changes due to water deficit stress (Fig. 1*A*,*B*). Only *H. annuus* experienced an increase in WUE_i under water deficit stress conditions (Fig. 1*C*). Additionally, water-stressed *H. annuus* also showed reductions of both g_m (Fig. 1*D*) and ETR, the latter being also slightly reduced in *G. biloba* (Fig. 1*E*). Finally, R_{light} only revealed differences at P=0.053 for the 'treatments' effect as it slightly decreased under water deficit stress (Fig. 1*F*).

Leaf water relations: No treatment effect was detected for both Ψ_{tlp} and π_o (P=0.337 and 0.139, respectively) (Fig. 2*A*,*C*). Although RWC_{tlp} was maintained in *G. biloba*, it increased in water-stressed *H. annuus* in comparison to control (Fig. 2*B*). However, water-stressed *G. biloba* leaves were almost three-folds more rigid than control ones (61.17 ± 14.32 and 21.15 ± 2.36 MPa, respectively; Fig. 2*D*). Water deficit stress increased a_f and C^*_{ft} in *H. annuus* [0.55 ± 0.03 and 1.96 ± 0.25 mol(H_2O) m^{-2} MPa^{-1}, respectively], but no changes were detected in *G. biloba* (Fig. 2*E*,*F*).

Leaf structural and anatomical traits: Under water deficit stress conditions, *H. annuus* and *G. biloba* experienced an increase in both LMA and LD, being more marked in the latter species as they doubled control values (Table 1). An opposite pattern was found for LA, which decreased significantly under water deficit stress conditions, especially in *G. biloba* (Table 1). However, water deprivation did not significantly change anatomical parameters (*i.e.*, f_{ias}, S_c/S, and T_{cw}) in none of the two species (Table 1), which were evaluated from similar pictures to those from Fig. 3.

Leaf cell wall composition: Water deficit stress induced different changes in cell wall composition in the two species. *G. biloba* significantly increased hemicelluloses while slightly decreasing cellulose, with no changes in the total AIR and pectins (Table 2). Instead, *H. annuus* significantly enhanced the total AIR with also increased amounts of cellulose, hemicelluloses, and pectins in a similar proportion (Table 2).

Discussion

A classic response to water deficit stress involves a reduction of P_N associated to decreased leaf overall CO_2 diffusion (*i.e.*, g_s and g_m) (Chaves *et al.* 2002, 2008; Flexas *et al.* 2004, 2012; Nadal and Flexas 2019), which promotes enhanced WUE_i due to larger descents in g_s than in g_m (Flexas *et al.* 2013). In the current study, this pattern was only observed in water-stressed *H. annuus* plants as P_N, g_s, and g_m did not significantly decrease in *G. biloba*

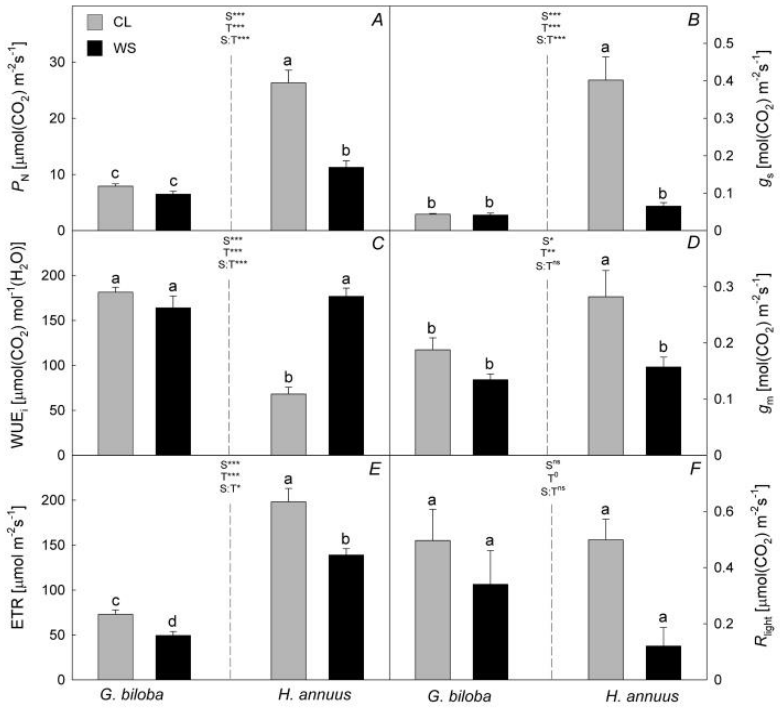

Fig. 1. (*A*) Net photosynthetic rate (P_N), (*B*) stomatal conductance (g_s), (*C*) intrinsic water-use efficiency (WUE_i), (*D*) mesophyll conductance (g_m), (*E*) electron transport rate (ETR), and (*F*) light respiration (R_{light}) in *Ginkgo biloba* and *Helianthus annuus* across conditions (CL – control, WS – water deficit stress). Species (S) and treatments (T) effects were quantified by two-way *ANOVA* and differences between groups were addressed by LSD test. *Different superscript letters* indicate significant differences. Significance: $^{***}P$<0.001; ** <0.01; * <0.05; ^{0} <0.1; ^{ns} >0.1. Values are means ± SE (n = 5–6).

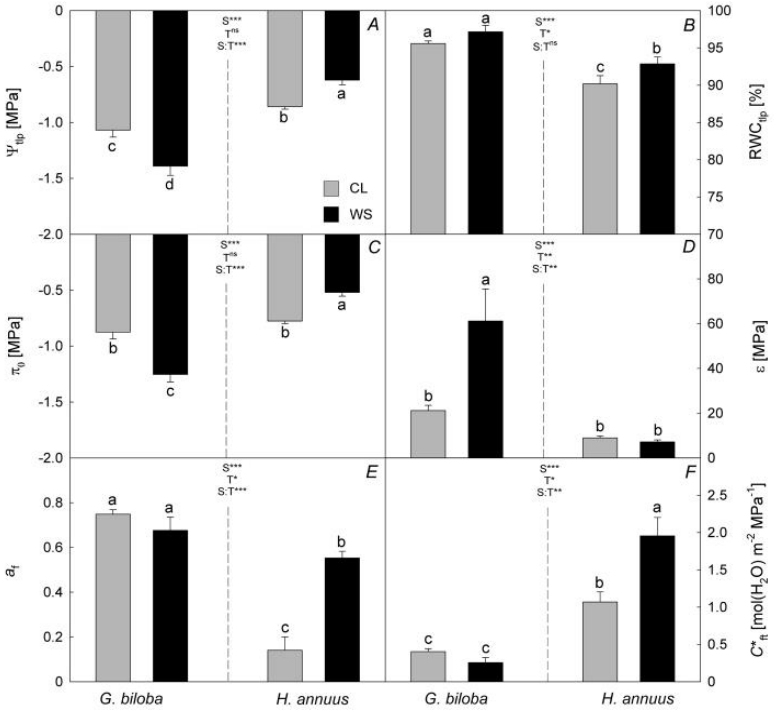

Fig. 2. (*A*) Water potential at turgor loss point (Ψ_{tlp}), (*B*) relative water content at turgor loss point (RWC_{tlp}), (*C*) osmotic potential at full turgor (π_o), (*D*) bulk modulus of elasticity (ε), (*E*) apoplastic water fraction (a_f), and (*F*) leaf area specific capacitance at full turgor (C^*_{ft}) in *Ginkgo biloba* and *Helianthus annuus* across conditions (CL – control, WS – water deficit stress). Species (S) and treatments (T) effects were quantified by two-way *ANOVA* and differences between groups were addressed by LSD test. Significance: $^{***}P<0.001$; $^{**}<0.01$; $^{*}<0.05$; $^{0}<0.1$; $^{ns}>0.1$. Values are means ± SE (n = 5–6).

Table 1. Leaf structural and anatomical traits of *Ginkgo biloba* and *Helianthus annuus* across conditions (CL – control, WS – water deficit stress). Average values ± SE are shown for leaf mass area (LMA), leaf density (LD), leaf area (LA), fraction of mesophyll intercellular air spaces (f_{ias}), chloroplasts surface area exposed to intercellular air spaces per leaf area (S_c/S) and cell wall thickness (T_{cw}). Species and treatments effects were quantified by two-way *ANOVA* and differences between groups were addressed by LSD test. *Different superscript letters* indicate significant differences. n = 5–6.

Species and treatments	LMA [g m^{-2}]	LD [g cm^{-3}]	LA [cm^2]	f_{ias} [%]	S_c/S [m^2 m^{-2}]	T_{cw} [µm]
G. biloba – CL	41.42 ± 1.22^{bc}	0.15 ± 0.00^{c}	85.36 ± 8.34^{a}	30.87 ± 3.95^{b}	9.73 ± 1.28^{b}	0.39 ± 0.01^{a}
G. biloba – WS	89.52 ± 5.16^{a}	0.31 ± 0.02^{a}	21.50 ± 9.61^{c}	25.13 ± 1.83^{b}	10.92 ± 1.13^{b}	0.42 ± 0.03^{a}
H. annuus – CL	32.04 ± 0.71^{c}	0.16 ± 0.00^{c}	40.79 ± 6.03^{b}	45.50 ± 2.39^{a}	17.24 ± 1.48^{a}	0.18 ± 0.01^{b}
H. annuus – WS	48.18 ± 1.02^{b}	0.22 ± 0.00^{b}	21.37 ± 0.49^{c}	40.31 ± 0.58^{a}	18.74 ± 1.59^{a}	0.16 ± 0.01^{b}
Species	< 0.001	0.010	0.016	< 0.001	< 0.001	< 0.001
Treatments	< 0.001	< 0.001	< 0.001	0.058	0.347	0.708
Species:Treatments	< 0.001	< 0.001	< 0.001	0.921	0.914	0.177

(Fig. 1*A–D*). Despite opposite patterns for photosynthesis regulation under water deficit stress, both species modified their foliage structure (*i.e.*, increased LMA and LD, *see* Table 1) as previously reported by Niinemets *et al.* (2009). Additionally, water deficit stress strongly limited leaf development in both species as LA decreased significantly (Table 1), which has been described as a typical response to water deficit stress (Chaves *et al.* 2002). However, although Chartzoulakis *et al.* (2002) and Hafez *et al.* (2020) reported modifications in leaf, mesophyll, and epidermis thicknesses as well as in f_{ias} testing avocado and barley, respectively, under water deprivation, Tomás *et al.* (2014) did not detect strong subcellular anatomical alterations in water-stressed grapevine cultivars. In fact, in the present study neither T_{cw} nor other subcellular anatomical traits classically affecting g_m were modified under water deficit stress (Table 1), suggesting that decreased g_m in water-stressed *H. annuus* might be due to other nonstudied characteristics (*e.g.*, aquaporins and/or carbonic anhydrases, *see* Pérez-Martín *et al.* 2014).

Poorter *et al.* (2009) proposed that LD could reflect, to some extent, the cell wall content per leaf. Nonetheless, AIR variations only followed the same pattern as LD in *H. annuus*, as the slight increase detected in *G. biloba*

was not significant (Table 2). AIR enhancement due to water deficit stress was previously detected in *N. sylvestris* (Clemente-Moreno *et al.* 2019) and *V. vinifera* (Roig-Oliver *et al.* 2020). Concerning specific cell wall main composition, it has been reported that variations in cellulose content may depend, for instance, on species, specific plant tissues, plants' age, and/or level of water deficit (Sweet *et al.* 1990, Zheng *et al.* 2014, Clemente-Moreno *et al.* 2019, Roig-Oliver *et al.* 2020). Thus, cellulose increased in *H. annuus* as previously shown for other species (Sweet *et al.* 1990, Clemente-Moreno *et al.* 2019, Roig-Oliver *et al.* 2020), but slightly decreased in *G. biloba* (Table 2). However, hemicelluloses have been found to either increase (Vicré *et al.* 1999), decrease (Sweet *et al.* 1990, Roig-Oliver *et al.* 2020), or stay constant (Clemente-Moreno *et al.* 2019) after exposure to water deficit stress. In our study, both species, especially *G. biloba*, presented increased amounts of hemicelluloses under water deficit stress (Table 2). Finally, pectins usually increase during water deficit because they play a key role in adjusting cell wall flexibility, thus, controlling cell wall hydric status (Sweet *et al.* 1990, Vicré *et al.* 1999, 2004; Cosgrove 2005, Leucci *et al.* 2008, Moore *et al.* 2008, 2013; Le Gall *et al.* 2015, Tenhaken 2015, Houston *et al.* 2016, Clemente-Moreno *et al.* 2019, Rui and Dinnery 2019, Roig-Oliver *et al.* 2020). However, in our study pectins were only enhanced in water-stressed *H. annuus* in a similar proportion to cellulose and hemicelluloses (Table 2). Additionally, the potential importance of pectins in determining ε adjustments has already been proposed (Moore *et al.* 2008, Solecka *et al.* 2008, Niinemets 2016) and Roig-Oliver *et al.* (2020) provided empirical evidence for this in grapevines. Surprisingly, *H. annuus* maintained ε under water deficit stress, while *G. biloba* – having kept pectins constant – drastically enhanced leaves rigidity once subjected to water deficit stress (Fig. 2*D*) as usually reported for other species (Bowman and Roberts 1985, Lo Gullo and Salleo 1988, Abrams 1990, Kloeppel *et al.* 1994). Although more experimental conditions should be tested to set concluding statements, our results suggest that ε adjustments in water-stressed *G. biloba* could be much more related to changes in leaf structure (*i.e.*, decreased LA and enhanced LMA and LD) and hemicelluloses rather than to other cell wall components. However, while increased ε and LD have been proposed to involve reductions in g_m (Niinemets *et al.* 2009, Nadal *et al.* 2018), *G. biloba* was able to maintain g_m at control values under water deficit stress conditions. Oppositely, *H. annuus* differed from the previous strategy as leaf structure and cell wall composition changes were not reflected in ε modifications. Instead, increased AIR, cellulose, hemicelluloses, and pectins under water deficit stress were reflected as an increase in a_f and C^*_{fi} (Fig. 2*E*, *F*).

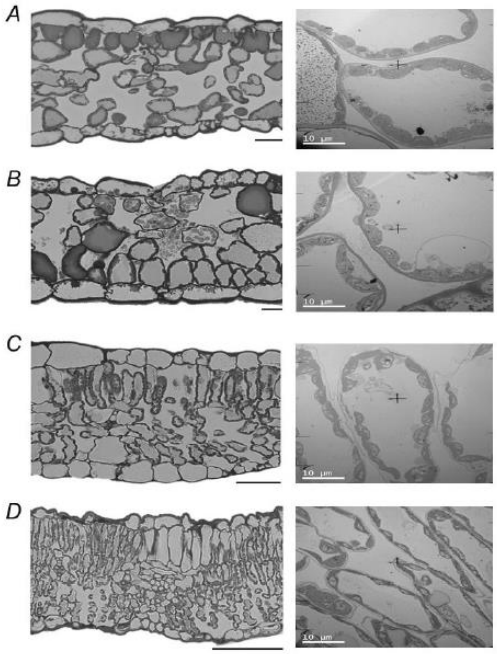

Fig. 3. Representative micrographs from semi-fine (*left*) and ultra-fine (*right*) cross-sections taken at 200× and at 1,500× magnifications, respectively, for *Ginkgo biloba* (*A*,*B*) and *Helianthus annuus* (*C*,*D*) under control and water deficit stress conditions, respectively. Black scale bars = 100 µm. Detailed quantitative analyses of studied anatomical parameters are reported in Table 1.

Table 2. Leaf cell wall composition of *Ginkgo biloba* and *Helianthus annuus* across conditions (CL – control, WS – water deficit stress). Average values ± SE are shown for alcohol insoluble residue (AIR), cellulose, hemicelluloses, and pectins contents. Species and treatments effects were quantified by two-way *ANOVA* and differences between groups were addressed by LSD test. *Different superscript letters* indicate significant differences. $n = 5–6$.

Species and treatments	AIR [g g^{-1}(DM)]	Cellulose [mg g^{-1}(AIR)]	Hemicelluloses [mg g^{-1}(AIR)]	Pectins [mg g^{-1}(AIR)]
G. biloba – CL	0.16 ± 0.03^{a}	125.2 ± 12.9^{a}	176.5 ± 18.3^{b}	71.27 ± 6.52^{b}
G. biloba – WS	0.19 ± 0.01^{a}	100.2 ± 11.6^{ab}	261.4 ± 30.6^{a}	79.60 ± 4.16^{b}
H. annuus – CL	0.09 ± 0.01^{b}	86.6 ± 8.8^{b}	79.7 ± 12.5^{c}	73.09 ± 12.09^{b}
H. annuus – WS	0.15 ± 0.01^{a}	128.7 ± 5.2^{a}	156.2 ± 9.8^{b}	103.68 ± 3.45^{a}
Species	< 0.001	0.622	< 0.001	0.051
Treatments	0.012	0.406	0.001	0.013
Species:Treatments	0.351	0.003	0.847	0.133

To our knowledge, this study provides the first evidence on how changes in cell wall main composition may play a role in determining different strategies to face water deficit stress by adjustments in ε and/or g_m testing species from different phylogenetic groups. Contrary to Clemente-Moreno *et al*. (2019) and Roig-Oliver *et al*. (2020), in the two species studied here, water deficit stress induced changes in cell wall composition that did not affect g_m and photosynthesis, but differently modified water relations parameters. Thus, more detailed studies using a larger range of species and treatments are required for a better understanding of how cell wall composition – including other cell wall compounds such as lignins and cell wall-bound phenolics – can involve changes in leaf physiology and to what extent these responses are species-dependent and/or change across plants phylogeny.

References

Abrams M.D.: Adaptations and responses to drought in *Quercus* species of North America. – Tree Physiol. **7***:* 227-238, 1990.

Álvarez-Arenas T.E.G., Sancho-Knapik D., Peguero-Pina J.J. *et al*.: Non-contact ultrasonic resonant spectroscopy resolves the elastic properties of layered plant tissues. – Appl. Phys. Lett. **113**: 253704, 2018.

Baldwin L., Domon J.M., Klimek J.F. *et al*.: Structural alteration of cell wall pectins accompanies pea development in response to cold. – Phytochemistry **104**: 37-47, 2014.

Bartels D., Classen B.: Structural investigations on arabino-galactan-proteins from a lycophyte and different monilophytes (ferns) in the evolutionary context. – Carbohydr. Polym. **172**: 342-351, 2017.

Bellasio C., Beerling D.J., Griffiths H.: An Excel tool for deriving key photosynthetic parameters from combined gas exchange and chlorophyll fluorescence: theory and practice. – Plant Cell Environ. **39**: 1180-1197, 2016.

Bernacchi C.J., Portis A.R., Nakano H. *et al*.: Temperature response of mesophyll conductance. Implications for the determination of Rubisco enzyme kinetics and for limitations to photosynthesis *in vivo*. – Plant Physiol. **130**: 1992-1998, 2002.

Blumenkrantz N., Asboe-Hansen G.: New method for quantitative determination of uronic acids. – Anal. Biochem. **54**: 484-489, 1973.

Bowman W.D.*,* Roberts S.W.: Seasonal changes in tissue elasticity in chaparral shrubs. – Physiol. Plantarum **65***:* 233-236*, 1985.*

Carpita N.C., Gibeaut D.M.: Structural models of primary cell walls in flowering plants: consistency of molecular structure with the physical properties of the walls during growth. – Plant J. **3**: 1-30, 1993.

Carriquí M., Cabrera H.M., Conesa M.À. *et al*.: Diffusional limitations explain the lower photosynthetic capacity of ferns as compared with angiosperms in a common garden study. – Plant Cell Environ. **38**: 448-460, 2015.

Carriquí M., Nadal M., Clemente-Moreno M.J. *et al*.: Cell wall composition strongly influences mesophyll conductance in gymnosperms. – Plant J. **103**: 1372-1385, 2020.

Carriquí M., Roig-Oliver M., Brodribb T.J. *et al*.: Anatomical constraints to nonstomatal diffusion conductance and photosynthesis in lycophytes and bryophytes. – New Phytol. **222**: 1256-1270, 2019.

Carvalho C.P., Hayashi A.H., Braga M.R., Nievola C.C.: Biochemical and anatomical responses related to the in vitro survival of the tropical bromeliad *Nidularium minutum* to low temperatures. – Plant Physiol. Bioch. **71**: 144-154, 2013.

Chartzoulakis K., Patakas A., Kofidis G. *et al*.: Water stress affects leaf anatomy, gas exchange, water relations and growth of two avocado cultivars. – Sci. Hortic.-Amsterdam **95**: 39-50, 2002.

Chaves M.M., Flexas J., Pinheiro C.: Photosynthesis under drought and salt stress: regulation mechanisms from whole plant to cell. – Ann. Bot.-London **103**: 551-560, 2008.

Chaves M.M., Pereira J.S., Maroco J. *et al*.: How plants cope with water stress in the field. Photosynthesis and Growth. – Ann. Bot.-London **89**: 907-916, 2002.

Clemente-Moreno M.J., Gago J., Díaz-Vivancos P. *et al*.: The apoplastic antioxidant system and altered cell wall dynamics influence mesophyll conductance and the rate of photosynthesis. – Plant J. **99**: 1031-1046, 2019.

Cosgrove D.J.: Relaxation in a high-stress environment: the molecular bases of extensible cell walls and cell enlargement. – Plant Cell **9**: 1031-1041, 1997.

Cosgrove D.J.: Growth of the plant cell wall. – Nat. Rev. Mol. Cell Biol. **6**: 850-861, 2005.

Dubois M., Gilles K.A., Hamilton J.K. *et al*.: Colorimetric method for determination of sugars and related substances. – Anal. Chem. **28**: 350-356, 1956.

Ellsworth P.V., Ellsworth P.Z., Koteyeva N.K., Cousins A.B.: Cell wall properties in *Oryza sativa* influence mesophyll CO_2 conductance. – New Phytol. **219**: 66-76, 2018.

Evans J.R., Kaldenhoff R., Genty B., Terashima I.: Resistance along the CO_2 diffusion pathway inside leaves. – J. Exp. Bot. **60**: 2235-2248, 2009.

Flexas J., Barbour M.M., Brendel O. *et al*.: Mesophyll conductance to CO_2: an unappreciated central player in photosynthesis. – Plant Sci. **193-194**: 70-84, 2012.

Flexas J., Bota J., Loreto F. *et al*.: Diffusive and metabolic limitations to photosynthesis under drought and salinity in C_3 plants. – Plant Biol. **6**: 269-279, 2004.

Flexas J., Díaz-Espejo A., Berry J.A. *et al*.: Analysis of leakage in IRGA's leaf chambers of open gas exchange systems: quantification and its effects in photosynthesis parameterization. – J. Exp. Bot. **58**: 1533-1543, 2007.

Flexas J., Niinemets Ü., Gallé A. *et al*.: Diffusional conductances to CO_2 as a target for increasing photosynthesis and photosynthetic water-use efficiency. – Photosynth. Res. **117**: 45-59, 2013.

Galmés J., Medrano H., Flexas J.: Acclimation of Rubisco specificity factor to drought in tobacco: discrepancies between *in vitro* and *in vivo* estimations. – J. Exp. Bot. **57**: 3659-3667, 2006.

Hafez Y., Attia K., Alamery S. *et al*.: Beneficial effects of biochar and chitosan on antioxidative capacity, osmolytes accumulation, and anatomical characters of water-stressed barley plants. – Agronomy **10**: 630, 2020.

Houston K., Tucker M.R., Chowdhury J. *et al*.: The plant cell wall: a complex and dynamic structure as revealed by the responses of genes under stress conditions. – Front. Plant Sci. **7**: 984, 2016.

Kloeppel B.D.*,* Kubiske M.E., Abrams *M.D.:* Seasonal tissue water relations of four successional Pennsylvania barrens species in open and understory environments. – Int. J. Plant Sci. **155***:* 73-79*, 1994.*

Le Gall H., Philippe F., Domon J.M. *et al*.: Cell wall metabolism in response to abiotic stress. – Plants-Basel **4**: 112-166, 2015.

Leucci M.R., Lenucci M.S., Piro G., Dalessandro G.: Water stress and cell wall polysaccharides in the apical root zone of wheat cultivars varying in drought tolerance. – J. Plant Physiol. **165**: 1168-1180, 2008.

Lo Gullo M.A., Salleo S.: Different strategies of drought

resistance in three Mediterranean sclerophyllous trees growing in the same environmental conditions. – New Phytol. **108**: 267-276, 1988.

Moore J.P., Farrant J.M., Driouich A.: A role for pectin-associated arabinans in maintaining the flexibility of the plant cell wall during water deficit stress. – Plant Signal. Behav. **3**: 102-104, 2008.

Moore J.P., Nguema-Ona E.E., Vicré-Gibouin M. *et al.*: Arabinose-rich polymers as an evolutionary strategy to plasticize resurrection plant cell walls against desiccation. – Planta **237**: 739-754, 2013.

Nadal M., Flexas J.: Variation in photosynthetic characteristics with growth form in a water-limited scenario: Implications for assimilation rated and water use efficiency in crops. – Agr. Water Manage. **216**: 457-472, 2019.

Nadal M., Flexas J., Gulías J.: Possible link between photosynthesis and leaf modulus of elasticity among vascular plants: A new player in leaf traits relationships? – Ecol. Lett. **21**: 1372-1379, 2018.

Niinemets Ü.: Global-scale climatic controls of leaf dry mass per area, density, and thickness in trees and shrubs. – Ecology **82**: 453-469, 2001.

Niinemets Ü.: Does the touch of cold make evergreen leaves tougher? – Tree Physiol. **36**: 267-272, 2016.

Niinemets Ü., Díaz-Espejo A., Flexas J. *et al.*: Role of mesophyll diffusion conductance in constraining potential photosynthetic productivity in the field. – J. Exp. Bot. **60**: 2249-2270, 2009.

Onoda Y., Wright I.J., Evans J.R. *et al.*: Physiological and structural tradeoffs underlying the leaf economics spectrum. – New Phytol. **214**: 1447-1463, 2017.

Peguero-Pina J.J., Sancho-Knapik D., Gil-Pelegrín E.: Ancient cell structural traits and photosynthesis in today's environment. – J. Exp. Bot. **68**: 1389-1392, 2017.

Pérez-Harguindeguy N., Díaz S., Garnier E. *et al.*: New handbook for standardised measurement of plant functional traits worldwide. – Aust. J. Bot. **61**: 167-234, 2013.

Pérez-Martín A., Michelazzo C., Torres-Ruiz J.M. *et al.*: Regulation of photosynthesis and stomatal and mesophyll conductance under water stress and recovery in olive trees: correlation with gene expression of carbonic anhydrase and aquaporins. – J. Exp. Bot. **65**: 3143-3156, 2014.

Poorter H., Niinemets Ü., Poorter L. *et al.*: Causes and consequences of variation in leaf mass per area (LMA): a meta-analysis. – New Phytol. **182**: 565-588, 2009.

Popper Z.A., Fry S.C.: Primary cell wall composition of pteridophytes and spermatophytes. – New Phytol. **164**: 165-174, 2004.

Popper Z.A., Michel G., Hervé C. *et al*: Evolution and diversity of plant cell walls: from algae to flowering plants. – Annu. Rev. Plant Biol. **62**: 567-590, 2011.

Roig-Oliver M., Nadal M., Clemente-Moreno M.J. *et al.*: Cell wall components regulate photosynthesis and leaf water relations of *Vitis vinifera* cv. Grenache acclimated to contrasting environmental conditions. – J. Plant Physiol. **244**: 153084, 2020.

Rui Y., Dinnery J.R.: A wall with integrity: surveillance and maintenance of the plant cell wall under stress. – New Phytol. **225**: 1428-1439, 2019.

Sack L., Cowan P.D., Jaikumar N., Holbrook N.M.: The 'hydrology' of leaves: coordination of structure and function in temperate woody species. – Plant Cell Environ. **26**: 1343-1356, 2003.

Sack L., Pasquet-Kok J.: Leaf pressure-volume curve parameters. PrometheusWiki contributors, 2011. *Available at*: http://prometheuswiki.org/tiki-pagehistory.php?page=Leaf%20pressure-volume%20curve%20parameters&preview=16.

Sarkar P., Bosneaga E., Auer M.: Plant cell walls throughout evolution: towards a molecular understanding of their design principles. – J. Exp. Bot. **60**: 3615-3635, 2009.

Schiraldi A., Fessas D., Signorelli M.: Water activity in biological systems – A review. – Pol. J. Food Nutr. Sci. **62**: 5-13, 2012.

Sharkey T.D.: What gas exchange data can tell us about photosynthesis. – Plant Cell Environ. **39**: 1161-1163, 2016.

Solecka D., Zebrowski J., Kacperska A.: Are pectins involved in cold acclimation and de-acclimation of winter oil-seed rape plants? – Ann. Bot.-London **101**: 521-530, 2008.

Somerville C., Bauer S., Brinistool G. *et al.*: Toward a systems approach to understanding plant cell walls. – Science **306**: 2206-2211, 2004.

Sørensen I., Domozych D., Williats W.G.T.: How have plant cell walls evolved? – Plant Physiol. **153**: 366-372, 2010.

Suwa R., Hakata H., Hara H. *et al.*: High temperature effects on photosynthate partitioning and sugar metabolism during ear expansion in maize (*Zea mays* L.) genotypes. – Plant Physiol. Bioch. **48**: 124-130, 2010.

Sweet W.J., Morrison J.C., Labavitch J.M., Matthews M.A.: Altered synthesis and composition of cell wall of grape (*Vitis vinifera* L.) leaves during expansion and growth inhibiting water deficit. – Plant Cell Physiol. **31**: 407-414, 1990.

Tenhaken R.: Cell wall remodelling under abiotic stress. – Front. Plant Sci. **5**: 771, 2015.

Terashima I., Miyazawa S.I., Hanba Y.T.: Why are sun leaves thicker than shade leaves? Consideration based on analyses of CO_2 diffusion in the leaf. – J. Plant Res. **114**: 93-105, 2001.

Thain J.F.: Curvature correlation factors in the measurements of cell surface areas in plant tissues. – J. Exp. Bot. **34**: 87-94, 1983.

Tomás M., Flexas J., Copolovici L. *et al.*: Importance of leaf anatomy in determining mesophyll diffusion conductance to CO_2 across species: quantitative limitations and scaling up by models. – J. Exp. Bot. **64**: 2269-2281, 2013.

Tomás M., Medrano H., Brugnoli E. *et al.*: Variability of mesophyll conductance in grapevine cultivars under water stress conditions in relation to leaf anatomy and water use efficiency. – Aust. J. Grape Wine Res. **20**: 272-280, 2014.

Tosens T., Nishida K., Gago J. *et al.*: The photosynthetic capacity in 35 ferns and fern allies: mesophyll CO_2 diffusion as a key trait. – New Phytol. **209**: 1576-1590, 2016.

Tyree M.T., Jarvis P.G.: Water in tissues and cells. – In: Lange O.L., Nobel P.S., Osmond C.B., Ziegler H. (ed.): Physiological Plant Ecology II. Encyclopedia of Plant Physiology (New Series). Pp. 35-77. Springer Verlag, Berlin-Heidelberg 1982.

Veromann-Jürgenson L.L., Tosens T., Laanisto L., Niinemets Ü.: Extremely thick cell walls and low mesophyll conductance: welcome to the world of ancient living! – J. Exp. Bot. **68**: 1639-1653, 2017.

Vicré M., Lerouxel O., Farrant J. *et al.*: Composition and desiccation-induced alterations of the cell wall in the resurrection plant *Craterostigma wilmsii*. – Physiol. Plantarum **120**: 229-239, 2004.

Vicré M., Sherwin H.W., Driouich A. *et al.*: Cell wall characteristics and structure of hydrated and dry leaves of the resurrection plant *Craterostigma wilmsii*, a microscopical study. – J. Plant Physiol. **155**: 719-726, 1999.

von Caemmerer S., Farquhar G., Berry J. *et al.*: Biochemical model of C_3 photosynthesis. – In: Laisk A., Nedbal L., Govindjee (ed.): Photosynthesis in Silico: Understanding Complexity from Molecules to Ecosystems. Pp. 209-230. Springer, Dordrecht 2009.

Yin X., Struik P.C., Romero P. *et al.*: Using combined measurements of gas exchange and chlorophyll fluorescence to estimate parameters of a biochemical C_3 photosynthesis

model: a critical appraisal and a new integrated approach applied to leaves in a wheat (*Triticum aestivum*) canopy. – Plant Cell Environ. **32**: 448-464, 2009.
Yin X., Sun Z., Struik P.C., Gu J.: Evaluating a new method to estimate the rate of leaf respiration in the light by analysis of combined gas exchange and chlorophyll fluorescence measurements. – J. Exp. Bot. **62**: 3489-3499, 2011.
Zheng M., Meng Y., Yang C. *et al*.: Protein expression changes during cotton fibre elongation in response to drought stress and recovery. – Proteomics **14**: 1776-1795, 2014.

Chapter 4

The importance of cell wall composition regulating species-specific responses to different environmental conditions

Cell wall components regulate photosynthesis and leaf water relations of *Vitis vinifera* cv. Grenache acclimated to contrasting environmental conditions

Margalida Roig-Oliver[1*], Miquel Nadal[1*], María José Clemente-Moreno[1+], Josefina Bota[1], Jaume Flexas[1]

[1]Research Group on Plant Biology under Mediterranean Conditions, Departament de Biologia, Universitat de les Illes Balears (UIB) – Agro-Environmental and Water Economics Institute (INAGEA). Carretera de Valldemossa Km 7.5, 07122 Palma, Illes Balears, Spain.

* Both authors contributed equally to this paper.

[+] Corresponding author.

Published in *Journal of Plant Physiology* in 2020.

Journal of Plant Physiology 244 (2020) 153084

Contents lists available at ScienceDirect

Journal of Plant Physiology

journal homepage: www.elsevier.com/locate/jplph

Cell wall components regulate photosynthesis and leaf water relations of *Vitis vinifera* cv. Grenache acclimated to contrasting environmental conditions

Margalida Roig-Oliver[1], Miquel Nadal[1], María José Clemente-Moreno*, Josefina Bota, Jaume Flexas

Research Group on Plant Biology under Mediterranean Conditions, Departament de Biologia, Universitat de les Illes Balears (UIB), INAGEA, Carretera de Valldemossa Km 7.5, 07122 Palma de Mallorca, Illes Balears, Spain

ARTICLE INFO

Keywords:
Cell wall composition
Bulk modulus of elasticity
Light-saturated CO_2 assimilation
Mesophyll conductance
Vitis vinifera cv. Grenache

ABSTRACT

Environmental conditions determine plants performance as they shape – among other key factors – leaf features and physiology. However, little is known regarding to the changes occurring in leaf cell wall composition during the acclimation to an environmental stress and, specially, if these changes have an impact on other leaf physiology aspects. In order to induce changes in photosynthesis, leaf water relations and cell wall main components (i.e., cellulose, hemicelluloses and pectins) and see how they co-vary, *Vitis vinifera* cv. Grenache was tested under four different conditions: (i) non-stress conditions (i.e., control, with high summer temperature and irradiance), (ii) growth chamber conditions, (iii) growth chamber under water stress and (iv) cold growth chamber. Plants developed in growth chambers decreased net CO_2 assimilation (A_N) and mesophyll conductance (g_m) compared to control. Although cold did not change the bulk modulus of elasticity (ε), it decreased in growth chamber conditions and water stress. Control treatment showed the highest values for photosynthetic parameters and ε as well as for leaf structural traits such as leaf mass area (*LMA*) and leaf density (*LD*). Whereas cellulose content correlated with photosynthetic parameters, particularly A_N and g_m, pectins and the amount of alcohol insoluble residue (*AIR*) – an approximation of the isolated cell wall fraction – correlated with leaf water parameters, specifically, ε. Although preliminary, our results suggest that cell wall modifications due to environmental acclimations can play a significant role in leaf physiology by affecting distinctly photosynthesis and water relations in a manner that might depend on environmental conditions.

1. Introduction

Photosynthesis is a complex phenomenon that encompasses diffusional and biochemical processes (Flexas et al., 2004; von Caemmerer et al., 2009v). Besides stomatal conductance (g_s) and biochemistry, the mesophyll conductance (g_m) is a key determinant establishing photosynthesis capacity amongst species and in response to different environmental conditions (Warren et al., 2004; Flexas et al., 2008, 2012; Nadal and Flexas, 2019). Mesophyll conductance represents the overall conductance of the pathway that CO_2 has to follow to reach its carboxylation sites in the chloroplast stroma from the substomatal cavity (Evans et al., 2009). Briefly, CO_2 has to diffuse from leaf mesophyll intercellular air spaces, entering into the liquid phase at the cell wall to then cross the lipidic plasma membrane, aqueous cytosol, chloroplast lipidic double membrane, until reaching Rubisco in the aqueous phase at chloroplast stroma. Along these steps, anatomical parameters such as the chloroplast distribution and the cell wall thickness have been identified as the most important limitations to CO_2 diffusion through the mesophyll (Terashima et al., 2001; Evans et al., 2009; Flexas et al., 2012; Tomás et al., 2013; Carriquí et al., 2015;

Abbreviations: A_N, light-saturated CO_2 assimilation; g_s, stomatal conductance; WUE_i, intrinsic water use efficiency; g_m, mesophyll conductance; *ETR*, electron transport rate; R_{light}, light respiration; Ψ_{tlp}, water potential at turgor loss point; RWC_{tlp}, relative water content at turgor loss point; π_o, osmotic potential at full turgor; ε, bulk modulus of elasticity; a_f, apoplastic water fraction; C^*_{ft}, leaf area specific capacitance at full turgor; *LMA*, leaf mass area; *LD*, leaf density; *AIR*, alcohol insoluble residue; *UA*, uronic acids

* Corresponding author at: Universitat de les Illes Balears (UIB), Carretera de Valldemossa, km 7.5, 07122 Palma de Mallorca, Illes Balears, Spain.
E-mail addresses: marga_9_3@hotmail.com (M. Roig-Oliver), miquel.nadal@uib.cat (M. Nadal), esojariam2@gmail.com (M.J. Clemente-Moreno), j.bota@uib.es (J. Bota), jaume.flexas@uib.es (J. Flexas).

[1] Both authors contributed equally to this paper.

https://doi.org/10.1016/j.jplph.2019.153084
Received 29 July 2019; Received in revised form 18 November 2019; Accepted 21 November 2019
Available online 26 November 2019

Tosens et al., 2016; Onoda et al., 2017; Peguero-Pina et al., 2017).

Because CO_2 and water share a significant fraction of this pathway in leaves and, particularly, the cell wall is thought to play a major role in leaf water relations (e.g., by determining the leaf bulk modulus of elasticity (ε; Tyree and Jarvis, 1982), it has been speculated that g_m should somehow coordinate with leaf hydraulics and water relations (Ferrio et al., 2012; Flexas et al., 2012, 2013; Pou et al., 2012). Recently, Nadal et al. (2018) experimentally reported the existence of a trade-off between g_m and A_n with ε in stress absence establishing a potential link between photosynthesis and leaf water relations properties. However, although ε varies widely across species (Bartlett et al., 2012; Nadal et al., 2018), its mechanical basis, intraspecific dynamics and/or acclimation to environmental conditions are not fully understood. Leaf structure has been proposed as its main driver as some studies found interspecific relationships between ε and both leaf mass area (*LMA*) and leaf density (*LD*) (Niinemets, 2001; Sack et al., 2003). Indeed, evergreen and sclerophyllous species, with high structural investments, usually present robust and rigid leaves with high ε (Salleo and Lo Gullo, 1990; Bartlett et al., 2012) possibly due to a large biomass investment in epidermis, cuticle and palisade tissue as well as in cell walls (Onoda et al., 2015; Álvarez-Arenas et al., 2018). Although it has been reported that elastic adjustments during water stress are usually mild to none (Bartlett et al., 2012) or species–dependent (Lo Gullo and Salleo, 1988), cold acclimation does often impose strong elastic adjustments. For instance, under winter conditions, ε increased in evergreen shrubs to prevent leaf injury from ice formation at freezing temperatures (Scholz et al., 2012; Zhang et al., 2016) and promoted freezing avoidance by enhancing super-cooling (Arias et al., 2015). Although the structural and/or biochemical changes driving elastic adjustments under cold stress are still largely unknown, cell wall composition has been suggested to play a key role in this issue (Niinemets, 2016). Hence, the relationship between ε and g_m suggests a common mechanistic basis that may involve cell wall characteristics (Nadal et al., 2018).

The cell wall has been suggested as a main structure determining ε and its adjustments in response to environmental changes (Moore et al., 2008; Solecka et al., 2008; Baldwin et al., 2014; Le Gall et al., 2015). Additionally, also g_m has been recently suggested to be modulated through modifications in the quantity and organisation of cell wall components (Ellsworth et al., 2018; Clemente-Moreno et al., 2019; Gago et al., 2019). The cell wall can be considered as a protective barrier mostly composed by cellulose microfibrils and non-cellulosic neutral polysaccharides (hereafter hemicelluloses) embedded in a pectin matrix containing cross-linked structural proteins (Cosgrove, 2005). By chemical and physical reorganisation of its components, the cell wall determines the shape and the size of the cells according to environmental conditions, which leads to different states of tissue and organ differentiation (Leucci et al., 2008; Moore et al., 2008; Solecka et al., 2008; Carvalho et al., 2013; Baldwin et al., 2014; Le Gall et al., 2015). Some studies testing different species have determined that cold (Solecka et al., 2008; Carvalho et al., 2013; Baldwin et al., 2014), water deprivation (Leucci et al., 2008; Moore et al., 2008, 2013; Clemente-Moreno et al., 2019) and heat and high sunlight irradiance (Suwa et al., 2010; Lima et al., 2013) alter sugars and pectin metabolism leading to modifications in cell wall components concentration, even in already fully-developed leaves.

Although Ellsworth et al. (2018) and Clemente-Moreno et al. (2019) have recently suggested the potential importance of cell wall composition in modulating g_m and thus photosynthesis, there is still scarce empirical evidence on this aspect. Thus, the main hypothesis of the present study is that cell wall modifications due to acclimation to different environmental conditions could be related to the regulation of photosynthetic and leaf water relations parameters, being g_m and ε key linking traits. Hence, we tested the woody *Vitis vinifera* cv. Grenache acclimated under different growing conditions in order to explore possible relationships between modifications in cell wall components and photosynthesis and leaf water relations.

2. Material and methods

2.1. Plant material and growth conditions

Twenty-four canes of *V. vinifera* cv. Grenache measuring ~30 cm were collected from mature vines of the experimental vineyard at the Universitat de les Illes Balears (Mallorca, Illes Balears). They contained, at least, two vegetative buds and a reproductive one. To ensure rooting, canes were disinfected with 2.5 g l^{-1} antifungal solution for 10 min and placed in 2 g l^{-1} indole butyric acid (IBA)/ethanol 50 % solution for 20 s. Canes were sewed individually in horticultural alveolus using a mixture of 3:1 substratum:perlite and they were set in a rooting chamber at 21 °C and 70 % humidity. Four months later, when each plant had more than 10 developed leaves, they were transplanted to 3 l pots containing the same mixture. These leaves were labelled to identify the onset of new ones during plants acclimation to different conditions.

Six individual replicates per treatment were subjected to four different growing conditions. Control treatment (i) consisted in letting the plants under summer outside conditions, receiving high temperatures and irradiance of typical Mediterranean summer. Specifically, the treatment was established during August 2018, when environmental conditions were characterized by mean maximum irradiance of 1535 μmol m^{-2} s^{-1} PPFD, mean temperature of 26.4 °C (20/33 °C min/max) and mean air relative humidity of 68.5 %. Two other treatments were evaluated in a growth chamber at 22 °C and 12/12 h light/darkness daily fluctuation: (ii) growth chamber conditions and (iii) water stress conditions. For cold treatment (iv), plants were placed in a growth chamber at 13 °C and 12/12 h light/darkness daily fluctuation. The plants belonging to these three treatments received an irradiance of 200–300 μmol m^{-2} s^{-1} PPFD. While water-stressed plants were monitored every two days to maintain pots at 50 % field capacity by replacing evapo-transpired water, plants belonging to other treatments were kept under well-watered conditions by daily irrigation at field capacity. In all cases, treatments lasted one month.

2.2. Gas exchange and fluorescence measurements

One month after establishing each treatment, simultaneous measurements of gas exchange and chlorophyll *a* fluorescence using an infrared gas analyser (IRGA) LI-6400XTR coupled with the fluorometer (Li-6400-40; Li-Cor Inc., Lincoln, NE, USA) were performed. For all measurements, new fully-expanded leaves unfolded after treatments imposition were used, except for the water-stressed as no new leaves emerged. In this case, the youngest fully-expanded leaf was used. Cold plants were moved to growth chamber at 22 °C when measured. Leaves were clamped into a 2 cm^2 cuvette. In all cases, leaf temperature was fixed at 25 °C and the vapour pressure deficit (VPD) was kept at around 1.5 kPa. Leaf steady-state conditions were induced at saturating photosynthetic photon flux density (PPFD 1250 μmol m^{-2} s^{-1}, 90-10 % red-blue light) and 400 μmol CO_2 mol^{-1} air. The flow rate within the chamber was kept at 300 mmol air min^{-1}. After 30 min, when steady-state conditions were reached, light-saturated CO_2 assimilation (A_N), stomatal conductance to CO_2 (g_s), CO_2 concentration at the sub-stomatal cavity (C_i) and photochemical yield of photosystem II (Φ_{PSII}) were recorded. The electron transport rate (*ETR*) was estimated by performing light curves under non-photorespiratory conditions provided by an atmosphere containing 1 % O_2 (Yin et al., 2009; Martins et al., 2013). The light respiration (R_{light}) was measured after leaving plants under darkness conditions for at least 20 min. Values for CO_2 compensation point in the absence of respiration (Γ^*) were obtained from A_N-C_i curves under non-photorespiratory conditions as described in Bellasio et al. (2016) for each treatment with the exception of water stress due to uncertainties of Γ^* estimation at low g_s (Galmés et al., 2006). Instead, a Γ^* in common with control plants was used. From all

previous parameters, mesophyll conductance to CO_2 (g_m) was estimated using the variable *J* method (Harley et al., 1992).

2.3. Pressure – volume curves

For all plants, a fully developed leaf neighbouring the one measured for gas exchange was cut, rehydrated in distilled water and kept under darkness conditions overnight for being measured the following day using the bench-dry method (Sack and Pasquet-Kok, 2011). Leaf water potential was measured with a pressure chamber (Model 600D; PMS Instrument Company, Albany, USA). Leaves were measured until obtaining pressure-volume curves of at least 10 points. From *P-V* curves, values for water potential at turgor loss point (Ψ_{tlp}), relative water content at turgor loss point (RWC_{tlp}), osmotic potential at full turgor (π_o), apoplastic water fraction (a_f) and leaf area-specific capacitance at full turgor (C^*_{ft}) were obtained following Sack and Pasquet-Kok (2011). ε was calculated from total relative water content over the full range above RWC_{tlp} as described in Melkonian et al. (1982). The apoplastic water fraction (a_f) was calculated as the *x*-intercept of the $-1/\Psi$ vs. RWC_{tlp} relationship.

2.4. Leaf structure

The same leaves used for *P-V* curves were used to calculate the leaf mass area (*LMA*) and the leaf density (*LD*) following Pérez-Harguindeguy et al. (2013). Leaf area (*LA*) was obtained after overnight rehydration. Pictures for leaf area (including the petiole) were analysed using ImageJ (Wayne Rasband/NIH). Then, leaves were placed in an oven at 70 °C for 72 h to obtain the dry weight. Leaf thickness was assessed from 6 measurements per leaf (avoiding main veins) with a digital caliper. Thickness per area was used as a proxy for *LD*.

2.5. Cell wall extraction and fractionation

To minimize leaf starch content, cell wall sampling was performed early in the morning in the same leaves used for gas-exchange. Thus, 1 g of fresh leaf tissue was cut in small pieces (1 cm^2, approximately) and placed in glass tubes containing absolute ethanol in a ratio 1:10 (w/v). Samples were boiled and ethanol-cleaned until bleached. They were cleaned twice with acetone > 95 % obtaining the alcohol insoluble residue (*AIR*), which represents an approximation of the total amount of isolated cell wall. They were grinded and a lugol determination was performed to evaluate starch presence. If positive, an α-amylase digestion was done to eliminate its residues. Once no starch remains were detected, 3 mg *AIR* belonging to each sample were taken per triplicate. They were hydrolysed with 2 M trifluoroacetic acid, heated at 121 °C for an hour and centrifuged at 13,000 *g* for 10 min obtaining two phases. The supernatant (non-cellulosic cell wall components) was directly kept at −20 °C for soluble sugars (hemicelluloses) and uronic acids (pectins) quantification and the pellet (cellulosic cell wall components) was cleaned twice with distilled water and acetone > 95 %. Once dried at room temperature, it was hydrolysed in 200 µl sulphuric acid 72 % (w/v) for an hour, diluted to 6 ml with distilled water and heated at 121 °C until pellet total degradation. Once cooled, the obtained aqueous samples were used for cellulose quantification.

2.6. Total sugars determination: cellulose and hemicelluloses

The phenol sulphuric acid method (Dubois et al., 1956) was used to determine sugars concentration. For cellulose, 0.4 ml phenol 5 % (w/v) and 2 ml sulphuric acid 98 % were added to 0.4 ml cellulose aqueous samples. For hemicelluloses, same reagents volume plus 0.35 ml distilled water were added to 50 µl aqueous samples. Mixtures were vortexed vigorously and cooled at room temperature before reading their absorbance at 490 nm using a Multiskan Sky Microplate Spectrophotometer (ThermoFisher Scientific). Both cellulose and hemicelluloses concentrations were obtained interpolating samples absorbance from a glucose calibration line.

2.7. Uronic acids determination

2.4 ml sodium tetraborate 75 mM prepared in concentrated H_2SO_4 were added to 0.2 ml of the same aqueous sample used for hemicelluloses determination. Mixtures were vortexed, boiled for 5 min and immediately cooled in a water-ice bath. Then 40 µl of 2-Hydroxybiphenyl 0.15 % prepared in sodium hydroxide 0.5 M were added. Samples were vortexed and absorbance was read at 520 nm using a Multiskan Sky Microplate Spectrophotometer (ThermoFisher Scientific). Uronic acids concentration was obtained interpolating samples values from a galacturonic acid calibration curve (Blumenkrantz and Asboe-Hansen, 1973).

2.8. Statistical analysis

Thompson test was performed to detect and eliminate outliers for all analysed parameters. Afterwards, one-way ANOVA and subsequent LSD test were performed to detect statistically significant differences for studied parameters among treatments ($P < 0.05$). Pearson's correlation matrices were performed to find correlations between all parameters, being significant when $P < 0.05$ and highly significant when $P < 0.01$. Finally, linear regressions between cell wall components and photosynthesis/water relations parameters were fitted using mean values per treatment. All analyses were performed using R software (ver. 3.2.2; R Core Team, Vienna, Austria).

3. Results

3.1. Physiological characterization

The highest A_N was obtained in control conditions (9.61 ± 0.76 µmol CO_2 m^{-2} s^{-1}), followed by cold and growth chamber conditions (Fig. 1A). However, A_N was strongly reduced by water stress (Fig. 1A), being accompanied by decreasing in g_s and g_m (Figs. 1B and 1D, respectively). Nevertheless, statistical differences were not found regarding the WUE_i between treatments (Fig. 1C). Control presented the highest g_m and *ETR* values (Figs. 1D and E, respectively). The light respiration did not differ statistically between treatments (Fig. 1F).

3.2. Leaf water relations

Leaf water relations showed two major responses across treatments. Control and cold treatments presented the highest values for both Ψ_{tlp} (Fig. 2A) and RWC_{tlp} (Fig. 2B) compared to growth chamber conditions and water stress through similar osmotic and elastic adjustments (Figs. 2C and D). ε was lower in water stress and growth chamber plants (11.2 ± 0.6 and 10.8 ± 1.0 MPa, respectively) and increased almost two-fold under control and cold conditions (Fig. 1D). Control and cold treatments achieved higher values for a_f (Fig. 2E), but growth chamber and water-stressed plants presented higher C^*_{ft} (Fig. 2F).

3.3. Leaf structure

Control had a *LMA* almost two times higher than cold treatment (Fig. 3A). Cold plants *LMA* was also lower than under water stress and growth chamber conditions (Fig. 3A). For *LD*, growth chamber, cold and water stress treatments were statistically equal, but differed from the highest value for control (Fig. 3B).

3.4. Leaf cell wall composition

The highest proportion of *AIR* was obtained in water stress

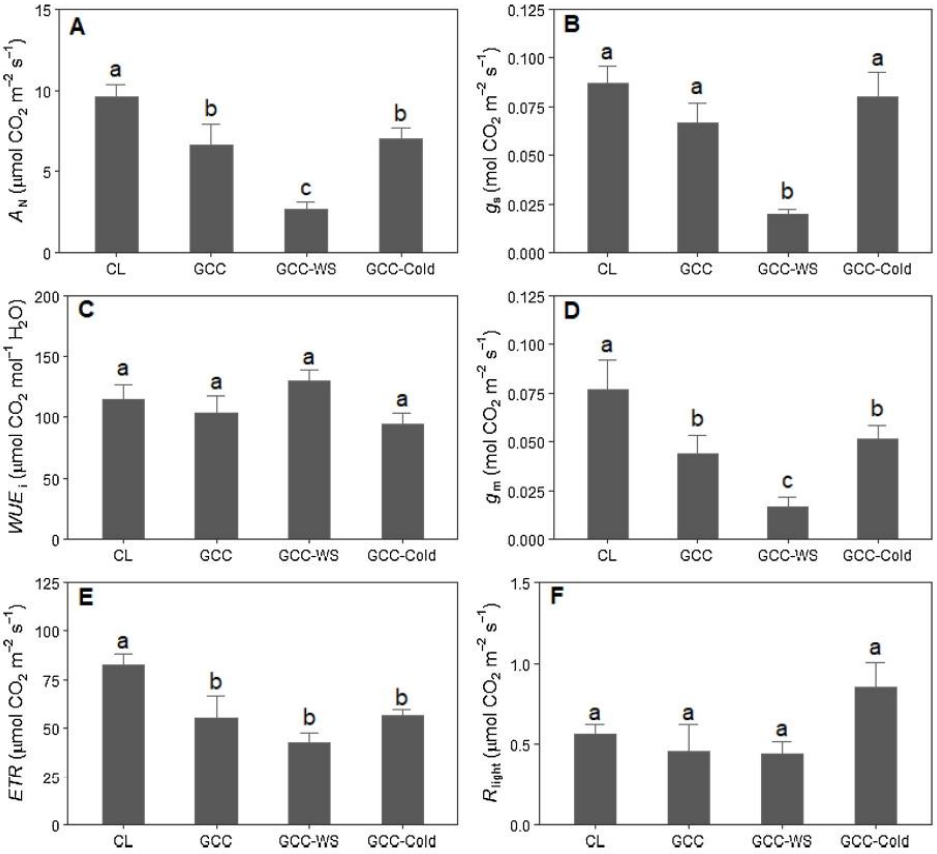

Fig. 1. (A) Light-saturated CO_2 assimilation, (B) stomatal conductance, (C) intrinsic water use efficiency, (D) mesophyll conductance from variable *J*, (E) electron transport rate and (F) light respiration in *V. vinifera* cv. Grenache across all conditions ("CL": control, "GCC": growth chamber conditions, "GCC-WS": growth chamber conditions under water stress, "GCC-Cold": growth chamber conditions under cold). *P*-values from One-Way ANOVA are shown. Different letters indicate differences among treatments. n = 5–6 (means ± SE).

treatment (0.30 ± 0.04 g g^{-1} dry weight) and the lowest in growth chamber and cold (0.19 ± 0.01 and 0.17 ± 0.01 g g^{-1} dry weight, respectively) (Table 1). Regarding to cellulose, water stress and growth chamber conditions presented the highest amounts (169.74 ± 12.17 and 141.99 ± 10.97 mg g^{-1} *AIR*, respectively), whilst the lowest quantity was found in control (Table 1). Oppositely, control presented the highest proportion of hemicelluloses (393.81 ± 8.69 mg g^{-1} *AIR*), achieving water stress and cold treatments the lowest (Table 1). For pectins, water stress and growth chamber were statistically equal and contained higher concentrations than control and cold (Table 1).

3.5. Relationships among parameters

Significant negative correlations were detected between cellulose and A_N (R^2 = 0.87, P = 0.046, Fig. 4A) and g_m (R^2 = 0.95, P = 0.015, Fig. 4B). ε also correlated negatively with total *AIR* (R^2 = 0.84, P = 0.053, Fig. 4C) and, particularly, with pectins content (R^2 = 0.95, P = 0.017, Fig. 4D). Additionally, other significant relationships were observed, such as that between cellulose and *ETR* or between pectin content and Ψ_{tlp} (Table S1).

4. Discussion

Environmental conditions are crucial for plants development and growth, as they regulate leaf features and, thus, physiology (Flexas et al., 2007; Chaves et al., 2008; Poorter et al., 2009; Bartlett et al., 2012; Tosens et al., 2012; Nadal and Flexas, 2019). Although the few datapoints used here do not allow us to draw conclusive statements, this study provides one of the first evidences of the potential relationships between photosynthesis (particularly, A_N and g_m) and leaf water relations (specifically, ε) with cell wall composition properties.

In our study, control plants achieved higher A_N, g_s, g_m and *ETR*, but also higher *LMA* and *LD*, as well as increased ε compared to other treatments (Figs. 1–3) due to higher irradiance and temperature during their growth. In fact, plants developed under high irradiance usually show a significant *LMA* enhancement (Poorter et al., 2009) because of greater thickness and palisade mesophyll investment (Niinemets and Sack, 2006; Tosens et al., 2012), which may in turn lead to an increased ε (Niinemets, 2001; Álvarez-Arenas et al., 2018). Nonetheless, control treatment achieved lower photosynthesis than in Flexas et al. (1998) testing the same species during Mediterranean summer conditions probably because our plants were younger and they were grown in pots which could limit their development, obtaining lower photosynthesis as in Moreno et al. (2010).

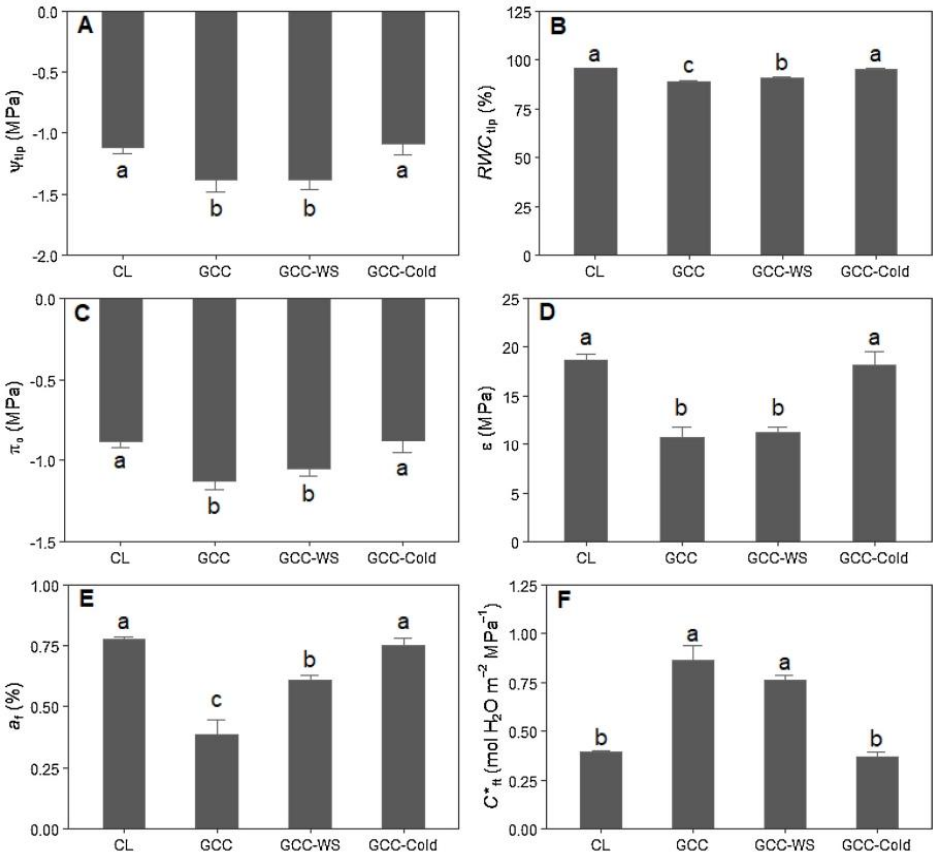

Fig. 2. (A) Water potential at turgor loss point, (B) relative water content at turgor loss point, (C) osmotic potential at full turgor, (D) bulk modulus of elasticity, (E) apoplastic water fraction and (F) leaf area specific capacitance at full turgor in *V. vinifera* cv. Grenache across all conditions ("CL": control, "GCC": growth chamber conditions, "GCC-WS": growth chamber conditions under water stress, "GCC-Cold": growth chamber conditions under cold). *P*-values from One-Way ANOVA are shown. Different letters indicate differences among treatments. n = 5–6 (means ± SE).

Water-stressed plants limited photosynthesis due to reduced overall CO_2 diffusion (i.e., decreased g_s and g_m) as often observed under water stress conditions (Flexas et al., 2004; Nadal and Flexas, 2019). The same happened for plants under growth chamber conditions, which decreased A_N because of lower g_m. Concomitantly, although Bartlett et al. (2012) reported that elastic adjustments are usually mild to none under water stress, changes in leaf water relations were detected, being opposite to the ones reported by Lo Gullo and Salleo (1988), who observed an increase of leaf rigidity in mature *Ceratonia siliqua* L. and *Laurus nobilis* L. leaves exposed to water stress. These changes followed the same pattern in growth chamber plants although being watered. As well as for water-stressed and growth chamber plants, photosynthesis was reduced by low temperature in our study, reflecting that grapevine photosynthesis is very sensitive to mild chilling conditions (Flexas et al.,

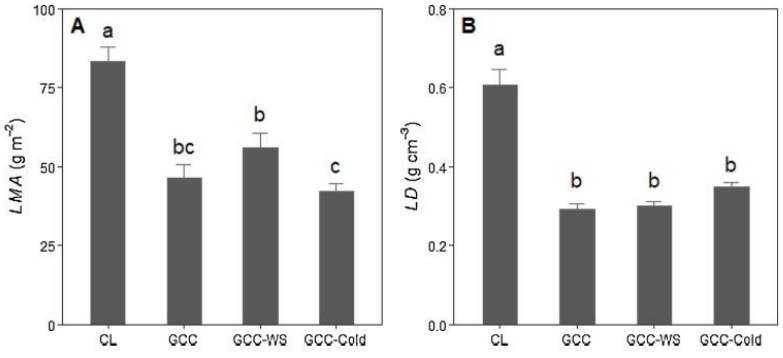

Fig. 3. (A) Leaf mass area and (B) leaf density in *V. vinifera* cv. Grenache across all conditions ("CL": control, "GCC": growth chamber conditions, "GCC-WS": growth chamber conditions under water stress, "GCC-Cold": growth chamber conditions under cold). *P*-values from One-Way ANOVA are shown. Different letters indicate differences among treatments. n = 5–6 (means ± SE).

Table 1
Leaf cell wall composition of *V. vinifera* cv. Grenache across all conditions ("CL": control, "GCC": growth chamber conditions, "GCC-WS": growth chamber conditions under water stress, "GCC-Cold": growth chamber conditions under cold). Average values ± SE are shown for alcohol insoluble residue, cellulose, hemicelluloses and pectins. *P*-values from One-Way ANOVA are shown. Different letters indicate differences among treatments. n = 4–6 (means ± SE).

Treatments	*AIR* (g g^{-1} dry weight)	Cellulose (mg g^{-1} *AIR*)	Hemicelluloses (mg g^{-1} *AIR*)	Pectins (mg g^{-1} *AIR*)
CL	0.25 ± 0.05^{ab}	83.82 ± 11.63^{b}	393.81 ± 8.69^{a}	79.97 ± 3.68^{b}
GCC	0.19 ± 0.01^{b}	141.99 ± 10.97^{a}	256.22 ± 18.39^{b}	109.82 ± 6.39^{a}
GCC-WS	0.30 ± 0.04^{a}	169.74 ± 12.17^{a}	163.61 ± 13.03^{c}	113.27 ± 8.73^{a}
GCC-Cold	0.17 ± 0.01^{b}	130.78 ± 13.12^{ab}	123.52 ± 11.25^{c}	74.84 ± 3.22^{b}

1999). Additionally, although it is thought that increased ε under cold temperature is an elastic adjustment that leads to the avoidance of leaf injury due to ice formation (Scholz et al., 2012; Arias et al., 2015), our cold treatment did not promote changes in leaf water relations compared to control plants, which is contrary to the reported for other species (Scholz et al., 2012; Arias et al., 2015; Zhang et al., 2016). This fact could be because our cold conditions were established at 13 °C instead of at zero or sub-zero temperatures, showing that mild temperature was not enough to promote changes in leaf water relations. However, water stress, cold and growth chamber conditions induced changes in *LMA* and *LD* (Fig. 3). Although it has been described that *LD* reflects to some extent the cell wall content per leaf (Poorter et al., 2009), variations in *AIR* quantities obtained in our experimental conditions (Table 1) did not follow the same pattern that *LD* changes. Therefore, when applying growth chamber and water stress conditions we obtained that photosynthesis and water relations changed compared to control plants. However, when applying cold, photosynthesis but not water relations were modified. This enables the possibility to check those changes in cell wall components that are specifically related to variations in photosynthesis and g_m as compared to other modifications specifically affecting water relations. A similar approach was recently proposed by Clemente-Moreno et al. (2019) studying short-term salinity or water stress and recovery in tobacco. The long-term water and cold stresses applied here plus an extra treatment (growth chamber conditions) were used to induce long-term changes in studied parameters, providing extended data for observed traits in acclimated plants.

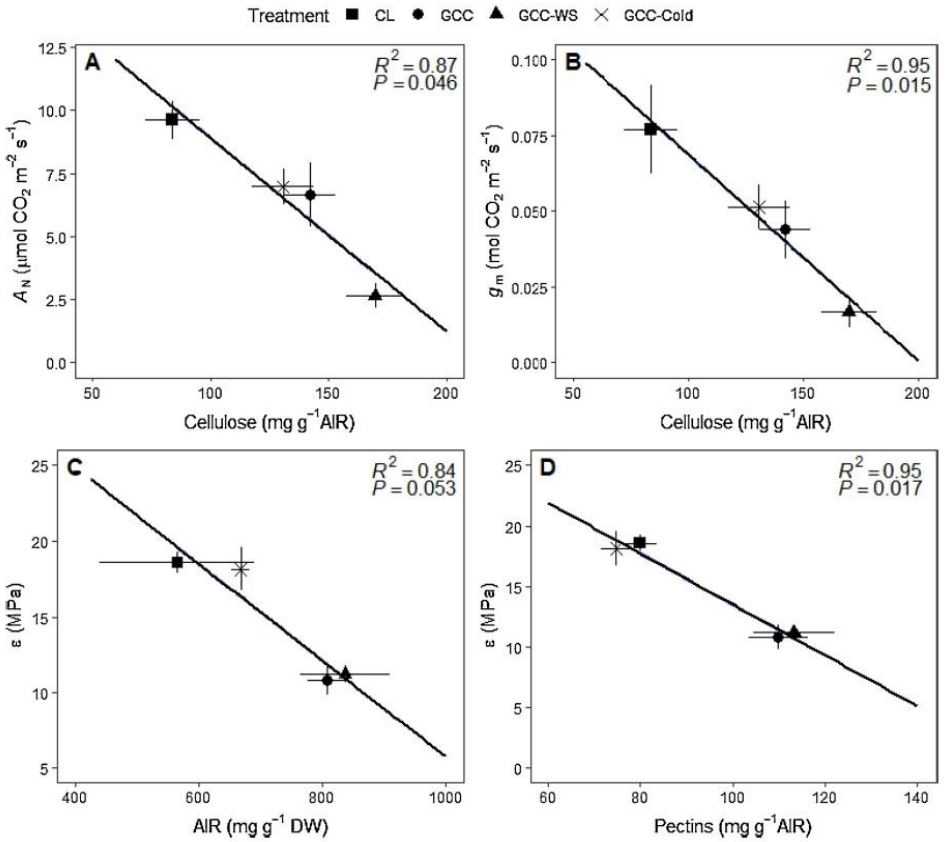

Fig. 4. (A) Relationship between light-saturated CO_2 assimilation and cellulose content, (B) relationship between mesophyll conductance and cellulose content, (C) relationship between elastic modulus of elasticity and *AIR* content and (D) relationship between elastic modulus of elasticity and pectins content in *V. vinifera* cv. Grenache across all conditions. n = 4–6 (means ± SE).

Once we had established four different treatments leading to distinct effects on photosynthetic, water relations and leaf structural traits, we could analyse how these changes were related to cell wall main composition. Cell wall composition experienced changes due to water stress in all analysed compounds (Table 1), following the same pattern described by Sweet et al. (1990) also in grapevines. In fact, higher amount of pectins are thought to be crucial to control the pectic matrix hydration status during water stress (Leucci et al., 2008; Moore et al., 2008). Additionally, some studies performed under cold conditions detected an enhancement in the pectin concentration as well as in the activities of pectin-modifying enzymes, suggesting they could be crucial for plant resistance to cold exposure (Solecka et al., 2008; Carvalho et al., 2013; Baldwin et al., 2014). For instance, testing the tropical species *Nidularium minutum* it was revealed that pectins increased growing plants at 10 °C and 15 °C compared to 25 °C (Carvalho et al., 2013). However, our results differed with the previous study as we detected no changes in pectin content in comparison to control (Table 1). As both studies were performed testing similar temperatures, different pectin behaviour could be attributed to species. While temperate plants are sometimes chilling-tolerant by activating strategies to withstand cold, tropical ones are more sensitive (Carvalho et al., 2013). Besides pectin modification, cold exposure sometimes promotes changes in sugars composition, but they do not follow a fixed pattern, as cellulose and hemicellulose concentrations have been reported to either increase or decrease (Le Gall et al., 2015). Our study detected a slightly increase in cellulose and a stronger reduction in hemicelluloses compared to control (Table 1).

Regarding to cell wall characterization of control treatment, although high irradiance may lead to hotter environmental conditions, these two conditions have been mainly tested individually to evaluate cell wall state (Le Gall et al., 2015). Furthermore, Masuda et al. (1981) and Suwa et al. (2010) detected that cell wall composition could also depend on studied genotypes, tissues and organs when considering high irradiance. Nonetheless, both heat and irradiance can affect cell wall sugars and pectin metabolisms. Whilst sugars behaviour is more varying, pectin concentration tends to increase once high irradiance is established and behaves oppositely when hotter conditions are settled (Le Gall et al., 2015). Nevertheless, our results (Table 1) followed the same pattern than the ones obtained in Lima et al. (2013) testing coffee leaves at 37 °C, where hemicelluloses and pectins significantly increased and decreased, respectively, as compared to growth chamber conditions (lower temperature and irradiance).

Despite the use of few datapoints do not allow us to assess definitive remarks, our results suggest a possible role of cell wall composition in determining both g_m and ε. The potential importance of cell wall in varying photosynthesis has recently been suggested by Ellsworth et al. (2018) testing rice *CslF6* mutants with disruptions in cell wall mixed-linkage glucans. In these mutants, lower g_m and, thus, A_N could be associated to changes in both cell wall porosity and tortuosity, which have been mainly explained due to modifications in the cell wall pectin fraction. However, mixed-linkage glucans are exclusive of grasses and few other plants, hence their role cannot be extended to other plant groups, including grapevine. Recently, Clemente-Moreno et al. (2019) found that both salt and water stress treatments significantly affected tobacco leaves cell wall composition, specifically pectins, which showed significant relationships with A_N and g_m. According to Moore et al. (2008), McKenna et al. (2010) and Solecka et al. (2008), cellulose and hemicelluloses are embedded in a complex pectin matrix. When the whole matrix contracts, pectins contract around cellulose and hemicelluloses microfibrils and the size of the cell wall pores may be altered making the CO_2 pathway through the cell wall more tortuous, thus contributing to lower g_m. In contrast, in our study cellulose was the only cell wall component significantly associated to photosynthetic traits, particularly, g_m (Fig. 4B). Considering the cell wall as a whole, changes in its compounds and in the way they organise have been reported as important facts regulating leaf mechanical traits (Kitajima et al., 2012; Le Gall et al., 2015; Farahi et al., 2017). We speculate that increases in cellulose amounts, particularly those achieved without changes in *LMA* or *LD* – such as those observed under growth chamber, cold and water stress conditions – may result in a tighter package of its microfibrils, limiting CO_2 flux through the mesophyll as observed by reduced g_m. These results provide further evidence that cell wall compounds can be involved in g_m regulation, but different compounds involvement could depend on species and/or environmental conditions.

Additionally, two significant correlations were found between cell wall composition and leaf water relations, i.e. between ε and *AIR* and between ε and pectin content (Figs. 4C and D, respectively). Cell wall thickness is one of the parameters affecting cell elasticity in single cells (Tyree and Jarvis, 1982) and it may also drive bulk tissue ε (Peguero-Pina et al., 2017). Nonetheless, it is not likely that cell wall thickness is responsible for rapid elastic adjustments. The first studies highlighting that cell wall compounds interactions and rearrangement could be crucial in determining short-term changes in ε were reported in Peltier and Marigo (1999) and Marshall and Dumbroff (1999), who found, respectively, fast decreasing of ε (< 24 h) in *Fraxinus excelsior* in response to ABA and pH treatments and an increased ε and cell wall stiffness in *Picea glauca* in response to paclobutrazol (a synthetic plant growth-regulator). Although more studies are required for a better understanding in how the increasing in cell wall rigidity occurs, some authors suggested that cellulose and hemicelluloses could modulate ε (Niinemets, 2016; Miranda-Apodaca et al., 2018). However, more agreement is found considering that an enhancement in pectins and in stronger polymers cross-linking in the pectic fraction could be involved in this process (Solecka et al., 2008; Baldwin et al., 2014). From our results, although few datapoints were used, we observed that pectins were the unique cell wall component driving ε in *V. vinifera* cv. Grenache (Fig. 4D) as no significant correlations were found between ε and the two other main cell wall components.

To the best of our knowledge, this study provides the first evidence of how cell wall composition could play a significant role in determining both ε and A_N – specially through g_m –, testing four different conditions at intraspecific level. While in our study A_N and g_m better correlated with cellulose and ε with pectins, more studies are required using a larger range of species and treatments, for a proper understanding of how cell wall composition can affect leaf physiology. Moreover, other minor cell wall components not considered thus far in previous studies concerning g_m (Ellsworth et al., 2018; Clemente-Moreno et al., 2019 and the present) such as lignins and phenols should be tested in further experiments as Sarkar et al. (2009) and Karabourniotis et al. (2014) suggested they could influence both water relations and photosynthesis.

Author contributions

MR-O, MN, JB and JF designed the study; MR-O and MN conducted the experiment; MR-O, MN and MJC performed the data analysis and MR-O and MN wrote the first manuscript version. All authors contributed to its following versions.

Declaration of Competing Interest

The authors declare no conflicts of interest.

Acknowledgments

This work was supported by the projects CTM2014-53902-C2-1-Pfrom the Ministerio de Economía y Competitividad (MINECO, Spain) and ERDF (FEDER) and PGC2018-093824-B-C41 from the Ministerio de Ciencia, Innovación y Universidades and ERDF (FEDER). MR-O and MN were supported by predoctoral fellowships FPU16/01544 and BES-2015-072578 from Ministerio de Economía y Competitividad (MINECO, Spain), respectively. Additionally, MN was co-supported by

the European Social Found. We thank Mr. Miquel Truyols and collaborators of the UIB Experimental Field and Glasshouses that are supported by the UIB Grant15/2015.

Appendix A. Supplementary data

Supplementary material related to this article can be found, in the online version, at doi:https://doi.org/10.1016/j.jplph.2019.153084.

References

Arias, N.S., Bucci, S.J., Scholz, F.G., Goldstein, G., 2015. Freezing avoidance by supercooling in *Olea europaea* cultivars: the role of apoplastic water, solute content and cell wall rigidity. Plant Cell Environ. 38, 2061–2070. https://doi.org/10.1111/pce.12529.

Álvarez-Arenas, T.E.G., Sancho-Knapik, D., Peguero-Pina, J.J., Gómez-Arroyo, A., Gil-Pelegrín, E., 2018. Non-contact ultrasonic resonant spectroscopy resolves the elastic properties of layered plant tissues. Appl. Phys. Lett. 113, 253704. https://doi.org/10.1063/1.5064517.

Baldwin, L., Domon, J.M., Klimek, J.F., Fournet, F., Sellier, H., Gillet, F., Pelloux, J., Lejeune-Hénaut, I., Carpita, N.C., Rayon, C., 2014. Structural alteration of cell wall pectins accompanies pea development in response to cold. Phytochemistry 104, 37–47. https://doi.org/10.1016/j.phytochem.2014.04.011.

Bartlett, M.K., Scoffoni, C., Sack, L., 2012. The determinants of leaf turgor loss point and prediction of drought tolerance of species and biomes: a global meta-analysis. Ecol. Lett. 15, 393–405. https://doi.org/10.1111/j.1461-0248.2012.01751.x.

Bellasio, C., Beerling, D.J., Griffiths, H., 2016. An Excel tool for deriving key photosynthetic parameters from combined gas exchange and chlorophyll fluorescence: theory and practice. Plant Cell Environ. 39, 1180–1197. https://doi.org/10.1111/pce.12560.

Blumenkrantz, N., AsboeHansen, G., 1973. New method for quantitative determination of uronic acids. Anal. Biochem. 54, 484–489. https://doi.org/10.1016/0003-2697(73)90377-1. Hansen.

Carriquí, M., Cabrera, H.M., Conesa, M.À., Coopman, R.E., Douthe, C., Gago, J., Gallé, A., Galmés, J., Ribas-Carbó, M., Tomás, M., Flexas, J., 2015. Diffusional limitations explain the lower photosynthetic capacity of ferns as compared with angiosperms in a common garden study. Plant Cell Environ. 38 (3), 448–460. https://doi.org/10.1111/pce.12402.

Carvalho, C.P., Hayashi, A.H., Braga, M.R., Nievola, C.C., 2013. Biochemical and anatomical responses related to the in vitro survival of the tropical bromeliad *Nidularium minutum* to low temperatures. Plant Physiol. Biochem. 71, 144–154. https://doi.org/10.1016/j.plaphy.2013.07.005.

Chaves, M.M., Flexas, J., Pinheiro, C., 2008. Photosynthesis under drought and salt stress: regulation mechanisms from whole plant to cell. Ann. Bot. 103, 551–560. https://doi.org/10.1093/aob/mcn125.

Clemente-Moreno, M.J., Gago, J., Díaz-Vivancos, P., Bernal, A., Miedes, E., Bresta, P., Liakopoulos, G., Fernie, A.R., Hernández, J.A., Flexas, J., 2019. The apoplastic antioxidant system and altered cell wall dynamics influence mesophyll conductance and the rate of photosynthesis. Plant J. https://doi.org/10.1111/tpj.14437.

Cosgrove, D.J., 2005. Growth of the plant cell wall. Nat. Rev. Mol. Cell Biol. 6, 850–861. https://doi.org/10.1038/nrm1746.

Dubois, M., Gilles, K.A., Hamilton, J.K., Rebers, P.A., Smith, F., 1956. Colorimetric method for determination of sugars and related substances. J. Anal. Chem. 28 (3), 350–356. https://doi.org/10.1021/ac60111a017.

Ellsworth, P.V., Ellsworth, P.Z., Koteyeva, N.K., Cousins, A.B., 2018. Cell wall properties in *Oryza sativa* influence mesophyll CO_2 conductance. New Phytol. 219, 66–76. https://doi.org/10.1111/nph.15173.

Evans, J.R., Kaldenhoff, R., Genty, B., Terashima, I., 2009. Resistance along the CO_2 diffusion pathway inside leaves. J. Exp. Bot. 60 (8), 2235–2248. https://doi.org/10.1093/jxb/erp117.

Farahi, R.H., Charrier, A.M., Tolbert, A., Lereu, A.L., Ragauskas, A., Davison, B.H., Passiah, A., 2017. Plasticity, elasticity, and adhesion energy of plant cell walls: nanometrology of lignin loss using atomic force microscopy. Sci. Rep. 7 (152). https://doi.org/10.1038/s41598-017-00234-4.

Ferrio, J.P., Pou, A., Flórez-Sarasa, I., Gessler, A., Kodama, N., Flexas, J., Ribas-Carbó, M., 2012. The *Péclet* effect on leaf water enrichment correlates with leaf hydraulic conductance and mesophyll conductance for CO_2. Plant Cell Environ. 169, 379–386. https://doi.org/10.1111/j.1365-3040.2011.02440.x.

Flexas, J., Escalona, J.M., Medrano, H., 1998. Down-regulation of photosynthesis by drought under field conditions in grapevine leaves. Aust. J. Plant Physiol. 25 (8), 8935–9000. https://doi.org/10.1071/pp98054.

Flexas, J., Badger, M., Chow, W.S., Medrano, H., Osmond, C.B., 1999. Analysis of the relative increase in photosynthetic O_2 uptake when photosynthesis in grapevine leaves is inhibited following low night temperatures and/or water stress. Plant Physiol. 121 (2), 675–684. https://doi.org/10.1104/pp.121.2.675.

Flexas, J., Bota, J., Loreto, F., Cornic, G., Sharkey, T.D., 2004. Diffusive and metabolic limitations to photosynthesis under drought and salinity in C_3 plants. Plant Biol. 6, 269–279. https://doi.org/10.1055/s-2004-820867.

Flexas, J., Díaz-Espejo, A., Galmés, J., Kaldenhoff, R., Medrano, H., Ribas-Carbó, M., 2007. Rapid variations of mesophyll conductance in response to changes in CO_2 concentration around leaves. Plant Cell Environ. 30, 1284–1298. https://doi.org/10.1111/j.1365-3040.2007.01700.x.

Flexas, J., Ribas-Carbó, M., Díaz-Espejo, A., Galmés, J., Medrano, H., 2008. Mesophyll conductance to CO_2: current knowledge and future prospect. Plant Cell Environ. 31, 602–621. https://doi.org/10.1111/j.1365-3040.2007.01757.x.

Flexas, J., Barbour, M.M., Brendel, O., Cabrera, H.M., Carriquí, M., Díaz-Espejo, A., Douthe, C., Dreyer, E., Ferrio, J.P., Gago, J., Gallé, A., Galmés, J., Kodama, N., Medrano, H., Niinemets, Ü., Peguero-Pina, J.J., Pou, A., Ribas-Carbó, M., Tomás, M., Tosens, T., Warren, C., 2012. Mesophyll conductance to CO_2: an unappreciated central player in photosynthesis. Plant Sci. 193–194, 70–84. https://doi.org/10.1016/j.plantsci.2012.05.009.

Flexas, J., Scoffoni, C., Gago, J., Sack, L., 2013. Leaf mesophyll conductance and leaf hydraulic conductance: an introduction to their measurement and coordination. J. Exp. Bot. 64 (13), 3965–3981. https://doi.org/10.1093/jxb/ert319.

Gago, J., Carriquí, M., Nadal, M., Clemente-Moreno, M.J., Coopman, R.E., Fernie, A., Flexas, J., 2019. Photosynthesis optimized across land plant's phylogeny. Trends Plant Sci. https://doi.org/10.1016/j.tplants.2019.07.002.

Galmés, J., Medrano, H., Flexas, J., 2006. Acclimation of Rubisco specificity factor to drought in tobacco: discrepancies between *in vitro* and *in vivo* estimations. J. Exp. Bot. 57 (14), 3659–3667. https://doi.org/10.1093/jxb/erl113.

Harley, P.C., Loreto, F., Di Marco, G., Sharkey, T.D., 1992. Theoretical considerations when estimating the mesophyll conductance to CO_2 flux by the analysis of the response of photosynthesis to CO_2. Plant Physiol. 98, 1429–1436. https://doi.org/10.1104/pp.98.4.1429.

Karabourniotis, G., Liakopoulos, G., Nikolopoulos, D., Bresta, P., Stavroulaki, V., Sumbele, S., 2014. Carbon gain vs. water saving, growth vs. defence: two dilemmas with soluble phenolics as a joker. Plant Sci. 227, 21–27. https://doi.org/10.1016/j.plantsci.2014.06.014.

Kitajima, K., Cordero, R.A., Wright, S.J., 2012. Leaf life span spectrum of tropical woody seedlings: effects of light and ontogeny and consequences for survival. Ann. Bot. 112 (4), 685–699. https://doi.org/10.1093/aob/mct036.

Le Gall, H., Philippe, F., Domon, J.M., Gillet, F., Pelloux, J., Rayon, C., 2015. Cell wall metabolism in response to abiotic stress. Planta 4, 112–166. https://doi.org/10.3390/plants4010112.

Leucci, M.R., Lenucci, M.S., Piro, G., Dalessandro, G., 2008. Water stress and cell wall polysaccharides in the apical root zone of wheat cultivars varying in drought tolerance. J. Plant Physiol. 165, 1168–1180. https://doi.org/10.1016/j.jplph.2007.09.006.

Lima, R.B., dos Santos, T.B., Vieira, L.G.E., de Lourdes, L.úcio, Ferrarese, M., Ferrarese-Filho, O., Donatti, L., Boeger, M.R.T., de Oliveira Petkowicz, C.L., 2013. Heat stress causes alterations in the cell-wall polymers and anatomy of coffee leaves (*Coffea Arabica* L.). Carbohydr. Polym. 93, 135–143. https://doi.org/10.1016/j.carbpol.2012.05.015.

Lo Gullo, M.A., Salleo, S., 1988. Different strategies of drought resistance in three Mediterranean sclerophyl-lous trees growing in the same environmental conditions. New Phytol. 108, 267–276. https://doi.org/10.1111/j.1469-8137.1988.tb04162.x.

Marshall, J.G., Dumbroff, E.B., 1999. Turgor regulation via cell wall adjustment in white spruce. Plant Physiol. 119, 313–319. https://doi.org/10.1104/pp.119.1.313.

Martins, S.C.V., Galmés, J., Molins, A., DaMatta, F.M., 2013. Improving the estimation of mesophyll conductance to CO_2: on the role of electron transport rate correction and respiration. J. Exp. Bot. 64, 3285–3298. https://doi.org/10.1093/jxb/ert168.

Masuda, Y., Kamisaka, S., Yanagisawa, H., Suzuki, H., 1981. Effect of light on growth and metabolic activities in pea seedlings I. Changes in cell wall polysaccharides during growth in the dark and in the light. Biochem. Physiol. Pflanz. 176, 23–34. https://doi.org/10.1016/S0015-3796(81)80005-4.

McKenna, B.A., Kopittke, P.M., Wehr, J.B., Blamey, F.P.C., Menzies, N.W., 2010. Metal ion effects on hydraulic conductivity of bacterial cellulose–pectin composites used as plant cell wall analogs. Physiol. Plant. 138, 205–214. https://doi.org/10.1111/j.1399-3054.2009.01306.x.

Melkonian, J.J., Wolfe, J., Steponkus, P.L., 1982. Determination of the volumetric modulus of elasticity of wheat leaves by pressure-volume relations and the effect of drought conditioning. Crop Sci. 22 (1), 116–123. https://doi.org/10.2135/cropsci1982.0011183X002200010027x.

Miranda-Apodaca, J., Pérez-López, U., Lacuesta, M., Mena-Petite, A., Muñoz-Rueda, A., 2018. The interaction between drought and elevated CO_2 in water relations in two grassland species is species-specific. J. Plant Physiol. 220, 193–202. https://doi.org/10.1016/j.jplph.2017.11.006.

Moore, J.P., Farrant, J.M., Driouich, A., 2008. A role for pectin-associated arabinans in maintaining the flexibility of the plant cell wall during water deficit stress. Plant Signal. Behav. 3 (2), 102–104. https://doi.org/10.4161/psb.3.2.4959.

Moore, J.P., Nguema-Ona, E.E., Vicré-Gibouin, M., Sørensen, I., Willats, W.G.T., Driouich, A., Farrant, J.M., 2013. Arabinose-rich polymers as an evolutionary strategy to plasticize resurrection plant cell walls against desiccation. Planta 237 (3), 739–754. https://doi.org/10.1007/s00425-012-1785-9.

Moreno, D., Berli, F.J., Piccoli, P.N., Bottini, R., 2010. Gibberellins and abscisic acid promote carbon allocation in roots and berries of grapevines. J. Plant Growth Regul. 30, 220–228. https://doi.org/10.1007/s00344-010-9186-4.

Nadal, M., Flexas, J., Gulías, J., 2018. Possible link between photosynthesis and leaf modulus of elasticity among vascular plants: a new player in leaf traits relationships? Ecol. Lett. 21, 1372–1379. https://doi.org/10.1111/ele.13103.

Nadal, M., Flexas, J., 2019. Variation in photosynthetic characteristics with growth form in a water-limited scenario: implications for assimilation rated and water use efficiency in crops. Agric. Water Manage. 216, 457–472. https://doi.org/10.1016/j.agwat.2018.09.024.

Niinemets, Ü., 2001. Global-scale climatic controls of leaf dry mass per area, density, and thickness in trees and shrubs. Ecology 82 (2), 453–469. https://doi.org/10.1890/0012-9658(2001)082[0453:GSCCOL]2.0.CO;2.

Niinemets, Ü., Sack, L., 2006. Structural determinants of leaf light-harvesting capacity

and photosynthetic potentials. In: In: Esser, K., Lüttge, U., Beyschlag, W., Murata, J. (Eds.), Progress in Botany (Genetics Physiology Systematics Ecology), vol 67. Springer, Berlin, Heidelberg, pp. 385–419.

Niinemets, Ü., 2016. Does the touch of cold make evergreen leaves tougher? Tree Physiol. 36, 267–272. https://doi.org/10.1093/treephys/tpw007.

Onoda, Y., Schieving, F., Anten, N.P.R., 2015. A novel method of measuring leaf epidermis and mesophyll stiffness shows the ubiquitous nature of the sandwich structure of leaf laminas in broad-leaved angiosperm species. J. Exp. Bot. 66 (9), 2487–2499. https://doi.org/10.1093/jxb/erv024.

Onoda, Y., Wright, I.J., Evans, J.R., Hikosaka, K., Kitajima, K., Niinemets, Ü., Poorter, H., Tosens, T., Westoby, M., 2017. Physiological and structural tradeoffs underlying the leaf economics spectrum. New Phytol. 214, 1447–1463. https://doi.org/10.1111/nph.14496.

Peguero-Pina, J.J., Sancho-Knapik, D., Gil-Pelegrín, E., 2017. Ancient cell structural traits and photosynthesis in today's environment. J. Exp. Bot. 68, 1389–1392. https://doi.org/10.1093/jxb/erx081.

Peltier, J.P., Marigo, G., 1999. Drought adaptation in *Fraxinus excelsior* L.: Physiological basis of the elastic adjustment. J. Plant Physiol. 154, 529–535. https://doi.org/10.1016/S0176-1617(99)80294-6.

Pérez-Harguindeguy, N., Díaz, S., Garnier, E., Lavorel, S., Poorter, H., Jaureguiberry, P., Harte, Bret, M.S, Gurvich, D.E., Urcelay, R.C., Funes, G., Quétier, F., Vaieretti, M.V., Conti, G., Poorter, L., Wright, I.A., Ray, P., Enrico, L., Pausas, J.G., de Vos, A.F., Buchman, N., Hodgson, J.G., Thompson, K., Morgan, H.D., ter Sttefe, H., Van Der Heijden, M.G.A., Sack, L., Blonder, B., Poschlod, P., Staver, M.C., Aquino, S., Cornelissen, J.H.C., 2013. New handbook for standardised measurement of plant functional traits worldwide. Austral. J. Bot. 61, 167–234. https://doi.org/10.1071/BT12225_CO.

Poorter, H., Niinemets, Ü., Poorter, L., Wright, I.J., Villar, R., 2009. Causes and consequences of variation in leaf mass per area (LMA): a meta-analysis. New Phytol. 182, 565–588. https://doi.org/10.1111/j.1469-8137.2009.02830.x.

Pou, A., Medrano, H., Flexas, J., Tyerman, S.D., 2012. A putative role for TIP and PIP aquaporins in dynamics of leaf hydraulic and stomatal conductances in grapevine under water stress and re-watering. Plant Cell Environ. 36 (4), 828–843.

Sack, L., Cowan, P.D., Jaikumar, N., Holbrook, N.M., 2003. The 'hydrology' of leaves: coordination of structure and function intemperate woody species. Plant Cell Environ. 26, 1343–1356. https://doi.org/10.1046/j.0016-8025.2003.01058.x.

Sack, L., Pasquet-Kok, J., 2011. Leaf pressure-volume curve parameters. Prometheus Wiki. (accessed 15 January 2019). http://prometheuswiki.org/tiki-pagehistory.php?page=Leaf%20pressure-volume%20curve%20parameters&preview=16.

Salleo, S., Lo Gullo, M.A., 1990. Sclerophylly and plant water relations in three Mediterranean *Quercus* species. Ann. Bot. 65, 259–270. https://doi.org/10.1093/oxfordjournals.aob.a087932.

Sarkar, P., Bosneaga, E., Auer, M., 2009. Plant cell walls throughout evolution: towards a molecular understanding of their design principles. J. Exp. Bot. 60 (13), 3615–3635. https://doi.org/10.1093/jxb/erp245.

Scholz, F.G., Bucci, S.J., Arias, N., Meinzer, F.C., Goldstein, G., 2012. Osmotic and elastic adjustments in cold desert shrubs differing in rooting depth: coping with drought and subzero temperatures. Oecologia 170, 885–897. https://doi.org/10.1007/s00442-012-2368-y.

Solecka, D., Zebrowski, J., Kacperska, A., 2008. Are pectins involved in cold acclimation and de-acclimation of winter oil-seed rape plants? Ann. Bot. 101, 521–530. https://doi.org/10.1093/aob/mcm329.

Suwa, R., Hakata, H., Hara, H., El-Shemy, H.A., Adu-Gyamfi, J.J., Nguyen, N.T., Kanai, S., Lightfoot, D.A., Mohapatra, P.K., Fujita, K., 2010. High temperature effects on photosynthate partitioning and sugar metabolism during ear expansion in maize (*Zea mays* L.) genotypes. Plant Physiol. Biochem. 48, 124–130. https://doi.org/10.1016/j.plaphy.2009.12.010.

Sweet, W.J., Morrison, J.C., Labavitch, J., Matthews, M.A., 1990. Altered synthesis and composition of cell wall of grape (*Vitis vinifera* L.) leaves during expansion and growth-inhibiting water deficits. Plant Cell Physiol. 31 (4), 407–414. https://doi.org/10.1093/oxfordjournals.pcp.a077924.

Terashima, I., Miyazawa, S.I., Hanba, Y.T., 2001. Why are sun leaves thicker than shade leaves? Consideration based on analyses of CO_2 diffusion in the leaf. J. Plant Res. 114 (1113), 93–105. https://doi.org/10.1007/PL00013972.

Tomás, M., Flexas, J., Copolovici, L., Galmés, J., Hallik, L., Medrano, H., Ribas-Carbó, M., Tosens, T., Vislap, V., Niinements, Ü., 2013. Importance of leaf anatomy in determining mesophyll diffusion conductance to CO_2 across species: quantitative limitations and scaling up by models. J. Exp. Bot. 64 (8), 2269–2281. https://doi.org/10.1093/jxb/ert086.

Tosens, T., Niinemets, Ü., Vislap, V., Eichelmann, H., Castro-Díez, P., 2012. Developmental changes in mesophyll diffusion conductance and photosynthetic capacity under different light and water availabilities in *Populus tremula*: how structure constrains function. Plant Cell Environ. 35, 839–856. https://doi.org/10.1111/j.1365-3040.2011.02457.x.

Tosens, T., Nishida, K., Gago, J., Coopman, R.E., Cabrera, H.M., Carriquí, M., Laanisto, L., Morales, L., Nadal, M., Rojas, R., Talts, E., Tomás, M., Hanba, Y., Niinemets, Ü., Flexas, J., 2016. The photosynthetic capacity in 35 ferns and fern allies: mesophyll CO_2 diffusion as a key trait. New Phytol. 209 (4), 1576–1590. https://doi.org/10.1111/nph.13719.

Tyree, M.T., Jarvis, P.G., 1982. Water in tissues and cells. In: Lange, O.L., Nobel, P.S., Osmond, C.B., Ziegler, H. (Eds.), Physiological Plant Ecology II. Springer, Berlin Heidelberg, pp. 35–77.

von Caemmerer, S., Farquhar, G., Berry, J., 2009v. Biochemical model of C_3 photosynthesis. In: Laisk, A., Nedbal, L., Govindjee (Eds.), Photosynthesis in Silico: Understanding Complexity from Molecules to Ecosystems. Springer Science + Business Media B.V., pp. 209–230.

Warren, C.R., Livingston, N.J., Turpin, D.H., 2004. Water stress decreases the transfer conductance of Douglas-fir (*Pseudotsuga menziesii)* seedlings. Tree Physiol. 24, 971–997. https://doi.org/10.1093/treephys/24.9.971.

Yin, X., Struik, P.C., Romero, P., Harbinson, J., Evers, J.B., Van der Putten, P.E., Vos, J., 2009. Using combined measurements of gas exchange and chlorophyll fluorescence to estimate parameters of a biochemical C_3 photosynthesis model: a critical appraisal and a new integrated approach applied to leaves in a wheat (*Triticum aestivum*) canopy. Plant Cell Environ. 32, 448–464. https://doi.org/10.1111/j.1365-3040.2009.01934.x.

Zhang, Y., Bucci, S.J., Arias, N.S., 2016. Freezing resistance in Patagonian woody shrubs: the role of cell wall elasticity and stem vessel size. Tree Physiol. 36 (8), 1007–1018. https://doi.org/10.1093/treephys/tpw036.

Table S1. Pearson correlation matrix of physiological, leaf water relations and cell wall parameters measured in *V. vinifera* cv. Grenache plants across all conditions. Values in bold and italics indicate significant ($P < 0.05$) and highly significant ($P < 0.01$) correlation coefficients, respectively.

	A_N	g_s	WUE_i	g_m	ETR	R_{light}	Ψ_{tlp}	RWC_{tlp}	π_o	ε	a_f	C^*_{ft}	LMA	LD	AIR	Cel	Hemicel	Pectin
A_N		**0.88**	-0.07	***0.98***	0.79	-0.31	0.24	-0.01	-0.04	0.28	-0.30	0.07	-0.14	0.39	-0.18	**0.87**	0.23	0.30
g_s			0.34	0.79	0.44	-0.02	0.36	0.01	-0.01	0.33	-0.33	0.14	-0.42	0.03	0.20	0.59	-0.17	0.45
WUE_i				-0.19	-0.45	0.27	-0.14	-0.42	-0.39	-0.27	-0.50	-0.31	-0.17	-0.49	***0.97***	-0.37	-0.46	-0.04
g_m					**0.89**	-0.30	0.36	0.15	0.11	0.43	-0.17	0.21	-0.01	0.57	-0.30	**0.95**	0.26	0.39
ETR						-0.47	0.15	0.09	0.02	0.28	-0.13	0.09	0.41	0.84	-0.48	***0.97***	0.58	0.14
R_{light}							0.52	0.28	0.36	0.34	0.05	0.43	-0.37	-0.48	0.09	-0.38	-0.28	0.56
Ψ_{tlp}								**0.88**	**0.90**	***0.98***	0.58	**0.96**	-0.37	0.14	-0.30	0.33	-0.46	***0.99***
RWC_{tlp}									***0.99***	**0.93**	**0.89**	***0.98***	-0.23	0.25	-0.49	0.22	-0.46	0.82
π_o										**0.92**	**0.87**	***0.98***	-0.29	0.17	-0.48	0.16	-0.48	0.83
ε											0.66	***0.97***	-0.25	0.31	-0.39	0.44	-0.40	**0.95**
a_f												0.78	-0.17	0.16	-0.46	-0.06	-0.48	0.48
C^*_{ft}													-0.32	0.17	-0.43	0.24	-0.47	**0.92**
LMA														0.72	-0.05	0.24	0.60	-0.41
LD															-0.45	0.78	0.49	0.08
AIR																-0.44	-0.45	-0.22
Cel																	0.40	0.33
Hemicel																		-0.46
Pectin																		

Adjustments in photosynthesis and leaf water relations are related to changes in cell wall composition in *Hordeum vulgare* and *Triticum aestivum* subjected to water deficit stress

Margalida Roig-Oliver[1*], Mateu Fullana-Pericàs[1], Josefina Bota[1], Jaume Flexas[1,2]

[1]Research Group on Plant Biology under Mediterranean Conditions, Departament de Biologia, Universitat de les Illes Balears (UIB) – Agro-Environmental and Water Economics Institute (INAGEA). Carretera de Valldemossa Km 7.5, 07122 Palma, Illes Balears, Spain.
[2]King Abdulaziz University, Jeddah, Saudi Arabia.

[*] Corresponding author.

Submitted to *Plant Science* on 3rd May 2021.

Adjustments in photosynthesis and leaf water relations are related to changes in cell wall composition in *Hordeum vulgare* and *Triticum aestivum* subjected to water deficit stress

Margalida Roig-Oliver[a], Mateu Fullana-Pericàs[a], Josefina Bota[a], Jaume Flexas[a,b]

[a]Research Group on Plant Biology under Mediterranean Conditions, Departament de Biologia, Universitat de les Illes Balears (UIB) – Agro-Environmental and Water Economics Institute (INAGEA). Carretera de Valldemossa Km 7.5, 07122 Palma, Illes Balears, Spain.
[b]King Abdulaziz University, Jeddah, Saudi Arabia.

Corresponding author: Margalida Roig-Oliver (margaroig93@gmail.com).

Abstract

In the current climate change scenario, understanding crops' physiologic performance under water shortage is crucial to overcome drought periods. Although the implication of leaf water relations maintaining leaf turgor and stomatal functioning under water deprivation has been suggested, the relationships between photosynthesis and osmotic and elastic adjustments remain misunderstood. Similarly, only few studies in dicotyledonous species analysed how changes in cell wall composition affected photosynthesis and leaf water relations under drought. To induce modifications in photosynthesis, leaf water relations and cell wall composition, *Hordeum vulgare* and *Triticum aestivum* were subjected to different water regimes: control (full irrigation, 100% field capacity; FC), 50% FC and 40% FC. Water shortage promoted photosynthesis reductions mainly attributed to stomatal conductance (g_s) declines, being accompanied by reduced osmotic potential at full turgor (π_o) and increased bulk modulus of elasticity (ε). Whereas both species enhanced pectins when intensifying water deprivation, species-dependent adjustments occurred for cellulose and hemicelluloses. From these results, we showed that π_o and ε adjustments influenced photosynthesis, particularly, g_s. Furthermore, the (Cellulose+Hemicelluloses)/Pectins ratio determined ε and mesophyll conductance (g_m) in grasses, presenting the lowest pectins content within angiosperms.

Thus, we highlight the relevance of cell wall composition regulating grasses physiology during drought acclimation.

Keywords

Cell wall composition, *Hordeum vulgare*, pectins, photosynthesis, *Triticum aestivum*, water deficit stress.

Abbreviations

a_f, apoplastic water fraction; AIR, alcohol insoluble residue; A_N, net CO_2 assimilation; C^*_{ft}, leaf area specific capacitance at full turgor; ε, bulk modulus of elasticity; *ETR*, electron transport rate; Ψ_{md}, midday water potential; Ψ_{pd}, pre-dawn water potential; Ψ_{tlp}, water potential at turgor loss point; g_m, mesophyll conductance; g_s, stomatal conductance; LD, leaf density; LMA, leaf mass per area; π_o, osmotic potential at full turgor; R_{light}, light respiration; RWC, leaf relative water content; RWC_{tlp}, relative water content at turgor loss point; WUE_i, intrinsic water use efficiency.

1. Introduction

Wheat (*Triticum aestivum* L.) and barley (*Hordeum vulgare* L.) are two of the most important grass crops worldwide, whose cultivars have been traditionally selected to enhance their production while increasing their drought tolerance [1-3]. In fact, water deprivation is one of the most relevant abiotic conditions limiting crops production in a climate change scenario, which is characterized by large variations in rainfalls amount, frequency, and duration [4-6]. Thus, one of the major challenges of plant physiology is to improve crops yield identifying those traits that can contribute to improve their drought tolerance [7-9]. Since photosynthesis is a crucial process influencing plants growth and productivity, it is important to understand how distinct levels of water deficit stress impose a limitation to photosynthesis performance [10-13]. Therefore, it has been described that severe water deficit stress imposition leads to important biochemical limitations to photosynthesis [11,14], whereas moderate levels of water shortage induce diffusional limitations [11,13]. Specifically, reductions in net CO_2 assimilation (A_N) are caused by diminishing in both stomatal and mesophyll conductances (g_s and g_m, respectively) [10-14], promoting an enhancement of the intrinsic water use efficiency (WUE_i) due to often larger declines in g_s than in g_m [15,16].

Photosynthesis performance may be related to leaf water relations under water deficit stress conditions [17]. Thus, pressure-volume (*P*–*V*) derived parameters – particularly, the water potential at turgor loss point (Ψ_{tlp}), the osmotic potential at full turgor (π_o), the bulk modulus of elasticity (ε) and the leaf capacitance– have been linked with photosynthesis across species [17-19]. Although modifications in both osmotic and elastic adjustments (i.e., changes in π_o and ε) have been proposed as mechanisms to face water deficit stress, their relationship with photosynthetic adjustments is still poorly understood. Hence, whereas an osmotic adjustment consisting in π_o reductions is a common response in those species submitted to water shortage [20-25], elastic adjustments could be species-specific and may involve different strategies [20,25-29]. Nevertheless, Sack et al. [30] and Niinemets [31] proposed that foliar traits –specifically, the leaf mass per area (LMA) and the leaf density (LD)– could determine ε. However, Moore et al. [32], Solecka et al. [33], Álvarez-Arenas et al. [34], Miranda-Apodaca et al. [35], Nadal et al. [18] and Roig-Oliver et al. [27,28] suggested that modifications in cell wall composition could be also important to regulate ε, but empirical evidences are for now restricted only to Roig-Oliver et al. [27].

The cell wall is a complex structure surrounding plant cells that is mainly composed of cellulose, hemicelluloses and pectins [36-40]. Of the previous, cellulose is the most abundant polysaccharide and conforms a microfibril matrix that provides mechanical strength to the wall [37-40]. Within those closely packed cellulose microfibrils, non-cellulosic polysaccharides (hereafter "hemicelluloses") are placed [36-37]. The resulting cellulose-hemicelluloses network is embedded in a pectin matrix containing cross-linking structural proteins [38-40], which is thought to be a relevant structure to maintain an appropriated cell wall hydric status, especially during water shortage [32,39,41,42]. Furthermore, changes in the amounts of pectins are also linked to photosynthesis –particularly, via g_m adjustments– in *Nicotiana sylvestris* and to ε in *Vitis vinifera* subjected to contrasting abiotic stressors including water deprivation [27,43]. Nonetheless, the relationships between changes in photosynthesis and leaf water relations derived parameters with modifications in cell wall composition seem to be complex and, perhaps, species-specific. In this sense, different patterns to adjust cell wall composition, leaf water relations and photosynthesis were found in *Ginkgo biloba* and *Helianthus annuus* subjected to water deficit stress [28]. Moreover, g_m was linked to lignins and cell wall bound phenolics in *H. annuus* submitted to contrasting water regimes, but instead no correlation between any cell wall compound and ε was observed [29].

To the best of our knowledge, studies focusing on the interactions between cell wall composition and changes in photosynthesis and leaf water relations parameters due to water deficit stress have been only performed in dicotyledonous species [27,29], with the exception of a dicotyledonous-gymnosperm comparison [28]. However, some of the most economically important crops worldwide are monocotyledonous and, particularly, grasses like maize, rice, sorghum, sugarcane, wheat, bamboo, oat, and barley [44,45]. In fact, monocotyledonous possess a specific cell wall composition within angiosperms as they may contain even larger proportions of cellulose and hemicelluloses –with changes in their cross-linking interactions as well as in the relative abundance of specific non-cellulosic polysaccharides–, but with a significant reduction of pectins [36,37,40,47,48]. Additionally, grasses represent a specific group within monocotyledonous from a cell wall compositional perspective because they also accumulate large quantities of mixed-linked glucans [36,37], which alterations were shown to affect g_m in mutant rice genotypes [49]. Thus, we evaluated *H. vulgare* and *T. aestivum* subjected to distinct levels of water deficit stress to detect potential relationships between changes in cell wall composition and adjustments in photosynthesis and in leaf water relations derived parameters, being g_s, g_m, π_o and ε key traits. The main hypothesis of the present study is that cell wall composition rearrangement due to water deprivation is linked to modifications in both photosynthetic and leaf water related parameters, which may have important implications for understanding grass crops physiology and management in a climate change scenario.

2. Materials and methods

2.1. Plant material and growth conditions

T. aestivum and *H. vulgare* seeds were sown in water-irrigated 3 l pots containing a substrate mixture of peat and perlite (3:1, v/v). They were placed in a growth chamber at 25 ºC receiving 300 µmol m^{-2} s^{-1} photosynthetic photon flux density (PPFD) for 12 h followed by 12 h of darkness. Plants were monitored to be watered to full capacity (FC) every two days, receiving Hoagland's solution 50% once a week. Three weeks after the sowing, three different treatments were imposed: control (i.e., full irrigation, 100% FC), 50% FC and 40% FC. Five individual replicates per species were randomly subjected to each treatment. Whereas control plants were maintained at 100% FC, plants belonging to 50% and 40% FC treatments were monitored daily to maintain each pot at specific FC by replacing evapo-transpired water. In all cases, treatments lasted three weeks.

2.2. Plants water status and foliar structure

At the end of the imposition of each treatment, pre-dawn (Ψ_{pd}) and midday (Ψ_{md}) leaf water potentials were measured in a fully developed leaf per plant using a pressure chamber (Model 600D; PMS Instrument Company, Albany, OR, USA). Additionally, in the same leaves used for Ψ_{md}, the leaf relative water content (RWC), the leaf mass per area (LMA) and the leaf density (LD) were determined. RWC was calculated as:

$$\mathrm{RWC} = \frac{\mathrm{FW} - \mathrm{DW}}{\mathrm{TW} - \mathrm{DW}} \text{ x } 100$$

where FW, DW and TW correspond to fresh, dry, and turgid weights, respectively. The FW was determined immediately after measuring Ψ_{md}. Then, leaves were rehydrated in distilled water for 24 h under darkness conditions at 4 ºC to obtain the TW. At this moment, leaves were photographed to calculate their area using ImageJ (Wayne Rasband/NIH). Also, their thickness was measured with a digital caliper from five measurements per leaf avoiding main veins. Finally, leaves were placed in an oven at 70 ºC for 72 h to determine their DW. LMA was calculated as the ratio of dry weight to leaf area, while LD was estimated as thickness per area.

2.3. Gas exchange and fluorescence measurements

An infrared gas analyser (IRGA) LI-6400XTR coupled with a fluorometer (Li-6400-40; Li-Cor Inc., Lincoln, NE, USA) was used for simultaneous gas exchange and chlorophyll *a* fluorescence (Chl *a*) measurements. The block temperature, the vapour pressure deficit (VPD) and the flow rate were fixed at 25 ºC, 1.5 kPa and 300 μmol air min^{-1}, respectively. One fully developed leaf per plant was clamped into a 2 cm^2 cuvette and steady-state conditions were induced at saturating photosynthetic photon flux density (PPFD 1500 μmol m^{-2} s^{-1}, 90–10% red-blue light) and 400 μmol CO_2 mol^{-1} air. When steady-state conditions were reached –usually after 15-20 min–, measurements for net CO_2 assimilation (A_N), stomatal conductance (g_s), CO_2 concentration at the sub-stomatal cavity (C_i) and steady-state fluorescence (F_s) were registered. Afterward, a saturating light flash of around 8000 μmol m^{-2} s^{-1} was applied to obtain the maximum fluorescence (F_m'). From these values, the real quantum efficiency of photosystem II (Φ_{PSII}) was recorded in the equipment as follows:

$$\Phi_{PSII} = \frac{F_{m\prime} - F_s}{F_{m\prime}}$$

Moreover, light curves under non-photorespiratory conditions (< 1% O_2) were performed to estimate the electron transport rate (*ETR*) following Valentini et al. [50]. Light respiration (R_{light}) was considered as half the dark-adapted respiration rate after plants exposition to darkness for, at least, 30 min [51]. As leaves did not cover the whole area of the IRGA cuvette, a picture of the leaf fraction enclosed in the cuvette was taken to recalculate the area with ImageJ. With all previous parameters, mesophyll conductance (g_m) was calculated as described in Harley et al. [52]. Species-specific values for the CO_2 compensation point in the absence of respiration (Γ^*) were obtained from Hermida-Carrera et al. [53].

2.4. Pressure-volume curves

A fully developed leaf adjacent to the one employed for gas exchange measurements was used to perform pressure-volume (*P–V*) curves. Hence, leaves were rehydrated in distilled water and kept under darkness conditions overnight. The next day, leaves water potential was measured with a pressure chamber (Model 600D; PMS Instrument Company) and they were subsequently weighted to determine their fresh weight. Thus, from complete *P–V* curves of at least 10 points, the leaf water potential at turgor loss point (Ψ_{tlp}), the relative water content at turgor loss point (RWC_{tlp}), the leaf osmotic potential at full turgor (π_o), the bulk modulus of elasticity (ε), the apoplastic water fraction (a_f), and the leaf area specific capacitance at full turgor (C^*_{ft}) were calculated [30,54].

2.5. Cell wall composition characterization

Those leaves used for gas exchange measurements were kept under darkness conditions overnight to minimize starch content. The next morning, around 500 mg of fresh leaf tissue per plant were cut in small pieces to be boiled until bleached in screwed-capped tubes containing absolute ethanol. They were cleaned twice with acetone >95% obtaining the alcohol insoluble (AIR), an approximation of the total isolated cell wall material. AIRs were dried at room temperature and then, an α-amylase digestion was performed to eliminate starch residues. Afterward, 3 analytical replicates per AIR weighting 3 mg, approximately, were hydrolysed with 2 M trifluoroacetic acid at 121 ºC for 1 h. After that, they were centrifuged obtaining two phases: a supernatant (non-cellulosic cell wall

components) and a pellet (cellulosic cell wall components). Whilst non-cellulosic cell wall components were used for hemicelluloses and pectins quantifications, the pellet was cleaned twice with distilled water and acetone >95%. The dry residue corresponding to cellulose was hydrolysed with 200 µl sulphuric acid 72% (w/v) for 1 h, diluted to 6 ml with distilled water and heated at 121 ºC until degradation. Both cellulose and hemicelluloses quantifications were performed by the phenol-sulphuric acid colorimetric procedure [55]. Hence, samples absorbance was read at 490 nm and both sugars contents were estimated interpolating samples values from a glucose calibration curve. For pectins quantification, the colorimetric method described in Blumenkrantz and Asboe-Hansen [56] was addressed using 2-hydroxybiphenil as a reagent. Thus, samples absorbance was read at 520 nm and pectins content was determined interpolating samples values from a galacturonic acid calibration curve. For all analyses, a Multiskan Sky Microplate spectrophotometer (ThermoFisher Scientific) was employed.

2.6. Statistical analysis

Prior to perform statistical analyses, Thompson test was addressed to detect and subtract outliers for all tested parameters. Then, two-way analysis of variance (ANOVA) and subsequent LSD test were performed to identify statistically significant (P<0.05) "species", "treatments" and "species:treatments" effects. Furthermore, Pearson's correlation matrices were done to find correlations between all studied parameters, which were considered as significant and highly significant when P<0.05 and P<0.01, respectively. Finally, linear regressions between photosynthetic, leaf water relations and cell wall composition parameters were fitted using mean values per species and treatment. In all cases, the R statistical software (ver. 3.2.2; R Core Team, Vienna, Austria) was employed.

3. Results

3.1. Plants water status

For both species, the reduction in water availability to 50% FC and 40% FC resulted in significant declines in plant water status parameters (Table 1). Thus, both species presented more negative values for Ψ_{pd} and Ψ_{md} as compared to control, being *T. aestivum* that species achieving the lowest values (Table 1). Instead, both species almost maintained RWC to control values under 50% FC, but significant reductions were found under 40% FC, being more accentuated in *T. aestivum* (Table 1).

3.2. Photosynthetic characterization

Under control conditions, both species presented similar A_N rates (25.92 ± 1.72 and 23.87 ± 1.18 μmol CO_2 m^{-2} s^{-1} for *H. vulgare* and *T. aestivum*, respectively), which were largely reduced due to 40% FC imposition (Fig. 1A). The same pattern was also found for g_s, presenting reductions of almost 90% and 80% in *H. vulgare* and *T. aestivum*, respectively (Fig. 1B). Because g_s was more reduced than A_N, WUE_i was significantly higher under water deficit stress conditions than under control in both species, especially in the 40% FC treatment (107.50 ± 5.08 and 93.75 ± 9.80 μmol CO_2 mol^{-1} H_2O for *H. vulgare* and *T. aestivum*, respectively; Fig. 1C). Although g_m only declined under 40% FC in *H. vulgare* (0.07 ± 0.02 mol CO_2 m^{-2} s^{-1}), it significantly increased under 50% FC in *T. aestivum* as compared to control (0.40 ± 0.06 and 0.23 ± 0.04 mol CO_2 m^{-2} s^{-1}, respectively), being then reduced to 0.13 ± 0.04 mol CO_2 m^{-2} s^{-1} under 40% FC (Fig. 1D). Regarding *ETR*, both "treatment" and "species" effects were significant (P=0.02 and P<0.001, respectively), being *H. vulgare* that species presenting more pronounced reductions due to water deficit stress treatments (Fig. 1E). Finally, only "species" effect was significant for R_{light} as *T. aestivum* presented slightly higher values than *H. vulgare* under all tested conditions (Fig. 1F).

3.3. Leaf water relations

Regarding *P–V* curves-derived parameters, water deficit stress imposed a significant shift towards more negative Ψ_{tlp} in comparison to control, whereas no "species" effect was detected (Fig. 2A). Again, these changes were more pronounced in *T. aestivum* as Ψ_{tlp} was significantly reduced during both water deprivation treatments imposition, whereas Ψ_{tlp} was similarly maintained to control values in *H. vulgare* subjected to 50% FC (Fig. 2A). Nonetheless, changes in RWC_{tlp} were specifically attributed to "treatments" effect (P<0.001) since water shortage promoted RWC_{tlp} increasing as compared to control (Fig. 2B). Concerning π_o, 50% FC imposition resulted in large declines in *T. aestivum*, whilst it was maintained at control values in *H. vulgare* (Fig. 2C). Nonetheless, both species presented significant reductions under 40% FC conditions, reaching -1.34 ± 0.12 and -1.20 ± 0.26 MPa in *T. aestivum* and *H. vulgare*, respectively (Fig. 2C). Regarding ε adjustments, changes were exclusively attributed to "treatments" effect (P<0.001) (Fig. 2D). Thus, under 40% FC, leaves rigidity (i.e., higher ε) was almost three times larger than under control in both species (11.33 ± 1.40 and 29.42 ± 0.30 MPa in *T. aestivum* and

10.49 ± 1.06 and 24.97 ± 3.78 MPa in *H. vulgare* under control and 40% FC, respectively; Fig. 2D). However, no significant changes were found for a_f (Fig. 2E). Finally, whereas 3.5-fold decreased C^*_{ft} was found in *T. aestivum* under 40% FC as compared to control (0.29 ± 0.12 and 0.95 ± 0.15 mol H_2O m^{-2} MPa^{-1}, respectively), it was maintained similarly to control values in *H. vulgare* (0.66 ± 0.00 and 0.78 ± 0.13 mol H_2O m^{-2} MPa^{-1}, respectively; Fig. 2F).

3.4. Leaf structure and cell wall composition

Water deficit stress treatments induced different changes in both species foliar structure and cell wall composition (Table 2). Whereas an enhancement of LMA and LD was detected under 50 and 40% FC conditions as compared to control in *H. vulgare*, no differences were observed in *T. aestivum* (Table 2). Regarding cell wall composition, *H. vulgare* increased the AIR content and the amounts of hemicelluloses with no changes in celluloses under 40% FC (Table 2). Instead, *T. aestivum* presented lower cellulose and hemicelluloses contents under both water shortage treatments than under control, with no changes in AIR (Table 2). Although pectins were gradually enhanced from control to 50% FC in *H. vulgare*, they decreased under 50% FC in *T. aestivum* as compared to control (Table 2). Nonetheless, both species displayed the highest amounts of pectins under 40% FC conditions (Table 2).

3.5. Correlations between parameters

Relationships between all studied parameters are found in Table S1. Particularly, significant negative correlations were found between ε and the (Cellulose+Hemicelluloses)/Pectins ratio (R^2=0.92, P<0.01, Fig. 3A) and g_s (R^2=0.60, P=0.04, Fig. 3B). However, g_s correlated positively with π_o (R^2=0.63, P=0.04, Fig. 3C) and with the (Cellulose+Hemicelluloses)/Pectins ratio (R^2=0.71, P=0.02, Fig. 3D). Additionally, other significant negative correlations were found between g_m and A_N with pectins (R^2=0.66, P=0.03, Fig. 4A and R^2=0.67, P=0.03, Fig. 4B, respectively).

4. Discussion

In the present study we tested two of the most relevant grass crops worldwide to examine the implications of distinct levels of water deficit stress promoting changes in their physiological performance. The classic response to water deprivation is characterized by A_N reductions due to decreasing in the overall CO_2 diffusion, resulting in enhanced WUE_i

[10,14]. Although g_s declines were already detected at 50% FC in both species, g_m was similarly maintained to control in *H. vulgare* whilst it was enhanced around 43% in *T. aestivum* (Figs. 1B,D). In fact, enhanced g_m under water deprivation was previously reported in sunflowers subjected to long term water deficit stress [29]. Given that g_s is a reference parameter to understand plants responses to progressive drought and that severe levels of water deficit stress usually occur when g_s drops below 0.03 mol CO_2 m^{-2} s^{-1} [57], our results may indicate that the water shortage treatments we applied just imposed a moderate stress. However, the application of apparently moderate water deficit stress treatments supposed significant changes in *P–V* derived parameters (Fig. 2).

Osmotic and elastic adjustments (i.e., changes in π_o and ε) are important mechanisms to face water deprivation [20-22,24.] Although *H. vulgare* maintained π_o to control value under 50% FC, significant declines were observed in *T. aestivum*, demonstrating that both species presented different mechanisms to face this level of water deficit stress. However, both of them achieved more negative π_o after their exposition to 40% FC. Nonetheless, elastic modifications were only observed under 40% FC, resulting in enlarged ε as previously reported in evergreen species subjected to drought periods [20] probably because of modifications in the foliar structure [58,59]. Since LMA and LD usually increase after plants exposition to water shortage, they have been correlated positively with ε across species [31,60,61]. However, in our study, the relationships between ε with LMA and LD were non-significant (Table S1), which implies that other traits were involved in ε adjustments in both grass species. Although it has been proposed that modifications in cell wall thickness may determine ε changes [62,63], it is improbable that such modifications are involved in fast ε adjustments. Thus, some studies proposed that changes in the cell wall proportion (i.e., the AIR) as well as in its compounds rearrangement may affect ε [27,32-35]. Of the previous, only Roig-Oliver et al. [27] provided empirical evidence on that issue, showing positive relationships between ε and AIR and pectins. In the present study, we also found that pectins content correlated with ε (Table S1), but an even more significant relationship emerged considering the (Cellulose+Hemicelluloses)/Pectins ratio (Fig. 3A), evidencing that modifications in pectins relative abundance determined elastic adjustments in grasses, even when they contain less than half pectins amounts than non-gramineous angiosperms [36,37,40,47,48]. Additionally, another two correlations between photosynthesis-related and leaf water-related parameters were further observed (Figs. 3B,C), being ε, π_o and g_s crucial traits. Lower π_o values were achieved while enhancing the level of water

deprivation, being accompanied by an increasing of leaves rigidity and by declines in g_s, all of them contributing to photosynthesis reductions. Since stomatal closure was in general the main photosynthesis limitation, this study provides one of the first evidences on the relationship between g_s adjustments due to modifications in leaf cell wall composition (Fig. 3D). In fact, Gago et al. [64] specifically proposed that changes in guard cells' cell wall composition –among other mechanisms such as specific sugars and organic acids accumulation and alterations in enzymatic processes– could influence stomatal movements, finally affecting photosynthesis. Particularly, it has been reported that pectin arabinans degradation blocked stomatal movements in the dicotyledonous *Commelina communis* [65] and high pectins deposition were found in the guard cells' cell wall of the grass species *Zea mays* [66]. Therefore, pectins have been proposed to strongly regulate guard cells' cell wall properties [67], which may potentially affect stomata functioning and, thus, photosynthesis. Although further studies exclusively evaluating guard cells' cell wall composition are needed to confirm this role for pectins, we show that even changes in their relative proportion considering the whole leaf cell wall were also responsible of photosynthetic reductions due to g_s modulation. Also, we demonstrate pectins relevance in determining g_m and, thus, photosynthesis (Figs. 4A,B). Although Ye et al. [68] did not report any cell wall composition effect on photosynthesis testing well-watered rice genotypes, Ellsworth et al. [49] and Zhang et al. [69] analysed different rice mutants and attributed photosynthesis reductions to alterations in mixed-linked glucans and to disrupted cellulose microfibrils orientation, respectively. However, those modifications in cell wall composition affecting photosynthesis –and, particularly, g_m– under distinct abiotic stressors including water shortage have just been explored in some dicotyledonous [27,29,43] and in a dicotyledonous-gymnosperm comparison [28]. Specifically, whilst Roig-Oliver et al. [28] found distinct patterns to face water deficit stress in *G. biloba* and *H. annuus*, cellulose and pectins were exclusively linked to g_m in grapevines and tobacco, respectively [27,43]. Thus, our results are in agreement with those reported in tobacco and are of special relevance since the effect of changes in cell wall composition regulating photosynthesis –specially, g_m– in grasses remained further unexplored.

5. Conclusions

To the best our knowledge, this study provides the first evidence on the role of cell wall composition determining both photosynthesis and leaf water relations adjustments in two

of the most relevant grass crops worldwide subjected to distinct water deficit stress regimes. Our results demonstrated the importance of osmotic and elastic adjustments influencing photosynthesis, being π_o, ε, and g_s key parameters. Also, we highlighted that changes in cell wall composition –particularly, in pectins content– determined leaf elasticity and both g_s and g_m. Besides these modifications in the amounts of the analysed leaf cell wall compounds, we speculate that they could be accompanied by changes in their physicochemical interactions resulting in differed guard cells movement and to altered wall porosity [65,66,70-73], which ultimately affected photosynthesis. However, further studies testing a larger number of grass crops subjected to more water shortage treatments as well as to recovery conditions are required to elucidate which physiologic strategies are activated during drought events that resemble those caused by the climate change.

Author contributions

MR-O, MF-P, JB and JF conceived and designed this study; MR-O and MF-P conducted the experiment; MR-O and JF performed the data analysis and MR-O wrote the first draft of the manuscript. All authors contributed to following versions, including the final one.

Funding

This work was supported by the project PGC2018-093824-B-C41 (Ministerio de Economía y Competitividad; MINECO, Spain) and the ERDF (FEDER). MR-O and MF-P were supported by pre-doctoral fellowships FPU16/01544 and FPI/1929/2016 through MINECO and Govern de les Illes Balears, respectively.

Declaration of Competing Interest

The authors declare they have no potential conflict of interest.

Acknowledgements

The authors thank Mr Joan Mestre for providing the seeds of both species. Also, we thank Dr Cyril Douthe for technical support during gas exchange performance and Dr Miquel Nadal for his advices with *P-V* curves.

References

[1] I.K. Dawson, J. Russell, W. Powell, B. Steffenson, W.T.B. Thomas, R. Waugh, Barley: a translational model for adaptation to climate change, New Phytol. 206 (2015) 913–931.

[2] A. Sallam, A.M. Alqudah, M.F.A. Dawood, P.S. Baenziger, A. Börner, Drought stress tolerance in wheat and barley: advances in physiology, breeding and genetics research, Int. J. Mol. Sci. 20 (2019) 3137.

[3] A. Gastaldi, S. Álvarez Prado, J.A. Arduini, D.J. Miralles, Optimizing wheat (*Triticum aestivum* L.) management under dry environments: a case study in the west pampas of Argentina, Agric. Water Manag. 2333 (2020) 106092.

[4] J. Lipiec, C. Doussan, A. Nosalewicz, K. Kondracka, Effect of drought and heat stresses on plant growth and yield: a review. Int. Agrophys. 27 (2013) 463–477.

[5] R.A. Richards, J.R. Hunt, J.A. Kirkegaard, J.B. Passioura, Yield improvement and adaptation of wheat to water-limited environments in Australia - a case study, Crop Pasture Sci. 65 (2014) 676–689.

[6] V.O. Sadras, R.A. Richards, Improvement of crop yield in dry environments: benchmarks, levels of organisation and the role of nitrogen, J. Exp. Bot. 65 (2014) 1981–1995.

[7] D. Tilman, K.G. Cassman, P.A. Matson, R. Naylor, S. Polasky, Agricultural sustainability and intensive production practices, Nature 418 (2002) 671–677.

[8] J.I.L. Morison, N.R. Baker, P.M. Mullineaux, W.J. Davies, Improving water use in crop production, Philos. Trans. Biol. Sci. 363 (2008) 639–658.

[9] H.R. Schultz, Global climate change, sustainability, and some challenges for grape and wine production, J. Wine Eco. 11 (2006) 181–200.

[10] M.M. Chaves, J.P. Maroco, J.S. Pereira, Understanding plant responses to drought – from genes to the whole plant, Funct. Plant Biol. 30 (2003) 239–264.

[11] M.M. Chaves, J. Flexas, C. Pinheiro, Photosynthesis under drought and salt stress: regulation mechanisms from whole plant to cell, Ann. Bot. 103 (2009) 551–560.

[12] J. Flexas, M.M. Barbour, O. Brendel, H.M. Cabrera, M. Carriquí, A. Díaz-Espejo, C. Douthe, E. Dreyer, J.P. Ferrio, J. Gago, A. Gallé, J. Galmés, N. Kodama, H. Medrano, Ü. Niinemets, J.J. Peguero-Pina, A. Pou, M. Ribas-Carbó, M. Tomás, T. Tosens, C. Warren, Mesophyll conductance to CO_2: an unappreciated central player in photosynthesis. Plant Sci. 193–194 (2012) 70–84.

[13] M. Nadal, J. Flexas, Variation in photosynthetic characteristics with growth form in a water-limited scenario: implications for assimilation rated and water use efficiency in crops, Agric. Water Manag. 216 (2019) 457–472.

[14] J. Flexas, J. Bota, F. Loreto, G. Cornic, T.D. Sharkey, Diffusive and metabolic limitations to photosynthesis under drought and salinity in C_3 plants, Plant Biol. 6 (2004) 269–279.

[15] J. Galmés, M.À. Conesa, J.M. Ochogavia, J.A. Perdomo, D.M. Francis, M. Ribas-Carbó, R. Savé, J. Flexas, H. Medrano, J. Cifre, Physiological and morphological adaptations in relation to water use efficiency in Mediterranean accessions of *Solanum lycopersicum*, Plant Cell Environ. 34 (2011) 245–260.

[16] J. Flexas, Ü. Niinemets, A. Gallé, M.M. Barbour, M. Centritto, A. Díaz-Espejo, C. Douthe, J. Galmés, M. Ribas-Carbó, P.L. Rodríguez, F. Rosselló, R. Soolanayakanahally, M. Tomás, I.J. Wright, G.D. Farquhar, H. Medrano, Diffusional conductances to CO_2 as a target for increasing photosynthesis and photosynthetic water-use efficiency, Photosynth. Res. 117 (2013) 45–59.

[17] D. Xiong, M. Nadal, Linking water relations and hydraulics with photosynthesis, Plant J. 101 (2020) 800–815.

[18] M. Nadal, J. Flexas, J. Gulías, Possible link between photosynthesis and leaf modulus of elasticity among vascular plants: a new player in leaf traits relationships? Ecol. Lett. 21 (2018) 1372–1379.

[19] S.D. Zhu, Y.J. Chen, Q. Ye, P.C. He, H. Liu, R.H. Li, P.L. Fu, G.F. Jiang, K.F. Cao, Leaf turgor loss point is correlated with drought tolerance and leaf carbon economics traits, Tree Physiol. 38 (2018) 658–663.

[20] M.A. Lo Gullo, S. Salleo, Different strategies of drought resistance in three Mediterranean sclerophyllous trees growing in the same environmental conditions, New Phytol. 108 (1988) 267–276.

[21] M.D. Abrams, Adaptations and responses to drought in *Quercus* species of North America, Tree Physiol. 7 (1990) 227–238.

[22] M.E. Kubiske, M.D. Abrams, Rehydration effects on pressure–volume relationships in four temperate woody species: variability with site, time of season and drought conditions, Oecologia 85 (1991) 537–542.

[23] M.K. Bartlett, C. Scoffoni, L. Sack, The determinants of leaf turgor loss point and prediction of drought tolerance of species and biomes: a global meta-analysis, Ecol. Lett. 15 (2012) 393–405.

[24] N.C. Turner NC, Turgor maintenance by osmotic adjustment: 40 years of progress, J. Exp. Bot. 69 (2018) 3223–3233.

[25] M. Nadal, M. Roig-Oliver, J. Bota, J. Flexas, Leaf age-dependent elastic adjustment and photosynthetic performance under drought stress in *Arbutus unedo* seedlings, Flora 271 (2020) 151662.

[26] M.A. Sobrado, N.C. Turner, A comparison of the water relations characteristics of *Helianthus annuus* and *Helianthus petiolaris* when subjected to water deficits, Oecologia 58 (1983) 309–313.

[27] M. Roig-Oliver, M. Nadal, M.J. Clemente-Moreno, J. Bota, J. Flexas, Cell wall components regulate photosynthesis and leaf water relations of *Vitis vinifera* cv. Grenache acclimated to contrasting environmental conditions, J. Plant Physiol. 244 (2020) 153084.

[28] M. Roig-Oliver, M. Nadal, J. Bota. J. Flexas, *Ginkgo Biloba* and *Helianthus annuus* show different strategies to adjust photosynthesis, leaf water relations, and cell wall composition under water deficit stress, Photosynthetica 58 (2020) 1098–1106.

[29] M. Roig-Oliver, P. Bresta, M. Nadal, G. Liakopoulos, D. Nikolopoulos, G. Karabourniotis, J. Bota, J. Flexas, Cell wall composition and thickness affect mesophyll conductance to CO_2 diffusion in *Helianthus annuus* under water deprivation, J. Exp. Bot. 71 (2020) 7198–7209.

[30] L. Sack, P.D. Cowan, N. Jaikumar, N.M. Holbrook, The 'hydrology' of leaves: coordination of structure and function intemperate woody species, Plant Cell Environ. 26 (2003) 1343–1356.

[31] Ü. Niinemets, Global-scale climatic controls of leaf dry mass per area, density, and thickness in trees and shrubs, Ecology 82 (2001) 453–469.

[32] J.P. Moore, J.M. Farrant, A. Driouich, A role for pectin-associated arabinans in maintaining the flexibility of the plant cell wall during water deficit stress, Plant Signal. Beh. 3 (2008) 102–104.

[33] D. Solecka, J. Zebrowski, A. Kacperska, Are pectins involved in cold acclimation and de-acclimation of winter oil-seed rape plants. Ann. Bot. 101 (2008) 521–530.

[34] T.E.G. Álvarez-Arenas, D. Sancho-Knapik, J.J. Peguero-Pina. A. Gómez-Arroyo, E. Gil-Pelegrín, Non-contact ultrasonic resonant spectroscopy resolves the elastic properties of layered plant tissues, Appl. Phys. Lett. 113 (2018) 253704.

[35] J. Miranda-Apodaca, U. Pérez-López, M. Lacuesta, A. Mena-Petite, A. Muñoz-Rueda, The interaction between drought and elevated CO_2 in water relations in two grassland species is species-specific, J. Plant Physiol. 220 (2018) 193–202.

[36] N.C. Carpita, D.M. Gibeaut DM, Structural models of primary cell walls in flowering plants: consistency of molecular structure with the physical properties of the walls during growth, Plant J. 3 (1993) 1–30.

[37] N.C. Carpita, M.C. McCann, The functions of cell wall polysaccharides in composition and architecture revealed through mutations, Plant Soil 247 (2002) 71–80.

[38] D.J. Cosgrove, Growth of the plant cell wall, Nat. Rev. Mol. Cell Biol. 6 (2005) 850–861.

[39] R. Tenhaken, Cell wall remodeling under abiotic stress, Front. Plant Sci. 5 (2015) 771.

[40] C.T. Anderson, J.J. Kieber, Dynamic construction, perception, and remodelling of plant cell walls, Ann. Rev. Plant Biol. 71 (2020) 39–69.

[41] M. Vicré, O. Lerouxel, J. Farrant. P. Lerouge, A. Driouich, Composition and desiccation-induced alterations of the cell wall in the resurrection plant *Craterostigma wilmsii*, Physiol. Plant. 120 (2004) 229–239.

[42] M.R. Leucci, M.S. Lenucci, G. Piro, G. Dalessandro, Water stress and cell wall polysaccharides in the apical root zone of wheat cultivars varying in drought tolerance, J. Plant Physiol. 165 (2008) 1168–1180.

[43] M.J. Clemente-Moreno, J. Gago, P. Díaz-Vivancos, A. Bernal, E. Miedes, P. Bresta, G. Liakopoulos, A.R. Fernie, J.A. Hernández, J. Flexas, The apoplastic antioxidant system and altered cell wall dynamics influence mesophyll conductance and the rate of photosynthesis, Plant J. 99 (2019) 1031–1046.

[44] J.L. Steiner, A.J. Flanzluebbers, Farming with grass – for people, for profit, for production, for protection, J. Soil Water Conserv. 64 (2009) 75A–80A.

[45] T.I. Odintsova, M.P. Slezina, E.A. Istomina, Defensins of grasses: a systematic review, Biomolecules 10 (2020) 1029.

[46] N.C. Carpita, Structure and biogenesis of the cell walls of grasses, Annu. Rev. Plant Physiol. Plant Mol. Biol. 47 (1996) 445–476.

[47] J. Vogel J, Unique aspects of the grass cell wall, Curr. Opi. Plant Biol. 11 (2008) 301–307.

[48] R.D. Hatfield, D.M. Rancour, J.M. Marita, Grass cell walls: a story of cross-linking, Front. Plant Sci. 7 (2017) 2056.

[49] P.V. Ellsworth, P.Z. Ellsworth, N.K. Koteyeva, A.B. Cousins, Cell wall properties in *Oryza sativa* influence mesophyll CO_2 conductance, New Phytol. 219 (2018) 66–76.

[50] R. Valentini, D. Epron, P.D. Angelis, G. Matteucci, E. Dreyer, In situ estimation of net CO_2 assimilation, photosynthetic electron flow and photorespiration of Turkey oak (*Q. cerris* L.) leaves: diurnal cycles under different water supply, Plant Cell Environ. 18 (1995) 631–664.

[51] Ü. Niinemets, A. Cescatti, M. Rodeghiero, T. Tosens, Leaf internal diffusion conductance limits photosynthesis more strongly in older leaves of Mediterranean evergreen broad-leaved species, Plant Cell Environ. 28 (2005) 1552–1566.

[52] P.C. Harley, F. Loreto, G. Di Marco, T.D. Sharkey, Theoretical considerations when estimating the mesophyll conductance to CO_2 flux by the analysis of the response of photosynthesis to CO_2, Plant Physiol. 98 (1992) 1429–1436.

[53] C. Hermida-Carrera, M.V. Kapralov, J. Galmés, Rubisco catalytic properties and temperature response in crops, Plant Physiol. 171 (2016) 2549–2561.

[54] L. Sack, J. Pasquet-Kok, Leaf pressure-volume curve parameters. Prometheus Wiki. Available at http://prometheuswiki.org/tiki-pagehistory.php?page=Leaf%20pressure-volume%20curve%20parameters&preview=16 (accessed 24 October 2020)

[55] M. Dubois, K.A. Gilles, J.K. Hamilton, P.A. Rebers, F. Smith F, Colorimetric method for determination of sugars and related substances, J. Anal. Chem. 28 (1956) 350–356.

[56] N. Blumenkrantz, G. Asboe-Hansen, New method for quantitative determination of uronic acids, Anal. Bioche. 54 (1973) 484–489

[57] H. Medrano, J.M. Escalona, J. Bota, J. Gulías, J. Flexas, Regulation of photosynthesis of C_3 plants in response to progressive drought: stomatal conductance as a reference parameter, Ann. Bot. 89 (2002) 895–905.

[58] S. Salleo, M.A. Lo Gullo, Sclerophylly and plant water relations in three Mediterranean *Quercus* species, Ann. Bot. 65 (1990) 259–27.

[59] T. Saito, K. Soga. T. Hoson, I. Terashima, The bulk elastic modulus and the reversible properties of cell walls in developing *Quercus* leaves, Plant Cell Physiol. 47 (2006) 715–725.

[60] I.J. Wright, P.B. Reich, J.H.C. Cornelissen, D.S. Falster, P.K. Groom, K. Hikosaka, W. Lee, C.H. Lusk, Ü. Niinemets, J. Oleksyn, N. Osada, H. Poorter, D.I. Warton, M. Westoby, Modulation of leaf economic traits and trait relationships by climate, Glob. Ecol. Biogeogr. 14 (2005) 411–421.

[61] H. Poorter, Ü. Niinemets, L. Poorter, I.J. Wright, R. Villar, Causes and consequences of variation in leaf mass per area (LMA): a meta-analysis, New Phytol. 182 (2009) 565–588.

[62] M.T. Tyree, P.G. Jarvis PG, Water in tissues and cells, in: O.L. Lange, P.S. Nobel, C.B. Osmond, H. Ziegler (Eds.), Physiological Plant Ecology II, Encyclopedia of Plant Physiology, Springer, Berlin, 1982, pp. 33–77.

[63] J.J. Peguero-Pina, D. Sancho-Knapik, E. Gil-Pelegrín, Ancient cell structural traits and photosynthesis in today's environment, J. Exp. Bot. 68 (2017) 1389–1392.

[64] J. Gago, D.M. Daloso, C.M. Figueroa, J. Flexas, A.R. Fernie, Z. Nikoloski Z, Relationships of leaf net photosynthesis, stomatal conductance, and mesophyll conductance to primary metabolism: a multispecies meta-analysis approach, Plant Physiol. 171 (2016) 265–279.

[65] L. Jones, J.L. Milne, D. Ashford, S.J. McQueen-Mason SJ, Cell wall arabinan is essential for guard cell function, Proc. Natl. Acad. Sci. USA 100 (2003) 11783–11788.

[66] L. Jones, J.L. Milne, D. Ashford, M.C. McCann, S.J. McQueen-Mason, A conserved functional role of pectic polymers in stomatal guard cells from a range of plant species, Planta 221 (2005) 255–264.

[67] I. Shtein, Y. Shelef, Z. Marom, E. Zelinger, A. Schwartz, Z.A. Popper, B. Bar-On, S. Harpaz-Saad, Stomatal cell wall composition: distinctive structural patterns associated with different phylogenetic groups, Ann. Bot. 119 (2017) 1021–1033.

[68] M. Ye, Z. Zhang, G. Huang, Z. Xiong, S. Peng, Y. Li Y, High leaf mass per area *Oryza* genotypes invest more leaf mass to cell wall and show a low mesophyll conductance, *Ao**BP* 12 (2020) plaa028

[69] R. Zhang, H. Hu, Y. Wang, Z. Hu, S. Ren, J. Li, B. He, Y. Wang, T. Xia, P. Chen, G. Xie, L. Peng, A novel rice fragile *culm* 24 mutant encodes a UDP-glucose epimerase that affects cell wall property and photosynthesis, J. Exp. Bot. 71 (2020) 2956–2969.

[70] N. Carpita, D. Sabularse, D. Montezinos, D.P. Delmer, Determination of the pore size of cell walls of living plant cells, Science 205 (1979) 1144–1147.

[71] O. Baron-Epel, P.K. Gharyal, M. Schindler, Pectins as mediators of wall porosity in soybean cells, Planta 175 (1988) 389–395

[72] L. Franková, S.C. Fry, Biochemistry and physiological roles of enzymes that 'cut and paste' plant cell-wall polysaccharides, J. Exp. Bot. 64 (2013) 3519–3550.

[73] J. Flexas, A. Díaz-Espejo, M.À.Conesa, R.E. Coopman, C. Douthe, J. Gago, A. Gallé, J. Galmés, H. Medrano, M. Ribas-Carbó, M. Tomás, Ü. Niinemets, Mesophyll

conductance to CO_2 and Rubisco as targets for improving intrinsic water use efficiency in C_3 plants, Plant Cell Environ. 39 (2015) 965–982.

Table 1. Water status of *H. vulgare* and *T. aestivum* plants subjected to different conditions (CL, control; 50% FC, 50% field capacity; 40% FC, 40% field capacity). Mean values ± SE are shown for pre-dawn leaf water potential (Ψ_{pd}), midday leaf water potential (Ψ_{md}) and RWC (leaf relative water content). Species and treatments effects were quantified by two-way ANOVA and differences between groups were addressed by LSD test. *P*-values are shown. n = 5 in all cases.

Species and treatments	**Ψ_{pd}** (MPa)	**Ψ_{md}** (MPa)	**RWC** (%)
H. vulgare – CL	-0.23 ± 0.01^{a}	-0.82 ± 0.04^{a}	90.62 ± 2.47^{a}
H. vulgare – 50% FC	-0.50 ± 0.09^{b}	-1.30 ± 0.09^{b}	88.39 ± 1.01^{ab}
H. vulgare – 40% FC	-1.80 ± 0.05^{c}	-2.15 ± 0.04^{c}	81.81 ± 2.39^{b}
T. aestivum – CL	-0.21 ± 0.03^{a}	-0.74 ± 0.08^{a}	94.15 ± 0.72^{a}
T. aestivum – 50% FC	-0.37 ± 0.01^{ab}	-1.40 ± 0.09^{b}	88.68 ± 0.31^{ab}
T. aestivum – 40% FC	-2.07 ± 0.11^{d}	-2.66 ± 0.16^{d}	67.44 ± 4.12^{c}
Species	0.369	0.023	0.046
Treatments	<0.001	<0.001	<0.001
Species:Treatments	0.012	0.018	0.002

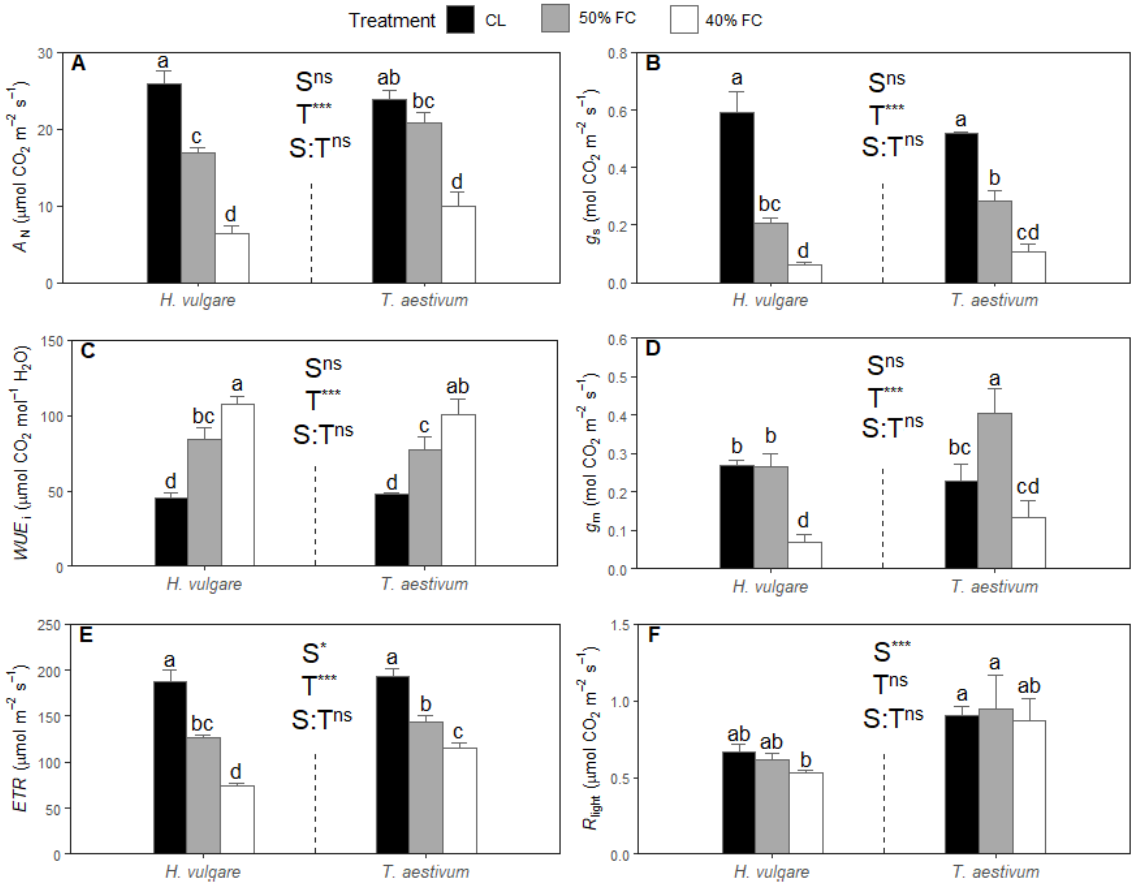

Fig. 1. Photosynthetic characterization of *H. vulgare* and *T. aestivum* plants subjected to different conditions (CL, control; 50% FC, 50% field capacity; 40% FC, 40% field capacity). (A) Net CO_2 assimilation (A_N), (B) stomatal conductance (g_s), (C) intrinsic water use efficiency (WUE_i), (D) mesophyll conductance (g_m), (E) electron transport rate (*ETR*) and (F) light respiration (R_{light}). Species (S) and treatments (T) effects were quantified by two-way ANOVA and differences between groups were addressed by LSD test. Different superscript letters indicate significant differences. Significance: *** P<0.001; ** <0.01; * <0.05; ^{ns} <0.5. Values are means ± SE (n = 5).

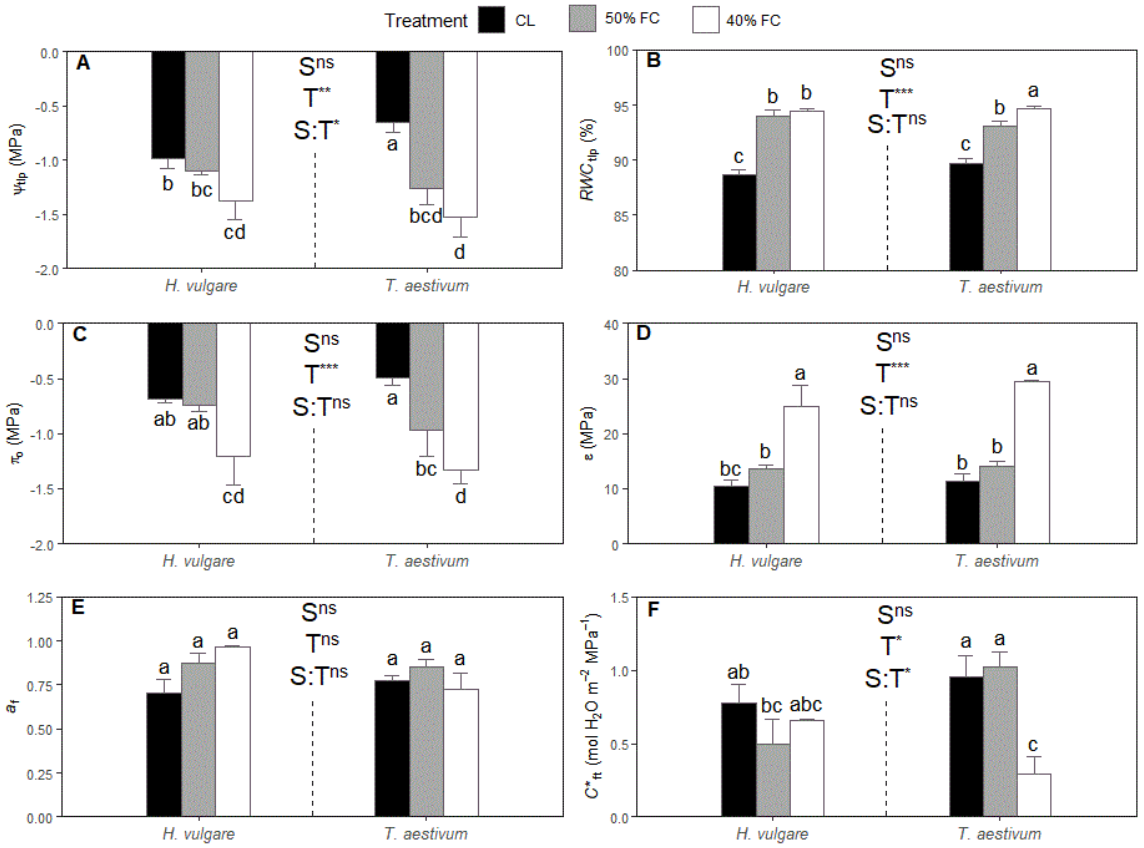

Fig. 2. Leaf water relations of *H. vulgare* and *T. aestivum* plants subjected to different conditions (CL, control; 50% FC, 50% field capacity; 40% FC, 40% field capacity). (A) Water potential at turgor loss point (Ψ_{tlp}), (B) relative water content at turgor loss point (RWC_{tlp}), (C) osmotic potential at full turgor (π_o), (D) bulk modulus of elasticity (ε), (E) apoplastic water fraction (a_f), and (F) leaf area specific capacitance at full turgor (C^*_{ft}). Species (S) and treatments (T) effects were quantified by two-way ANOVA and differences between groups were addressed by LSD test. Different superscript letters indicate significant differences. Significance: *** P<0.001; ** <0.01; * <0.05; ^{ns} <0.5. Values are means ± SE (n = 5).

Table 2. Leaf structural traits and cell wall composition of *H. vulgare* and *T. aestivum* plants subjected to different conditions (CL, control; 50% FC, 50% field capacity; 40% FC, 40% field capacity). Mean values ± SE are shown for leaf mass per area (LMA), leaf density (LD), alcohol insoluble residue (AIR), cellulose, hemicelluloses and pectins. Species and treatments effects were quantified by two-way ANOVA and differences between groups were addressed by LSD test. Different superscript letters indicate significant differences. *P*-values are shown. n = 5 in all cases.

Species and treatments	LMA ($g\ m^{-2}$)	LD ($g\ cm^{-3}$)	AIR (% extracted)	Cellulose ($mg\ g^{-1}$ AIR)	Hemicelluloses ($mg\ g^{-1}$ AIR)	Pectins ($mg\ g^{-1}$ AIR)
H. vulgare – CL	29.35 ± 0.99^{b}	0.11 ± 0.01^{b}	15.23 ± 2.47^{b}	228.99 ± 9.79^{b}	176.81 ± 15.19^{b}	26.75 ± 3.48^{c}
H. vulgare – 50% FC	40.18 ± 3.17^{a}	0.15 ± 0.02^{a}	18.72 ± 0.71^{b}	245.07 ± 12.25^{b}	179.66 ± 22.12^{b}	30.80 ± 1.15^{bc}
H. vulgare – 40% FC	41.40 ± 3.14^{a}	0.17 ± 0.01^{a}	24.88 ± 1.70^{a}	233.94 ± 4.26^{b}	229.37 ± 6.25^{a}	37.93 ± 0.52^{a}
T. aestivum – CL	41.83 ± 2.88^{a}	0.18 ± 0.01^{a}	16.41 ± 0.16^{b}	292.93 ± 3.78^{a}	227.71 ± 8.34^{a}	33.20 ± 0.77^{ab}
T. aestivum – 50% FC	38.49 ± 1.73^{a}	0.16 ± 0.01^{a}	17.38 ± 0.19^{b}	222.69 ± 12.37^{b}	207.00 ± 15.14^{ab}	29.02 ± 1.44^{bc}
T. aestivum – 40% FC	38.85 ± 1.99^{a}	0.17 ± 0.02^{a}	18.67 ± 0.79^{b}	227.08 ± 15.98^{b}	177.20 ± 15.78^{b}	36.49 ± 0.34^{a}
Species	0.292	0.023	0.075	0.214	0.607	0.326
Treatments	0.277	0.184	<0.001	0.026	0.644	<0.001
Species:Treatments	0.015	0.021	0.053	0.002	0.004	0.033

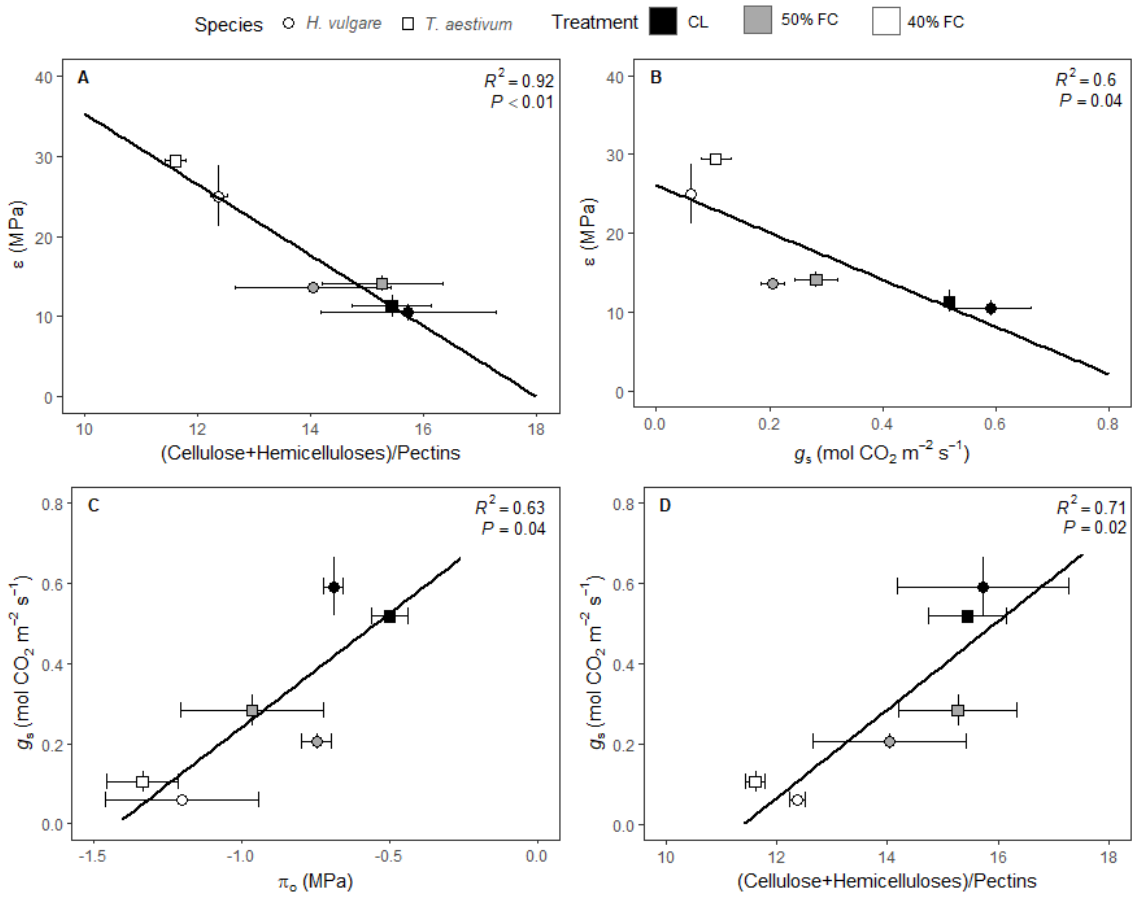

Fig. 3. Relationships between bulk modulus of elasticity (ε) and (A) (Cellulose+Hemicelluloses)/Pectins ratio and (B) stomatal conductance (g_s) and relationships between g_s and (C) osmotic potential at full turgor (π_o) and (D) (Cellulose+Hemicelluloses)/Pectins ratio in *H. vulgare* and *T. aestivum* plants subjected to different conditions (CL, control; 50% FC, 50% field capacity; 40% FC, 40% field capacity). n = 5 (means ± SE).

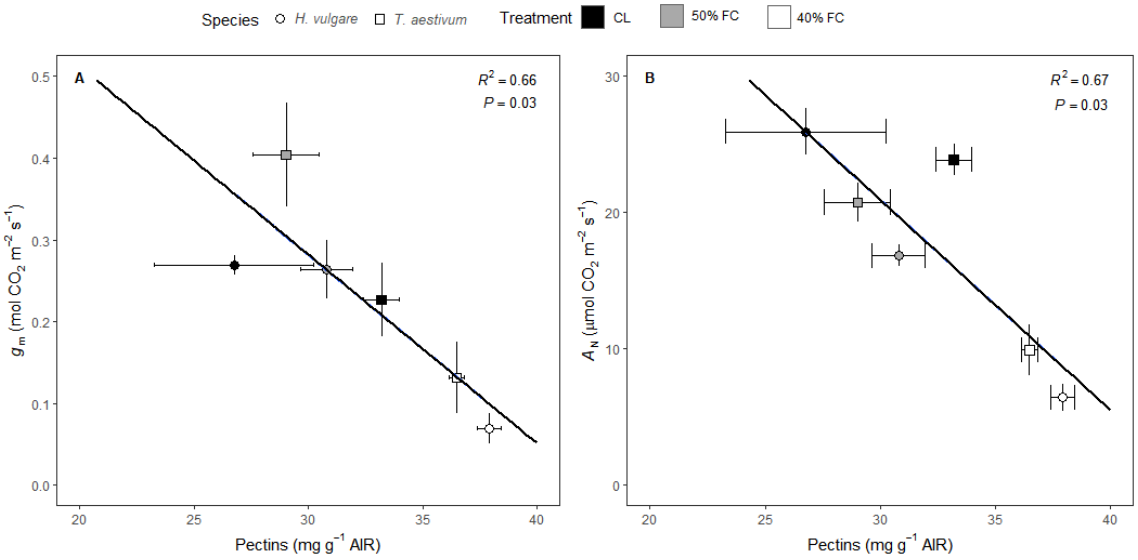

Fig. 4. (A) Relationship between mesophyll conductance (g_m) and pectins content and (B) relationship between net CO_2 assimilation (A_N) and pectins content in *H. vulgare* and *T. aestivum* plants subjected to different conditions (CL, control; 50% FC, 50% field capacity; 40% FC, 40% field capacity). n = 5 (means ± SE).

Table S1. Pearson correlation matrix of photosynthetic, leaf water relations and cell wall parameters measured in *T. aestivum* and *H. vulgare* plants subjected to different conditions. Values in italics and bold indicate significant (P<0.05) and highly significant (P<0.01) correlation coefficients, respectively.

	A_N	g_s	*WUE*	g_m	*ETR*	R_{light}	AIR	Cel	Hemicel	Pectin	(Cel+Hemicel) /Pectin	π_o	RWC_{tlp}	π_{tlp}	ε	a_f	C^*_{ft}	LMA	LD
A_N		***0.94***	***-0.96***	0.74	***0.95***	0.38	*-0.89*	0.35	-0.14	*-0.86*	***0.95***	*0.85*	0.44	0.79	*-0.91*	-0.55	0.65	-0.51	-0.49
gs			***-0.99***	0.49	***0.96***	0.26	-0.81	0.43	-0.06	-0.72	*0.88*	*0.84*	0.4	*0.83*	*-0.82*	-0.62	0.6	-0.57	-0.52
WUE				-0.53	***-0.97***	-0.29	*0.82*	-0.49	0.04	0.72	*-0.9*	*-0.88*	-0.45	*-0.87*	*0.86*	0.59	-0.62	0.5	0.46
g_m					0.56	0.49	-0.68	-0.08	-0.2	*-0.85*	0.77	0.49	0.38	0.34	-0.73	-0.2	0.6	-0.3	-0.29
ETR						0.47	*-0.91*	0.49	-0.12	-0.7	*0.84*	*0.82*	0.51	*0.82*	-0.79	-0.71	0.54	-0.46	-0.39
R_{light}							-0.58	0.21	0.05	-0.16	0.26	0.09	0.79	0.14	-0.1	-0.49	0.35	0.11	0.36
AIR								-0.22	0.45	0.77	-0.71	-0.63	-0.36	-0.56	0.66	*-0.82*	-0.33	0.54	0.47
Cel									0.49	0.12	0.33	0.67	0.59	0.8	-0.39	-0.09	0.32	0.55	0.37
Hemicel										0.43	0.07	0.09	0.61	0.25	-0.01	0.55	0.57	0.6	0.68
Pectin											*-0.85*	-0.63	-0.07	-0.46	*0.83*	0.39	-0.48	0.69	0.73
(Cel+Hemicel)/ Pectin													0.47	0.8	***-0.97***	-0.28	0.81	-0.41	-0.41
π_o													0.39	***0.97***	***-0.93***	-0.26	0.57	-0.19	-0.31
RWC_{tlp}														0.5	-0.34	-0.14	0.73	0.33	0.52
π_{tlp}															*-0.84*	-0.27	0.59	-0.08	-0.16
ε																0.19	-0.69	0.35	0.44
a_f																	0.07	0.6	0.44
*C*ft*																		-0.08	0.04
LMA																			***0.93***
LD																			

Distinct photosynthetic regulation under water shortage and recovery in tomato genotypes: water relations, leaf anatomy, and cell wall composition

Margalida Roig-Oliver[1*], Mateu Fullana-Pericàs[1], Josefina Bota[1], Jaume Flexas[1,2]

[1]Research Group on Plant Biology under Mediterranean Conditions, Departament de Biologia, Universitat de les Illes Balears (UIB) – Agro-Environmental and Water Economics Institute (INAGEA). Carretera de Valldemossa Km 7.5, 07122 Palma, Illes Balears, Spain.
[2]King Abdulaziz University, Jeddah, Saudi Arabia.

[*] Corresponding author.

Submitted to *Plant, Cell & Environment* on 23rd May 2021.

Distinct photosynthetic regulation under water shortage and recovery in tomato genotypes: water relations, leaf anatomy, and cell wall composition

Margalida Roig-Oliver[1], Mateu Fullana-Pericàs[1], Josefina Bota[1], Jaume Flexas[1,2]

Running head: Tomato genotypes differently face water shortage.

[1]Research Group on Plant Biology under Mediterranean Conditions, Departament de Biologia, Universitat de les Illes Balears (UIB) – Agro-Environmental and Water Economics Institute (INAGEA). Carretera de Valldemossa Km 7.5, 07122 Palma, Illes Balears, Spain.
[2]King Abdulaziz University, P.O. Box 80200 Jeddah 21589, Saudi Arabia.

Corresponding author: margaroig93@gmail.com

Funding
This work was supported by the project PGC2018-093824-B-C41 from Ministerio de Economía y Competitividad (MINECO, Spain) and the ERDF (FEDER). MR-O was supported by a predoctoral fellowship FPU16/01544 from MINECO.

Abstract
Water shortage strongly affects plants physiological performance. Since tomato (*Solanum lycopersicum*) non-long shelf-life (nLSL) and long shelf-life (LSL) genotypes differently face water deprivation, we subjected a nLSL and a LSL genotype to four treatments: control (i.e., well-watering), short-term water deficit stress at 40% field capacity (ST 40% FC), short-term water deficit stress at 30% FC (ST 30% FC) and short-term water deficit stress at 30% FC followed by recovery (ST 30% FC-Rec). Treatments imposition promoted genotypic-dependent elastic adjustments that were accompanied by distinct photosynthetic responses. Whilst the nLSL genotype largely modified mesophyll conductance (g_m) across experimental conditions, it was kept within a narrow range in the LSL. Particularly, modifications in the relative abundance between cell wall compounds and in sub-cellular anatomic parameters such as the chloroplasts surface area exposed to intercellular air spaces per leaf area (S_c/S) and the cell wall thickness (T_{cw}),

regulated g_m in the LSL genotype. Instead, only changes in foliar structure at supra-cellular level influenced g_m in the nLSL genotype. Thus, we demonstrate for the first time that even genotypes of the same species can present different elastic, anatomic and cell wall composition mediated-mechanisms to regulate g_m and photosynthesis when subjected to distinct water regimes.

Key words

Bulk modulus of elasticity, cell wall composition, cell wall thickness, genotype, mesophyll conductance, pectins, photosynthesis, tomato, water deficit stress.

Acknowledgements

We thank Dr Miquel À. Conesa for his help with genotypes selection.

Introduction

Water scarcity is one of the most relevant abiotic stresses limiting photosynthesis and, thus, plants growth and productivity (Flexas, Bota, Loreto, Cornic, & Sharkey, 2004; Chaves, Flexas, & Pinheiro, 2009; Nadal & Flexas, 2019). In the present scenario of climate change, which is mainly characterized by increased temperatures and large reductions in the water supply, agriculture is one of the most affected sectors (Morison, Baker, Mullineaux, & Davies, 2008). Together with the desertification of several regions, global population is predicted to rise during the next decades, enhancing the demand from crops production (Tilman, Cassman, Matson, Naylor, & Polasky, 2002; Schultz, 2016). Since one of the major challenges for plant physiology is to improve crops' productivity (Evans, 1997; Long, Zhu, Naidu, & Ort, 2006; Wu, Hammer, Doherty, von Caemmerer, & Farquhar, 2019), there is a need to select drought-resistant genotypes to ensure food requirements (Mickelbart, Hasegawa, & Bailey-Serres, 2015).

Tomato (*Solanum lycopersicum* L.) is among the most produced and consumed horticultural crops worldwide, accounting for more than 83000 available genotypes (FAO, 2021). During centuries, tomato has undergone diverse cultivation practices partially based on the conditions of each region, leading to the distinctive adaptation of different landraces to specific areas (Cebolla-Cornejo, Rosselló, & Nuez, 2013; Bota et al., 2014; Cortés-Olmos, Valcárcel, Rosselló, Díez, & Cebolla-Corneho, 2015; Flores, Sánchez, Fenoll, & Hellin, 2017; Fullana-Pericàs et al., 2017, 2019; Conesa, Fullana-Pericàs, Granell, & Galmés, 2020). Particularly, the Western Mediterranean long shelf-

life (LSL) tomato landraces have been traditionally selected according to their fruit phenotype, which remain without signs of deterioration for more than 6-12 months after harvested (Saladié et al., 2007; Bota et al., 2014; Conesa et al., 2014; Manzo et al., 2018). Besides this particularity regarding fruits conservation, LSL genotypes in their vegetative state have been also related to drought tolerance because of molecular, morphological, physiological, and biochemical adaptations (Galmés et al., 2011, 2013; Fullana-Pericàs et al., 2017, 2019; Tranchida-Lombardo et al., 2018). Specifically, Galmés et al. (2011) demonstrated that LSL genotypes exhibited larger intrinsic water use efficiency (WUE_i) than non-long shelf-life (nLSL) ones when subjected to water deficit stress, minimizing reductions in net CO_2 assimilation (A_N) as compared to stomatal conductance (g_s) declines. In fact, this enlarged WUE_i has been correlated positively with the ratio between mesophyll and stomatal conductances (i.e., the g_m/g_s ratio), with stomatal traits and distribution as well as with mesophyll anatomical properties (Galmés et al., 2011, 2013; Fullana-Pericàs et al., 2017; Conesa et al., 2020). Besides the gas-exchange perspective, drought also induced changes in the foliar structure and in leaf water relations parameters, particularly, in the leaf mass per area (LMA) and in the bulk modulus of elasticity (ε) (Galmés et al., 2011). However, the existence of other strategies which could distinctively affect the physiological performance of tomato LSL and nLSL genotypes subjected to water deficit stress are still unknown (Conesa et al., 2020).

Recent studies have demonstrated that modifications in cell wall composition determined photosynthesis performance, leaf water relations and/or anatomical adjustments in different species subjected to contrasting abiotic conditions such as water deprivation (Clemente-Moreno et al., 2019, Roig-Oliver et al., 2020a; Roig-Oliver, Nadal, Bota, & Flexas, 2020b; Roig-Oliver, Nadal, Clemente-Moreno, Bota, & Flexas, 2020c). From their results, it has been shown that each species presented changes in g_m, ε and cell wall thickness (T_{cw}) which were differently related to modifications in specific cell wall compounds, suggesting that these relationships could be species-specific (Flexas et al., 2021). Nevertheless, to the best of our knowledge, only the study by Ye et al. (2020) evaluated how changes in cell wall composition influenced g_m and T_{cw} in distinct genotypes of the same species. Particularly, they did not find correlations among these parameters analysing eight rice genotypes subjected to well-watering conditions. However, grasses present a very characteristic cell wall composition within angiosperms (Carpita, 1996; Carpita & McCann, 2002), which makes their results difficult to extrapolate to other species. Since water deprivation affects cell wall composition (Sweet,

Morrison, Labavitch, & Matthews, 1999; Tenhaken, 2015; Rui & Dinnery, 2019; Clemente-Moreno et al., 2019; Nadal, Roig-Oliver, Bota, & Flexas, 2020; Roig-Oliver et al., 2020a,b,c) and induces changes in photosynthesis, leaf water relations and anatomical characteristics even at genotype level (Galmés et al., 2011, 2013; Fullana-Pericàs et al., 2017, 2019), we tested a tomato LSL with a nLSL genotype subjected to distinct levels of water shortage. Additionally, a recovery treatment was applied to separate the commonly proportional responses between g_s and g_m (Flexas et al., 2013) to exclusively connect cell wall, anatomic and elastic modifications to g_m. Thus, our hypothesis is that cell wall thickness and composition change more plastically in the LSL genotype in response to distinct water availability treatments, differentially determining g_m, ε and T_{cw} in both genotypes.

Materials and methods

Plant material selection and preparation

Tomato genotypes selection was based on their leaf morphology and growth type since these traits influence their physiological performance (Galmés et al., 2011). The 'Ailsa Craig' genotype was used as nLSL genotype, whilst a 'de Ramellet' genotype (accession UIB1-28 according to the University of the Balearic Islands seed bank code) was employed as LSL genotype. Whilst seeds of nLSL genotype were kindly provided by Dr Eva Domínguez (EELM-CSIC, Malaga), LSL seeds were obtained from the University of the Balearic Islands seed bank. Both genotypes presented indeterminate growth and the common divided tomato leaf morphology.

Following Fullana-Pericàs et al. (2019), an antiviral treatment was addressed to all seeds before the sowing. They were submerged in a 10% sodium triphosphate solution for 3 h to be subsequently cleaned with distilled water. Then, seeds were submerged in a 30% commercial bleach solution for 1 h, they were washed again with distilled water and they were air-dried at room temperature for 24 h. Seeds were kept in a hermetic container filled with silica gel for, at least, 24 h before been placed in an oven at 70ºC for 24 h.

Growth conditions and experimental design

After the application of the antiviral treatment, seeds were sown individually in water-irrigated 3 L pots containing a substrate mixture of peat and perlite (3:1, v/v). All pots were placed in a growth chamber at 25ºC receiving 300 µmol m^{-2} s^{-1} photosynthetic photon flux density (PPFD) for 12 h followed by 12 h of darkness. Pots were daily

monitored to be watered to 100% field capacity (FC) by replacing evapo-transpired water, receiving Hoagland's solution 50% once a week. Twenty-eight days after the sowing –when all plants presented, at least, 3-4 fully developed leaves–, four treatments were established: (i) control (CL, i.e., without stress), (ii) short-term water deficit stress at 40% FC (ST 40% FC), (iii) short-term water deficit stress at 30% FC (ST 30% FC) and (iv) short-term water deficit stress at 30% FC followed by a recovery (ST 30% FC-Rec). Five individual replicates per genotype were randomly subjected to each treatment. Control plants were always maintained at 100% FC. For other treatments, a cessation of water irrigation was imposed until reaching 40% FC (ST 40% FC) or 30% FC (ST 30% FC and ST 30% FC-Rec). Once a specific FC was reached –near after 6 days for ST 40% FC and 9 days for ST 30% and ST 30%-Rec–, it was maintained. ST 30% FC-Rec was identical to ST 30% FC treatment, but a 2-days recovery until reaching 100% FC was applied. In all cases, plants water status was monitored every day weighing the pots to be maintained at a specific FC by replacing evapo-transpired water. All measurements were performed when plants were 40-days old.

Plants water status

The pre-dawn and the midday leaf water potentials (Ψ_{pd} and Ψ_{md}, respectively) of each plant were determined in fully developed leaves using a pressure chamber (Model 600D; PMS Instrument Company, Albany, OR, USA). Additionally, those leaves used to determine Ψ_{md} were employed for the leaf relative water content (RWC) estimation. Thus, leaves were immediately weighted after measuring the Ψ_{md}, obtaining the fresh weight (FW). Afterward, they were rehydrated overnight in distilled water under darkness at 4ºC. The next morning, leaves were weighted to determine the turgid weight (TW). Finally, they were placed in an oven at 70ºC for, at least, 72 h to obtain the dry weight (DW). From these measurements, RWC was calculated as:

$$\mathrm{RWC} = \frac{\mathrm{FW} - \mathrm{DW}}{\mathrm{TW} - \mathrm{DW}} \times 100$$

Foliar structure

Those leaves used to determine Ψ_{md} and RWC were also employed to estimate the leaf mass per area (LMA) and the leaf density (LD). Thus, when leaves were rehydrated, they were photographed to calculate the leaf area with ImageJ software (Wayne

Rasband/NIH). Additionally, leaves thickness was estimated from five measurements per leaf avoiding main veins with a digital caliper. Whilst LMA was calculated from the relationship between DW and leaf area, LD was estimated as thickness per area.

Gas exchange and fluorescence measurements

A fully developed leaf per plant (second or third from the apex) was chosen to perform gas exchange and chlorophyll *a* fluorescence measurements using an infrared gas analyser coupled with a 2 cm^2 fluorometer chamber (Li-6400-40; Li-Cor Inc., Lincoln, NE, USA). The block temperature was kept at 25ºC, the vapour pressure deficit (VPD) at around 1.5 kPa, the air flow rate at 300 μmol air min^{-1}, the light-saturating photosynthetic active radiation (PAR) at 1500 μmol m^{-2} s^{-1} (90–10% red-blue light) and the CO_2 ambient concentration (C_a) at 400 μmol CO_2 mol^{-1} air. When steady-state conditions were achieved (usually after 15-20 minutes), measurements for net CO_2 assimilation (A_N), stomatal conductance (g_s), CO_2 concentration at the sub-stomatal cavity (C_i) and steady-state fluorescence (F_s) were registered in the gas exchange system. Then, a saturating light flash was applied to obtain the maximum fluorescence (F_m'). From these values, the real quantum efficiency of photosystem II (Φ_{PSII}) was recorded. According to Valentini, Epron, Angelis, Matteucci, & Dreyer (1995), light curves under non-photorespiratory conditions (1% O_2) were performed for the electron transport rate (*ETR*) calculation. The light respiration (R_{light}) was calculated as half the dark-adapted mitochondrial respiration after plants exposition to darkness for 30 minutes (Niinemets, Cescatti, Rodeghiero, & Tosens, 2005). With previous values, mesophyll conductance (g_m) was calculated as described in Harley, Loreto, Di Marco, & Sharkey (1992) using the tomato value for the CO_2 compensation point in the absence of respiration (Γ^*) reported by Hermida-Carrera, Kapralov, & Galmés (2016).

Photosynthesis limitations analysis

Photosynthesis limitations were estimated following Grassi & Magnani (2005). On one hand, *absolute* stomatal (l_s), mesophyll (l_m) and biochemical (l_b) limitations were calculated per each genotype and treatment. Additionally, *relative* stomatal (*SL*), mesophyll (*ML*) and biochemical (*BL*) contributions to d*A*/*A* from a control to a water deficit stress state and during recovery were calculated assuming that the maximum A_N per genotype corresponded to that measured under control conditions.

Anatomical characterization

At the end of gas exchange performance, small portions of those leaves enclosed in the IRGA cuvette were cut avoiding main veins. They were fixed under vacuum pressure with a glutaraldehyde 4% and paraformaldehyde 2% solution prepared in a 0.01 M phosphate buffer (pH 7.4). Then, samples were post-fixed for 2 h in 2% buffered osmium tetroxide to be dehydrated by a graded ethanol series. Obtained pieces were embedded in LR resin (London Resin Company) and were placed in an oven at 60ºC for 48 h (Tosens, Niinemets, Vislap, Eichelmann, & Castro-Díez, 2012; Tomás et al., 2013).

Semi-fine and ultra-fine (0.8 μm and 90 nm, respectively) cross sections were cut with an ultramicrotome (Leica UC6, Vienna, Austria). Semi-fine cross sections were dyed with 1% toluidine blue to be photographed at 200X magnifications with a digital camera (U-TVO.5XC; Olympus, Tokyo, Japan) coupled with an Olympus BX60 optic microscope. From these pictures, leaf thickness (T_{leaf}), mesophyll thickness (T_{mes}), and fraction of mesophyll intercellular air spaces (f_{ias}) were calculated. Ultra-fine cross sections were contrasted with uranyl acetate and lead citrate to be photographed at 1500X and 30000X magnifications with a transmission electron microscopy (TEM H600; Hitachi, Tokyo, Japan). Pictures at 1500X magnifications were used to calculate chloroplasts thickness (T_{chl}), chloroplasts length (L_{chl}), mesophyll and chloroplasts surface area exposed to intercellular air spaces per leaf area (S_m/S and S_c/S, respectively) and the S_c/S_m ratio. From pictures at 30000X magnifications, the cell wall thickness (T_{cw}) was calculated. Following Thain (1983), a cell curvature correction factor was determined performing an average length-width ratio of 5 cells per mesophyll type (palisade or spongy). Values for all parameters were averaged from 10 measurements addressed in randomly selected cell structures using ImageJ. Finally, g_m was calculated based on anatomical particularities according to Tomás et al. (2013).

Pressure-volume curves

A fully developed leaf per plant adjacent to that employed for gas exchange measurements was chosen to perform pressure-volume (*P–V*) curves. Entire leaves (including the petiole) were cut to be rehydrated in distilled water under darkness overnight. The next morning, leaves water potential was measured with a pressure chamber (Model 600D; PMS Instrument Company), being subsequently weighted. From *P–V* curves, the leaf water potential at turgor loss point (Ψ_{tlp}), the relative water content at turgor loss point (RWC_{tlp}), the leaf osmotic potential at full turgor (π_o), the bulk

modulus of elasticity (ε), the apoplastic water fraction (a_f), and the leaf area specific capacitance at full turgor (C^*_{ft}) were calculated (Sack, Cowan, Jaikumar, & Holbrook, 2003; Sack & Pasquet-Kok, 2011).

Cell wall extraction and fractionation

The same leaves employed for gas exchange measurements were kept under darkness overnight to minimize starch accumulation. The following morning, around 700 mg of fresh foliar tissue per plant were cut in small portions to be boiled until bleached in screwed-capped tubes filled with absolute ethanol. Then, they were cleaned twice with acetone >95% to obtain the alcohol insoluble residue (AIR), an approximation of the total isolated cell wall material. AIRs were dried at room temperature and an α-amylase digestion was addressed to remove starch remains. Then, 3 analytical replicates of each AIR weighting 3 mg, approximately, were hydrolysed with 2 M trifluoroacetic acid (TFA) at 121ºC. After 1 h, samples were centrifuged obtaining an aqueous supernatant and a pellet. Whilst supernatants were directly employed for hemicelluloses and pectins quantifications, pellets were cleaned twice with distilled water and acetone >95% to eliminate TFA residues. The dry pellet (i.e., cellulose) was hydrolysed with 200 µl sulphuric acid 72% (w/v) for 1 h, diluted to 6 ml with distilled water and heated at 121ºC until degradation. Cellulose and hemicelluloses quantifications were performed by the phenol-sulphuric acid colorimetric procedure (Dubois, Gilles, Hamilton, Rebers, & Smith, 1956). Samples absorbance was read at 490 nm and cellulose and hemicelluloses contents were calculated interpolating samples values from a glucose calibration curve. Pectins quantification was addressed by the colorimetric method of Blumenkrantz & Asboe-Hansen (1973) using 2-hydroxybiphenil as a reagent. Samples absorbance was read at 520 nm and pectins content was estimated interpolating samples values from a galacturonic acid calibration curve. A Multiskan Sky Microplate spectrophotometer (ThermoFisher Scientific) was employed in all cases.

Statistical analysis

Prior to perform statistics, Thompson test was used to detect and eliminate outliers in the database. Then, two-way analysis of variance (ANOVA) with subsequent LSD test was addressed to identify statistically significant ($P<0.05$) "genotypes", "treatments" and "genotypes:treatments" effects. Also, Pearson's correlation matrices were performed in each genotype to find correlations between all tested parameters, being significant and

highly significant when $P<0.05$ and $P<0.01$, respectively. Finally, linear regressions between photosynthetic, leaf water relations, anatomical and cell wall composition parameters were fitted using mean values per genotypes and treatments. All these analyses were done with R software (ver. 3.2.2; R Core Team, Vienna, Austria).

Results

Plants water status

Both genotypes presented non-significant differences for Ψ_{pd} between CL and ST 40% FC (Table 1). However, an almost 4-fold decrease was detected under ST 30% FC in both cases (Table 1). Although the nLSL genotype presented significant Ψ_{md} reductions under ST 40% FC as compared to CL (-0.96 ± 0.03 and -0.40 ± 0.01 MPa, respectively), these declines were only significant under ST 30% FC in the LSL (Table 1). Despite that RWC reductions were only significant under ST 30% FC in the nLSL genotype, it was progressively reduced during the imposition of water deficit stress treatments in the LSL (Table 1). Remarkably, RWC reduction under ST 30% FC was much larger in the nLSL genotype than in LSL (Table 1). In all cases, both genotypes restored previous parameters to CL values after ST 30% FC-Rec (Table 1).

Pressure-volume curves

In both genotypes, decreasing in Ψ_{tlp} was specifically attributed to treatments effect, achieving the lowest values under ST 30% FC (Fig. 1A). Whereas recovery almost restored Ψ_{tlp} to CL in the LSL, it remained significantly lower in the nLSL (-0.62 ± 0.02 and -0.53 ± 0.03 MPa; Fig. 1A). RWC_{tlp} gradually increased after the application of water shortage treatments, being almost restored to CL in both genotypes upon recovery (Fig. 1B). Notice that, despite the previously mentioned difference regarding RWC in both genotypes under ST 30% FC, both were below the wilting point according to RWC_{tlp} values (Table 1, Fig. 1B). Although the pattern for π_o resembled that of Ψ_{tlp}, both genotypes achieved similar values under ST 30% FC-Rec, remaining significantly lower than under CL (-0.45 ± 0.04 and -0.44 ± 0.03 MPa for nLSL and LSL, respectively; Fig. 1C). Concerning ε, ST 30% FC imposition increased 28% and 81% leaves rigidity in nLSL and LSL genotypes, respectively, as compared to CL (Fig. 1D). Even though recovery restored ε to CL in the nLSL, it rested slightly enhanced in the LSL (6.93 ± 2.61 MPa; Fig. 1D). The nLSL genotype significantly increased a_f in all tested conditions in comparison to CL, whilst it was similarly maintained across all treatments in the LSL

(Fig. 1E). A significant C^*_{ft} decrease from 2.32 ± 0.40 to 1.21 ± 0.05 mol H_2O m^2 MPa^{-1} was observed in the LSL genotype under ST 30% FC in comparison to CL, resting almost similar to ST 30% FC upon recovery (Fig. 1F). However, C^*_{ft} was almost maintained across all tested conditions in the nLSL genotype (Fig. 1F).

Photosynthetic characterization

The highest A_N was found in the LSL genotype under CL (20.23 ± 0.17 µmol CO_2 m^{-2} s^{-1}), being followed by the nLSL under the same condition (17.64 ± 0.86 µmol m^{-2} s^{-1}; Fig. 2A). ST 40% FC promoted A_N declines of around 67% and 60% in nLSL and LSL, respectively, in comparison to CL (Fig. 2A). Nonetheless, both genotypes reached similar A_N under ST 30% FC (1.18 ± 0.09 and 1.61 ± 0.21 µmol CO_2 m^{-2} s^{-1} for nLSL and LSL, respectively) and upon recovery, remaining significantly lower than under CL (Fig. 2A). Both genotypes achieved similar g_s under ST 40% FC and ST 30% FC, the latter representing 97% CL reductions (Fig. 2B). Even though g_s did not reach CL values under ST 30% FC-Rec, the LSL genotype exhibited larger g_s than the nLSL under this condition (0.32 ± 0.02 and 0.20 ± 0.01 mol CO_2 m^{-2} s^{-1}; Fig. 2B). Although both genotypes presented similar WUE_i under CL, the nLSL reached the highest under ST 40% FC (109.21 ± 8.82 µmol CO_2 mol^{-1} H_2O; Fig. 2C). However, the LSL progressively enhanced WUE_i during the application of water shortage treatments, reaching the largest value under ST 30% FC (125.04 ± 8.50 µmol CO_2 mol^{-1} H_2O; Fig. 2C). The LSL restored WUE_i to CL upon recovery, whereas it rested significantly larger than CL in the nLSL (61.42 ± 2.00 and 43.63 ± 0.82 µmol CO_2 mol^{-1} H_2O; Fig. 2C). The nLSL genotype presented the highest g_m under CL (0.24 ± 0.02 mol CO_2 m^{-2} s^{-1}), which was almost 2-fold larger than that of LSL under the same condition (Fig. 2D). Also, the nLSL showed 54% and 95% lower g_m than CL under ST 40% FC and ST 30% FC, respectively (Fig. 2D). However, in the LSL, g_m reductions were only found under ST 30% FC, representing 5-fold larger g_m than that of the nLSL under the same condition (Fig. 2D). Whilst ST 30% FC-Rec restored g_m to CL in the LSL genotype, it rested similarly to FC 40% FC in the nLSL (Fig. 2D). The largest *ETR* was detected in the LSL under CL (198.50 ± 14.14 µmol m^{-2} s^{-1}), being followed by the nLSL under this condition (140.27 ± 9.07 µmol m^{-2} s^{-1}; Fig. 2E). Nonetheless, water deficit stress treatments significantly reduced *ETR* in both genotypes, reaching the lowest values under ST 30% FC (40.40 ± 2.17 and 45.05 ± 0.18 µmol m^{-2} s^{-1} for nLSL and LSL, respectively; Fig. 2E). Although recovery almost restored *ETR* to CL in the nLSL genotype, declines of around 40% were detected in the LSL (Fig. 2E).

Whilst LSL genotype presented the largest R_{light} under CL (1.43 ± 0.07 µmol CO_2 m^{-2} s^{-1}), it decreased due to water shortage treatments in both genotypes, reaching the lowest value in the nLSL under ST 30% FC (0.71 ± 0.15 µmol CO_2 m^{-2} s^{-1}; Fig. 2F). Recovery restored R_{light} to CL value in the nLSL, but it rested significantly lower in the LSL (Fig. 2F).

Photosynthesis limitations analyses are found in Table 2. Whilst l_b was the main photosynthesis *absolute* limitation in the nLSL genotype under CL, both l_m and l_b similarly co-limited A_N in the LSL. Under ST 40% FC and upon recovery, only l_b limited photosynthesis in both genotypes. Although l_m was the main photosynthesis limitation in the nLSL genotype under ST 30% FC, l_s and l_b co-limited A_N in the LSL. Concerning *relative* limitations contribution to d*A*/*A*, *SL* and *BL* co-limited A_N under ST 40% FC in both genotypes. However, under ST 30% FC, only *ML* limited photosynthesis in the nLSL genotype, whereas *SL* was the main photosynthetic determinant in the LSL. Upon recovery, A_N was similarly co-limited by *ML* and *BL* in both genotypes.

Cell wall composition characterization

Differences in leaf cell wall composition were mainly attributed to genotypes effect (Table 3). The highest AIR amount was detected in the LSL genotype under CL, whereas the lowest were found in the nLSL across all conditions (Table 3). Although nLSL genotype presented larger cellulose than LSL, slightly higher amounts of hemicelluloses were detected in the LSL across all tested conditions as compared to the nLSL, especially under CL (Table 3). Finally, pectins were the unique cell wall component presenting significant differences due to genotypes and treatments effects as well as in the interaction term (Table 3). Whereas a tendency to increase pectins content was found in both genotypes when applying water deprivation, larger pectins quantity was observed in the nLSL genotype (Table 3). Upon recovery, pectins were similarly maintained to water shortage treatments in nLSL genotype, whilst they remained significantly higher than CL in the LSL (Table 3).

Foliar structure and anatomical characterization

Concerning foliar structure, LMA changes were exclusively attributed to a genotype effect since LSL presented slightly larger values than the nLSL (Table 4). However, no significant differences were found for LD (Table 4). Regarding anatomical characterization from semi-fine cross sections, both genotypes presented the largest T_{leaf}

under CL, being slightly higher in the LSL (238.03 ± 3.77 µm; Table 4). Although T_{leaf} was gradually reduced in the nLSL genotype due to water shortage application, the lowest value in the LSL was observed under ST 40% FC (187.66 ± 5.27 µm; Table 4). Upon recovery, T_{leaf} rested 20% and 12% lower than under CL in nLSL and LSL, respectively (Table 4). A similar pattern was found for T_{mes} (Table 4). Finally, only a significant genotype effect was detected for f_{ias} since the nLSL presented larger porosity than the LSL (Table 4). In relation to the analysis of ultra-fine cross sections, water deprivation treatments and ST 30% FC-Rec promoted declines in T_{chl} and L_{chl} as compared to CL in both genotypes (Table 5). Also, water deficit stress reduced S_m/S and S_c/S in both genotypes, being almost restored to CL upon recovery in the LSL (Table 5). Instead, ST 30% FC-Rec presented even lower S_m/S and S_c/S than water shortage treatments in the nLSL (Table 5). Both genotypes exhibited the largest S_c/S_m under CL (Table 5). Although nLSL achieved the lowest S_c/S_m under ST 40% FC, it was gradually reduced during water deprivation in the LSL (Table 5). Upon recovery, S_c/S_m was almost restored to CL in the nLSL, whilst it rested significantly lower in the LSL (Table 5). Changes in T_{cw} were exclusively attributed to treatments effect (Table 5). Even though water shortage treatments decreased T_{cw} in the LSL genotype, it was maintained to CL in the nLSL (Table 5). Nonetheless, whereas the CL value was almost restored upon recovery in the LSL genotype, T_{cw} increased in the nLSL under the same condition (Table 5). Finally, the statistical analysis performed for g_m estimation based on anatomical measurements revealed that only the treatment effect was significant since g_m significantly decreased under water deficit stress as well as upon recovery in comparison to CL in both genotypes (Table S1).

Relationships between parameters

Correlations between all tested parameters for each genotype are found in Tables S2 and S3. Notoriously, despite non-significant correlations were detected between photosynthetic, leaf water relations, sub-cellular anatomic and cell wall composition parameters in the nLSL genotype, significant relationships were observed for the LSL (Figs. 3 and 4). Hence, whilst g_m correlated positively with the (Cellulose+Hemicelluloses)/Pectins ratio (R^2=0.99, P<0.01, Fig. 3A), a negative relationship with ε was found (R^2=0.97, P=0.01, Fig. 3B). In turn, ε and the (Cellulose+Hemicelluloses)/Pectins ratio were linked negatively (R^2=0.95, P=0.02, Fig. 3C). Positive correlations between g_m and S_c/S and T_{cw} were detected (R^2=0.92, P=0.03,

Fig. 4A and R^2=0.99, P<0.01, Fig. 4B, respectively). Although ε and S_c/S were non-significantly linked (Fig. 4C), a negative relationship between ε and T_{cw} was observed (R^2=0.95, P=0.02, Fig. 4D). Finally, a positive relationship between S_c/S and the (Cellulose+Hemicelluloses)/Pectins ratio was found (R^2=0.94, P=0.02, Fig. 4E), as well as for T_{cw} and the (Cellulose+Hemicelluloses)/Pectins ratio (R^2=0.99, P<0.01, Fig. 4F). Regarding those significant correlations exclusively detected in the nLSL genotype, g_m was linked negatively with LMA (R^2=0.98, P<0.01, Fig. 5A). However, positive relationships between g_m and T_{leaf} and T_{mes} were found (R^2=0.92, P=0.03, Fig. 5C and R^2=0.97, P=0.01, Fig. 5D, respectively).

Discussion

Water shortage is recognized as one of the most important abiotic stresses affecting plants physiological performance (Flexas et al., 2004; Chaves et al., 2009; Nadal & Flexas, 2019). In fact, changes in leaf water relations –particularly, osmotic and elastic adjustments– usually occur under water deficit stress (Lu Gullo & Salleo, 1988; Abrams, 1990; Kubiske & Abrams, 1991; Galmés et al., 2011; Bartlett, Scoffoni, & Sack, 2012; Turner, 2018; Nadal et al., 2020; Xiong & Nadal, 2020). In our study, we detected π_o declines in both genotypes once subjected to water deprivation, as commonly described (Lu Gullo & Salleo, 1988; Abrams, 1990; Kubiske & Abrams, 1991; Bartlett et al., 2012; Turner, 2018; Nadal et al., 2020). Although both genotypes presented similar π_o reductions under water shortage, elastic modifications were of higher relevance in the LSL (Fig. 1), allowing to keep much larger RWC under ST 30% FC than in the nLSL. Nonetheless, RWC values under this condition were below the RWC_{tlp} in both genotypes. In fact, ε adjustments occurring under water deficit stress are variable (see, for instance, Sobrado & Turner, 1983; Lo Gullo & Salleo, 1988; Bartlett et al., 2012; Nadal et al., 2020; Roig-Oliver et al., 2020a,b,c), suggesting that they could be species-dependent. Furthermore, Galmés et al. (2011) reported genotype-dependent elastic adjustments testing well-watered and water-stressed nLSL and LSL tomato genotypes. Whilst they demonstrated that most of the analysed genotypes increased leaves rigidity (i.e., higher ε) during water deprivation probably to avoid excessive water losses (Bartlett et al., 2012), ε was not modified in others. Hence, our results provide further evidence on the genotype-dependent elastic adjustments occurring in tomato genotypes (Fig. 1).

Besides modifications in leaf water relations, the application of treatments differing in their water availability also promoted distinct photosynthetic responses in the

tested genotypes (Fig. 2). Under CL conditions, the LSL genotype achieved larger A_N than the nLSL because of enhancements in both g_s and *ETR* even when presenting lower g_m. This photosynthetic behaviour in the LSL genotype was linked to a co-balanced photosynthesis limitation attributed to similar l_m and l_b, whereas in the nLSL genotype only l_b mainly limited A_N (Table 2). In fact, Nadal & Flexas (2019) highlighted that enhancements in biochemical processes rather than only increasing g_m could improve significantly A_N in well-watered crops. Even though both genotypes reduced g_s to the same extend under ST 40% FC, the LSL presented lower *ETR* reductions than the nLSL. Also, the LSL maintained g_m close to CL value, whereas significant declines were observed in the nLSL. These different photosynthetic adjustments occurring in both genotypes promoted that the LSL achieved larger A_N than the nLSL under ST 40% FC. Although both genotypes exhibited similar A_N, g_s and *ETR* under ST 30% FC, the LSL presented larger WUE_i than the nLSL because of lower g_m declines. Overall, these different photosynthetic adjustments allowed the LSL genotype to achieve higher A_N under CL and to increase WUE_i under both water deficit stress treatments, being linked to less variable g_m across experimental conditions as compared to the nLSL. Nonetheless, similar photosynthetic enhancements were observed in both genotypes after ST 30% FC-Rec, which were mostly driven by g_s increasing. However, the full recovery of g_s and A_N was not achieved (Fig. 2).

Recent studies have demonstrated that changes in cell wall composition during abiotic stresses application regulate g_m and/or ε adjustments in a species-specific way (Clemente-Moreno et al., 2019; Roig-Oliver et al., 2020a,b,c). However, here we show for the first time that the involvement of cell wall composition determining these functional traits differently occur even when comparing genotypes of the same species, being mainly attributed to changes in pectins relative proportion (Fig. 3). In fact, pectins are thought to be of crucial relevance maintaining an appropriated degree of cell wall hydration during water shortage (Tenhaken, 2015; Rui & Dinnery, 2019). Moreover, modifications in their amounts are probably accompanied by changes in their physicochemical structure and in their enzymatic performance, which could potentially influence elasticity, thickness and porosity, key traits affecting g_m (Flexas et al., 2021). Besides the relevance of cell wall composition, sub-cellular anatomical traits – specifically, T_{cw} and S_c/S– also determined g_m from a species-dependent perspective during acclimation to distinct environmental stresses (Hanba, Kogami, & Terashima, 2002; Tholen et al., 2008; Tosens et al., 2012; Galmés et al., 2013). Here, we show that

the correlations between g_m and S_c/S and T_{cw} differently occurred at genotype level (Figs. 4A, B), as similarly happened with those between ε and S_c/S and T_{cw} (Figs. 4C, D). Particularly, they were only significant for the LSL genotype, which increased g_m and reduced ε while enhancing T_{cw}, contradicting that thicker cell walls impose a resistance for CO_2 diffusion (Gago et al., 2019; Flexas & Carriquí, 2020) and imply more rigid leaves (Peguero-Pina, Sancho-Knapik, & Gil-Pelegrín, 2017; Nadal, Flexas, & Gulías, 2018). However, we speculate that the LSL experimented T_{cw} reductions during water deprivation which were accompanied by dynamic changes in cell wall composition – specifically, increased pectins– that enabled to partially maintain g_m. This may represent a case of fine anatomical-physiological plasticity that allows for increasing WUE_i. Instead, the nLSL similarly maintained T_{cw} and cell wall composition across treatments, promoting strong g_m declines once subjected to water shortage which were attributed to changes in foliar traits and to supra-cellular anatomy, particularly, enhancements in LMA and reductions in T_{leaf} and T_{mes} (Fig. 5). These results suggest that the nLSL genotype adjusted g_m by supra-cellular adjustments and/or because of mesophyll collapse due to very large depression in RWC (Table 1). Actually, the latter is more compatible with the fact that it seems a collapse more than a regulation in the sense that nLSL plants decreased photosynthesis as well as WUE_i. Nevertheless, since different g_m values were obtained from fluorescence and anatomical measurements (Table S1), we cannot discard that other traits not studied here such as aquaporins or carbonic anhydrases could be involved in g_m regulation across experimental conditions, as already observed during water deprivation (Pérez-Martín et al., 2014). However, even in this case, it appears that LSL plants achieved larger benefits –at least, at leaf level– from their regulation syndrome than nLSL ones.

To the best of our knowledge, this study demonstrates for the first time that the relationship between cell wall composition and physiological behaviour in plants subjected to distinct water regimes is genotype-dependent within a single and thoroughly selected crop species. Whilst the LSL genotype maintained g_m within a narrow range across experimental conditions due to elastic, sub-cellular anatomic and cell wall composition adjustments, the nLSL experienced large g_m variations that were linked to changes in foliar traits as well as in supra-cellular anatomical characteristics. Since both genotypes exhibited contrasting responses for most of the analysed parameters, we suggest that cell wall composition modifications occurring in the LSL might be crucial

during their adaptation to drought environments and could sustain their productivity under the climate change scenario.

Conflicts of interest

The authors declare no conflicts of interest.

Author contributions

MR-O, JB and JF conceived and designed the study; MR-O and MF-P conducted the experiment; MR-O and JF performed the data analysis, and MR-O wrote the first version of the manuscript with the inputs of all co-authors.

References

Abrams, M. D. (1990). Adaptations and responses to drought in *Quercus* species of North America. *Tree Physiology*, 7, 227–238.

Bartlett, M. K., Scoffoni, C., & Sack, L. (2015). The determinants of leaf turgor loss point and prediction of drought tolerance of species and biomes: A global meta-analysis. *Ecology Letters*, 15, 393–405.

Blumenkrantz, N., & Asboe-Hansen, G. (1973). New method for quantitative determination of uronic acids. *Analytical Biochemistry*, 54, 484–489.

Bota, J., Conesa, M. À., Ochogavía, J. M., Medrano, H., Francis, D. M., & Cifre, J. (2014). Characterization of a landrace collection for Tomàtiga de Ramellet (*Solanum lycopersicum* L.) from the Balearic Islands. *Genetic Resources and Crop Evolutio n*, 61, 1131–1146.

Carpita, N. C. (1996). Structure and biogenesis of the cell walls of grasses. *Annual Review of Plant Physiology and Plant Molecular Biology*, 47, 445–476.

Carpita, N. C., & McCann, M. C. (2002). The functions of cell wall polysaccharides in composition and architecture revealed through mutations. *Plant and Soil*, 247, 71–80.

Cebolla-Cornejo, J., Rosselló, S., & Nuez, F. (2013). Phenotypic and genetic diversity of Spanish tomato landraces. *Scientia Horticulturae*, 162, 150–164.

Chaves, M. M., Flexas, J., & Pinheiro, C. (2009). Photosynthesis under drought and salt stress: regulation mechanisms from whole plant to cell. *Annals of Botany*, 103, 551–560.

Clemente-Moreno M. J., Gago, J., Díaz-Vivancos, P., Bernal, A., Miedes, E., Bresta, P., Liakopoulos, G., Fernie, A. R., Hernández, J. A., & Flexas, J. (2019). The apoplastic

antioxidant system and altered cell wall dynamics influence mesophyll conductance and the rate of photosynthesis. *The Plant Journal*, 99, 1031–1046.

Conesa, M. À., Galmés, J., Ochogavía, J. M., March, J., Jaume, J., Martorell, A., Francis, D. M., Medrano, H., Rose, J. K. C., & Cifre, J. (2014). The postharvest tomato fruit quality of long shelf-life Mediterranean landraces is substantially influenced by irrigation regimes. *Postharvest Biology and Technology*, 93, 114–121.

Conesa, M. À., Fullana-Pericàs, M., Granell, A., & Galmés, J. (2020). Mediterranean long shelf-life landraces: an untapped genetic resource for tomato improvement. *Frontiers in Plant Science*, 10, 1651.

Cortés-Olmos, C., Valcárcel, J. V., Rosselló, J., Díez, M. J., & Cebolla-Cornejo, J. (2015). Traditional eastern Spanish varieties of tomato. *Scientia Agriculturae*, 5, 420–431.

Dubois, M., Gilles, K. A., Hamilton, J. K., Rebers, P. A., & Smith, F. (1956). Colorimetric method for determination of sugars and related substances. *Analytical Chemistry*, 28, 350–356.

Evans, L.T. (1997). Adapting and improving crops: the endless task. *Philosophical Transactions of the Royal Society of London. Series B: Biological Sciences*, 352, 901–906.

FAO. (2021). htttp://fao.org/faostat (Accessed 8th May 2021).

Flexas, J., Bota, J., Loreto, F., Cornic, G., & Sharkey, T. D. (2004). Diffusive and metabolic limitations to photosynthesis under drought and salinity in C_3 plants. *Plant Biology*, 6, 269–279.

Flexas, J., Niinemets, Ü., Gallé, A., Barbour, M. M., Centritto, M., Díaz-Espejo, A., Douthe, C., Galmés, J., Ribas-Carbó, M., Rodríguez, P. L., Rosselló, F., Soolanayakanahally, R., Tomás, M., Wright, I. J., Farquhar, G. D., & Medrano, H. (2013). Diffusional conductances to CO_2 as a target for increasing photosynthesis and photosynthetic water-use efficiency. *Photosynthesis Research*, 117, 45–59.

Flexas, J., & Carriquí, M. (2020). Photosynthesis and photosynthetic efficiencies along the terrestrial plant's phylogeny: lessons for improving crop photosynthesis. *The Plant Journal*, 101, 964–978.

Flexas, J., Clemente-Moreno, M. J., Bota, J., Brodribb, T. J., Gago, J., Mizokami, Y., Nadal M., Perera-Castro A. V., Roig-Oliver, M., Sugiura, D., Xiong, D., & Carriquí, M. (2021). Cell wall thickness and composition are involved in photosynthetic limitation. *Journal of Experimental Botany*, erab144.

Flores, P., Sánchez, E., Fenoll, J., & Hellin, P. (2017). Genotypic variability of carotenoids in traditional tomato cultivars. *Food Research International*, 100, 510–516.

Fullana-Pericàs, M., Conesa, M. À., Soler, S., Ribas-Carbó, M., Granell, A., & Galmés, J. (2017). Variations of leaf morphology, photosynthetic traits and water-use efficiency in Western-Mediterranean tomato landraces. *Photosynthetica*, 55, 121–133.

Fullana-Pericàs, M., Conesa, M. À., Douthe, C., El Aou-ouad, H., Ribas-Carbó, M., & Galmés, J. (2019). Tomato landraces as a source to minimize yield losses and improve fruit quality under water deficit conditions. *Agricultural Water Management*, 223, 105722.

Gago, J., Carriquí, M., Nadal, M., Clemente-Moreno, M. J., Coopman, R. E., Fernie, A. R., & Flexas, J. (2019). Photosynthesis optimized across land plant phylogeny. *Trends in Plant Science*, 24, 947–958.

Galmés, J., Conesa, M. À., Ochogavía, J. M., Perdomo, J. A., Francis, D. M., Ribas-Carbó, M., Savé, R., Flexas, J., Medrano, H., & Cifre, J. (2011). Physiological and morphological adaptations in relation to water use efficiency in Mediterranean accessions of *Solanum lycopersicum*. *Plant, Cell & Environment*, 34, 245–260.

Galmés, J., Ochogavía, J. M., Gago, J., Roldán, E. J., Cifre, J., & Conesa, M. À. (2013). Leaf responses to drought stress in Mediterranean accessions of *Solanum lycopersicum*: Anatomical adaptations in relation to gas exchange parameters. *Plant, Cell & Environment*, 36, 920–935.

Grassi, G., & Magnani, F. (2005). Stomatal, mesophyll conductance and biochemical limitations to photosynthesis as affected by drought and leaf ontogeny in ash and oak trees. *Plant, Cell & Environment*, 28, 834–849.

Hanba, Y., Kogami, H., & Terashima, I. (2002). The effect of growth irradiance on leaf anatomy and photosynthesis in *Acer* species differing in light demand. *Plant, Cell & Environment*, 25, 1021–1030.

Harley, P. C., Loreto, F., Di Marco, G., & Sharkey, T. D. (1992). Theoretical considerations when estimating the mesophyll conductance to CO_2 flux by the analysis of the response of photosynthesis to CO_2. *Plant Physiology*, 98, 1429–1436.

Hermida-Carrera, C., Kapralov, M. V., & Galmés, J. (2016). Rubisco catalytic properties and temperature response in crops. *Plant Physiology*, 171, 2549–2561.

Kubiske, M. E., & Abrams, M. D. (1991). Rehydration effects on pressure–volume relationships in four temperate woody species: variability with site, time of season and drought conditions. *Oecologia*, 85, 537–542.

Lo Gullo, M. A., & Salleo, S. (1988). Different strategies of drought resistance in three Mediterranean sclerophyllous trees growing in the same environmental conditions. *New Phytologist*, 108, 267–276.

Long, S. P., Zhu, X. G., Naidu, S. L., & Ort, D. R. (2006). Can improvement in photosynthesis increase crop yields? *Plant, Cell & Environment*, 29, 315–330.

Manzo, N., Pizzolongo, F., Meca, G., Aiello, A., Marchetti, N., & Romano, R. (2018). Comparative chemical compositions of fresh and stored vesuvian PDO "Pomodorino Del Piennolo" tomato and the ciliegino variety. *Molecules* 23, 2871.

Mickelbart, M. V., Hasegawa, P. M., & Bailey-Serres, J. (2015). Genetic mechanisms of abiotic stress tolerance that translate to crop yield stability. *Nature Reviews Genetics*, 16, 237–251.

Morison, J. I. L., Baker, N. R., Mullineaux, P. M., & Davies, W. J. (2008). Improving water use in crop production. *Philosophical Transactions of the Royal Society of London. Series B: Biological Sciences*, 363, 639–658.

Nadal, M., Flexas, J., & Gulías, J. (2018). Possible link between photosynthesis and leaf modulus of elasticity among vascular plants: a new player in leaf traits relationships? *Ecology Letters*, 21, 1372–1379.

Nadal, M., & Flexas, J. (2019). Variation in photosynthetic characteristics with growth form in a water-limited scenario: implications for assimilation rated and water use efficiency in crops. *Agricultural Water Management*, 216, 457–472.

Nadal, M., Roig-Oliver, M., Bota, J., & Flexas, J. (2020). Leaf age-dependent elastic adjustment and photosynthetic performance under drought stress in *Arbutus unedo* seedlings. *Flora*, 271, 151662.

Niinemets, Ü., Cescatti, A., Rodeghiero, M., & Tosens, T. (2005). Leaf internal diffusion conductance limits photosynthesis more strongly in older leaves of Mediterranean evergreen broadleaved species. *Plant, Cell & Environment*, 28, 1552–1566.

Peguero-Pina, J. J., Sancho-Knapik, D., & Gil-Pelegrín, E. (2017). Ancient cell structural traits and photosynthesis in today's environment. *Journal of Experimental Botany*, 68, 1389–1392.

Pérez-Martín, A., Michelazzo, C., Torres-Ruiz, J. M., Flexas, J., Fernández, J. E., Sebastiani, L., & Díaz-Espejo, A. (2014). Regulation of photosynthesis and stomatal and mesophyll conductance under water stress and recovery in olive trees: correlation with gene expression of carbonic anhydrase and aquaporins. *Journal of Experimental Botany*, 65, 3143–3156.

Roig-Oliver, M., Bresta, P., Nadal, M., Liakopoulos, G., Nikolopoulos, D., Karabourniotis, G., Bota, J., & Flexas, J. (2020*a*). Cell wall composition and thickness affect mesophyll conductance to CO_2 diffusion in *Helianthus annuus* under water deprivation. *Journal of Experimental Botany*, 71, 7198–7209.

Roig-Oliver, M., Nadal, M., Bota, J., & Flexas, J. (2020*b*). *Ginkgo Biloba* and *Helianthus annuus* show different strategies to adjust photosynthesis, leaf water relations, and cell wall composition under water deficit stress. *Photosynthetica*, 58, 1098–1106.

Roig-Oliver, M., Nadal, M., Clemente-Moreno, M. J., Bota, J., & Flexas, J. (2020*c*). Cell wall components regulate photosynthesis and leaf water relations of *Vitis vinifera* cv. Grenache acclimated to contrasting environmental conditions. *Journal of Plant Physiology*, 244, 153084.

Sack, L., Cowan, P. D., Jaikumar, N., & Holbrook, N. M. (2003). The 'hydrology' of leaves: coordination of structure and function intemperate woody species. *Plant, Cell & Environment*, 26, 1343–1356.

Sack, L., & Pasquet-Kok, J. (2011). Leaf pressure-volume curve parameters. Prometheus Wiki. http://prometheuswiki.org/tiki-pagehistory.php?page=Leaf%20pressure-volume%20curve%20parameters&preview=16 (Accessed 28th March 2021).

Sobrado, M. A., & Turner, N. C. (1983). A comparison of the water relations characteristics of *Helianthus annuus* and *Helianthus petiolaris* when subjected to water deficits. *Oecologia*, 58, 309–313.

Saladié, M., Matas, A. J., Isaacson, T., Jenks, M. A., Goodwin, S. M., Niklas, K. J., Xiaolin, R., Labavitch, J. M., Shackel, K. A., Fernie, A. R., Lytovchenko, A., O'Neill, M. A., Watkins, C. B., & Rose, J. K. C. (2007). A reevaluation of the key factors that influence tomato fruit softening and integrity. *Plant Physiology*, 144, 1012–1028.

Schultz, H. R. (2016). Global climate change, sustainability, and some challenges for grape and wine production. *Journal of Wine Ecology*, 11, 181–200.

Sweet, W. J., Morrison, J. C., Labavitch, J., Matthews, M. A. (1990). Altered synthesis and composition of cell wall of grape (*Vitis vinifera* L.) leaves during expansion and growth-inhibiting water deficits. *Plant and Cell Physiology*, 31, 407–414.

Tenhaken, R. (2015). Cell wall remodeling under abiotic stress. *Frontiers in Plant Science*, 5, 771.

Thain, J. F. (1983). Curvature correlation factors in the measurements of cell surface areas in plant tissues. *Journal of Experimental Botany*, 34, 87–94.

Tholen, D., Boom, C., Noguchi, K., Ueda, S., Katase, T., & Terashima, I. (2008). The chloroplast avoidance response decreases internal conductance to CO_2 diffusion in *Arabidopsis thaliana* leaves. *Plant, Cell & Environment*, 11, 1688–1700.

Tilman, D., Cassman, K. G., Matson, P. A., Naylor, R., & Polasky, S. (2002). Agricultural sustainability and intensive production practices. *Nature*, 418, 671–677.

Tomás, M., Flexas, J., Copolovici, L., Galmés, J., Hallik, L., Medrano, H., Ribas-Carbó, M., Tosens, T., Vislap, V., & Niinemets, Ü. (2013). Importance of leaf anatomy in determining mesophyll diffusion conductance to CO_2 across species: quantitative limitations and scaling up by models. *Journal of Experimental Botany*, 64, 2269–2281.

Tosens T., Niinemets Ü., Vislap V., Eichelmann H., & Castro-Díez, P. (2012). Developmental changes in mesophyll diffusion conductance and photosynthetic capacity under different light and water availabilities in *Populus tremula*: how structure constrains function. *Plant, Cell & Environment*, 35, 839–856.

Tranchida-Lombardo, V., Aiese Cigliano, R., Anzar, I., Landi, S., Palombieri, S., Colantuono, C., Bostan, H., Termolino, P., Aversano, R., Batelli, G., Cammareri, M., Carputo, D., Chiusano, M. L., Conicella, C., Consiglio, F., D'Agostino, N., De Palma, M., Di Matteo, A., Grandillo, S., Sanseverino, W., Tucci, M., & Grillo, S. (2018). Whole-genome re-sequencing of two Italian tomato landraces reveals sequence variations in genes associated with stress tolerance, fruit quality and long shelf-life traits. *DNA Research*, 25, 149–160.

Turner, N. C. (2018). Turgor maintenance by osmotic adjustment: 40 years of progress. *Journal of Experimental Botany*, 69, 3223–3233.

Valentini, R., Epron, D., Angelis, P. D., Matteucci, G., & Dreyer, E. (1995). In situ estimation of net CO_2 assimilation, photosynthetic electron flow and photorespiration of Turkey oak (*Q. cerris* L.) leaves: diurnal cycles under different water supply. *Plant, Cell & Environment*, 18, 631–664.

Wu, A., Hammer, G. L., Doherty, A., von Caemmerer, S., & Farquhar, G. D. (2019). Quantifying impacts of enhancing photosynthesis on crop yield. *Nature Plants*, 5, 380–388.

Xiong, D., & Nadal, M. (2020). Linking water relations and hydraulics with photosynthesis. *The Plant Journal*, 101, 800–815.

Ye, M., Zhang, Z., Huang, G., Xiong, Z., Peng, S., & Li, Y. (2020). High leaf mass per area *Oryza* genotypes invest more leaf mass to cell wall and show a low mesophyll conductance. *AoB Plants*, 12, plaa028.

Table 1. Plants water status of tomato non-long shelf-life (nLSL) and long shelf-life (LSL) genotypes subjected to different conditions (control, CL; short-term water deficit stress at 40% FC, ST 40% FC; short-term water deficit stress at 30% FC, ST 30% FC; short-term water deficit stress at 30% FC followed by recovery, ST 30% FC-Rec). Mean values ± SE are shown for pre-dawn leaf water potential (Ψ_{pd}), midday leaf water potential (Ψ_{md}) and leaf relative water content (RWC). Genotypes (G) and treatments (T) effects were quantified by two-way ANOVA and differences between groups were addressed by LSD test. n = 5 in all cases.

Genotypes and treatments	**Ψ_{pd}** (MPa)	**Ψ_{md}** (MPa)	**RWC** (%)
nLSL – CL	-0.24 ± 0.01^{a}	-0.40 ± 0.01^{a}	86.51 ± 0.05^{ab}
nLSL – ST 40% FC	-0.43 ± 0.02^{a}	-0.96 ± 0.03^{b}	82.07 ± 2.63^{ab}
nLSL – ST 30% FC	-0.89 ± 0.19^{b}	-1.34 ± 0.22^{c}	57.37 ± 5.12^{d}
nLSL – ST 30% FC-Rec	-0.32 ± 0.00^{a}	-0.43 ± 0.01^{a}	84.24 ± 1.20^{ab}
LSL – CL	-0.31 ± 0.03^{a}	-0.42 ± 0.02^{a}	88.33 ± 0.32^{a}
LSL – ST 40% FC	-0.42 ± 0.02^{a}	-0.54 ± 0.05^{a}	80.48 ± 2.01^{b}
LSL – ST 30% FC	-1.05 ± 0.09^{b}	-1.30 ± 0.05^{c}	70.22 ± 2.86^{c}
LSL – ST 30% FC-Rec	-0.26 ± 0.02^{a}	-0.43 ± 0.02^{a}	84.36 ± 1.73^{ab}
G	0.628	0.045	0.046
T	<0.001	<0.001	<0.001
G:T	0.588	0.071	0.040

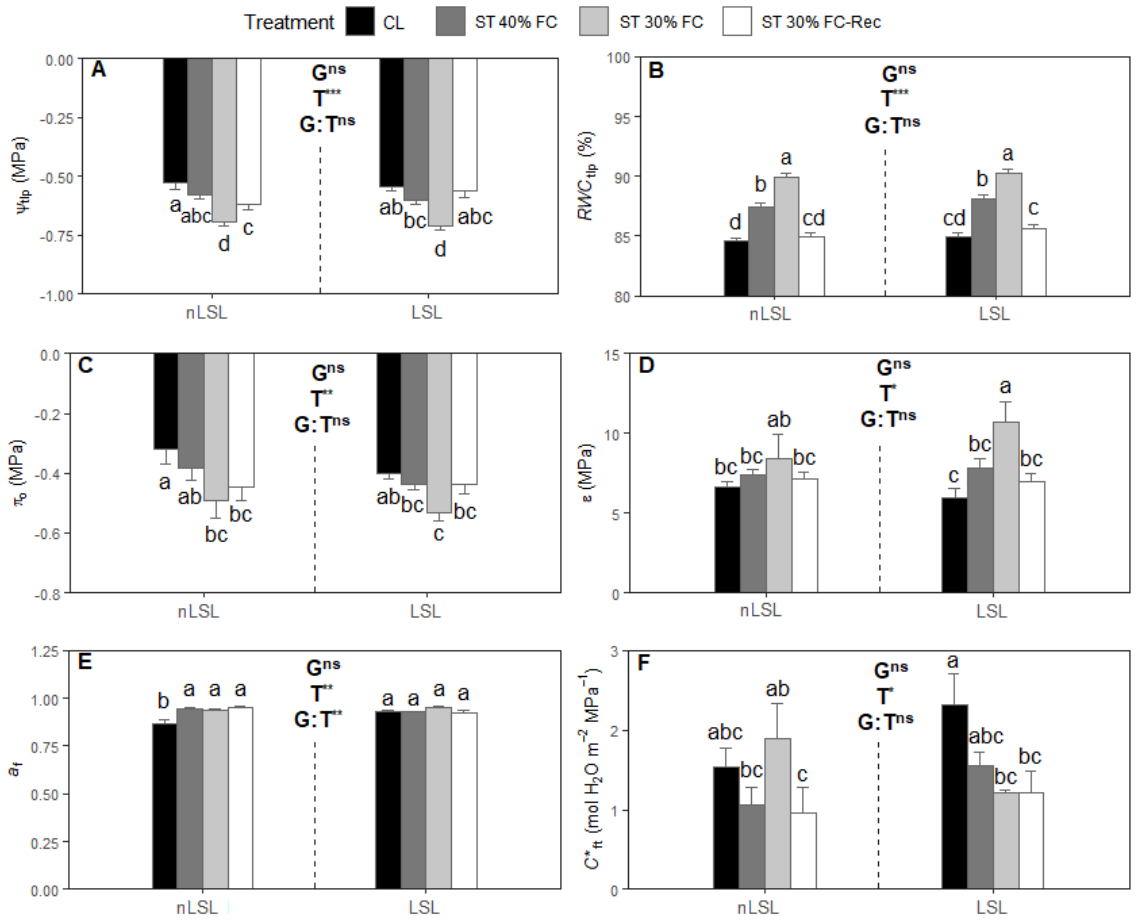

Fig. 1. Leaf water relations of tomato non-long shelf-life (nLSL) and long shelf-life (LSL) genotypes subjected to different conditions (control, CL; short-term water deficit stress at 40% FC, ST 40% FC; short-term water deficit stress at 30% FC, ST 30% FC; short-term water deficit stress at 30% FC followed by recovery, ST 30% FC-Rec). (A) Water potential at turgor loss point (Ψ_{tlp}), (B) relative water content at turgor loss point (RWC_{tlp}), (C) osmotic potential at full turgor (π_o), (D) bulk modulus of elasticity (ε), (E) apoplastic water fraction (a_f), and (F) leaf area specific capacitance at full turgor (C^*_{ft}). Genotypes (G) and treatments (T) effects were quantified by two-way ANOVA and differences between groups were addressed by LSD test. Different superscript letters indicate significant differences. Significance: *** P<0.001; ** <0.01; * <0.05; ^{ns} >0.05. Values are means ± SE (n = 5).

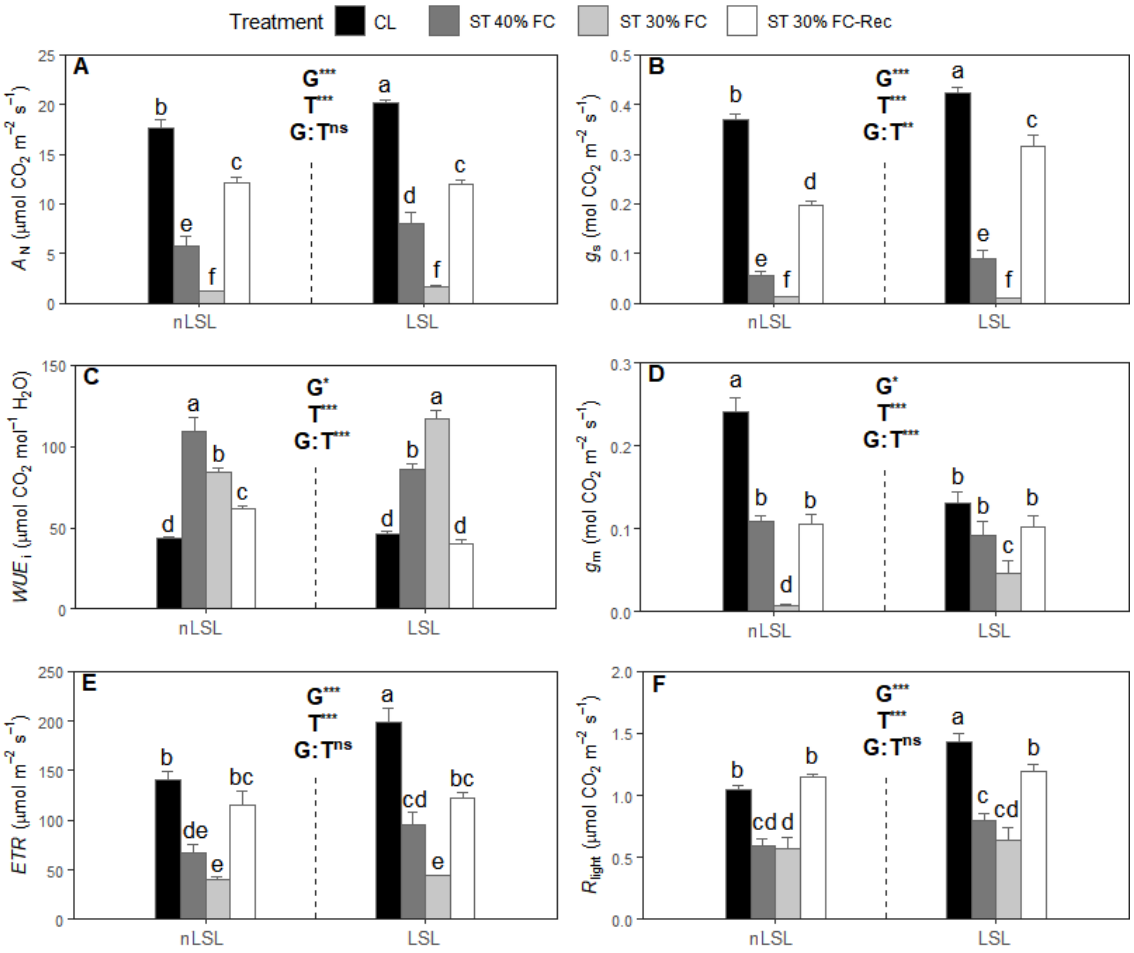

Fig. 2. Photosynthetic characterization of tomato non-long shelf-life (nLSL) and long shelf-life (LSL) genotypes subjected to different conditions (control, CL; short-term water deficit stress at 40% FC, ST 40% FC; short-term water deficit stress at 30% FC, ST 30% FC; short-term water deficit stress at 30% FC followed by recovery, ST 30% FC-Rec). (A) Net CO_2 assimilation (A_N), (B) stomatal conductance (g_s), (C) intrinsic water use efficiency (WUE_i), (D) mesophyll conductance (g_m), (E) electron transport rate (ETR) and (F) light respiration (R_{light}). Genotypes (G) and treatments (T) effects were quantified by two-way ANOVA and differences between groups were addressed by LSD test. Different superscript letters indicate significant differences. Significance: *** P<0.001; ** <0.01; * <0.05; ^{ns} >0.05. Values are means ± SE (n = 5).

Table 2. Photosynthesis limitations analysis of tomato non-long shelf-life (nLSL) and long shelf-life (LSL) genotypes subjected to different conditions (control, CL; short-term water deficit stress at 40% FC, ST 40% FC; short-term water deficit stress at 30% FC, ST 30% FC; short-term water deficit stress at 30% FC followed by recovery, ST 30% FC-Rec). Mean values ± SE are shown for stomatal (l_s), mesophyll (l_m) and biochemical (l_b) *relative* limitations as well as for stomatal (*SL*), mesophyll (*ML*) and biochemical limitations (*BL*) contributions to d*A*/*A* according to Grassi and Magnani (2005). Genotypes (G) and treatments (T) effects were quantified by two-way ANOVA and differences between groups were addressed by LSD test. n = 5 in all cases.

Genotypes and treatments	l_s	l_m	l_b	***SL*** (%)	***ML*** (%)	***BL*** (%)
nLSL – CL	0.12 ± 0.00	0.22 ± 0.02	0.65 ± 0.03			
nLSL – ST 40% FC	0.34 ± 0.03	0.19 ± 0.02	0.46 ± 0.02	29.44 ± 3.48	9.97 ± 0.85	24.28 ± 3.36
nLSL – ST 30% FC	0.25 ± 0.02	0.50 ± 0.04	0.25 ± 0.02	24.35 ± 2.32	48.46 ± 3.96	18.66 ± 0.97
nLSL – ST 30% FC-Rec	0.18 ± 0.01	0.29 ± 0.05	0.51 ± 0.05	8.37 ± 0.57	15.34 ± 4.69	14.77 ± 4.57
LSL – CL	0.13 ± 0.01	0.43 ± 0.02	0.44 ± 0.02			
LSL – ST 40% FC	0.26 ± 0.01	0.32 ± 0.01	0.43 ± 0.02	23.25 ± 3.53	9.39 ± 4.13	22.29 ± 2.85
LSL – ST 30% FC	0.40 ± 0.03	0.26 ± 0.06	0.37 ± 0.06	38.59 ± 3.59	18.46 ± 6.26	28.32 ± 4.18
LSL – ST 30% FC-Rec	0.11 ± 0.01	0.34 ± 0.01	0.54 ± 0.02	3.00 ± 0.73	12.83 ± 5.15	19.87 ± 2.03
G	0.047	0.304	0.176	0.239	0.006	0.155
T	<0.001	0.021	<0.001	<0.001	<0.001	0.107
G:T	<0.001	<0.001	<0.001	0.003	0.007	0.230

Table 3. Leaf cell wall composition of tomato non-long shelf-life (nLSL) and long shelf-life (LSL) genotypes subjected to different conditions (control, CL; short-term water deficit stress at 40% FC, ST 40% FC; short-term water deficit stress at 30% FC, ST 30% FC; short-term water deficit stress at 30% FC followed by recovery, ST 30% FC-Rec). Mean values ± SE are shown for alcohol insoluble residue (AIR), cellulose, hemicelluloses, and pectins contents. Genotypes (G) and treatments (T) effects were quantified by two-way ANOVA and differences between groups were addressed by LSD test. n = 5 in all cases.

Genotypes and treatments	**AIR** ($g\ g^{-1}$ DW)	**Cellulose** ($mg\ g^{-1}$ AIR)	**Hemicelluloses** ($mg\ g^{-1}$ AIR)	**Pectins** ($mg\ g^{-1}$ AIR)
nLSL – CL	0.08 ± 0.01^{c}	120.39 ± 9.00^{ab}	283.43 ± 7.81^{c}	41.01 ± 3.16^{bc}
nLSL – ST 40% FC	0.09 ± 0.01^{bc}	108.89 ± 4.58^{abc}	346.64 ± 45.35^{abc}	68.28 ± 2.78^{a}
nLSL – ST 30% FC	0.07 ± 0.01^{c}	109.83 ± 3.85^{abc}	377.42 ± 61.20^{abc}	62.22 ± 3.75^{a}
nLSL – ST 30% FC-Rec	0.07 ± 0.01^{c}	130.42 ± 12.00^{a}	306.65 ± 31.23^{bc}	64.57 ± 2.26^{a}
LSL – CL	0.12 ± 0.01^{a}	80.96 ± 6.37^{d}	456.61 ± 60.49^{a}	27.87 ± 1.09^{d}
LSL – ST 40% FC	0.10 ± 0.01^{ab}	101.29 ± 15.63^{bcd}	402.25 ± 30.99^{abc}	33.75 ± 1.89^{cd}
LSL – ST 30% FC	0.08 ± 0.01^{abc}	92.28 ± 10.09^{cd}	443.10 ± 36.28^{ab}	44.18 ± 4.56^{b}
LSL – ST 30% FC-Rec	0.09 ± 0.01^{abc}	102.72 ± 5.76^{bcd}	415.12 ± 56.31^{ab}	39.04 ± 1.02^{bc}
G	<0.001	<0.001	<0.001	<0.001
T	0.076	0.240	0.706	<0.001
G:T	0.820	0.335	0.571	0.003

Table 4. Leaf structural and anatomical characterization from semi-fine cross sections of tomato non-long shelf-life (nLSL) and long shelf-life (LSL) genotypes subjected to different conditions (control, CL; short-term water deficit stress at 40% FC, ST 40% FC; short-term water deficit stress at 30% FC, ST 30% FC; short-term water deficit stress at 30% FC followed by recovery, ST 30% FC-Rec). Mean values ± SE are shown for leaf mass per area (LMA), leaf density (LD), leaf thickness (T_{leaf}), mesophyll thickness (T_{mes}), and fraction of mesophyll intercellular air spaces (f_{ias}). Genotypes (G) and treatments (T) effects were quantified by two-way ANOVA and differences between groups were addressed by LSD test. n = 5 in all cases.

Genotypes and treatments	**LMA** ($g\ m^{-2}$)	**LD** ($g\ cm^{-3}$)	T_{leaf} (µm)	T_{mes} (µm)	f_{ias} (%)
nLSL – CL	47.53 ± 5.12^{b}	0.11 ± 0.01^{a}	222.01 ± 17.76^{ab}	173.85 ± 15.88^{ab}	29.04 ± 2.53^{abc}
nLSL – ST 40% FC	53.57 ± 6.54^{ab}	0.13 ± 0.02^{a}	193.21 ± 5.11^{cd}	147.15 ± 0.57^{bcd}	34.04 ± 2.50^{a}
nLSL – ST 30% FC	60.34 ± 1.94^{ab}	0.16 ± 0.01^{a}	163.12 ± 11.04^{e}	118.78 ± 9.26^{e}	32.84 ± 2.21^{ab}
nLSL – ST 30% FC-Rec	54.84 ± 9.20^{ab}	0.15 ± 0.03^{a}	179.04 ± 7.70^{de}	138.79 ± 3.35^{de}	34.68 ± 3.25^{a}
LSL – CL	60.80 ± 5.54^{ab}	0.14 ± 0.01^{a}	238.03 ± 3.77^{a}	193.47 ± 2.22^{a}	24.10 ± 1.21^{c}
LSL – ST 40% FC	64.97 ± 9.13^{ab}	0.15 ± 0.02^{a}	187.66 ± 5.27^{cde}	145.85 ± 2.77^{cd}	25.00 ± 3.39^{c}
LSL – ST 30% FC	71.05 ± 2.73^{a}	0.17 ± 0.01^{a}	212.77 ± 7.71^{abc}	165.12 ± 8.45^{bc}	26.95 ± 2.73^{bc}
LSL – ST 30% FC-Rec	59.51 ± 3.65^{ab}	0.17 ± 0.00^{a}	207.71 ± 9.02^{bc}	162.02 ± 5.47^{bcd}	23.12 ± 0.86^{c}
G	0.030	0.159	0.003	0.002	<0.001
T	0.252	0.079	<0.001	<0.001	0.514
G:T	0.890	0.973	0.060	0.093	0.532

Table 5. Leaf anatomical characterization from ultra-fine cross sections of tomato non-long shelf-life (nLSL) and long shelf-life (LSL) genotypes subjected to different conditions (control, CL; short-term water deficit stress at 40% FC, ST 40% FC; short-term water deficit stress at 30% FC, ST 30% FC; short-term water deficit stress at 30% FC followed by recovery, ST 30% FC-Rec). Mean values ± SE are shown for chloroplasts thickness (T_{chl}), chloroplasts length (L_{chl}), mesophyll and chloroplasts surface area exposed to intercellular air spaces per leaf area (S_m/S and S_c/S, respectively), S_c/S_m ratio, and cell wall thickness (T_{cw}). Genotypes (G) and treatments (T) effects were quantified by two-way ANOVA and differences between groups were addressed by LSD test. n = 5 in all cases.

Genotypes and treatments	T_{chl} (μm)	L_{chl} (μm)	S_m/S ($m^2\ m^{-2}$)	S_c/S ($m^2\ m^{-2}$)	S_c/S_m	T_{cw} (μm)
nLSL – CL	5.53 ± 0.05^{a}	2.91 ± 0.15^{ab}	17.86 ± 0.74^{a}	16.10 ± 0.91^{a}	0.90 ± 0.02^{a}	0.11 ± 0.00^{b}
nLSL – ST 40% FC	4.63 ± 0.05^{b}	2.72 ± 0.14^{ab}	15.98 ± 0.25^{abc}	$12.\ 30 \pm 0.18^{bcd}$	0.79 ± 0.02^{bc}	0.11 ± 0.01^{b}
nLSL – ST 30% FC	4.52 ± 0.15^{b}	2.58 ± 0.24^{b}	14.31 ± 0.87^{bc}	12.47 ± 1.01^{bcd}	0.86 ± 0.02^{ab}	0.11 ± 0.01^{b}
nLSL – ST 30% FC-Rec	4.74 ± 0.13^{b}	2.27 ± 0.13^{b}	13.72 ± 1.57^{c}	10.23 ± 1.11^{d}	0.84 ± 0.02^{abc}	0.13 ± 0.00^{a}
LSL – CL	5.95 ± 0.27^{a}	3.23 ± 0.28^{a}	17.28 ± 1.85^{ab}	15.29 ± 1.54^{ab}	0.88 ± 0.03^{a}	0.13 ± 0.01^{a}
LSL – ST 40% FC	4.75 ± 0.25^{b}	2.68 ± 0.31^{ab}	15.96 ± 0.33^{abc}	12.58 ± 0.77^{bcd}	0.79 ± 0.05^{bc}	0.12 ± 0.01^{ab}
LSL – ST 30% FC	4.62 ± 0.20^{b}	2.64 ± 0.12^{ab}	15.10 ± 0.10^{abc}	11.16 ± 0.40^{cd}	0.75 ± 0.01^{c}	0.10 ± 0.02^{b}
LSL – ST 30% FC-Rec	4.87 ± 0.33^{b}	2.38 ± 0.28^{b}	15.63 ± 0.96^{abc}	13.31 ± 0.95^{abc}	0.78 ± 0.04^{bc}	0.12 ± 0.00^{ab}
G	0.112	0.394	0.406	0.470	0.044	0.149
T	<0.001	0.016	0.042	0.001	0.005	0.047
G:T	0.863	0.886	0.710	0.158	0.237	0.150

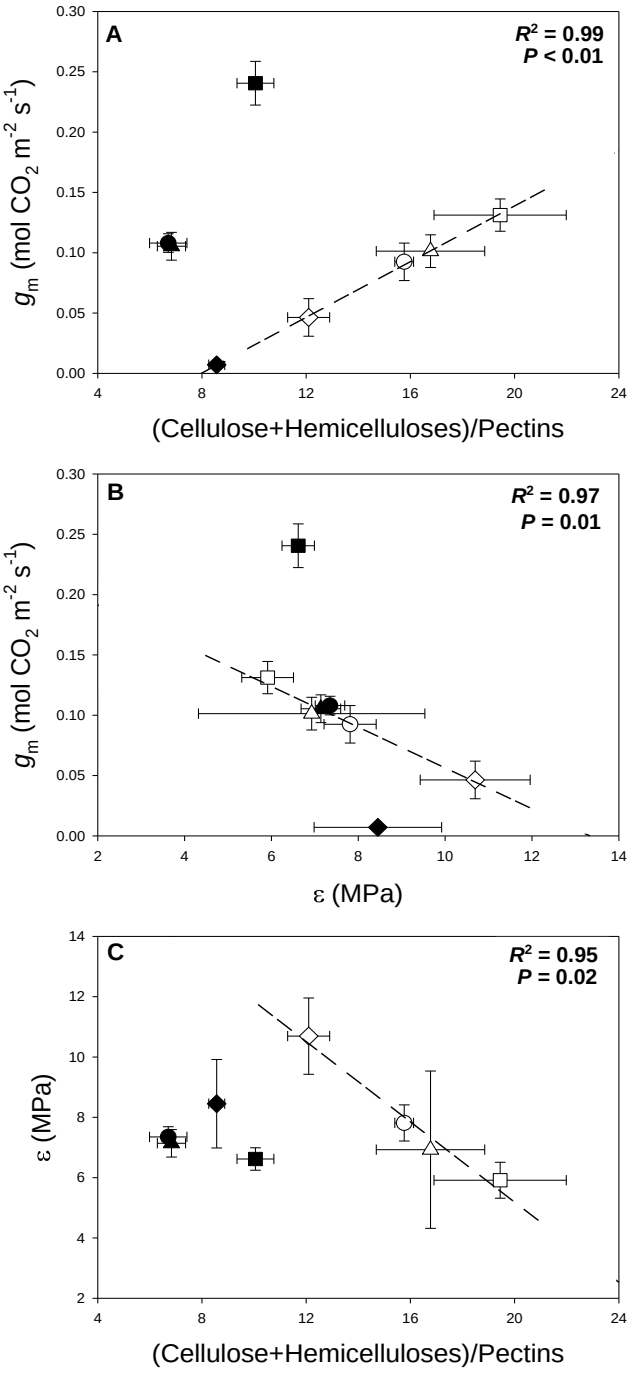

Fig. 3. (A) Relationship between mesophyll conductance (g_m) and the (Cellulose+Hemicelluloses)/Pectins ratio, (B) relationship between mesophyll conductance (g_m) and the bulk modulus of elasticity (ε) and (C) relationship between the bulk modulus of elasticity (ε) and the (Cellulose+Hemicelluloses)/Pectins ratio. When significant, discontinuous regression lines, regression square coefficients and significances are shown for the LSL genotype. nLSL genotype values are represented by black-filled points, whereas LSL genotype values are represented by white-filled points. Dots, squares, rhombus, and triangles correspond to CL, ST 40% FC, ST 30% FC, and ST 30%-Rec treatments, respectively. n = 5 (means ± SE).

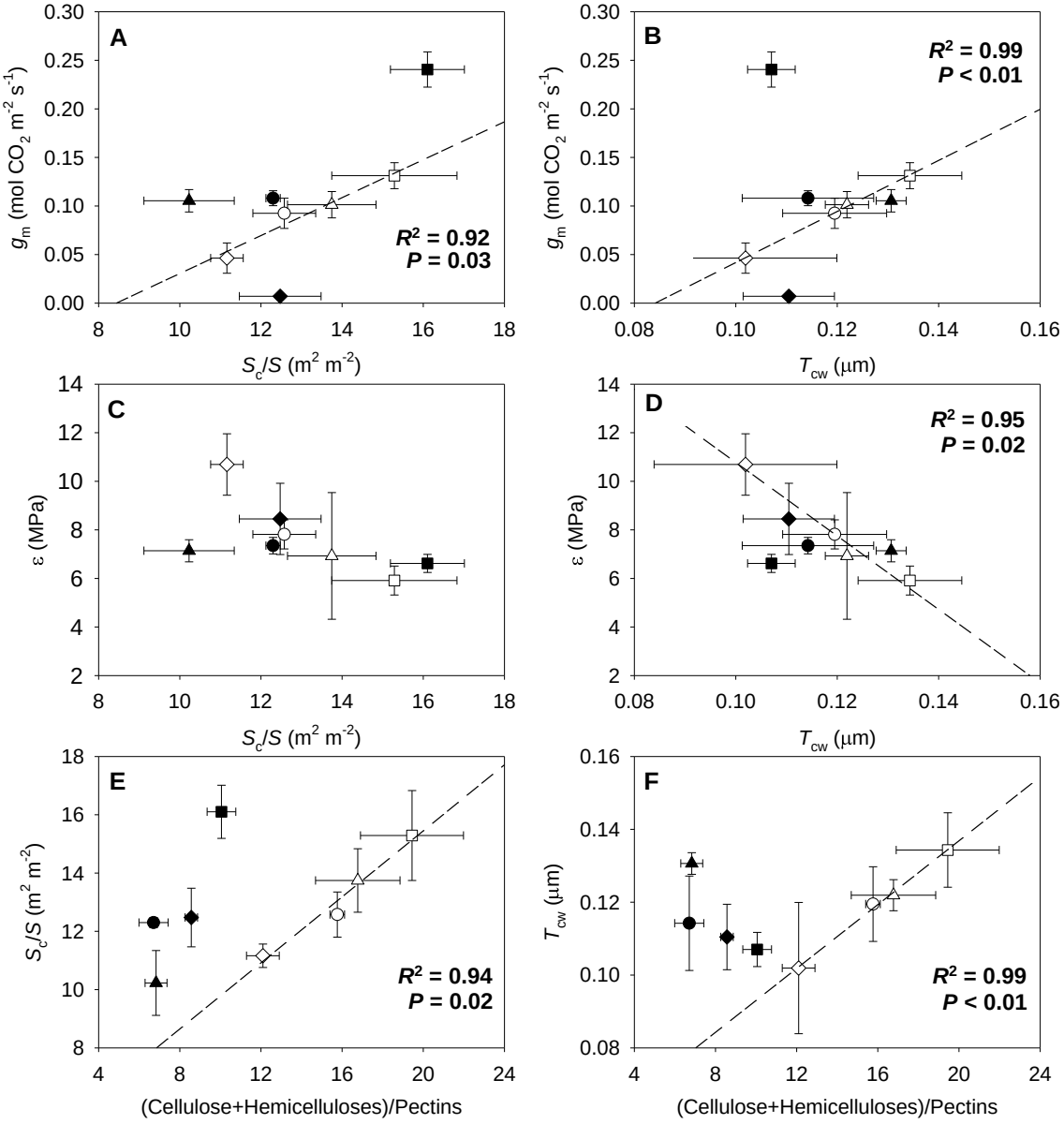

Fig. 4. Relationships between mesophyll conductance (g_m) and (A) chloroplasts surface area exposed to intercellular air spaces per leaf area (S_c/S) and (B) cell wall thickness (T_{cw}). Relationships between the bulk modulus of elasticity (ε) and (C) chloroplasts surface area exposed to intercellular air spaces per leaf area (S_c/S) and (D) cell wall thickness (T_{cw}). Relationships between (E) chloroplasts surface area exposed to intercellular air spaces per leaf area (S_c/S) and (F) cell wall thickness (T_{cw}) with the (Cellulose+Hemicelluloses)/Pectins ratio. When significant, discontinuous solid regression lines, regression square coefficients and significances are shown for the LSL genotype. nLSL genotype values are represented by black-filled points, whereas LSL genotype values are represented by white-filled points. Dots, squares, rhombus, and triangles correspond to CL, ST 40% FC, ST 30% FC, and ST 30%-Rec treatments, respectively. n = 5 (means ± SE).

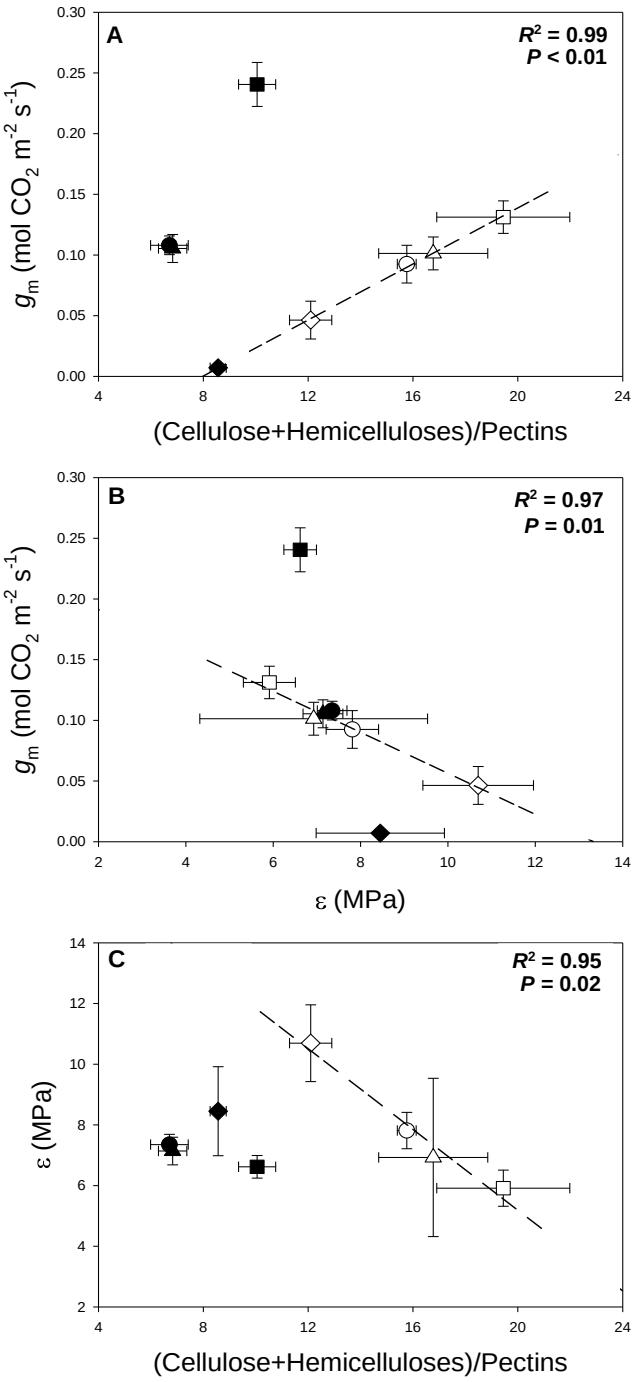

Fig. 5. Relationships between mesophyll conductance (g_m) and (A) leaf mass pear area (LMA), (B) leaf thickness (T_{leaf}) and (C) mesophyll thickness (T_{mes}). When significant, solid regression lines, regression square coefficients and significances are shown for the nLSL genotype. nLSL genotype values are represented by black-filled points, whereas LSL genotype values are represented by white-filled points. Dots, squares, rhombus, and triangles correspond to CL, ST 40% FC, ST 30% FC, and ST 30%-Rec treatments, respectively. n = 5 (means ± SE).

Supplementary Information

Table S1. Mesophyll conductance (g_m) calculated from fluorescence and anatomical measurements performed in tomato non-long shelf-life (nLSL) and long shelf-life (LSL) genotypes subjected to different conditions (control, CL; short-term water deficit stress at 40% FC, ST 40% FC; short-term water deficit stress at 30% FC, ST 30% FC; short-term water deficit stress at 30% FC followed by recovery, ST 30% FC-Rec). Whilst g_m_fluorescence was calculated according to Harley et al. (1992), g_m_anatomy was estimated following Tomás et al. (2013). Mean values ± SE values are shown. Genotypes (G) and treatments (T) effects were quantified by two-way ANOVA and differences between groups were addressed by LSD test. n = 5 in all cases.

Genotypes and treatments	**g_m_fluorescence** (mol CO_2 m^{-2} s^{-1})	**g_m_anatomy** (mol CO_2 m^{-2} s^{-1})
nLSL – CL	0.24 ± 0.02^{a}	0.10 ± 0.00^{a}
nLSL – ST 40% FC	0.11 ± 0.01^{b}	0.08 ± 0.01^{bc}
nLSL – ST 30% FC	0.01 ± 0.00^{d}	0.08 ± 0.00^{bc}
nLSL – ST 30% FC-Rec	0.11 ± 0.01^{b}	0.06 ± 0.00^{cd}
LSL – CL	0.13 ± 0.01^{b}	0.09 ± 0.01^{ab}
LSL – ST 40% FC	0.09 ± 0.02^{b}	0.08 ± 0.00^{bcd}
LSL – ST 30% FC	0.05 ± 0.02^{c}	0.08 ± 0.00^{bc}
LSL – ST 30% FC-Rec	0.10 ± 0.01^{b}	0.06 ± 0.01^{d}
G	0.021	0.190
T	<0.001	<0.001
G:T	<0.001	0.574

Table S2. Pearson correlation matrix of physiological, leaf water relations, cell wall and anatomical parameters measured in *S. lycopersicum* nLSL genotype across all experimental conditions. Values in italics and bold indicate significant (P<0.05) and highly significant (P<0.01) correlation coefficients, respectively.

	A_N	g_s	WUE_i	g_m	ETR	R_{light}	Ψ_{pd}	Ψ_{md}	RWC	AIR	Cel.	Hemicel.	Pectins	(C+H)/P	π_o	RWC_{tlp}	Ψ_{tlp}	ε	a_f	C^*_{ft}	LMA	LD	T_{leaf}	T_{mes}	f_{ias}	T_{chl}	L_{chl}	S_m/S	S_c/S	S_c/S_m	T_{cw}
A_N		*0.98*	-0.8	0.93	*1*	0.87	0.89	*0.95*	0.82	0.37	0.7	***-1***	-0.73	0.4	0.76	*-0.96*	0.82	-0.94	-0.67	-0.31	-0.9	-0.77	0.82	0.87	-0.57	0.89	0.25	0.57	0.47	0.47	0.34
g_s			-0.87	0.92	*0.97*	0.83	0.79	0.89	0.7	0.27	0.64	*-0.96*	-0.85	0.57	0.74	-0.89	0.77	-0.87	-0.79	-0.12	-0.87	-0.76	0.82	0.86	-0.7	0.95	0.34	0.61	0.59	0.63	0.24
WUE_i				-0.61	-0.82	-0.84	-0.47	-0.72	-0.35	0.23	-0.73	-0.78	0.8	-0.65	-0.35	0.69	-0.36	0.55	0.69	-0.15	0.52	0.37	-0.46	-0.51	0.63	-0.77	-0.06	-0.28	-0.43	-0.84	-0.36
g_m					0.89	0.62	0.87	0.82	0.82	0.62	0.39	-0.9	-0.77	0.47	0.95	-0.85	*0.96*	-0.94	-0.78	-0.24	***-0.99***	*-0.95*	*0.97*	***0.99***	-0.69	0.94	0.56	0.82	0.68	0.4	0.01
ETR						0.91	0.89	*0.97*	0.82	0.31	0.76	***-1***	-0.69	0.35	0.7	*-0.97*	0.77	-0.92	-0.61	-0.35	-0.85	-0.71	0.76	0.82	-0.5	0.85	0.16	0.48	0.39	0.46	0.43
R_{light}							0.75	0.94	0.68	-0.01	*0.96*	-0.89	-0.46	0.15	0.35	-0.91	0.46	-0.74	-0.34	-0.41	-0.57	-0.36	0.43	0.51	-0.22	0.6	-0.25	0.08	0.04	0.4	0.74
Ψ_{pd}								0.93	***0.99***	0.65	0.62	-0.92	-0.4	0.01	0.78	*-0.96*	0.88	*-0.98*	-0.37	-0.67	-0.88	-0.78	0.79	0.85	-0.25	0.68	0.15	0.49	0.23	0.03	0.41
Ψ_{md}									0.88	0.34	0.83	*-0.98*	-0.5	0.13	0.62	***-1***	0.73	-0.93	-0.42	-0.54	-0.79	-0.63	0.67	0.75	-0.29	0.71	-0.02	0.34	0.19	0.27	0.59
RWC										0.72	0.55	-0.86	-0.29	-0.1	0.77	-0.91	0.87	-0.96	-0.28	-0.75	-0.85	-0.76	0.76	0.81	-0.16	0.59	0.14	0.47	0.17	-0.11	0.4
AIRg											-0.18	-0.37	-0.11	-0.13	0.81	-0.41	0.82	-0.65	-0.22	-0.53	-0.71	-0.79	0.72	0.71	-0.17	0.37	0.56	0.68	0.35	-0.39	-0.26
Cel.												-0.74	-0.23	-0.05	0.09	-0.79	0.23	-0.57	-0.08	-0.47	-0.33	-0.1	0.17	0.27	0.03	0.35	-0.51	-0.2	-0.23	0.27	0.89
Hemicel.													0.66	-0.31	-0.73	*0.98*	-0.8	0.95	0.6	0.39	0.87	0.74	-0.79	-0.84	0.48	-0.84	-0.17	-0.5	-0.38	-0.4	-0.43
Pectins														-0.92	-0.67	0.51	-0.6	0.55	0.99	-0.41	0.71	0.69	-0.75	-0.74	*0.97*	-0.94	-0.65	-0.76	-0.88	-0.87	0.24
(C+H)/P															0.41	-0.13	0.29	-0.17	-0.92	0.74	-0.4	-0.43	0.5	0.45	*-0.95*	0.74	0.67	0.64	0.88	0.92	-0.47
π_o																-0.67	*0.98*	-0.86	-0.73	-0.22	*-0.97*	***-1***	***0.99***	*0.98*	-0.67	0.84	0.74	0.92	0.74	0.22	-0.24
RWC_{tlp}																		*0.95*	0.44	0.56	0.83	0.68	-0.72	-0.79	0.31	-0.73	-0.04	-0.39	-0.22	-0.24	-0.54
Ψ_{tlp}																		-0.93	-0.64	-0.38	*-0.98*	*-0.98*	*0.97*	*0.98*	-0.56	0.82	0.6	0.84	0.61	0.14	-0.07
ε																			0.53	0.54	0.95	0.86	-0.87	-0.92	0.41	-0.79	-0.3	-0.62	-0.39	-0.17	-0.29
a_f																				-0.43	0.73	0.74	-0.79	-0.76	*0.99*	-0.93	-0.76	-0.84	-0.95	-0.81	0.38
C^*_{ft}																					0.3	0.2	-0.16	-0.24	-0.54	0.09	0.4	0.15	0.5	0.66	-0.64
LMA																						*0.97*	-0.98	***-1***	0.64	-0.9	-0.58	-0.83	-0.66	-0.3	0.02
LD																							***-0.99***	*-0.99*	0.68	-0.86	-0.74	-0.93	-0.75	-0.25	0.23
T_{leaf}																								***0.99***	-0.73	0.91	0.72	0.92	0.77	0.34	-0.2
T_{mes}																									-0.69	0.91	0.64	0.87	0.71	0.32	-0.09
f_{ias}																										-0.88	-0.8	-0.83	*-0.97*	-0.82	0.48
T_{chl}																											0.62	0.82	0.82	0.69	-0.09
L_{chl}																												0.93	0.92	0.34	0.36
S_m/S																													0.92	0.37	-0.56
S_c/S																														0.66	-0.64
S_c/S_m																															-0.13
T_{cw}																															

Table S3. Pearson correlation matrix of physiological, leaf water relations, cell wall and anatomical parameters measured in *S. lycopersicum* LSL genotype across all experimental conditions. Values in italics and bold indicate significant (P<0.05) and highly significant (P<0.01) correlation coefficients, respectively.

	A_N	g_s	WUE_i	g_m	ETR	R_{light}	Ψ_{pd}	Ψ_{md}	RWC	AIR	Cel.	Hemicel.	Pectins	(C+H)/P	π_o	RWC_{tlp}	Ψ_{tlp}	ε	a_f	C^*_{ft}	LMA	LD	T_{leaf}	T_{mes}	f_{ias}	T_{chl}	L_{chl}	S_m/S	S_c/S	S_c/S_m	T_{cw}
A_N		*0.96*	-0.87	*0.97*	***1***	*0.97*	0.8	0.82	*0.95*	0.68	-0.5	0.33	-0.87	*0.98*	0.91	-0.94	0.91	-0.94	-0.71	0.82	-0.85	-0.81	0.62	0.69	-0.76	0.91	0.63	0.92	***1***	0.95	*0.97*
g_s			-0.94	0.91	0.94	***1***	0.78	0.77	0.92	0.44	-0.42	0.34	-0.69	0.92	0.83	*-0.97*	0.89	-0.9	-0.71	0.65	-0.89	-0.6	0.66	0.71	-0.83	0.84	0.46	0.78	0.95	0.83	0.9
WUE_i				-0.89	-0.84	-0.93	-0.91	-0.88	-0.94	-0.34	0.08	-0.01	0.06	-0.89	-0.86	*0.99*	-0.95	0.93	0.88	-0.44	*0.99*	0.46	-0.38	-0.43	*0.97*	-0.62	-0.18	-0.63	-0.85	-0.67	-0.87
g_m					0.97	0.91	0.9	0.93	*0.99*	0.74	-0.33	0.11	-0.9	***1***	*0.98*	-0.94	*0.97*	*-0.99*	-0.83	0.77	-0.89	-0.82	0.43	0.51	-0.82	0.82	0.54	0.9	*0.97*	0.9	***1***
ETR						*0.95*	0.77	0.8	0.94	0.71	-0.54	0.36	-0.88	*0.98*	0.9	-0.92	0.89	-0.93	-0.67	0.85	-0.81	-0.83	0.64	0.71	-0.72	0.93	0.68	0.94	***1***	*0.96*	*0.97*
R_{light}							0.78	0.77	0.92	0.47	-0.44	0.35	-0.71	0.93	0.83	*-0.97*	0.89	-0.91	-0.7	0.68	-0.88	-0.63	0.67	0.72	-0.81	0.85	0.49	0.8	*0.96*	0.85	0.91
Ψ_{pd}								***0.99***	0.95	0.54	0.11	-0.29	-0.71	0.89	0.95	-0.91	*0.98*	*-0.95*	*-0.99*	0.44	*-0.96*	-0.57	0.06	0.14	*-0.95*	0.5	0.14	0.63	0.79	0.63	0.89
Ψ_{md}									*0.95*	0.62	0.05	-0.27	-0.78	0.91	*0.97*	-0.89	*0.98*	*-0.96*	*-0.97*	0.52	-0.94	-0.65	0.08	0.16	-0.91	0.55	0.23	0.69	0.81	0.68	0.92
RWC										0.64	-0.22	0.03	-0.83	*0.99*	*0.98*	*-0.97*	***0.99***	***-1***	-0.89	0.67	-0.95	-0.73	0.37	0.45	-0.9	0.75	0.42	0.82	0.95	0.84	*0.98*
AIRg											-0.47	0.12	*-0.96*	0.72	0.75	-0.48	0.59	-0.66	-0.43	0.89	-0.39	*-0.98*	0.23	0.33	-0.28	0.71	0.79	0.88	0.71	0.82	0.76
Cel.												-0.93	0.48	-0.36	-0.17	0.22	-0.1	0.19	-0.26	-0.79	-0.02	0.6	-0.89	-0.9	-0.16	-0.81	-0.91	-0.67	-0.53	-0.7	-0.35
Hemicel.													-0.17	0.16	-0.07	-0.11	-0.08	0	0.42	0.53	0.12	-0.29	0.93	0.9	0.24	0.65	0.7	0.42	0.34	0.48	0.13
Pectins														-0.89	-0.89	0.71	-0.79	0.84	0.61	-0.92	0.62	0.98	-0.37	-0.48	0.52	-0.83	-0.77	*-0.96*	-0.88	-0.93	-0.92
(C+H)/P															*0.97*	*-0.95*	*0.96*	*-0.98*	-0.81	0.78	-0.89	-0.82	0.47	0.55	-0.82	0.84	0.56	0.9	*0.98*	0.91	***1***
π_o																-0.91	*0.98*	*-0.99*	-0.89	0.7	-0.9	-0.8	0.25	0.34	-0.84	0.71	0.44	0.84	0.91	0.82	*0.98*
RWC_{tlp}																	*-0.97*	*0.97*	0.85	-0.58	*0.97*	0.6	-0.47	-0.53	0.93	-0.74	-0.34	-0.75	-0.93	-0.78	-0.93
Ψ_{tlp}																		***-0.99***	-0.94	0.59	*-0.97*	-0.67	0.27	0.35	-0.94	0.67	0.31	0.76	0.9	0.76	*0.96*
ε																			0.9	-0.67	0.95	0.74	-0.34	-0.42	0.9	-0.74	-0.41	-0.82	-0.94	-0.83	*-0.98*
a_f																				-0.3	0.94	0.45	0.06	-0.01	*0.96*	-0.36	0.01	-0.51	-0.69	-0.5	-0.81
C^*_{ft}																					-0.41	*-0.96*	0.65	0.73	-0.28	0.94	0.95	0.97	0.84	*0.96*	0.79
LMA																						0.48	-0.25	-0.31	*0.99*	-0.56	-0.13	-0.61	-0.83	-0.64	-0.88
LD																							-0.43	-0.53	0.36	-0.85	-0.86	*-0.96*	-0.83	-0.93	-0.84
T_{leaf}																								***0.99***	-0.14	0.82	0.71	0.61	0.63	0.69	0.44
T_{mes}																									-0.19	0.88	0.76	0.7	0.7	0.76	0.52
f_{ias}																										-0.43	0.02	-0.49	-0.73	-0.52	-0.8
T_{chl}																											0.87	*0.95*	0.93	*0.98*	0.83
L_{chl}																												0.86	0.66	0.85	0.57
S_m/S																													0.94	***0.99***	0.91
S_c/S																														*0.96*	*0.97*
S_c/S_m																															0.91
T_{cw}																															

Chapter 5

The use of mutant plants to elucidate the effect of specific cell wall disruptions affecting photosynthesis

Reduced photosynthesis in *Arabidopsis thaliana atpme17.2* and *atpae11.1* mutants is associated to altered cell wall composition

Margalida Roig-Oliver[1*], Catherine Rayon[2], Romain Roulard[2], François Fournet[2], Josefina Bota[1], Jaume Flexas[1]

[1]Research Group on Plant Biology under Mediterranean Conditions, Departament de Biologia, Universitat de les Illes Balears (UIB) – Agro-Environmental and Water Economics Institute (INAGEA). Carretera de Valldemossa Km 7.5, 07122 Palma, Illes Balears, Spain.
[2]EA 3900-BIOPI, Biologie des Plantes et Innovation, Université de Picardie Jules Verne, Amiens 80039, France.

[*] Corresponding author.

Published in *Physiologia Plantarum* in 2020.

Physiologia Plantarum
An International Journal for Plant Biology

Physiologia Plantarum 0: 0–0. 2020

Reduced photosynthesis in *Arabidopsis thaliana atpme17.2* and *atpae11.1* mutants is associated to altered cell wall composition

Margalida Roig-Oliver[a,*], Catherine Rayon[b], Romain Roulard[b], François Fournet[b], Josefina Bota[a] and Jaume Flexas[a]

[a]Research Group on Plant Biology under Mediterranean Conditions, Departament de Biologia, Universitat de les Illes Balears (UIB) – Agro-Environmental and Water Economics Institute (INAGEA), Palma 07122, Spain
[b]EA 3900-BIOPI, Biologie des Plantes et Innovation, Université de Picardie Jules Verne, Amiens 80039, France

Correspondence
*Corresponding author,
e-mail: margaroig93@gmail.com

Received 28 May 2020
revised 31 July 2020

doi:10.1111/ppl.13186

The cell wall is a complex and dynamic structure that determines plants' performance by constant remodeling of its compounds. Although cellulose is its major load-bearing component, pectins are crucial to determine wall characteristics. Changes in pectin physicochemical properties, due to pectin remodeling enzymes (PRE), induce the rearrangement of cell wall compounds, thus, modifying wall architecture. In this work, we tested for the first time how cell wall dynamics affect photosynthetic properties in *Arabidopsis thaliana* pectin methylesterase *atpme17.2* and pectin acetylesterase *atpae11.1* mutants in comparison to wild-type Col-0. Our results showed maintained PRE activities comparing mutants with wild-type and no significant differences in cellulose, but cell wall non-cellulosic neutral sugars contents changed. Particularly, the amount of galacturonic acid (GalA) – which represents to some extent the pectin cell wall proportion – was reduced in the two mutants. Additionally, physiological characterization revealed that mutants presented a decreased net CO_2 assimilation (A_N) because of reductions in both stomatal (g_s) and mesophyll conductances (g_m). Thus, our results suggest that *atpme17.2* and *atpae11.1* cell wall modifications due to genetic alterations could play a significant role in determining photosynthesis.

Introduction

The plant cell wall is a complex structure surrounding plant cells that determines plant morphology by defining cells' shape and size due to the maintenance of an appropriated turgor pressure (Cosgrove 2005, Ali and Traas 2016). It is mainly composed of cellulose microfibrils cross-linked to non-cellulosic polysaccharides, hemicelluloses. This network consisting of cellulose and hemicelluloses is embedded in a matrix of pectins, another specific type of non-cellulosic polysaccharides

Abbreviations – AE, acetylesterase; A_N, net CO_2 assimilation; C_i, CO_2 concentration at the sub-stomatal cavity; CWPE, cell wall protein extract; DCW, dry cell wall; ETR, electron transport rate; f_{ias}, fraction of mesophyll intercellular air spaces; GalA, galacturonic acid; g_m, mesophyll conductance; g_s, stomatal conductance; HG, homogalacturonans; N_{PAL}, number of palisade layers; PAE, pectin acetylesterase; PME, pectin methylesterase; PRE, pectin remodeling enzymes; RG-I, rhamnogalacturonan type 1; RG-II, rhamnogalacturonan type 2; R_{light}, light respiration; T_{LE}, lower epidermis thickness; T_{LEAF}, leaf thickness; T_{MES}, mesophyll thickness; T_{UE}, upper epidermis thickness; WUE_i, intrinsic water use efficiency; XGA, xylogalacturonan.

(Carpita and Gibeaut 1993, Carpita and McCann 2002, Cosgrove 2005, Lampugnani et al. 2018). By constant remodeling of its components and because of the action of cell wall remodeling enzymes, the cell wall is a highly dynamic structure for the synthesis of new polysaccharides during cell elongation and differentiation and/or in response to stress (Carpita and McCann 2002, Cosgrove 2005, 2016, Tenhaken 2015, Hocq et al. 2017, Kong et al. 2019, Rui and Dinnery 2019).

Although cell wall mechanical properties are often related to the interaction between cellulose and hemicelluloses (Baskin 2005, Geitmann and Ortega 2009), the importance of pectins physicochemical modifications in determining cell wall traits during plants growth and in response to biotic and abiotic stresses – for instance, porosity, hydric status and elasticity – has also been demonstrated (Cosgrove 2005, 2016, Pelloux et al. 2007, Moore et al. 2008, Solecka et al. 2008, McKenna et al. 2010, Gou et al. 2012, Palin and Geitmann 2012, Turbant et al. 2016, Hocq et al. 2017, Kong et al. 2019, Roig-Oliver et al. 2020). Pectins are complex non-cellulosic polysaccharides rich in galacturonic acid (GalA) that can be divided into four main polymers according to their chemical structure: rhamnogalacturonans types 1 and 2 (RG-I and RG-II, respectively), homogalacturonans (HG) and xylogalacturonan (XGA) (Caffall and Mohnen 2009, Atmodjo et al. 2013). Although the ratio between these polysaccharides depends on species, tissues and plant developmental stages, HG are the most abundant ones and consist in linear regions of up to 200 α-1,4-linked GalA residues (Carpita and McCann 2002, Caffall and Mohnen 2009) secreted to the cell wall in a highly methyl-esterified form (70–80%; Pelloux et al. 2007, Guénin et al. 2017). Pectin methylesterases (PME, EC 3.1.1.11) are enzymes which remove HG methyl groups (Pelloux et al. 2007, Turbant et al. 2016, Guénin et al. 2017). Whilst low levels of PME activity have been related to an increase of cell wall rigidity and to alterations in seed germination, plant growth and reproduction (Parre and Geitmann 2005, Bosch and Hepler 2005, Derbyshire et al. 2007, Pelletier et al. 2010, Müller et al. 2013, Leroux et al. 2015, Levesque-Tremblay et al. 2015, Scheler et al. 2015, Turbant et al. 2016, Guénin et al. 2017), enhanced PME activity could lead to cell wall loosening (Peaucelle et al. 2008, 2011). On the other hand, pectin acetylesterases (PAE, EC 3.1.1.6) control the pectin acetylesterification status by regulating the degree of GalA acetylation in both HG and RG-I residues, which can also interfere with plants growth and development (Gou et al. 2008, 2012, de Souza et al. 2014, de Souza and Pauly 2015). However, little is still known regarding the specific biological implications of different acetylation degrees (Gou et al. 2012, de Souza et al. 2014, de Souza and Pauly 2015, Philippe et al. 2017). Thus, the action of pectin remodeling enzymes (PRE) – which includes PME and (P)AE activities – involves changes in pectins physicochemical properties that confer them the ability to rearrange the pectin matrix as well as to modify their interaction between other cell wall compounds modifying wall architecture, thickness and porosity (Cosgrove 2005, Solecka et al. 2008, de Souza and Pauly 2015, Houston et al. 2006, Turbant et al. 2016, Hocq et al. 2017, Kong et al. 2019, Rui and Dinnery 2019). Some of these cell wall characteristics, particularly thickness and porosity, have actually been identified as key traits determining mesophyll conductance (g_m) and, thus, photosynthesis (Terashima et al. 2001, Evans et al. 2009, Flexas et al. 2012, Tomás et al. 2013, Carriquí et al. 2015, 2019, 2020, Tosens et al. 2016, Onoda et al. 2017, Peguero-Pina et al. 2017, Veromann-Jürgenson et al. 2017). As these cell wall characteristics are likely influenced by dynamic changes in its composition, cell wall components rearrangements have been recently shown to affect g_m at an interspecific level under non-stress conditions (Carriquí et al. 2020) and at an intraspecific level in response to environmental stresses (Clemente-Moreno et al. 2019, Roig-Oliver et al. 2020).

The use of mutants has demonstrated that cell wall modifications could involve changes in photosynthesis. Particularly, Ellsworth et al. (2018) tested *Oryza sativa* mutants with disruptions in cell wall mixed-linkage glucan biosynthesis leading to slower growth and phenotypic disruptions such as thinner stems with reduced flexibility. Additionally, Zhang et al. (2020) tested other mutants of the same species in which cellulose microfibrils orientation was disrupted affecting plant growth and photosynthesis as shown by a lower chlorophyll content. Although these studies demonstrate that cell wall modifications alter photosynthesis, their results are difficult to extrapolate to the rest of angiosperms as monocots present specific cell wall composition (Carpita and McCann 2002, Pooper and Tuohy 2010, Sørensen et al. 2010). Thus, the use of *Arabidopsis thaliana* L. (Heynh) as a model plant is more adequate for a better understanding of how cell wall modifications affect photosynthesis. After the completion of its genome sequence (Arabidopsis Genome Initiative 2000), *Arabidopsis* has gained importance because it is relatively easy to generate mutants to study how specific genetic alterations modify both biochemical and physiological processes. Although Weraduwage et al. (2016) have already tested *A. thaliana* mutants with alterations in pectin methyltransferases showing that they changed both PME activity and photosynthesis, further information regarding other relevant enzyme activities – such as pectin acetylesterases – is necessary for a better understanding of how

cell wall dynamics can affect photosynthesis, especially g_m. Thus, we provide a study in which *A. thaliana atpme17.2*, a type I PME (Sénéchal et al. 2014), and *atpae11.1* (Philippe et al. unpublished) mutants were tested for the first time in comparison to wild-type Col-0 in order to evaluate the role of cell wall composition and PRE activities in determining photosynthetic efficiency.

Materials and methods

Plant material and growth conditions

A. thaliana atpme17.2 (SALK_059908) and *atpae11.1* (GK 505H02) mutants from wild-type Columbia (Col-0) were isolated from SALK (SIGnAL, USA) and GABI (CeBiTec, Germany) T-DNA insertion collections, respectively, using gene-specific forward and reverse primers and T-DNA left border specific primers (Sénéchal et al. 2014, Philippe et al. unpublished data). Whilst the T-DNA insertion was localized in the first intron for *atpme17.2*, it was localized in the tenth for *atpae11.1*. Twelve seeds of each studied genotype were sown individually in horticultural alveolus with a substrate mixture containing peat and perlite (3:1, v/v). Horticultural alveolus with plastic trays for sub-irrigation were placed in a growth chamber at 22°C with 12/12 h light/darkness daily fluctuation receiving 200–250 µmol m^{-2} s^{-1} photosynthetic photon flux density (PPFD) and they were watered three times per week with Hoagland solution 50%. Three weeks later, six individual replicates per genotype were randomly selected to be transplanted to individual pots filled with the same substrate mixture following the 'ice-cream cone-like' method (Flexas et al. 2007a). Thus, plants grew with their bases on the top of the 'cone', with their rosette spreading downwards to facilitate gas-exchange measurements. In all cases, plants were subjected to these conditions for 40 days.

Gas-exchange and fluorescence measurements

Forty days after the sowing, a fully developed leaf per plant from the third to last pair of the rosette was selected for simultaneous gas-exchange and chlorophyll *a* fluorescence (Chl *a*) measurements using an infrared gas analyzer (IRGA) LI-6400XTR equipped with a fluorometer (Li-6400-40; Li-Cor Inc.). Measurements were performed from 09:00 to 15:00 h. Leaves were clamped into a 2 cm^2 cuvette. The block temperature was kept at 25°C and the vapor pressure deficit (VPD) at around 1.5 kPa. Leaf steady-state conditions were induced at saturating photosynthetic photon flux density (PPFD 1250 µmol m^{-2} s^{-1}, 90–10% red-blue light) and 400 µmol CO_2 mol^{-1} air. The flow rate was fixed at 300 µmol air min^{-1}. When steady-state conditions were reached, A_N-C_i curves were performed increasing ambient CO_2 concentrations (C_a) from 50 to 1500 µmol CO_2 mol^{-1} air. Measurements for net CO_2 assimilation (A_N), stomatal conductance (g_s), CO_2 concentration at the sub-stomatal cavity (C_i) and steady-state fluorescence (F_s) were registered after the stabilization of the gas-exchange rates in a given C_a in a period comprised between 180 and 240 s. Then, a saturating light flash was applied to obtain the maximum fluorescence (F_m'). From these values, the real quantum efficiency of photosystem II (Φ_{PSII}) was registered. All A_N-C_i data was corrected for CO_2 leakage in and out of the IRGA chamber following Flexas et al. (2007b). Light curves under non-photorespiratory conditions were assessed as described in Valentini et al. (1995) to calculate the electron transport rate (ETR). Light respiration (R_{light}) was assumed as half the dark respiration rate, determined after plants exposure to full darkness for, at least, 20 min (Niinemets et al. 2005). From all these parameters, mesophyll conductance (g_m) was calculated according to Harley et al. (1992) using the value for CO_2 compensation point in the absence of respiration (Γ^*) reported by Whitney et al. (2011) for *A. thaliana*.

Anatomical measurements

After gas-exchange measurements, one randomly selected plant per genotype was used to collect samples for anatomy. Thus, small pieces of those leaves used for gas-exchange measurements were cut avoiding main foliar structures and were fixed under vacuum pressure with glutaraldehyde 4% and paraformaldehyde 2% in a 0.01 M phosphate buffer (pH 7.4). Afterward, they were post-fixed in 2% buffered osmium tetroxide for 2 h and dehydrated by a graded ethanol series. Obtained pieces were embedded in LR white resin (London Resin Company) and were placed in an oven at 60°C for 48 h (Tomás et al. 2013, Carriquí et al. 2015, 2019). Semi-fine (0.8 µm) cross-sections were cut with an ultramicrotome (Leica RM2265, Leica Biosystems) and were stained with toluidine blue 0.1% to be observed in bright field with a light microscope (Nikon-Eclipse-90i). Pictures at ×100 magnifications were taken to determine leaf thickness (T_{LEAF}), upper epidermis thickness (T_{UE}), lower epidermis thickness (T_{LE}), mesophyll thickness (T_{MES}), number of palisade layers (N_{PAL}) and fraction of mesophyll intercellular air spaces (f_{ias}). Values for all parameters were obtained as an average of 10 measurements from randomly selected cell structures using the ImageJ software (Wayne Rasband/NIH).

Cell wall composition

Sampling for cell wall analysis was performed in those leaves adjacent to the one used for gas-exchange measurements after leaving plants under dark conditions overnight to minimize starch content. Around 0.5–1 g of fresh leaf tissue per plant were frozen in liquid nitrogen, freeze-dried, ground to fine powder in a ball mill and stored at −80°C. Plant cell wall material was prepared from 10 mg of dry leaf powder according to Peña et al. (2004). Dry cell wall material (DCW) was digested with α-amylase according to Fleischer et al. (1999). Following Foster et al. (2010), 3 mg of each α-amylase-digested DCW were placed in screw-capped glass tubes to be hydrolysed with 1 ml of 2 N trifluoroacetic acid at 100°C for 90 min, cooled down at room temperature and centrifuged obtaining two phases: the supernatant (non-cellulosic cell wall sugars, i.e. hemicelluloses and pectins) and the pellet (cellulosic cell wall sugars). Trifluoroacetic acid remains from the supernatant were evaporated under nitrogen flow to quantify specific neutral sugars from hemicelluloses cell wall fraction (i.e. fucose, rhamnose, arabinose, galactose, glucose, xylose and mannose) and from pectin fraction (i.e. galacturonic acid) as described in Turbant et al. (2016). After evaporated, hydrolysates were dissolved with 1 ml of deionized water and each one was diluted (1:10, v/v) to determine its specific non-cellulosic neutral sugars composition by high-performance anion-exchange chromatography coupled with a pulsed electrochemical detection (HPAEC-PAD; Dionex ICS-3000, Dionex Corporation).

Cellulose content was estimated following Foster et al. (2010). Thus, pellets were cleaned three times with deionized water and subsequently freeze-dried overnight. Freeze-dried samples were resuspended in 1 ml Updegraff reagent (acetic acid: nitric acid: deionized water, 8:1:2 v/v) to be heated at 100°C for 30 min. Once cooled, samples were centrifuged at 10 000 *g* and pellets were cleaned twice with deionized water and three times with absolute acetone. Then, they were freeze-dried overnight. The following morning, 175 µl sulfuric acid 72% were added and samples were incubated at 30°C for 45 min. Afterward, 825 µl deionized water was added and the mixtures were centrifuged at 10 000 *g*. Finally, 200 µl anthrone reagent prepared in sulfuric acid 100% (2:1, w:v) plus 90 µl deionized water was added to 10 µl of each supernatant. Samples absorbance was read at 625 nm using a Microplate Spectrophotometer (BioTek PowerWave). Cellulose concentration was determined by interpolating samples absorbance from a glucose calibration curve.

Protein extraction and cell wall enzyme activity assays

Enriched weakly bound cell wall proteins (CWP) were extracted to perform PME and (P)AE enzyme activities assays. Briefly, around 0.7–1 g fresh leaf tissue from leaves adjacent to the one used for gas-exchange measurements were sampled, grounded to fine powder using a ball mill and stored at −80°C. Then, 50 mg of frozen plant powder were homogenized in 150 µl of 50 mM sodium dihydrogen phosphate (pH 7.5) containing 2 M sodium chloride. Samples were incubated at 4°C under constant agitation for 30 min before centrifugation at 13 000 *g*. The supernatants were recovered and a second extraction was performed on pellets following the same methodology. The supernatants were combined and desalted on Amicon Ultra-0.5 Centrifugal Filter Unit 3Kda cut-off (Merck Millipore) using McIlvaine buffer (0.2 M disodium hydrogen phosphate prepared in 0.1 M citric acid, pH 6.5) containing 100 mM sodium chloride. Protein concentration was determined according to Bradford (1976). Thus, samples absorbance was read at 595 nm using a spectrophotometer (BioTek PowerWave) and CWP concentration was determined by interpolating samples values from a bovine serum albumin calibration curve.

The overall PME enzyme activity was determined by measuring the methanol released from pectin methyl ester content (Baldwin et al. 2014). Briefly, 5 µl of each CWP were incubated with 85 µl of 50 mM sodium phosphate buffer (pH 7.5) containing 0.025 U alcohol oxidase and 100 µg methyl-esterified citrus pectin solution 90%. Samples were incubated at 28°C for 30 min and, then, 100 µl of staining solution (2 M ammonium acetate and 20 mM pentane-2,4-dione prepared in 50 mM glacial acetic acid) were added. They were incubated at 68°C under darkness conditions for 15 min and their absorbance was read at 420 nm with a spectrophotometer (BioTek PowerWave). PME enzyme activity was determined by interpolating samples values from a methanol calibration curve.

AE and PAE enzyme activities were estimated by measuring acetate release using triacetin and sugar beet as a substrate, respectively (Baldwin et al. 2014, Remoroza et al. 2014). Thus, 20 µg of CWP extract in a final volume of 30 µl were incubated with 0.2 M sodium dihydrogen phosphate prepared in 100 mM sodium chloride and 0.1 M citric acid (pH 6.5). Then, 120 µl of 100 mM triacetin (Sigma) or 10 mg ml^{-1} of sugar beet pectin (42% methylesterification and 31% acetylation degrees, CP Kelco) prepared in McIlvaine buffer containing 100 mM sodium chloride were added to samples for AE or PAE assays, respectively. They were incubated at 40°C under

constant agitation for 2 h. Once cooled, the acetate concentration of each sample was determined with the Acetic Acid Kit (Megazyme, K-ACETRM). Samples absorbance was read at 340 nm with a spectrophotometer (BioTek PowerWave). AE and PAE enzyme activities were determined by interpolating samples values from an acetic acid calibration curve.

Statistical analysis

Thompson test was performed to detect and eliminate outliers for all tested parameters. Then, one-way ANOVA and subsequent LSD test were assessed to detect statistically significant differences for the studied parameters between genotypes ($P < 0.05$). All analyses were performed with R software (ver. 3.2.2; R Core Team, Austria).

Results

Pectin remodeling enzymes activities

No significant changes in PRE activities were observed comparing *atpme17.2* and *atpae11.1* mutants with the wild-type Col-0 (Fig. 2). Particularly, all tested genotypes presented similar amount of PME enzyme activity (0.18 ± 0.01, 0.19 ± 0.02 and 0.18 ± 0.01 nmol methanol µg protein^{-1} min^{-1} for Col-0, *atpae11.1* and *atpme17.2*, respectively; Fig. 2A). A similar pattern was detected for both AE and PAE enzyme activities (Fig. 2B,C, respectively).

Cell wall cellulosic and non-cellulosic sugars characterization

Cellulose content did not differ between the studied genotypes (Fig. 3A). However, there was a strong reduction in the cell wall pectin fraction, expressed by the amounts of galacturonic acid, in both *atpae11.1* and *atpme17.2* mutants (34.55 ± 3.96 and 66.27 ± 5.78 % WT, respectively; Fig. 3A). Regarding the hemicellulosic cell wall fraction, although both mutants presented increased fucose content in comparison to Col-0, these changes were only significant for *atpae11.1* (Fig. 3B). Nonetheless, no significant modifications were detected comparing the amount of other non-cellulosic neutral sugars belonging to hemicelluloses (i.e. rhamnose, arabinose, galactose, glucose, xylose and mannose) among genotypes (Fig. 3B).

Photosynthetic characterization

The analysis of A_N-C_i curves revealed that both *atpae11.1* and *atpme17.2* mutants showed strong reductions in photosynthetic capacity accompanied by diminished C_i (Supporting Information, Fig. S1). At ambient CO_2 concentration, mutants presented more than a two-fold decrease in A_N compared to wild-type (4.95 ± 1.19, 3.24 ± 0.58 and 10.05 ± 0.63 µmol CO_2 m^{-2} s^{-1} for *atpae11.1*, *atpme17.2* and Col-0, respectively; Fig. 4A). Additionally, decreases in g_s were also detected, being more pronounced in *atpme17.2* (0.11 ± 0.02 mol CO_2 m^{-2} s^{-1}; Fig. 4B). However, these A_N and g_s reductions in both mutants did not lead to differing WUE_i in comparison to Col-0 (Fig. 4C). Again, g_m reductions were found in both mutants, especially in *atpme17.2* with a g_m eight-fold lower than Col-0 (Fig. 4D). Finally, no significant differences among genotypes were found for ETR and R_{light} (Fig. 4E,F, respectively).

Anatomical characterization

The preliminary analysis of leaf anatomic features indicated a reduction in T_{LEAF} which was observed in both mutants in comparison to Col-0 (Table S1). However, they presented slightly increased and reduced T_{UE} and T_{LE}, respectively, than the wild-type (Table S1). Additionally, in both mutants there were indications of a decrease in T_{MES}, but even more marked in *atpae11.1*, which also obtained lower N_{PAL} than Col-0 (Table S1). Finally, changes in f_{ias} suggested an increase of porosity in *atpme17.2* and *atpae11.1* in comparison to Col-0 (Table S1).

Discussion

Cell wall rearrangement is an important feature determining plants' development during their entire life (Carpita and McCann 2002, Cosgrove 2005, 2016, Tenhaken 2015, Hocq et al. 2017, Lampugnani et al. 2018, Kong et al. 2019, Rui and Dinnery 2019). In this work, *A. thaliana atpme17.2* and *atpae11.1* mutants were studied in comparison to wild-type Col-0 to assess for the first time whether potential differences in their cell wall composition – including PRE activities – could affect photosynthesis.

Several studies have evidenced phenotypic effects occurring in specific *Arabidopsis* mutants (for instance, Hernández-Blanco et al. 2007, Kong et al. 2014, López-Calcagno et al. 2017, Zhao et al. 2018), which were also detected in this study as mutant plants reduced their rosette diameter as well as their foliar size in comparison to wild-type (Fig. 1). In fact, alterations of PRE activities could be involved in several physiological processes due to the remodeling of cell wall architecture, which could modify the plants' phenotype (Carpita and McCann 2002, Cosgrove 2005, 2016, Hocq et al. 2017, Kong et al. 2019). Particularly, the effects of altered PME have been widely studied and, in *Arabidopsis*, they are implicated in seed germination (Müller et al. 2013),

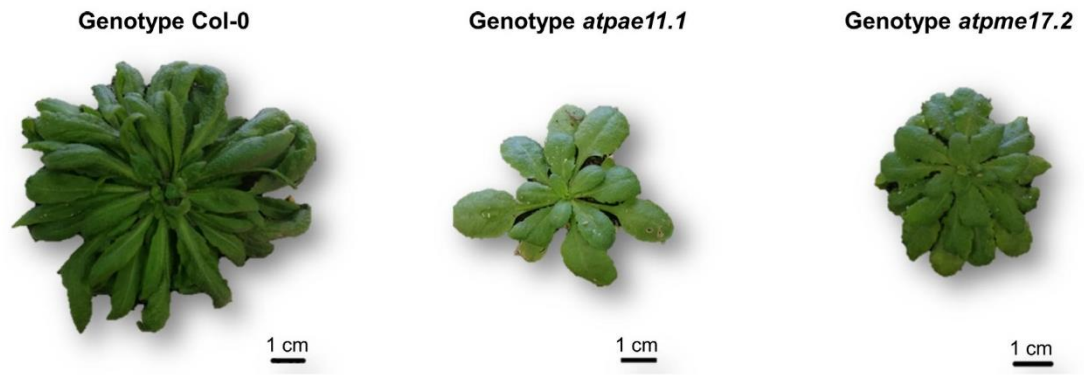

Fig. 1. Representative phenotypical alterations of 40-day-old wild-type Col-0 in comparison to *atpae11.1* and *atpme17.2* mutant genotypes.

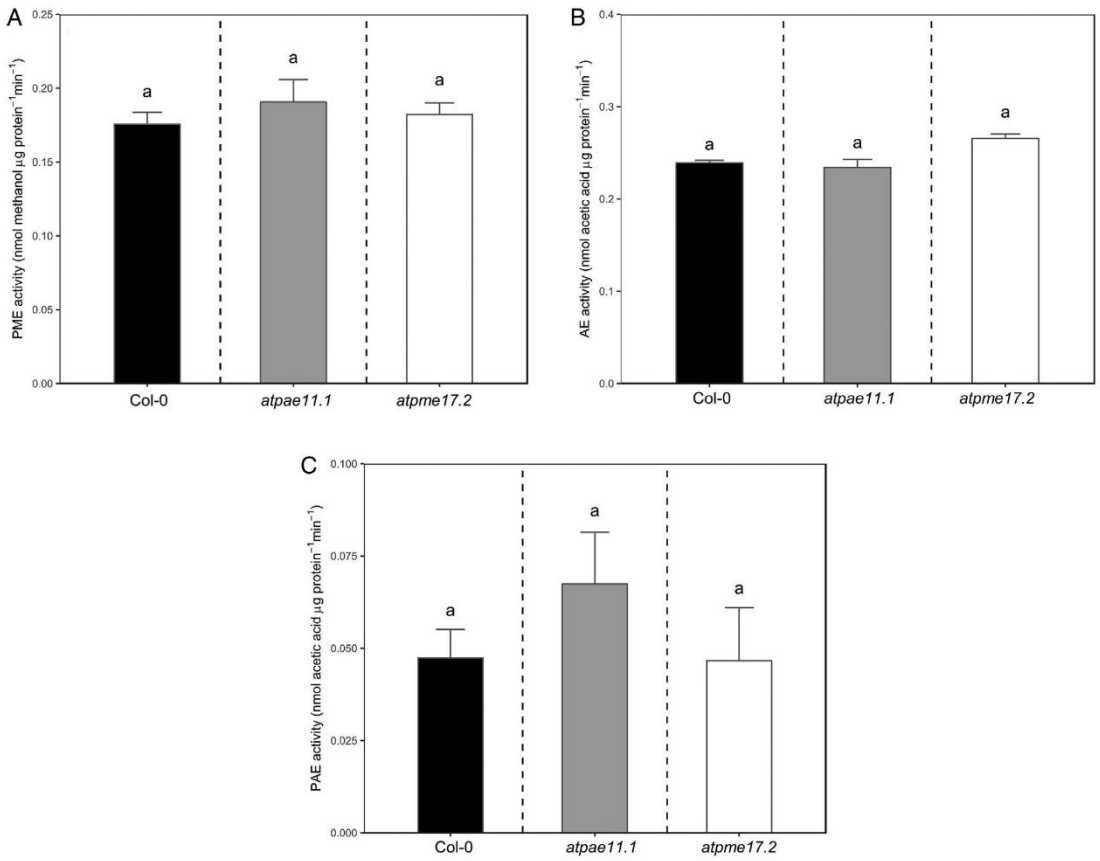

Fig. 2. Enzyme activities in *Arabidopsis thaliana* Col-0, *atpae11.1* and *atpme17.2* genotypes. (A) Pectin methylesterase, (B) acetylesterase and (C) pectin acetylesterase. Different superscript letters indicate significant difference ($P < 0.05$) between genotypes according to LSD test. n = 4–6 (means ± SE).

seed mucilage adhesion (Turbant et al. 2016), reduction of root hair production (Guénin et al. 2017), pollen grain maturation and germination (Leroux et al. 2015), dark-grown hypocotyls (Derbyshire et al. 2007, Pelletier et al. 2010) or even in stomatal function (Amsbury et al. 2016). On the other hand, although there is limited information regarding specific biological effects of PAE on plants growth and development, it seems that it could be involved in determining *Arabidopsis* inflorescence stem height (de Souza et al. 2014) and in regulating pollen tube growth and plant reproduction in other species (Gou et al. 2012). However, we did not observe any significant differences in PRE activities comparing mutant genotypes with Col-0 (Fig. 2). Although Sénéchal et al. (2014) and Philippe et al. (unpublished data) reported that *AtPME17* and *AtPAE11*, respectively, were highly expressed in older leaves and roots, there is no obvious correlation between high transcript levels and translation into high protein levels and/or high enzymes activities (Bosch and Hepler 2005, Jamet et al. 2009). Additionally, although *atpme17.2* and *atpae11.1* exhibited mutations in the same genes than those mutants used in Sénéchal et al. (2014) and Philippe et al. (unpublished data), the ones studied here presented alterations in introns, while those used in the above-mentioned studies were localized in exons. Thus, we suggest that different positions of the T-DNA insertions used for our mutant genotypes could be involved in differing PRE activities in comparison to previous reports. Furthermore, our tested mutants could contain specific PME and/or PAE proteins which may not be present in Col-0, thus, compensating PME and PAE activities. In *A. thaliana*, pectin methylesterases belong to a multigenic family of 66 isoforms (Pelloux et al. 2007). Therefore, as it has been proposed that some genes could control the same processes (Bosch and Hepler 2005), those alterations related to *AtPME17.2* could be supplied for other similar or related genes. Similarly, pectin acetylesterases belong to a multigenic family of 12 isoforms in *A. thaliana*, but their implications are not fully understood (Gou et al. 2012, Philippe et al. 2017). For instance, de Souza et al. (2014) reported a genetic characterization of null *atpae8* and *atpae9* mutants showing that they presented 20% more acetate in their cell wall. Moreover, the double mutant showed an even more enhanced acetate cell wall proportion (37%). However, Orfila et al. (2012) overexpressed an ortholog *Arabidopsis AtPAE8* from *Vigna unguiculata* in potato and found a decreased degree of pectin acetylation. Following previous studies, we expected changes in PAE activity, but it was maintained at similar levels in all tested genotypes perhaps due to genetic redundancy.

Despite enzymatic activities were maintained, the two mutants presented alterations of cell wall composition which could explain the phenotypic differences. However, our results for cell wall non-cellulosic neutral sugars analyses differed from previous reports by Mertz et al. (2012) and Engelsdorf et al. (2017). Particularly, Mertz et al. (2012) determined that galacturonic acid (GalA) was the most abundant non-cellulosic neutral sugar in *A. thaliana mur* mutants. Additionally, Engelsdorf et al. (2017) tested *A. thaliana pgm*, *adg1-1* and *sex1-1* mutants and showed that neutral sugars from the hemicellulosic cell wall fraction significantly changed in comparison to wild-type Col-0, whilst GalA amounts were maintained. Nonetheless, our results differed from the previous studies probably because, apart from testing

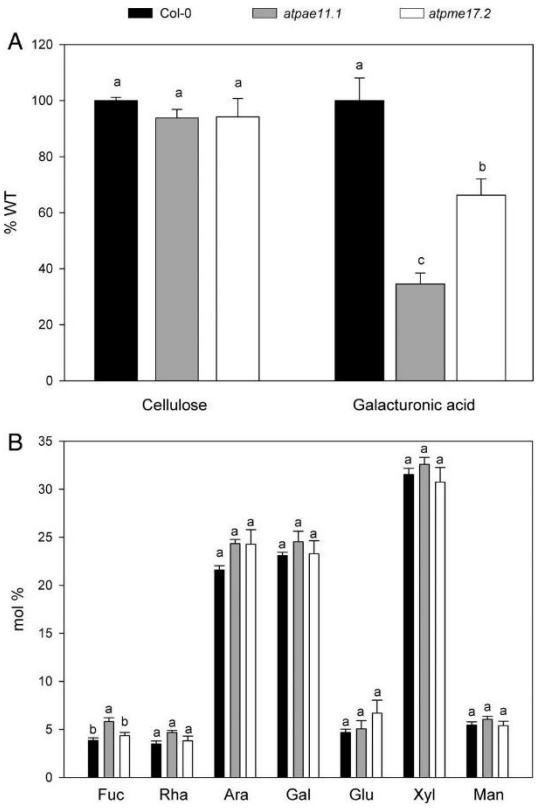

Fig. 3. Cell wall composition of *A. thaliana* Col-0, *atpae11.1* and *atpme17.2* genotypes. (A) Cellulose and galacturonic acid content and (B) non-cellulosic neutral sugars content from hemicellulosic cell wall fraction: L-fucose (Fuc), L-rhamnose (Rha), L-arabinose (Ara), D-galactose (Gal), D-glucose (Glu), D-xylose (Xyl) and D-mannose (Man). Different superscript letters indicate significant difference ($P < 0.05$) between genotypes according to LSD test. n = 4–6 (means ± SE).

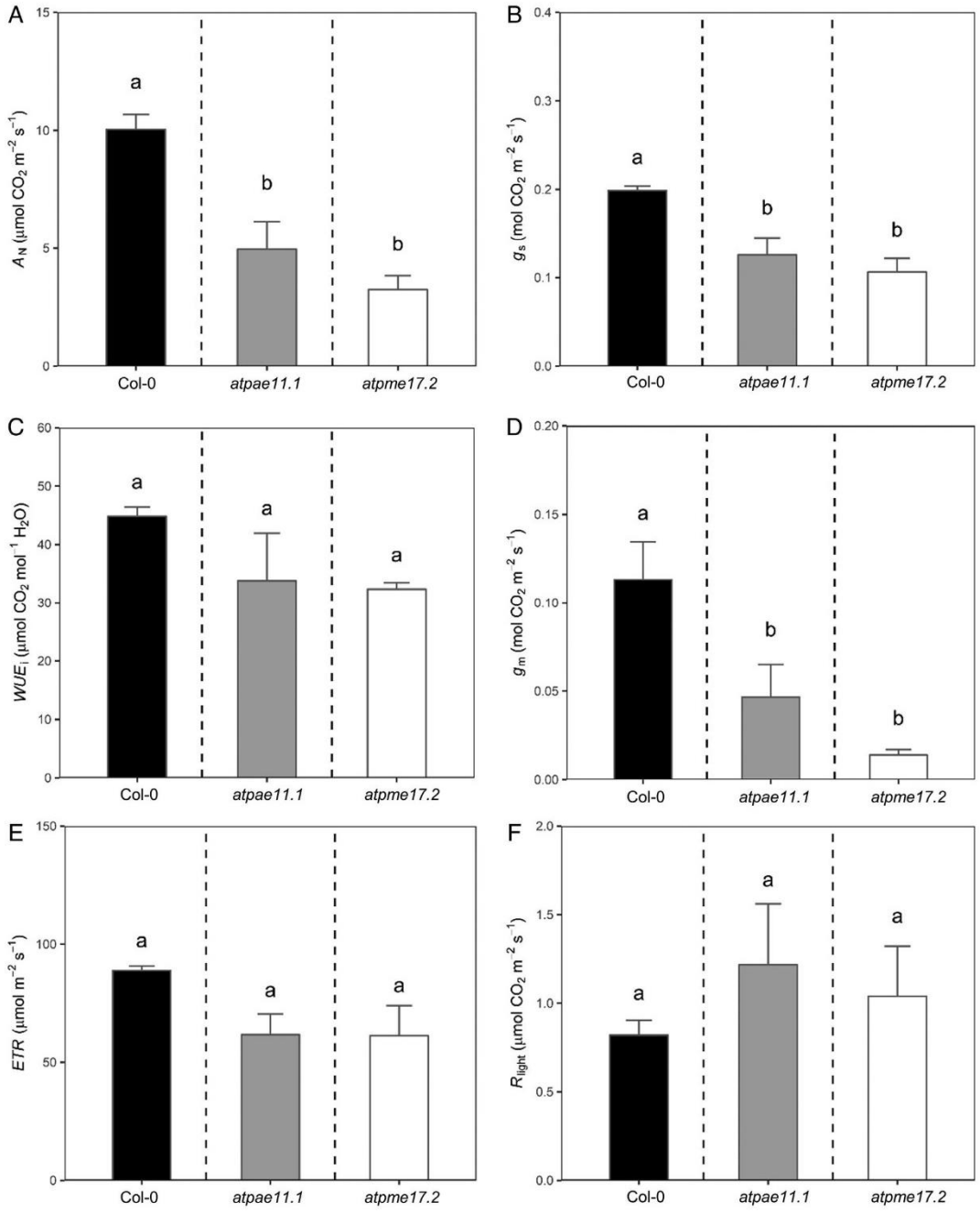

Fig. 4. Photosynthetic characterization of *A. thaliana* Col-0, *atpae11.1* and *atpme17.2* genotypes. (A) Net CO_2 assimilation (A_N), (B) stomatal conductance (g_s), (C) intrinsic water use efficiency (WUE_i), (D) mesophyll conductance (g_m), (E) electron transport rate (ETR) and (F) light respiration (R_{light}). Different superscript letters indicate significant difference ($P < 0.05$) between genotypes according to LSD test. n = 5–6 (means ± SE).

other mutants, our plants were grown under different conditions, for instance, different photoperiod, light intensity and soil composition. Additionally, we performed the trifluoroacetic acid hydrolysis at 100°C instead of at 121°C, which may have resulted in higher resistance to the acid hydrolysis of the linkages between GalA-GalA and rhamnose-GalA, thus, obtaining lower amounts of both non-cellulosic neutral sugars than expected. However, our results showed that both mutants experienced decreased amounts of GalA (i.e. pectins) compared to wild-type (Fig. 3A) with maintained PRE activities. In fact, there is no obvious correlation between altered PRE activities and modified pectins quantity probably because they determine pectins physicochemical properties, not their amount (Pelloux et al. 2007, Gou et al. 2012, Palin and Geitmann 2012, Turbant et al. 2016, Hocq et al. 2017, Kong et al. 2019). Therefore, this descent in pectins as well as some additional mutant-specific alterations in the hemicellulosic cell wall fraction such as increased fucose in *atpae11.1* (Fig. 3B), could explain the diminished photosynthetic capacity (Figs 4 and S1) as previously reported (Weraduwage et al. 2016), especially, via altered g_m (Ellsworth et al. 2018, Clemente-Moreno et al. 2019, Carriquí et al. 2020, Roig-Oliver et al. 2020). Of the previous studies, Clemente-Moreno et al. (2019) and Roig-Oliver et al. (2020) demonstrated a cell wall composition-mediated effect on g_m based on correlative evidence after stress-inducing changes in both g_m and cell wall composition testing tobacco and grapevines, respectively. Particularly, Clemente-Moreno et al. (2019) found a negative relationship between non-cellulosic sugars, specifically pectins, with g_m. Although Weraduwage et al. (2016) did not focus on modifications of g_m, they also highlighted the importance of pectins as possible drivers of altered photosynthesis in *A. thaliana* cell wall mutants. However, only Ellsworth et al. (2018) used cell wall mutants to directly demonstrate the role of cell wall composition on g_m. Specifically, they used rice mutants with disruptions in cell wall mixed-linkage glucan – a compound specific of grasses – production and showed a reduction in g_m of 83%, which was only partially explained by changes in observed anatomical properties. In fact, Weraduwage et al. (2016) also reported that anatomical alterations derived from cell wall modifications were important determinants of photosynthesis. The results provided in these previous studies lead to the suggestion that altered cell wall composition may induce changes in cell wall effective porosity and CO_2 diffusion path length and/or chemical properties, thus, changing photosynthesis. Nonetheless, our results follow a different pattern than those reported by Clemente-Moreno et al. (2019) probably because they only tested one single genotype after short-term water and salt stresses induction. As our tested genotypes were grown under non-stressing conditions and the observed phenotypical differences are likely to be constitutive, we believe that our data on *atpme17.2* and *atpae11.1* mutants could be much more comparable with that from Carriquí et al. (2020). Particularly, while they demonstrated that pectins themselves did not correlate with g_m testing seven conifers species, they found a strong positive relationship between g_m and the ratio of pectins to celluloses and hemicelluloses. Even though in this study we do not have enough data to calculate this ratio, the fact that celluloses were equally maintained among genotypes, and pectins were not, suggests that g_m reductions in *atpme17.2* and *atpae11.1* mutants could also be related to a diminished fraction of pectins to celluloses and, perhaps, hemicelluloses. Additionally, although anatomical traits were studied only preliminarily in this work, we hypothesize that together with non-cellulosic sugars alterations they could also be involved in photosynthesis reduction in both mutants as they display, for instance, decreased T_{LEAF} and T_{MES} as compared to wild-type (Table S1). However, more detailed anatomical studies of *atpme17.2* and *atpae11.1* mutants using more replicates would be necessary to confirm this point. Finally, and contrary to Ellsworth et al. (2018), the mutants also showed a significant decrease of g_s (although of lower magnitude than that of g_m). Whether this is an indirect consequence of co-adjustment with reduced g_m (Flexas et al. 2013) or a direct effect of cell wall composition on stomata (Jones et al. 2003) remains to be elucidated.

This study provides insights on how different cell wall architecture could influence the photosynthetic efficiency in *A. thaliana atpme17.2* and *atpae11.1* mutants in comparison to wild-type Col-0. Thus, we established that cell wall composition modification could lead to reduced photosynthetic traits in *atpme17.2* and *atpae11.1* mutants maybe because of alterations in leaf chemistry and, perhaps, in anatomical traits. However, more studies are required to establish the potential implications of *AtPME17.2* and *AtPAE11.1* in whole plant dynamics using mutants where the T-DNA insertion is localized in their specific catalytic sites.

Author contributions

M.R.-O., C.R., J.B. and J.F. designed the study; M.R.-O., C.R., R.R. and F.F. conducted the experiment; M.R.-O. performed the data analysis and M.R.-O., J.B. and J.F. wrote the first manuscript version. All authors contributed to its following versions.

Acknowledgements – This work was supported by the project PGC2018-093824-B-C41 from Ministerio de Economía y Competitividad (MINECO, Spain). M.R.-O. was supported by a predoctoral fellowship FPU16/01544. We thank Ms. Maïté Leschevin for her help during enzymatic activities assays performance.

Data Availability Statement

Data sharing is not applicable to this article as no new data were created or analyzed in this study.

References

Ali O, Traas J (2016) Force-driven polymerization and turgor-induced wall expansion. Trends Plant Sci 21: 398–409

Amsbury S, Hunt L, Elhaddad N, Baillie A, Lundgren M, Verhertbruggen Y, Scheller HV, Knox JP, Fleming AJ, Gray JE (2016) Stomatal function requires pectin de-methyl-esterification of the guard cell wall. Curr Biol 26: 2899–2906

Arabidopsis Genome Initiative (2000) Analysis of the genome sequence of the flowering plant *Arabidopsis thaliana*. Nature 408: 796–815

Atmodjo MA, Zhangying H, Mohnen D (2013) Evolving views of pectin biosynthesis. Annu Rev Plant Biol 64: 747–779

Baldwin L, Domon JM, Klimek JF, Fournet F, Sellier H, Gillet F, Pelloux J, Lejeune-Hénaut I, Carpita NC, Rayon C (2014) Structural alteration of cell wall pectins accompanies pea development in response to cold. Phytochemistry 104: 37–47

Baskin TI (2005) Anisotropic expansion of the plant cell wall. Annu Rev Cell Dev Biol 21: 203–222

Bosch M, Hepler PK (2005) Pectin methylesterases and pectin dynamics in pollen tubes. Plant Cell 17: 3219–3226

Bradford MM (1976) A rapid and sensitive method for the quantitation of microgram quantities of protein utilizing the principle of protein-dye binding. Anal Biochem 72: 248–254

Caffall KH, Mohnen D (2009) The structure, function, and biosynthesis of plant cell wall pectic polysaccharides. Carbohydr Res 344: 1879–1900

Carpita NC, Gibeaut DM (1993) Structural models of primary cell walls in flowering plants: consistency of molecular structure with the physical properties of the walls during growth. Plant J 3: 1–30

Carpita NC, McCann MC (2002) The functions of cell wall polysaccharides in composition and architecture revealed through mutations. Plant and Soil 247: 71–80

Carriquí M, Cabrera HM, Conesa MÀ, Coopman RE, Douthe C, Gago J, Gallé A, Galmés J, Ribas-Carbó M, Tomás M, Flexas M (2015) Diffusional limitations explain the lower photosynthetic capacity of ferns as compared with angiosperms in a common garden study. Plant Cell Environ 38: 448–460

Carriquí M, Roig-Oliver M, Brodribb TJ, Coopman R, Gill W, Mark K, Niinemets Ü, Perera-Castro AV, Ribas-Carbó M, Sack L, Tosens T, Waite M, Flexas J (2019) Anatomical constraints to nonstomatal diffusion conductance and photosynthesis in lycophytes and bryophytes. New Phytol 222: 1256–1270

Carriquí M, Nadal M, Clemente-Moreno MJ, Gago J, Miedes E, Flexas J (2020) Cell wall composition strongly influences mesophyll conductance in gymnosperms. Plant J, 103: 1372–1385. https://doi.org/10.1111/tpj.14806

Clemente-Moreno MJ, Gago J, Díaz-Vivancos P, Bernal A, Miedes E, Bresta P, Liakopoulos G, Fernie AR, Hernández JA, Flexas J (2019) The apoplastic antioxidant system and altered cell wall dynamics influence mesophyll conductance and the rate of photosynthesis. Plant J 99: 1031–1046

Cosgrove DJ (2005) Growth of the plant cell wall. Nat Rev Mol Cell Biol 6: 850–861

Cosgrove DJ (2016) Plant cell wall extensibility: connecting plant cell growth with cell wall structure, mechanics, and the action of wall-modifying enzymes. J Exp Bot 67: 463–476

de Souza AJ, Hull PA, Gille S, Pauly M (2014) Identification and functional characterization of the distinct plant pectin esterases PAE8 and PAE9 and their deletion mutants. Planta 240: 1123–1138

de Souza AJ, Pauly M (2015) Comparative genomics of pectinacetylesterases: insight on function and biology. Plant Signal Behav 10: e1055434

Derbyshire P, McCann MC, Roberts K (2007) Restricted cell elongation in *Arabidopsis* hypocotyls is associated with a reduced average pectin esterification level. BMC Plant Biol 7: 31

Ellsworth PV, Ellsworth PZ, Koteyeva NK, Cousins AB (2018) Cell wall properties in *Oryza sativa* influence mesophyll CO_2 conductance. New Phytol 219: 66–76

Engelsdorf T, Will C, Hofmann J, Schmitt C, Merritt BB, Rieger L, Frenger MS, Marschall A, Franke RB, Pattathil S, Voll LM (2017) Cell wall composition and penetration resistance against the fungal pathogen *Colletotrichum higginsianum* are affected by impaired starch turnover in *Arabidopsis* mutants. J Exp Bot 68: 701–713

Evans JR, Kaldenhoff R, Genty B, Terashima I (2009) Resistance along the CO_2 diffusion pathway inside leaves. J Exp Bot 60: 2235–2248

Fleischer A, O'Neill MA, Ehwald R (1999) The pore size of non-graminaceous plant cell walls is rapidly decreased by borate ester cross-linking of the pectic polysaccharide rhamnogalacturonan II. Plant Physiol 121: 829–838

Flexas J, Ortuño MF, Ribas-Carbó M, Díaz-Espejo A, Flórez-Saraza ID, Medrano H (2007a) Mesophyll conductance to CO_2 in *Arabidopsis thaliana*. New Phytol 175: 501–511

Flexas J, Díaz-Espejo A, Berry JA, Cifre J, Galmés J, Kaldenhoff R, Medrano H, Ribas-Carbó M (2007b) Analysis of leakage in IRGA's leaf chambers of open gas exchange systems: quantification and its effects in photosynthesis parameterization. J Exp Bot 58: 1533–1543

Flexas J, Barbour MM, Brendel O, Cabrera HM, Carriquí M, Díaz-Espejo A, Douthe C, Dreyer E, Ferrio JP, Gago J, Gallé A, Galmés J, Kodama N, Medrano H, Niinemets Ü, Peguero-Pina JJ, Pou A, Ribas-Carbó M, Tomás M, Tosens T, Warren CR (2012) Mesophyll conductance to CO_2: an unappreciated central player in photosynthesis. Plant Sci 193-194: 70–84

Flexas J, Niinemets Ü, Gallé A, Barbour MM, Centritto M, Díaz-Espejo A, Douthe C, Galmés J, Ribas-Carbó M, Rodríguez PL, Rosselló F, Soolanayakanahally R, Tomás M, Wright IJ, Farqujar GD, Medrano H (2013) Diffusional conductances to CO_2 as a target for increasing photosynthesis and photosynthetic water-use efficiency. Photosynth Res 117: 45–59

Foster CE, Martin TM, Pauly M (2010) Comprehensive compositional analysis of plant cell walls (lignocellulosic biomass) part II: carbohydrates. JoVE 37: 1837

Geitmann A, Ortega JKE (2009) Mechanics and modelling of plant cell growth. Trends Plant Sci 14: 467–478

Gou JY, Park S, Yu XH, Miller LM, Liu CJ (2008) Compositional characterization and imaging of "wall-bound" acylesters of *Populus trichocarpa* reveal differential accumulation of acyl molecules in normal and reactive woods. Planta 229: 15–24

Gou JY, Miller LM, Hou G, Yu XH, Chen XY, Liu CJ (2012) Acetylesterase-mediated deacetylation of pectin impairs cell elongation, pollen germination, and plant reproduction. Plant Cell 24: 50–65

Guénin S, Hardouin J, Paynel F, Müller K, Mongelard G, Driouich A, Lerouge P, Kermode AR, Lehner A, Mollet JC, Pelloux J, Gutiérrez L, Mareck A (2017) AtPME3, a ubiquitous cell wall pectin methylesterase of *Arabidopsis thaliana*, alters the metabolism of cruciferin seed storage proteins during post-germinative growth of seedlings. J Exp Bot 68: 1083–1095

Harley PC, Loreto F, Di Marco G, Sharkey TD (1992) Theoretical considerations when estimating the mesophyll conductance to CO_2 flux by the analysis of the response of photosynthesis to CO_2. Plant Physiol 98: 1429–1436

Hernández-Blanco C, Feng DX, Hu J, Sánchez-Vallet A, Deslandes L, Llorente F, Berrocal-Lobo M, Keller H, Barlet X, Sánchez-Rodríguez C, Anderson LK, Somerville S, Marco Y, Molina A (2007) Impairment of cellulose synthase required for *Arabidopsis* secondary cell wall formation enhances disease resistance. Plant Cell 19: 890–903

Hocq L, Sénéchal F, Lefebvre V, Lehner A, Domon JM, Mollet JC, Dehors J, Pageau K, Marcelo P, Guérineau F, Kolšek K, Mercadante D, Pelloux J (2017) Combined experimental and computational approaches reveal distinct pH dependence of pectin methylesterase inhibitors. Plant Physiol 173: 1075–1093

Houston K, Tucker MR, Chowdhury J, Shirley N, Little A (2006) The plant cell wall: a complex and dynamic structure as revealed by the responses of genes under stress conditions. Front Plant Sci 7: 984

Jamet E, Roujol D, San-Clemente H, Irshad M, Soubigou-Taconnat L, Renou JP, Pont-Lezica R (2009) Cell wall biogenesis of *Arabidopsis thaliana* elongating cells: transcriptomics complements proteomics. BMC Genomics 10: 505

Jones L, Milne JL, Ashford D, McQueen-Mason SJ (2003) Cell wall arabinan is essential for guard cell function. Proc Natl Acad Sci U S A 100: 11783–11788

Kong Y, Peña MJ, Renna L, Avci U, Pattathil S, Tuomivaara ST, Li X, Reiter WD, Brandizzi F, Hahn MG, Darvill AG, York WS, O'Neill MA (2014) Galactose-depleted xyloglucan is dysfunctional and leads to dwarfism in *Arabidopsis*. Plant Physiol 167: 1296–1306

Kong G, Wan L, Deng YZ, Yang W, Li W, Jiang L, Situ J, Xi P, Li M, Jiang Z (2019) Pectin acetylesterase PAE5 is associated with the virulence of plant pathogenic oomycete *Peronophythora litchii*. Physiol Mol Plant Path 106: 16–22

Lampugnani ER, Khan GA, Somssich M, Persson S (2018) Building a plant cell wall at a glance. J Cell Sci 131: jcs207373

Leroux C, Bouton S, Kiefer-Meyer MC, Fabrice TN, Mareck A, Guénin S, Fournet F, Ringli C, Pelloux J, Drioich A, Lerouge P, Lehner MJC (2015) Pectin methylesterase48 is involved in *Arabidopsis* pollen grain germination. Plant Physiol 167: 367–380

Levesque-Tremblay G, Pelloux J, Braybrook SA, Müller K (2015) Tuning of pectin methylesterification: consequences for cell wall biomechanics and development. Planta 242: 791–811

López-Calcagno PE, Abuzaid AO, Lawson T, Raines CA (2017) *Arabidopsis* CP12 mutants have reduced levels of phosphoribulokinase and impaired function of the Calvin-Benson cycle. J Exp Bot 68: 2285–2298

McKenna BA, Kopittke PM, Wehr JB, Blamey FPC, Menzies NW (2010) Metal ion effects on hydraulic conductivity of bacterial cellulose–pectin composites used as plant cell wall analogs. Physiol Plant 138: 205–214

Mertz RA, Olek AT, Carpita NC (2012) Alterations in cell-wall glycosyl linkage structure of *Arabidopsis* murus mutants. Carbohydr Polym 89: 331–339

Moore JP, Farrant JM, Driouich A (2008) A role for pectin-associated arabinans in maintaining the flexibility of the plant cell wall during water deficit stress. Plant Signal Behav 3: 102–104

Müller K, Levesque-Tremblay G, Bartels S, Weitbrecht K, Wormit A, Usadel B, Haughn G, Kermode AR (2013) Demethylesterification of cell wall pectins in *Arabidopsis* plays a role in seed germination. Plant Physiol 161: 305–316

Niinemets Ü, Cescatti A, Rodeghiero M, Tosens T (2005) Leaf internal diffusion conductance limits photosynthesis more strongly in older leaves of Mediterranean evergreen broad-leaved species. Plant Cell Environ 28: 1552–1566

Onoda Y, Wright IJ, Evans JR, Hikosaka K, Kitajima K, Niinemets Ü, Poorter H, Tosens T, Westoby M (2017) Physiological and structural tradeoffs underlying the leaf economics spectrum. New Phytol 214: 1447–1463

Orfila C, Dal Degan F, Jorgensen B, Scheller HV, Ray PM, Ulvskov P (2012) Expression of mung bean pectin acetyl esterase in potato tubers: effect on acetylation of cell wall polymers and tuber mechanical properties. Planta 236: 185–196

Palin R, Geitmann A (2012) The role of pectin in plant morphogenesis. Biosystems 109: 397–402

Parre E, Geitmann A (2005) Pectin and the role of the physical properties of the cell wall in pollen tube growth of *Solanum chacoense*. Planta 220: 582–592

Peaucelle A, Louvet R, Johansen JN, Höfte H, Laufs P, Pelloux J, Mouille G (2008) *Arabidopsis* phyllotaxis is controlled by the methylesterification status of cell-wall pectins. Curr Biol 18: 1943–1948

Peaucelle A, Braybrook SA, Le Guillou L, Bron E, Kuhlemeier C, Höfte H (2011) Pectin-induced changes in cell wall mechanics underlie organ initiation in *Arabidopsis*. Curr Biol 21: 1720–1726

Peguero-Pina JJ, Sancho-Knapik D, Gil-Pelegrín E (2017) Ancient cell structural traits and photosynthesis in today's environment. J Exp Bot 68: 1389–1392

Pelletier S, Van Orden J, Wolf S, Vissenberg K, Delacourt J, Ndong YA, Pelloux J, Bischoff V, Urbain A, Mouille G, Lemonnier G, Renou JP, Höfte H (2010) A role for pectin de-methylesterification in a developmentally regulated growth acceleration in dark-grown *Arabidopsis* hypocotyls. New Phytol 188: 726–739

Pelloux J, Rustérucci C, Mellerowicz EJ (2007) New insights into pectin methylesterase structure and function. Trends Plant Sci 12: 267–277

Peña MJ, Ryden P, Madson M, Smith AC, Carpita NC (2004) The galactose residues of xyloglucan are essential to maintain mechanical strength of the primary cell walls in Arabidopsis during growth. Plant Physiol 134: 443–451

Philippe F, Pelloux J, Rayon C (2017) Plant pectin acetylesterase structure and function: new insights from bioinformatic analysis. BMC Genomics 18: 456

Pooper ZA, Tuohy MG (2010) Beyond the green: understanding the evolutionary puzzle of plant and algal cell walls. Plant Physiol 153: 373–383

Remoroza C, Wagenknecht M, Gu F, Buchholt HC, Moerschbacher BM, Schols H, Gruppen H (2014) A *Bacillus licheniformis* pectin acetylesterase is specific for homogalacturonan acetylated at O-3. Carbohydr Polym 107: 85–93

Roig-Oliver M, Nadal M, Clemente-Moreno MJ, Bota J, Flexas J (2020) Cell wall components regulate photosynthesis and leaf water relations of *Vitis vinifera* cv. Grenache acclimated to contrasting environmental conditions. J Plant Physiol 244: 153084

Rui Y, Dinnery JR (2019) A wall with integrity: surveillance and maintenance of the plant cell wall under stress. New Phytol 225: 1428–1439

Scheler C, Weitbrecht K, Pearce SP, Hampstead A, Büttner-Mainik A, Lee KJD, Voegele A, Oracz K, Dekkers BJW, Wang X, Wood ATA, Bentsink L, King JR, Knox JP, Holdsworth MJ, Müller K, Leubner-Metzger G (2015) Promotion of testa rupture during garden cress germination involves seed compartment-specific expression and activity of pectin methylesterases. Plant Physiol 167: 200–215

Sénéchal F, Graff L, Surcouf O, Marcelo P, Rayon C, Bouton S, MAreck A, Mouille G, Stintzi A, Höfte H, Lerouge P, Schaller A, Pelloux J (2014) *Arabidopsis* PECTIN METHYLESTERASE17 is co-expressed with and processed by SBT3.5, a subtilisin-line serine protease. Ann Bot 114: 1161–1175

Solecka D, Zebrowski J, Kacperska A (2008) Are pectins involved in cold acclimation and de-acclimation of winter oil-seed rape plants? Ann Bot 101: 521–530

Sørensen I, Domozych D, Williats WGT (2010) How have plant cell walls evolved? Plant Physiol 153: 366–372

Tenhaken R (2015) Cell wall remodelling under abiotic stress. Front Plant Sci 5: 771

Terashima I, Miyazawa SI, Hanba YT (2001) Why are sun leaves thicker than shade leaves? Consideration based on analyses of CO_2 diffusion in the leaf. J Pl Res 114: 93–105

Tomás M, Flexas J, Copolovici L, Galmés J, Hallik L, Medrano H, Ribas-Carbó M, Tosens T, Vislap V, Niinements Ü (2013) Importance of leaf anatomy in determining mesophyll diffusion conductance to CO_2 across species: quantitative limitations and scaling up by models. J Exp Bot 64: 2269–2281

Tosens T, Nishida K, Gago J, Coopman RE, Cabrera HM, Carriquí M, Laanisto L, Morales L, Nadal M, Rojas R, Talts E, Tomás M, Hanba Y, Niinemets Ü, Flexas J (2016) The photosynthetic capacity in 35 ferns and fern allies: mesophyll CO_2 diffusion as a key trait. New Phytol 209: 1576–1590

Turbant A, Fournet F, Lequart M, Zabijak L, Pageau K, Bouton S, Wuytswinkel V (2016) PME58 plays a role in pectin distribution during seed coat mucilage extrusion through homogalacturonan modification. J Exp Bot 67: 2177–2190

Valentini R, Epron D, Angelis PD, Matteucci G, Dreyer E (1995) In situ estimation of net CO_2 assimilation, photosynthetic electron flow and photorespiration of

Turkey oak (*Q. cerris* L.) leaves: diurnal cycles under different water supply. Plant Cell Environ 18: 631–664
Veromann-Jürgenson LL, Tosens T, Laanisto L, Niinemets Ü (2017) Extremely thick cell walls and low mesophyll conductance: welcome to the world of ancient living! J Exp Bot 68: 1639–1653
Weraduwage SM, Kim SJ, Renna L, Anozie FC, Sharkey TD, Brandizzi F (2016) Pectin methylesterification impacts the relationship between photosynthesis and plant growth in *Arabidopsis thaliana*. Plant Physiol 171: 833–848
Whitney SM, Houtz RL, Alonso H (2011) Advancing our understanding and capacity to engineer nature's CO_2-sequestering enzyme, Rubisco. Plant Physiol 155: 27–35
Zhang R, Hu H, Wang Y, Hu Z, Ren S, Li J, He B, Wang Y, Xia T, Chen P, Xie G, Peng L (2020) A novel rice *fragile culm 24* mutant encodes a UDP-glucose epimerase that affects cell wall property and photosynthesis. J Exp Bot 71: 2956–2969. https://doi.org/10.1093/jxb/eraa044
Zhao X, Liu N, Shang N, Zeng W, Ebert B, Rautengarten C, Zeng QY, Li H, Chen X, Beahan C, Bacic A, Heazlewood JL, Wu AM (2018) Three UDP-xylose transporters participate in xylan biosynthesis by conveying cytosolic UDP-xylose into the Golgi lumen in *Arabidopsis*. J Exp Bot 69: 1125–1124

Supporting information

Additional supporting information may be found online in the Supporting Information section at the end of the article.

Table S1. Anatomical characterization from semi-fine cross-sections of *Arabidopsis thaliana* Col-0, *atpae11.1* and *atpme17.2* genotypes.

Fig. S1. Net CO_2 assimilation at different CO_2 concentrations at the sub-stomatal cavity (A_N-C_i curves) of *Arabidopsis thaliana* Col-0, *atpae11.1* and *atpme17.2* genotypes.

Edited by R. Rivero

Supplementary Information

Table S1. Anatomical characterization from semi-fine cross sections of *A. thaliana* Col-0, *atpae11.1* and *atpme17.2* genotypes. Average values ± SE from ten measurements are shown for leaf thickness (T_{LEAF}), upper epidermis thickness (T_{UE}), lower epidermis thickness (T_{LE}), mesophyll thickness (T_{MES}), number of palisade layers (N_{PAL}) and fraction of mesophyll intercellular air spaces (f_{ias}). n = 1 in all cases.

Genotypes	**Parameters**					
	T_{LEAF} (μm)	T_{UE} (μm)	T_{LE} (μm)	T_{MES} (μm)	N_{PAL}	f_{ias} (%)
Col-0	188.8 ± 2.4	16.6 ± 1.3	14.9 ± 1.4	149.6 ± 3.0	1.8 ± 0.3	19.2
atpae11.1	157.9 ± 3.8	19.0 ± 1.6	11.7 ± 0.4	115.8 ± 5.9	1.3 ± 0.3	38.6
atpme17.2	165.2 ± 4.9	21.5 ± 2.1	11.5 ± 0.6	130.0 ± 4.6	1.8 ± 0.1	25.9

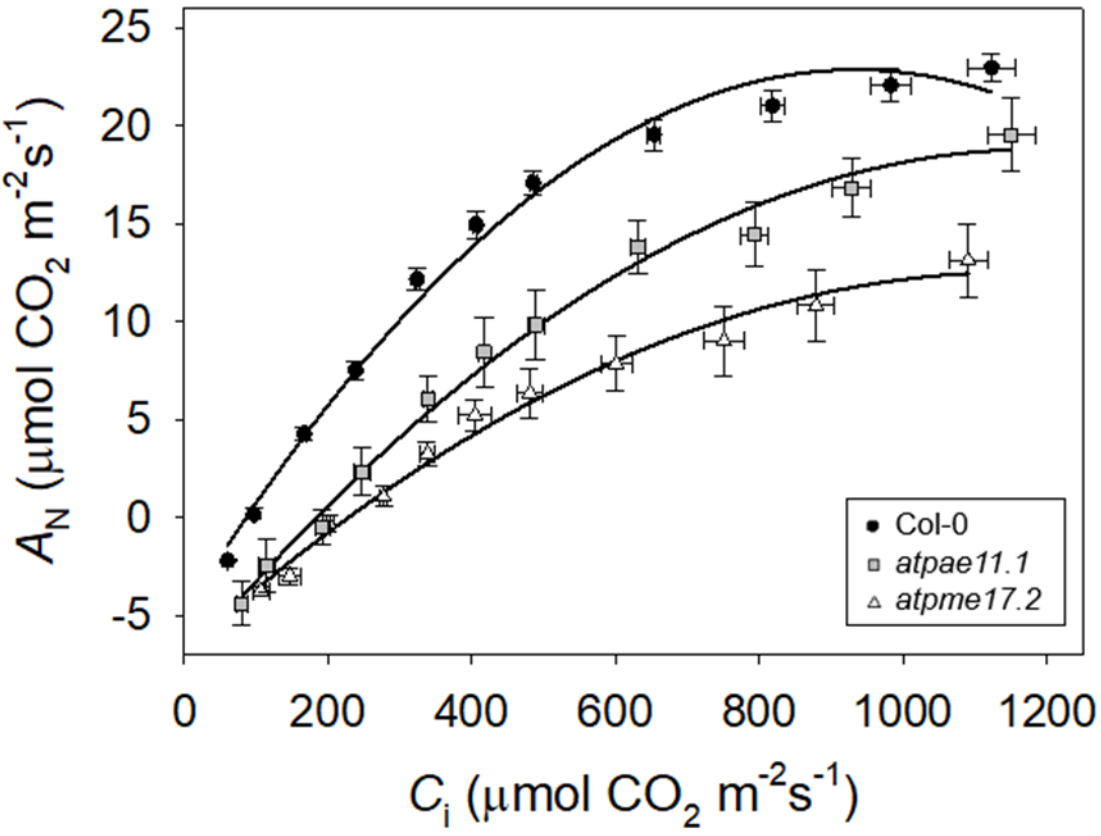

Fig. S1. Net CO_2 assimilation at different CO_2 concentrations at the sub-stomatal cavity (A_N-C_i curves) of *A. thaliana* Col-0, *atpae11.1* and *atpme17.2* genotypes. Each point represents average values ± SE of independent gas-exchange measurements conducted with different plants. n = 5–6.

Chapter 6

Cell wall composition: an important photosynthesis determinant conserved in the most primitive land plant lineage

Cell wall thickness and composition are related to photosynthesis in Antarctic mosses

Margalida Roig-Oliver[1*], Cyril Douthe[1], Josefina Bota[1], Jaume Flexas[1,2]

[1]Research Group on Plant Biology under Mediterranean Conditions, Departament de Biologia, Universitat de les Illes Balears (UIB) – Agro-Environmental and Water Economics Institute (INAGEA). Carretera de Valldemossa Km 7.5, 07122 Palma, Illes Balears, Spain.
[2]King Abdulaziz University, Jeddah, Saudi Arabia.

[*] Corresponding author.

Submitted to *Physiologia Plantarum* on 27th May 2021.

Cell wall thickness and composition are related to photosynthesis in Antarctic mosses

Margalida Roig-Oliver[1*], Cyril Douthe[1], Josefina Bota[1], Jaume Flexas[1,2]

[1]Research Group on Plant Biology under Mediterranean Conditions, Departament de Biologia, Universitat de les Illes Balears (UIB) – Agro-Environmental and Water Economics Institute (INAGEA). Carretera de Valldemossa Km 7.5, 07122 Palma, Illes Balears, Spain.
[2]King Abdulaziz University, Jeddah, Saudi Arabia.

*Corresponding author: Margalida Roig-Oliver, margaroig93@gmail.com

Abstract

Cell wall thickness (T_{cw}) is an important anatomical trait determining photosynthesis through land plants' phylogeny, being bryophytes the plant group presenting the thickest walls and the lowest photosynthetic rates. Recently, the potential involvement of cell wall composition influencing both thickness and mesophyll conductance (g_m) has been suggested, representing a novel trait that could ultimately affect photosynthesis. However, only a few studies testing spermatophytes have demonstrated that issue. In order to explore the role of cell wall composition in determining both T_{cw} and g_m in mosses, we tested six species growing under field conditions in Antarctica. We performed gas exchange and chlorophyll fluorescence measurements, an anatomical characterization, and a quantitative analysis of cell wall main composition (i.e., cellulose, hemicelluloses and pectins) in the six species. We reported different photosynthetic rates for the studied species, which also presented differences in anatomical characteristics and in cell wall composition. Whilst g_m correlated negatively with T_{cw} and pectins content, a positive relationship between T_{cw} and pectins emerged, suggesting that pectins could contribute to determine cell wall porosity. Our results show for the first time that cell wall composition –with pectins playing a key role– strongly influences T_{cw} and g_m in Antarctic mosses, ultimately defining photosynthesis.

Key words

Cell wall composition, cell wall thickness, mesophyll conductance, mosses, pectins.

Introduction

Antarctica is considered the most extreme region on Earth since it is the coldest, driest, highest, windiest, and most isolated continent, in which large seasonal temperature extremes as well as fluctuations in solar radiation and in water availability occur (Robinson et al., 2003; Bramley-Alves et al., 2014). Because of these harsh conditions and an extremely short growing season, the Antarctic flora is dominated by algae, lichens, and bryophytes. Of these, bryophytes (i.e., hornworts, liverworts, and mosses) constitute one of the most diverse groups of land plants as they comprehend more than 12.500 extant species, being surpassed only by angiosperms (Hedderson et al., 1996; Goffinet et al., 2001; Shaw & Renzaglia, 2004; Frey & Stech, 2009). In Antarctica, at least 111 bryophyte species are present (Ochyra et al., 2008; Bramley-Alves et al., 2014), representing one of the few regions in which they predominate because their biological characteristics allows them to inhabit those areas where vascular plants are sparse or absent (Buck & Goffinet, 2000; Newton et al., 2000; Hyvönen et al., 2004; Proctor et al., 2007; Roberts et al., 2012; Huttunen et al, 2018).

A recent study has shown that photosynthesis and photosynthesis-related traits are correlated with species distribution and fitness in Antarctica (Perera-Castro et al., 2020a). Although bryophyte photosynthesis –i.e., photosynthetic efficiency and limitations– has been scarcely studied in comparison to that of spermatophytes, there is enough evidence on how low are their net CO_2 assimilation (A_N) rates as compared to other land plants groups (Alpert & Oechel, 1987; Williams & Flanagan, 2002; Brodribb et al., 2007, 2020; Waite & Sack, 2010; Hanson et al., 2014; Wang et al., 2014; Carriquí et al., 2019; Gago et al. 2019; Fan et al., 2020; Flexas & Carriquí, 2020; Perera-Castro et al., 2020a,b,c).

Recently, Carriquí et al. (2019) performed a detailed study analysing which traits limited photosynthesis in the gametophytes of several bryophyte species, evidencing that CO_2 diffusive limitations are more significant than biochemical ones. These CO_2 diffusive limitations were exclusively related to mesophyll conductance (g_m), since gametophytes lack stomata (Shaw & Renzaglia, 2004; Huttunen et al., 2018). Additionally, it was shown that g_m limitation to photosynthesis was driven by anatomical characteristics, particularly, extremely thick cell walls (T_{cw}) and low chloroplasts surface area exposed to intercellular air spaces (S_c/S), important traits determining photosynthesis through land plants' phylogeny (Flexas et al., 2018; Carriquí et al., 2019; Gago et al., 2019; Flexas & Carriquí, 2020). Besides cell wall thickness, the leaf cell wall is a complex and dynamic three-dimensional structure surrounding plants cells which is compounded

by several types of polysaccharides, phenolic compounds, and proteins (Carpita & McCann, 2002; Somerville et al., 2004; Cosgrove, 2005; Anderson & Kieber, 2020). These components interact with each other determining cell wall mechanical properties at each developmental stage (Somerville et al., 2004; Cosgrove, 2005; Sarkar et al., 2009; Anderson & Kieber, 2020; Lundgren & Fleming, 2020). Cellulose represents its main compound and consists in multiple β-1,4-linked glucan-bounded chains forming microfibrils, providing strength to the wall (Carpita & McCann, 2002; Somerville et al., 2004; Cosgrove, 2005; Anderson & Kieber, 2020). Within closely packed cellulose microfibrils, short non-cellulosic polysaccharides (i.e., hemicelluloses) are located (Carpita & McCann, 2002; Somerville et al., 2004; Cosgrove, 2005; Anderson & Kieber, 2020). Additionally, pectins are acidic polysaccharides rich in galacturonic acid that conform a network in which the cellulose-hemicelluloses matrix is embedded (Carpita & McCann, 2002; Somerville et al., 2004; Cosgrove, 2005; Moore et al., 2008; Anderson & Kieber, 2020). This pectin matrix has been suggested to be an important structure influencing several cell wall properties such as elasticity, degree of hydrophobicity, porosity and thickness (Carpita & McCann, 2002; Somerville et al., 2004; Vicré et al., 1999; Moore et al., 2008; Cosgrove, 2005; Schiraldi et al., 2012; Houston et al., 2016; Rui & Dinnery, 2019; Carriquí et al., 2020; Roig-Oliver et al., 2020a,b).

Whereas it is known that phylogenetic groups present specific particularities regarding cell wall composition (Popper & Fry, 2003, 2004; Sarkar et al., 2009; Sørensen et al., 2010; Popper et al., 2011), the relationship between cell wall composition and photosynthesis –particularly, g_m–, remains misunderstood (Lundgren & Fleming, 2020). However, some studies in spermatophytes have recently provided some light on that issue. In this sense, the first evidence for changes in cell wall composition affecting g_m was demonstrated in mutant rice genotypes (Ellsworth et al., 2018). Similar conclusions were reached testing *Arabidopsis thaliana* mutants, being g_m variations specifically attributed to modifications in pectins and/or in the (Cellulose+Hemicelluloses)/Pectins ratio (Roig-Oliver et al., 2020c). Additionally, Clemente-Moreno et al. (2019) and Roig-Oliver et al. (2020b) evidenced specific relationships between modifications in cell wall composition and g_m in tobacco and vines, respectively, acclimated to contrasting environmental conditions. Also, Roig-Oliver et al. (2020*a*) showed that T_{cw} variations were closely linked to changes in cell wall composition in sunflower subjected to different water availability. Nonetheless, to the best of our knowledge, only Carriquí et al. (2020)

performed an interspecific study demonstrating the importance of cell wall composition in determining differences in both g_m and T_{cw} among seven conifer species.

Although specific cell wall compositional traits have been characterized in some moss species (Popper & Fry, 2003; Matsunaga et al., 2004; Peña et al., 2008), to the best of our knowledge, there is no information regarding how their cell wall composition could influence both photosynthesis and T_{cw}. Thus, the main hypothesis of the current study is that cell wall composition is involved in regulating T_{cw}, g_m, and, thus, photosynthesis in mosses, which present the lowest photosynthesis and g_m values and the highest T_{cw} across land plants' phylogeny. Given the high diversity of moss species in Antarctica (Ochyra et al., 2008; Bramley-Alves et al., 2014) and the fact that photosynthesis and photosynthesis-related traits have been shown to influence their distribution and fitness in this region (Perera-Castro et al., 2020a), we analysed six Antarctic moss species belonging to distinct families from photosynthetic, anatomical and cell wall composition perspectives.

Materials and Methods

Experimental site and plant material

The present study was performed in Livingston Island (South Shetland Islands, Antarctica; 62º39'94''S, 60º23'20''W, 12 masl), where mean annual precipitation in summer season (from December to February) is 44.1 ± 11 mm and mean min/max annual temperatures are 5.4 ± 1.4 ºC and 13.8 ± 2.4 ºC, respectively (Bañón & Vasallo, 2015). Gas exchange measurements and sample collection for anatomical and cell wall composition analyses were performed in six moss species (Table 1) during February 2020, i.e., the high Antarctic summer.

Gas exchange and fluorescence measurements

Mosses were collected in the field and were subsequently transported to the laboratory to perform simultaneous gas exchange and chlorophyll *a* fluorescence (Chl *a*) measurements using a LiCOR 6800 system (LiCOR Biosciences, Lincoln, NE, USA). Per each species, 8 or 9 replicates were measured. Following Carriquí et al. (2019), shoots from distinct moss species, litter and dead tissues were removed carefully. Then, photosynthetic tissues were hydrated to guarantee their optimal status during gas exchange measurements performance. Excessive water was gently removed with a paper and, then, photosynthetic tissues were placed avoiding overlapping in a 6 cm^2 cuvette with a gasket affixed to a thin

stocking piece (Perera-Castro et al., 2020b,c). To prevent dehydration to affect gas exchange measurements, those individual parts remaining outside of the cuvette were carefully covered with a wet paper and, if necessary, they were watered. For all species, the flow rate was kept at 350 μmol air min^{-1}, the vapour pressure deficit (VPD) at around 1.5 kPa, the block temperature at 20 ºC and the air relative humidity at 60-65 %. Steady-state conditions were induced in phyllidia (hereafter "leaves") at saturating photosynthetic photon flux density (PPFD from 800 to 1250 μmol m^{-2} s^{-1}, depending on each species, 90-10 % red-blue light) and 400 μmol CO_2 mol^{-1} air. Once steady-state conditions were reached, usually after 5-10 min, measurements for net CO_2 assimilation (A_N), CO_2 atmospheric concentration (C_a) and steady-state fluorescence (F_s) were registered in the equipment. Subsequently, a saturating light flash was applied to determine the maximum fluorescence (F_m') and the real quantum effective of photosystem II (Φ_{PSII}). From these values, the electron transport rate (*ETR*) was estimated as $ETR = \text{PPFD} \times \Phi_{PSII} \times \alpha \times \beta$, where α is the leaf absorbance and β is the electron partitioning between photosystems I and II (Genty et al. 1989). Due to logistic restrictions to perform light curves under non-photorespiratory conditions (Valentini et al., 1995), $\alpha \times \beta$ values were compiled from bibliography. Thus, $\alpha \times \beta$ values for *Bryum pseudotriquetrum*, *Polytrichum juniperinum* and *Sanionia uncinata* were compiled from Carriquí et al. (2019). For *Polytrichum alpinum*, the $\alpha \times \beta$ product was taken as the average of those values described for other *Polytrichum* species (Carriquí et al., 2019). For the rest of species (i.e., *Brachytecium austrosalebrosum* and *Warnstorfia sarmentosa*) a mean of all $\alpha \times \beta$ values reported in Carriquí et al. (2019) for numerous mosses was used. The light respiration (R_{light}) was assumed to be the half the dark respiration rate, measured after plants exposure to darkness for, at least, 30 min (Niinemets et al., 2005). With all previous values, the mesophyll conductance (g_m) was estimated according to Harley et al. (1992) considering that the CO_2 compensation point in the absence of respiration (Γ^*) was that of tobacco at 25 ºC (Bernacchi et al., 2001), because no published values are available for mosses. Additionally, as mosses lack stomata, the CO_2 concentration at the sub-stomatal cavity (C_i) of the original equation was replaced by C_a as previously assumed by Carriquí et al. (2019):

$$g_m = \frac{A_N}{C_a - \frac{\Gamma^*((ETR + 8(A_N + R_L))}{ETR - 4(A_N + R_L)}}$$

Since individuals did not totally cover the whole cuvette area, a photograph of the photosynthetic tissues inside of the cuvette was taken after finishing gas exchange measurements to recalculate the area. Those species presenting photosynthetic tissues resembling true leaves, i.e., *P. alpinum* and *P. juniperinum*, were dissected and the real photosynthetic leaf area was calculated. For other species, the entire shoot was used. All area estimations were done with ImageJ software (Wayne Rasband/NIH, Bethesda, MD, USA).

Anatomical characterization

After the performance of gas exchange measurements, small pieces of those leaves enclosed in the cuvette were quickly fixed under vacuum pressure with a solution of glutaraldehyde 4 % and paraformaldehyde 2 % prepared in a 0.01 M phosphate buffer (pH 7.4). Four replicates per each species were prepared. Afterward, samples were post-fixed in 2 % buffered osmium tetroxide for 2 h to be subsequently dehydrated by a graded ethanol series. Dehydrated portions were embedded in LR white resin (London Resin Company) and were kept in an oven at 60 ºC for 48 h (Tosens et al., 2016; Carriquí et al., 2019).

Semi-fine (0.8 μm) and ultra-fine (90 nm) cross sections were cut with an ultramicrotome (Leica UC6, Vienna, Austria) to characterize each species from an anatomical perspective according to mosses' particularities (Carriquí et al., 2019). Thus, semi-fine sections were dyed with 1 % toluidine blue to be viewed with an Olympus BX60 optic microscope. Samples were photographed at 200 and/or 500X magnifications with a digital camera (U-TVO.5XC; Olympus, Tokyo, Japan). From these pictures, the estimation of leaf thickness (T_{leaf}) was addressed in all replicates. Additionally, mesophyll thickness (T_{mes}) and the fraction of mesophyll intercellular air spaces (f_{ias}) were also measured when species characteristics allowed for their determination. Ultra-fine cross sections were contrasted with uranyl acetate and lead citrate to take pictures at 1500X and 30000X magnifications with a transmission electron microscopy (TEM H600; Hitachi, Tokyo, Japan). From those images at 1500X magnifications, chloroplasts thickness (T_{chl}), chloroplasts length (L_{chl}), mesophyll and chloroplasts surface area exposed to intercellular air spaces (S_m/S and S_c/S, respectively) and the ratio S_c/S_m were calculated. From those images at 30000X magnifications, cell wall and cytoplasm thickness (T_{cw} and T_{cyt}, respectively) were estimated. Finally, a cell curvature correction factor was determined for each species according to Thain (1983) performing an average length/width ratio of

five randomly selected cells. In all cases, final values per each parameter were obtained as a mean of 10 measurements from randomly selected cell structures using ImageJ.

Foliar structure

Five individuals per species neighbouring the ones used for gas exchange characterization were hydrated. After removing shoots belonging to different moss species, dead tissues and litter, individuals were photographed to estimate the leaf or the canopy mass per area (LMA and CMA, respectively) with ImageJ. Similar to the recalculation of the photosynthetic area after gas exchange measurements, *P. alpinum* and *P. juniperinum* were dissected carefully as their structural characteristics allowed for leaves separation from thalli. For the rest of species, the entire shoot was used. Then, all samples were placed in an oven at 70 ºC for, at least, 72 h to determine their dry weight. From these values, LMA was calculated for both *Polytrichum* species and CMA for the other species as the ratio of dry mass to leaf area.

Cell wall extraction and fractionation

Per each species, six individuals neighbouring those used for gas exchange measurements were watered to prevent dehydration once shoots of different moss species, dead tissues and litter have been removed. Subsequently, they were stored overnight under darkness conditions to minimize leaf starch accumulation. The following morning, sampling for cell wall analyses was addressed. Whilst only leaves were collected for *P. alpinum* and *P. juniperinum*, entire shoots were sampled for the rest of species. For all replicates, around 700 mg of leaf fresh tissue were collected to be stored at -80 ºC until used. At the laboratory, each sample was boiled with absolute ethanol until bleached. Afterward, they were cleaned twice with acetone >95 % obtaining the alcohol insoluble residue (AIR), an approximation of the total isolated cell wall material. Prior to perform the analysis of cell wall main compounds, all AIRs were α-amylase-digested in order to eliminate starch remains. Once no starch residues were further observed, 3 analytical replicates of each AIR weighing around 3 mg were hydrolysed with 2 M trifluoroacetic acid at 121 ºC for 1 h. Then, they were centrifuged at 13000 g obtaining an aqueous supernatant (non-cellulosic cell wall fraction, corresponding to hemicelluloses and pectins) and a pellet (cellulosic cell wall fraction). Whilst supernatants were stored at -20 ºC for hemicelluloses and pectins quantifications, pellets were cleaned twice with distilled water and twice more with acetone >95 %. After air-dried, pellets were hydrolysed with 200 µl

sulphuric acid 72 % (w/v) at room temperature for 1 h, diluted to 6 ml with distilled water and heated at 121 ºC until an aqueous solution containing cellulose was obtained. Hemicelluloses and cellulose contents were estimated from a glucose calibration curve by the phenol sulphuric acid method (Dubois et al., 1956). Pectins quantification was performed from a galacturonic acid calibration curve (Blumenkrantz & Asboe-Hansen, 1973). All these colorimetric reactions were read with a Multiskan Sky Microplate Spectrophotometer (ThermoFisher Scientific).

Statistical analysis

Prior to perform statistics, Thompson test was addressed to identify and eliminate outliers for all evaluated parameters. Then, one-way ANOVA and subsequent LSD test were performed to detect statistically significant differences ($P < 0.05$) for each studied parameter between species. Furthermore, Pearson's correlation matrices were addressed to find correlations between parameters, being significant at $P < 0.05$ and highly significant at $P < 0.01$. Finally, linear regressions between photosynthetic traits, anatomical particularities and cell wall compositional features were fitted using mean values per species. All these analyses were done with R software (ver. 3.2.2; R Core Team, Vienna, Austria).

Results

Physiological characterization

Net CO_2 assimilation (A_N) of the studied Antarctic moss species ranged from 0.74 ± 0.05 to 4.26 ± 0.34 μmol CO_2 m^{-2} s^{-1} in *S. uncinata* and *P. juniperinum*, respectively (Table 2). Together with *P. alpinum*, the later species achieved the largest g_m (11.65 ± 0.93 and 9.69 ± 0.82 mmol CO_2 m^{-2} s^{-1}, respectively), whereas *B. austrosalebrosum* presented almost 7-fold diminished g_m (1.59 ± 0.31 mmol CO_2 m^{-2} s^{-1}; Table 2). Similarly, *P. juniperinum* achieved the largest *ETR* (121.35 ± 8.01 μmol m^{-2} s^{-1}) and was followed by *P. alpinum*, which had reductions of around 30% as compared to the previous species (Table 2). Nonetheless, similar *ETR* values were found in the rest of species, being significantly lower than those measured in both *Polytrichum* species (Table 2). Finally, *B. austrosalebrosum*, *B. pseudotriquetrum* and *P. juniperinum* achieved the highest R_{light}, whereas the lowest was found in *S. uncinata* (Table 2).

Foliar structure and anatomical characterization

Regarding mosses' foliar structure, non-significant differences in LMA were detected between *Polytrichum* species (Table 3). Similarly, the rest of mosses did not present statistically significant differences for CMA (Table 3).

Anatomical features of each studied species can be found in Fig. S1. Concerning those traits estimated from light microscopy pictures, *P. alpinum* and *P. juniperinum* presented the highest T_{leaf}, being statistically different from the rest of species, which presented around 13-fold thinner leaves (Table 3). Additionally, T_{mes} and f_{ias} were only measured in these two species due to *Polytrichum* anatomical particularities (Fig. S1). Thus, whereas *P. alpinum* presented significantly higher T_{mes} than *P. juniperinum*, similar f_{ias} was observed in both species (Table 3). Regarding those traits estimated from pictures at 1500X and 30000X magnifications, *P. alpinum* achieved the highest S_m/S (17.39 ± 0.69 m^2 m^{-2}), being followed by *P. juniperinum* (Table 4). However, the rest of mosses presented similarly lower S_m/S values, ranging from 1.21 ± 0.14 to 1.67 ± 0.35 m^2 m^{-2} in *W. sarmentosa* and *B. pseudotriquetrum*, respectively (Table 4). Both *Polytrichum* species showed significantly higher S_c/S in comparison to the rest of species, which had, at least, 10-fold lower S_c/S (Table 4). *B. austrosalebrosum*, *P. alpinum* and *P. juniperinum* achieved the highest values for the S_c/S_m ratio, which was reduced around 40% in *W. sarmentosa*, that species presenting the lowest S_c/S_m (0.49 ± 0.06; Table 4). No statistical differences among species were found for L_{chl} and T_{chl} (Table 4). *B. austrosalebrosum* exhibited the largest T_{cyt} (0.84 ± 0.06 μm), being followed by *B. pseudotriquetrum* and *W. sarmentosa* (Table 4). Nonetheless, *S. uncinata* showed almost 4-fold lower T_{cyt} than *B. austrosalebrosum* (Table 4). Finally, the largest T_{cw} was found in *B. pseudotriquetrum* and *S. uncinata*, being up to 4-fold larger than in *P. juniperinum* and *P. alpinum*, which presented the thinnest cell walls (Table 4).

Cell wall composition characterization

The highest isolated AIR proportion was found in *W. sarmentosa*, whilst the lowest was detected in both *S. uncinata* and *B. austrosalebrosum* (Table 5). The later species presented the largest cellulose content (12.90 ± 1.18 g glc m^{-2}), being followed by *W. sarmentosa* (Table 5). Nonetheless, *P. juniperinum* contained the lowest cellulose amounts, being almost 2.5-fold lower than in *B. austrosalebrosum* (Table 5). Regarding hemicelluloses, no statistic significant differences among species were detected (Table 5). Finally, *S. uncinata*, *B. pseudotriquetrum* and *B. austrosalebrosum* presented almost

three times higher pectins content than *P. alpinum*, that species containing the lowest (1.20 ± 0.08 g gal ac m^{-2}, Table 5).

Relationships among parameters

Several significant correlations were detected among all studied parameters (Table S1). Concerning relationships between photosynthetic parameters, positive correlations were found between A_N and g_m (R^2 = 0.94, P < 0.01, Fig. 1A) and *ETR* (R^2 = 0.98, P < 0.01, Fig. 1B). Nonetheless, g_m correlated negatively with T_{cw} (R^2 = 0.67, P = 0.03, Fig. 2). Since cellulose and hemicelluloses contents were less variable than pectins among species (Table 5), pectins were the unique cell wall main compound related with the (Cellulose+Hemicelluloses)/Pectins ratio (i.e., (C+H)/P; Table S1). Consequently, those parameters that correlate positively with the (Cellulose+Hemicelluloses)/Pectins ratio were linked negatively with pectins (Table S1). Particularly, we detected a positive correlation between T_{cw} and pectins (R^2 = 0.95, P < 0.01, Fig. 3) and a negative one between g_m and pectins (R^2 = 0.59, P = 0.05, Fig. 4).

Discussion

Changes in cell wall composition have been linked to g_m rates in different spermatophyte species (Ellsworth et al., 2018; Clemente-Moreno et al., 2019; Carriquí et al., 2020; Roig-Oliver et al., 2020a,b,c). In this study, we analysed six Antarctic moss species showing that interspecific variations in both g_m and T_{cw} were strongly related with differences in cell wall composition.

The photosynthetic rates reported in the present study are comprised within the ranges previously reported for mosses (Alpert & Oechel, 1987; Williams & Fanagan, 2002; Brodribb et al., 2007, 2020; Waite & Sack, 2010; Hanson et al., 2014; Wang et al., 2014; Carriquí et al., 2019; Fan et al., 2020; Perera-Castro et al., 2020a,b,c). The two *Polytrichum* species achieved the largest A_N and g_m due to their specific characteristics, as already shown by Carriquí et al. (2019). In fact, the family Polytrichaceae is placed in the highest position along bryophytes' phylogeny since they exhibit structural, morphological, and anatomical traits differing from the rest of mosses (Hébant, 1977; Ligrone et al., 2002; Hyvönen et al., 2004; Bell & Hyvönen, 2010; Huttunen et al., 2018). First, they present a well-developed internal conducting system with specialized water-conducting cells (i.e., hydroids) (Hébant, 1977; Ligrone et al., 2002; Bell & Hyvönen 2010; Huttunen et al., 2018) which is functionally similar to the vascular system of higher

plants (Brodribb et al., 2020). Additionally, their phyllidia resemble true leaves with a "pseudo-mesophyll" that increases the area for CO_2 uptake (Proctor, 2005; Hyvönen et al., 2004; Bell & Hyvönen, 2010; Huttunen et al., 2018). Together with thinner cell walls (see Fig. S1 for anatomical details), all these traits resulted in enhanced A_N and g_m as compared to other moss species (Table 2). Despite the fact that plants were measured during the most favourable growing season, it is possible that the measured photosynthetic rates do not represent the maximum achievable photosynthetic capacity. Indeed, especially for the two *Polytrichum* species, the measured *ETR* would allow for larger A_N rates than those reached (Table 2). In fact, Carriquí et al. (2019) reported larger A_N rates than those presented in our study for *B. pseudotriquetrum*, *P. juniperinum* and *S. uncinata*. Nevertheless, the three species rank equally in both studies, with *P. juniperinum* and *S. uncinata* presenting the largest and the lowest A_N values, respectively.

Specific cell wall composition characteristics have been studied along land plants' phylogeny, evidencing those traits specifically related to each plant lineage (Popper & Fry 2003, 2004; Sarkar et al., 2009; Sørensen et al., 2010; Popper et al., 2011). Although mosses cell wall composition has not been deeply studied as compared to other groups, Popper & Fry (2003) determined that they contain high quantities of cellulose and mannose, the latter representing the most abundant hemicellulosic sugar. Additionally, mosses usually contain high amounts of pectins, which are thought to provide protection against desiccation (Popper & Fry 2003). However, these major cell wall components present some structural differences as compared to spermatophytes (Matsunaga et al., 2004; Peña et al., 2008; Popper, 2008), suggesting a prior stage before the appearance of flowering plants (Popper, 2008). Surprisingly, in our study pectins were the less abundant cell wall compound, while hemicelluloses were the most abundant (Table 5). Similar to Popper & Fry (2003) and Peña et al. (2008), we used the AIR as an approximation of the total isolated cell wall fraction from which we quantified the relative proportion of each cell wall compound. However, whereas Popper & Fry (2003) performed a qualitative analysis of cell wall composition and Peña et al. (2008) determined the presence of very specific components by NMR spectroscopic analysis and MALDI-TOF-MS procedures, we made a quantitative determination of cell wall compounds. Thus, we suggest that contrasting results regarding the relative abundance of hemicelluloses and pectins may be attributed to different specificities of the used methodologies. Nevertheless, since the method we used here is well contrasted (Ibarz et al., 2005; Masuko et al., 2005) and it

was employed identically for all species, we expect that at least the relative differences among species are fully trustable.

Recently, Carriquí et al. (2019) confirmed the existence of a negative trade-off between g_m and T_{cw} in mosses, which was also detected in the present study (Fig. 2). Although it has been suggested that modifications in cell wall composition could influence T_{cw} (Carpita & McCann, 2002; Cosgrove, 2005; Moore et al., 2008; Rui & Dinnery, 2019), to the best of our knowledge, only two studies evidence that issue. At intraspecific level, Roig-Oliver et al. (2020a) showed that the (Cellulose+Hemicelluloses)/Pectins ratio was linked to T_{cw} adjustments in sunflowers subjected to different water availability conditions. Nonetheless, at interspecific level, Carriquí et al. (2020) found that hemicelluloses and pectins absolute concentrations correlated negatively with T_{cw} in seven conifers acclimated to the same environmental conditions. Whilst our results demonstrate that changes in the (Cellulose+Hemicelluloses)/Pectins ratio determined T_{cw} across species (Table S1), the existence of this relationship was specifically attributed to pectins (Fig. 3) since these were the larger contributors to the interspecific variability in the (Cellulose+Hemicelluloses)/Pectins ratio. In fact, pectins are thought to be crucial defining several cell wall characteristics that could finally affect the CO_2 diffusion (Cosgrove, 2005; Moore et al., 2008; Houston et al., 2016). In this sense, we found that increased pectins amounts resulted in diminished g_m (Fig. 4), which agrees with the results in water-stressed tobacco (Clemente-Moreno et al., 2019). However, this relationship seems to be species-specific because Roig-Oliver et al. (2020b) showed that only cellulose was related to g_m in vines. Nevertheless, these studies were done evaluating single angiosperms acclimated to varying environmental stressors. Thus, our results are more comparable with those reported by Carriquí et al. (2020) since they performed a multi-species analysis. Particularly, they found that both hemicelluloses and cellulose determined g_m rates across conifers. Furthermore, they showed that g_m was associated to the proportion between cell wall main compounds, highlighting pectins potential importance in regulating g_m. Even though our results do not allow to draw conclusive statements, we suggest that the direct effect of different cell wall composition –with pectins playing a key role– on T_{cw} across species strongly influenced g_m rates because of different wall porosity, thus, modifying the CO_2 diffusivity through the wall. However, even comparable, contrasting results between gymnosperms and mosses reflect the

importance of specific cell wall composition determining g_m in a different manner in distinct phylogenetic groups.

In conclusion, this interspecific study evidences the importance of cell wall composition in influencing cell wall thickness and photosynthesis in Antarctic mosses. Low A_N and g_m values were achieved due to extremely thick cell walls, which in turn, were determined by different cell wall composition, specifically, pectins. Nonetheless, further studies testing more species are necessary to elucidate the relationship between cell wall composition and g_m in order to improve our current knowledge regarding the mechanistic basis of g_m and to detect a general role of cell wall composition influencing CO_2 diffusivity through cell walls along land plants' phylogeny.

Authors contributions

MR-O, JF and JB designed the experiment; MR-O and CD conducted the experiment and performed the data analysis; MR-O wrote the first draft of the manuscript. All authors contributed to its following versions to produce the final version.

Acknowledgements

This work was supported by the project PGC2018-093824-B-C41 from Ministerio de Economía y Competitividad (MINECO, Spain). MR-O was supported by a predoctoral fellowship FPU16/01544. We thank Ms Alicia V. Perera-Castro for her help in identifying moss species. We also thank María Teresa Mínguez (Universitat de València, Secció de Microscòpia Electrònica – SCSIE) and Dr Ferran Hierro (Universitat de les Illes Balears, Serveis Cientificotècnics) for technical support during microscopic analyses, as well as Dr Marc Carriquí for his advices during anatomical measurements. Finally, we thank Comité Polar Español (CPE), CSIC's Unidad de Tecnología Marina (UTM) and the personnel at Base Juan Carlos I and at Hespérides vessel for their help during the Antarctic campaign.

Conflicts of interest

The authors declare no conflicts of interest.

Data availability statement

The data supporting the findings of this study are available from the corresponding author (Margalida Roig-Oliver) upon request.

References

Alpert, P. & Oechel, W.W. (1987) Comparative patterns of net photosynthesis in an assemblage of mosses with contrasting microdistributions. *American Journal of Botany*, 74 (12), 1787–1796

Anderson, C.T. & Kieber, J.J. (2020) Dynamic construction, perception, and remodelling of plant cell walls. *Annual Review of Plant Biology*, 71, 39–69

Bañón, M. & Vasallo, F. (2015) AEMET en la Antártida: Climatología y meteorología sinóptica en las estaciones meteorológicas españolas en la Antártida. *Ministerio de Agricultura, Alimentación y Medio Ambiente. Agencia Estatal de Meteorología, Madrid.*

Bell, N.E. & Hyvönen, J. (2010) Phylogeny of the moss class Polytrichopsida (Bryophyta): Generic-level structure and incongruent gene trees. *Molecular Phylogenetics and Evolution*, 55, 381–398

Bernacchi, C.J., Singsaas, E.L., Pimentel, C., Portis, A.R. Jr & Long, S.P. (2001) Improved temperature response functions for models of Rubisco-limited photosynthesis. *Plant, Cell and Environment*, 24, 253–259

Blumenkrantz, N. & Asboe-Hansen, G. (1973) New method for quantitative determination of uronic acids. *Analytical Biochemistry*, 54, 484–489

Bramley-Alves, J., King, D.H., Robinson, S.A. & Miller, R.E. (2014) Dominating the Antarctic Environment: Bryophytes in a Time of Change. In: Hanson, D. & Rice, S. (Eds.) Photosynthesis in Bryophytes and Early Land Plants. Advances in Photosynthesis and Respiration (Including Bioenergy and Related Processes), pp. 309–324.

Brodribb, T.J., Carriquí, M., Delzon, S., McAdam, S.A.M. & Holbrook, N.M. (2020) Advanced vascular function discovered in a widespread moss. *Nature Plants*, 6, 273–279

Brodribb, T.J., Feild, T.S. & Jordan, G.J. (2007) Leaf maximum photosynthetic rate and venation are linked by hydraulics. *Plant Physiology*, 144, 1890–1898

Buck, W.R., Goffinet, B. & Shaw, A.J. (2000) Testing morphological concepts of orders of pleurocarpous mosses (Bryophyta) using phylogenetic reconstructions based on *trnL-trnF* and *rps4* sequences. *Molecular Phylogenetics and Evolution*, 16, 180–198

Carpita, N.C. & McCann, M.C. (2002) The functions of cell wall polysaccharides in composition and architecture revealed through mutations. *Plant and Soil*, 247, 71–80

Carriquí, M., Nadal, M., Clemente-Moreno, M.J., Gago, J., Miedes, E. & Flexas, J. (2020) Cell wall composition strongly influences mesophyll conductance in gymnosperms. *The Plant Journal*, 103, 1372–1385

Carriquí, M., Roig-Oliver, M., Brodribb, T.J., Coopman, R.E., Gill, W., Mark, K., Niinemets, Ü., Perera-Castro, A., Ribas-Carbó, M., Sack, L., Tosens, T., Waite, M. & Flexas, J. (2019) Anatomical constraints to nonstomatal diffusion conductance and photosynthesis in lycophytes and bryophytes. *New Phytologist*, 222, 1256–1270

Clemente-Moreno, M.J., Gago, J., Díaz-Vivancos, P., Bernal, A., Miedes, E., Bresta, P., Liakopoulos, G., Fernie, A.R., Hernández, J.A. & Flexas, J. (2019) The apoplastic antioxidant system and altered cell wall dynamics influence mesophyll conductance and the rate of photosynthesis. *The Plant Journal*, 99, 1031–1046

Cosgrove, D.J. (2005) Growth of the plant cell wall. *Nature Reviews. Molecular Cell Biology*, 6, 850–861

Dubois, M., Gilles, K.A., Hamilton, J.K., Rebers, P.A. & Smith, F. (1956) Colorimetric method for determination of sugars and related substances. *Analytical Chemistry*, 28, 350–356

Ellsworth, P.V., Ellsworth, P.Z., Koteyeva, N.K. & Cousins, A.B. (2018) Cell wall properties in *Oryza sativa* influence mesophyll CO_2 conductance. *New Phytologist*, 219, 66–76

Evans, J.R. (2009a) Potential errors in electron transport rates calculated from chlorophyll fluorescence as revealed by a multilayer leaf model. *Plant Cell and Physiology*, 50, 698–706

Evans, J.R., Kaldenhoff, R., Genty, B. & Terashima, I. (2009b) Resistances along the CO_2 diffusion pathway inside leaves. *Journal of Experimental Botany*, 60, 2235–2248

Fan, X.Y., Liu, W.Y., Song, L., Liu, S., Shi, X.M. & Yuan, G.D. (2020) A combination of morphological and photosynthetic functional traits maintains the vertical distribution of bryophytes in a subtropical cloud forest. *American Journal of Botany*, 107 (5), 761–772

Flexas, J., Carriquí, M., Cano, F.J., Coopman, R.E., Mizokami, Y., Tholen, D. & Xiong, D. (2018) CO_2 diffusion inside photosynthetic organs. In: Adams, W. III & Terashima, I. (Eds.) The leaf: a platform for performing photosynthesis. Advances in Photosynthesis and Respiration (Including Bioenergy and Related Processes). Springer, Cham, pp. 163-208.

Flexas, J. & Carriquí, M. (2020) Photosynthesis and photosynthetic efficiencies along the terrestrial plant's phylogeny: lessons for improving crop photosynthesis. *The Plant Journal*, 101, 964–978

Frey, W. & Stech, M. (2009) Division of Bryophyta Schimp. (Musci, Mosses). In Syllabus of Plant Families. Adolf Engler's Syllabus der Pflanzenfamilien, 13th edition. Part 3. Bryophytes and Seedless Vascular Plants; Frey, W. Ed. Gebr€uder Borntraeger: Berlin, pp 116–257.

Gago, J., Carriquí, M., Nadal, M., Clemente-Moreno, M.J., Coopman, R.E., Fernie, A.R. & Flexas, J. (2019) Photosynthesis optimized across land plant phylogeny. *Trends in Plant Science*, 24, 947–958

Genty, B., Briantais, J.M. & Baker, N.R. (1989). The relationship between the quantum yield of photosynthetic electron-transport and quenching of chlorophyll fluorescence. *Biochimica et Biophysica Acta*, 990, 87–92

Goffinet, B., Cox, C., Shaw, J. & Hedderson, T.A. (2001). The Bryophyta (Mosses): systematic and evolutionary inferences from an rps4 gene (cpDNA) phylogeny. *Annals of Botany*, 87, 191–208

Hanson, D.T., Renzaglia, K. & Villarreal, J.C. (2014). Diffusional limitations to CO_2 concentrating mechanisms in bryophytes. In: Hanson, D.T. & Rice, S.K. (Eds.) Photosynthesis in bryophytes and early land plants. Berlin, Germany: Springer, pp. 95-111.

Harley, P.C., Loreto, F., Di Marco, G. & Sharkey, T.D. (1992). Theoretical considerations when estimating the mesophyll conductance to CO_2 flux by analysis of the response of photosynthesis to CO_2. *Plant Physiology*, 98, 1429–1436

Hébant, C. (1977) The conducting tissues of Bryophytes. Vaduz: J. Cramer, Lehre, Germany.

Hedderson, T.A.J. & Longton, R.E. (1996) Life history variation in mosses: water relations, size and phylogeny. *Oikos*, 77, 31–43

Houston, K., Tucker, M.R., Chowdhury, J., Shirley, N. & Little, A. (2016). The plant cell wall: a complex and dynamic structure as revealed by the responses of genes under stress conditions. *Frontiers in Plant Science*, 7:984

Huttunen, S., Bell, N. & Hedenäs, L. (2018). The evolutionary diversity of mosses – taxonomic heterogeneity and its ecological drivers. *Critical Reviews in Plant Sciences*, 37(2-3), 128–174

Hyvönen, J., Koskinen, S., Merrill, S., Hedderson, T.A. & Stenroos, S. (2004) Phylogeny of the Polytrichales (Bryophyta) based on simultaneous analysis of molecular and morphological data. *Molecular Phylogenetics and Evolution*, 31, 915–928

Ibarz, A., Pagán, A., Tribaldo, F. & Pagán, J. (2005) Improvement in the measurement of spectrophotometric data in the *m*-hydroxydiphenyl pectin determination methods. *Food Control*, 17, 890–893

Kenrick, P. & Crane, C. (1996) Embryophytes. Land plants. Version 01 January 1996. Available from: http://tolweb.org/Embryophytes/20582/1996.01.01 in The Tree of Life Web Project, http://tolweb.org/. [Accessed 10 October 2020].

Ligrone, R., Vaughn, K.C., Renzaglia, K.S., Know, J.P. & Duckett, J.G. (2002) Diversity in the distribution of polysaccharide and glycoprotein epitopes in the cell walls of bryophytes: new evidence for the multiple evolution of water-conducting cells. *New Phytologist*, 156, 491–508

Lundgren, M.R. & Fleming, A.J. (2020) Cellular perspectives for improving mesophyll conductance. *The Plant Journal*, 101 (4), 845–847

Masuko, T., Minami, A., Iwasaki, N., Majima, T., Nishimura, S.I. & Lee, Y.C. (2005) Carbohydrate analysis by a phenol-sulfuric acid method in microplate format. *Analytical Biochemistry*, 339(1), 69–72

Matsunaga, T., Ishii, T., Matsumoto, S., Higushi, M., Darvill, A., Albersheim, P. & O'Neill, M.A. (2004) Occurrence of the primary cell wall polysaccharide rhamnogalacturonan II in pteridophytes, lycophytes, and bryophytes. Implications for the evolution of vascular plants. *Plant Physiology*, 134, 339–351

Moore, J.P., Farrant, J.M. & Driouich, A. (2008) A role for pectin-associated arabinans in maintaining the flexibility of the plant cell wall during water deficit stress. *Plant Signaling & Behavior*, 3, 102–104

Newton, A.E., Cox, C.J., Duckett, J.G., Wheeler, J.A., Goffinet, B., Hedderson, T.A.J. & Mishler, B.D. (2000) Evolution of the major moss lineages: phylogenetic analyses based on multiple gene sequences and morphology. *The Bryologist*, 103 (2), 187–211

Niinemets, Ü., Cescatti, A., Rodeghiero, M. & Tosens, T. (2005) Leaf internal diffusion conductance limits photosynthesis more strongly in older leaves of Mediterranean evergreen broadleaved species. *Plant, Cell and Environment*, 28, 1552–1566

Ochyra, R., Lewis, S. & Bednarek-Ochyra, H. (2008) The illustrated moss flora of Antarctica. Cambridge: Cambridge University Press.

Peña, M.J., Darvill, A.G., Eberhard, S., York, W.S. & O'Neill, M.A. (2008) Moss and liverwort xyloglucans contain galacturonic acid and are structurally distinct from the xyloglucans synthesized by hornworts and vascular plants. *Glycobiology*, 18(11), 891–904

Perera-Castro, A.V., Flexas, J., González-Rodríguez, Á.M. & Fernández-Marín, B. (2020a) Photosynthesis on the edge: photoinhibition, desiccation and freezing tolerance of Antarctic bryophytes. *Photosynthesis Research* https://doi.org/10.1007/s11120-020-00785-0

Perera-Castro, A.V., Nadal, M. & Flexas, J. (2020b) What drives photosynthesis during desiccation? Mosses and other outliers from the photosynthesis-elasticity trade-off. *Journal of Experimental Botany*, 71(20), 6460–6470

Perera-Castro, A.V., Waterman, M.J., Tumbull, J.D., Ashcroft, M.B., McKinley, E., Watling, J.R., Bramley-Alves, J., Casanova-Katny, A., Zuniga, G., Flexas, J. & Robinson, S.A. (2020c) It is hot in the sun: Antarctic mosses have high temperature optima for photosynthesis despite cold climate. *Frontiers in Plant Science*, 11, 1178

Popper, Z.A. & Fry, S.C. (2003) Primary cell wall composition of Bryophytes and Charophytes. *Annals of Botany*, 91, 1–12

Popper, Z.A. & Fry, S.C. (2004) Primary cell wall composition of pteridophytes and spermatophytes. *New Phytologist*, 164, 165–174

Popper, Z.A. (2008) Evolution and diversity of green plant cell walls. *Current Opinion in Plant Biology*, 11(3), 286–292

Popper, Z.A., Michel, G., Hervé, C., Domozych, D.S., Willats, W.G.T., Tuohy, M.G., Kloareg, B & Stengel, D.B. (2011) Evolution and diversity of plant cell walls: from algae to flowering plants. *Annual Review of Plant Biology*, 62, 567–590

Proctor, M.C.F. (2005) Why do Polytrichaceae have lamellae? *Journal of Bryology*, 27, 221–229

Proctor, M.C.F., Oliver, M.J., Wood, A.J., Apert, P., Stark, L.R., Cleavitt, N.L. & Mishler, B.D. (2007) Desiccation-tolerance in bryophytes: a review. *The Bryologist*, 110, 595–621

Renzaglia, K.S., Schuette, S., Duff, R.J., Ligrone, R., Shaw, A.J., Mishler, B.D. & Duckett, J.G. (2007) Bryophyte phylogeny: advancing the molecular and morphological frontiers. *The Bryologist*, 110, 179–213

Roberts, A.W., Roberts, E.M. & Haigler, C.H. (2012) Moss cell walls: structure and biosynthesis. *Frontiers in Plant Science,* 3:166

Robinson, S.A., Wasley, J. & Tobin, A.K. (2003) Living on the edge – plants and global change in continental and maritime Antarctica. *Glogal Change Biology*, 9, 1681–1717

Roig-Oliver, M., Bresta, P., Nadal, M., Liakopoulos, G., Nikolopoulos, D., Karabourniotis, G., Bota, J. & Flexas, J. (2020a) Cell wall composition and thickness

affect mesophyll conductance to CO_2 diffusion in *Helianthus annuus* under water deprivation. *Journal of Experimental Botany*, 71(22), 7198–7209

Roig-Oliver, M., Nadal, M., Clemente-Moreno, M.J., Bota, J. & Flexas, J. (2020b) Cell wall components regulate photosynthesis and leaf water relations of *Vitis vinifera* cv. Grenache acclimated to contrasting environmental conditions. *Journal of Plant Physiology*, 244, 153084

Roig-Oliver, M., Rayon, C., Roulard, R., Fournet, F., Bota, J. & Flexas, J. (2020c) Reduced photosynthesis in *Arabidopsis thaliana atpme17.2* and *atpae11.1* mutants is associated to altered cell wall composition. *Physiologia Plantarum*, 10.1111/ppl.13186

Rui, Y. & Dinneny, J.R. (2019) A wall with integrity: surveillance and maintenance of the plant cell wall under stress. *New Phytologist*, 225, 1428–1439

Sarkar, P., Bosneaga, E. & Auer, M. (2009) Plant cell walls throughout evolution: towards a molecular understanding of their design principles. *Journal of Experimental Botany*, 60, 3615–3635

Schiraldi, A., Fessas, D. & Signorelli, M. (2012) Water activity in biological systems–a review. *Polish Journal of Food and Nutrition Sciences*, 62, 5–13

Shaw, J. & Renzaglia, K. (2004) Phylogeny and diversification of bryophytes. *American Journal of Botany*, 91, 1557–1581

Somerville, C., Bauer, S., Brininstool, G., Facette, M., Hamann, T., Milne, J., Osborne, E., Paredez, A., Persson, S., Raab, T., Vorweek, S. & Youngs, H. (2004). Toward a systems approach to understanding plant cell walls. *Science*, 306 (5705), 2206–2211

Sørensen, I., Domozych, D. & Williats, W.G.T. (2010) How have plant cell walls evolved? *Plant Physiology*, 153, 366–372

Thain, J.F. (1983) Curvature correlation factors in the measurements of cell surface areas in plant tissues. *Journal of Experimental Botany*, 34, 87–94

Tosens, T., Nishida, K., Gago, J., Coopman, R.E., Cabrera, H.M., Carriquí, M., Laanisto, L., Morales, L., Nadal, M., Rojas, R., Talts, E., Tomàs, M., Hanba, Y., Niinemets, Ü. & Flexas, J. (2016) The photosynthetic capacity in 35 ferns and fern allies: mesophyll CO_2 diffusion as a key trait. *New Phytologist*, 209, 1576–1590

Valentini, R., Epron, D., Angelis, P.D., Matteucci, G. & Dreyer, E. (1995) In situ estimation of net CO_2 assimilation, photosynthetic electron flow and photorespiration of Turkey oak (*Q. cerris* L.) leaves: diurnal cycles under different water supply. *Plant, Cell and Environment*, 18, 631–664

Vicré, M., Sherwin, H.W., Driouich, A., Jaffer, M.A. & Farrant, J.M. (1999) Cell wall characteristics and structure of hydrated and dry leaves of the resurrection plant *Craterostigma wilsmii*, a microscopical study. *Journal of Plant Physiology*, 155, 719–726

Wagner, S., Zotz, G., Salazar, A.N. & Bader, M.Y. (2013) Altitudinal changes in temperature responses of net photosynthesis and dark respiration in tropical bryophytes. *Annals of Botany*, 111, 455–465

Waite, M. & Sack, L. (2010) How does moss photosynthesis relate to leaf and canopy structure? Trait relationships for 10 Hawaiian species of contrasting light habitats. *New Phytologist*, 185, 156–172

Wang, Z., Bao, W., Feng, D. & Lin, H. (2014) Functional trait scaling relationships across 13 temperate mosses growing in wintertime. *Ecological Research*, 29, 629–639

Wang, Z. & Bader, M.Y. (2018) Associations between shoot-level water relations and photosynthetic responses to water and light in 12 moss species. *AoB Plants*, 10 (3), ply034

Williams, T.G. & Flanagan, L.B. (2002) Measuring and modelling environmental influences on photosynthetic gas exchange in *Sphagnum* and *Pleurozium*. *Plant, Cell and Environment*, 21 (6), 555–564

Table 1. Classification the studied moss species in relation to their phylogeny and habitat occupation in Antarctica according to Kenrick & Crane (1996) and Ochyra et al. (2008).

Species	Family	Habitat in Antarctica
Brachytecium austrosalebrosum	Brachytheciaceae	Wet rock faces or rocky/sandy soils limiting with melt water paths
Bryum pseudotriquetrum	Briaceae	Ubiquitous
Polytrichum alpinum	Polytrichaceae	Rocky soil and humus
Polytrichum juniperinum	Polytrichaceae	Rocky soil and humus
Sanionia uncinata	Amblystegiaceae	Ubiquitous
Warnstorfia sarmentosa	Amblystegiaceae	Wet soils or wet rock faces

Table 2. Photosynthetic characterization of the studied species. Average values ± SE are shown for net CO_2 assimilation (A_N), mesophyll conductance (g_m), electron transport rate (*ETR*) and light respiration (R_{light}). Different superscript letters indicate significant differences ($P < 0.05$) between species according to LSD test. In all cases, n = 8–9.

Species	A_N (μmol CO_2 m^{-2} s^{-1})	g_m (mmol CO_2 m^{-2} s^{-1})	*ETR* (μmol m^{-2} s^{-1})	R_{light} (μmol CO_2 m^{-2} s^{-1})
B. austrosalebrosum	1.12 ± 0.03^{cd}	1.59 ± 0.31^{c}	5.96 ± 0.60^{c}	0.59 ± 0.04^{a}
B. pseudotriquetrum	1.33 ± 0.07^{c}	4.72 ± 0.25^{b}	14.69 ± 0.68^{c}	0.60 ± 0.05^{a}
P. alpinum	3.49 ± 0.28^{b}	9.69 ± 0.82^{a}	88.54 ± 3.74^{b}	0.52 ± 0.04^{ab}
P. juniperinum	4.26 ± 0.34^{a}	11.65 ± 0.93^{a}	121.35 ± 8.01^{a}	0.55 ± 0.05^{a}
S. uncinata	0.74 ± 0.05^{d}	2.78 ± 0.83^{bc}	4.49 ± 0.36^{c}	0.36 ± 0.02^{c}
W. sarmentosa	1.39 ± 0.08^{c}	3.61 ± 0.75^{bc}	10.25 ± 1.05^{c}	0.41 ± 0.04^{bc}

Table 3. Structural and anatomical characterization from semi-fine cross sections of studied species. Average values ± SE are shown for leaf mass per area (LMA), dry canopy mass per area (CMA), leaf thickness (T_{leaf}), mesophyll thickness (T_{mes}) and fraction of mesophyll intercellular air spaces (f_{ias}). Superscript letters indicate significant difference ($P < 0.05$) between species according to LSD test. In all cases, n = 4–5.

Species	LMA ($g\ m^{-2}$)	CMA ($g\ m^{-2}$)	T_{leaf} (µm)	T_{mes} (µm)	f_{ias} (%)
B. austrosalebrosum	-	43.53 ± 3.36^{a}	16.31 ± 1.00^{b}	-	-
B. pseudotriquetrum	-	41.22 ± 1.70^{a}	17.86 ± 4.52^{b}	-	-
P. alpinum	79.35 ± 4.45^{a}	-	164.49 ± 5.11^{a}	92.32 ± 1.16^{a}	16.67 ± 3.63^{a}
P. juniperinum	73.55 ± 6.46^{a}	-	166.61 ± 1.93^{a}	83.22 ± 0.77^{b}	16.43 ± 2.76^{a}
S. uncinata	-	52.74 ± 5.59^{a}	12.44 ± 1.35^{b}	-	-
W. sarmentosa	-	38.66 ± 3.43^{a}	14.02 ± 0.30^{b}	-	-

Table 4. Anatomical characterization from ultra-fine cross sections of studied species. Average values ± SE are shown for mesophyll and chloroplasts surface area exposed to intercellular air spaces (S_m/S and S_c/S, respectively), S_c/S_m ratio, chloroplasts thickness (T_{chl}), chloroplasts length (L_{chl}), cytoplasm thickness (T_{cyt}) and cell wall thickness (T_{cw}). Superscript letters indicate significant difference ($P < 0.05$) between species according to LSD test. In all cases, $n = 4$.

Species	S_m/S ($m^2\ m^{-2}$)	S_c/S ($m^2\ m^{-2}$)	S_c/S_m	T_{chl} (µm)	L_{chl} (µm)	T_{cyt} (µm)	T_{cw} (µm)
B. austrosalebrosum	1.50 ± 0.07^{c}	1.28 ± 0.14^{b}	0.80 ± 0.01^{a}	2.21 ± 0.06^{a}	5.27 ± 0.07^{a}	0.84 ± 0.06^{a}	1.09 ± 0.12^{b}
B. pseudotriquetrum	1.67 ± 0.35^{c}	1.17 ± 0.28^{b}	0.68 ± 0.03^{b}	1.71 ± 0.30^{a}	4.44 ± 0.89^{a}	0.47 ± 0.10^{b}	1.43 ± 0.14^{a}
P. alpinum	17.38 ± 0.69^{a}	13.91 ± 0.85^{a}	0.80 ± 0.02^{a}	2.92 ± 0.86^{a}	5.09 ± 0.26^{a}	0.40 ± 0.00^{bc}	0.35 ± 0.02^{c}
P. juniperinum	15.64 ± 0.89^{b}	12.11 ± 1.18^{a}	0.82 ± 0.01^{a}	2.50 ± 0.06^{a}	5.56 ± 0.30^{a}	0.35 ± 0.01^{bc}	0.46 ± 0.03^{c}
S. uncinata	1.30 ± 0.18^{c}	1.01 ± 0.19^{b}	0.76 ± 0.01^{ab}	1.88 ± 0.12^{a}	4.28 ± 0.46^{a}	0.23 ± 0.04^{c}	1.53 ± 0.13^{a}
W. sarmentosa	1.21 ± 0.14^{c}	0.56 ± 0.06^{b}	0.49 ± 0.06^{c}	2.22 ± 0.18^{a}	3.75 ± 0.37^{a}	0.52 ± 0.11^{b}	1.27 ± 0.01^{ab}

Table 5. Cell wall composition of studied species. Average values ± SE are shown for alcohol insoluble residue (AIR), cellulose, hemicelluloses and pectins contents. Cellulose and hemicelluloses are expressed as glucose (glc) grams per area, whereas pectins are expressed as galacturonic acid (gal ac) grams per area. Superscript letters indicate significant difference ($P < 0.05$) between species according to LSD test. In all cases, $n = 6$.

Species	**AIR** (% extracted)	**Cellulose** (g glc m^{-2})	**Hemicelluloses** (g glc m^{-2})	**Pectins** (g gal ac m^{-2})
B. austrosalebrosum	14.67 ± 0.31^{c}	12.90 ± 1.18^{a}	15.77 ± 1.32^{a}	2.43 ± 0.19^{a}
B. pseudotriquetrum	16.51 ± 1.06^{bc}	7.05 ± 0.52^{bc}	10.50 ± 0.51^{a}	2.88 ± 0.08^{a}
P. alpinum	23.33 ± 2.18^{ab}	7.46 ± 0.26^{bc}	17.04 ± 1.18^{a}	1.20 ± 0.08^{c}
P. juniperinum	23.08 ± 2.95^{ab}	5.47 ± 1.42^{c}	13.68 ± 3.76^{a}	1.51 ± 0.30^{bc}
S. uncinata	16.37 ± 1.01^{c}	7.69 ± 1.04^{bc}	16.47 ± 3.56^{a}	3.25 ± 0.60^{a}
W. sarmentosa	25.64 ± 1.68^{a}	9.38 ± 1.03^{b}	13.74 ± 1.98^{a}	2.36 ± 0.28^{ab}

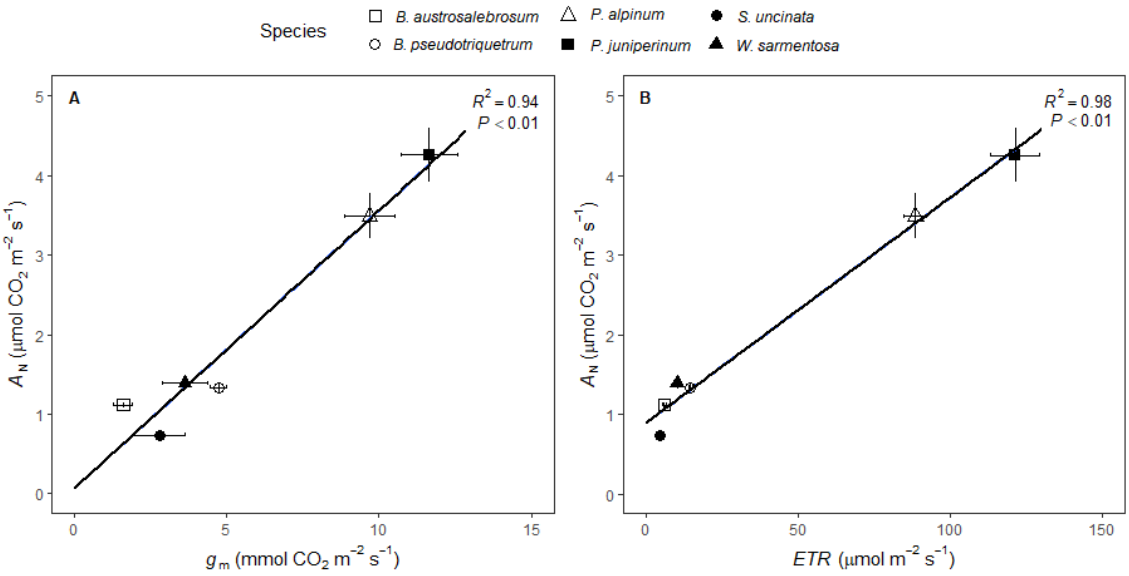

Fig. 1. Relationships between (A) net CO_2 assimilation (A_N) and mesophyll conductance (g_m) and (B) net CO_2 assimilation (A_N) and electron transport rate (*ETR*) in studied moss species. n = 8–9 (means ± SE).

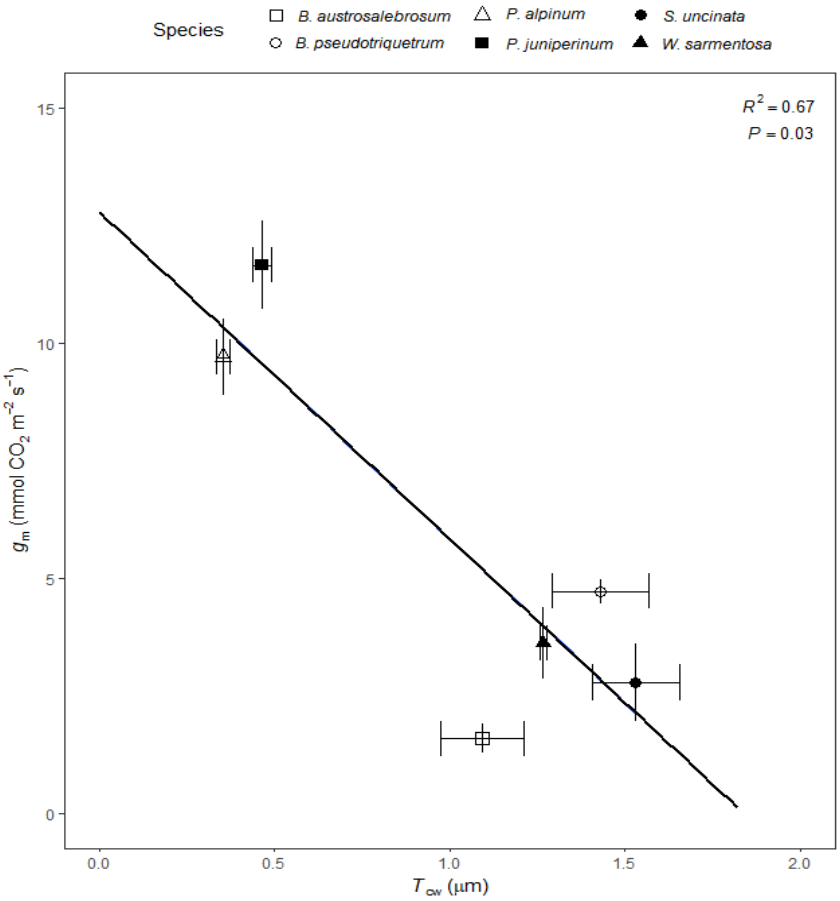

Fig. 2. Relationship between mesophyll conductance (g_m) and cell wall thickness (T_{cw}) in studied moss species. n = 4–9 (means ± SE).

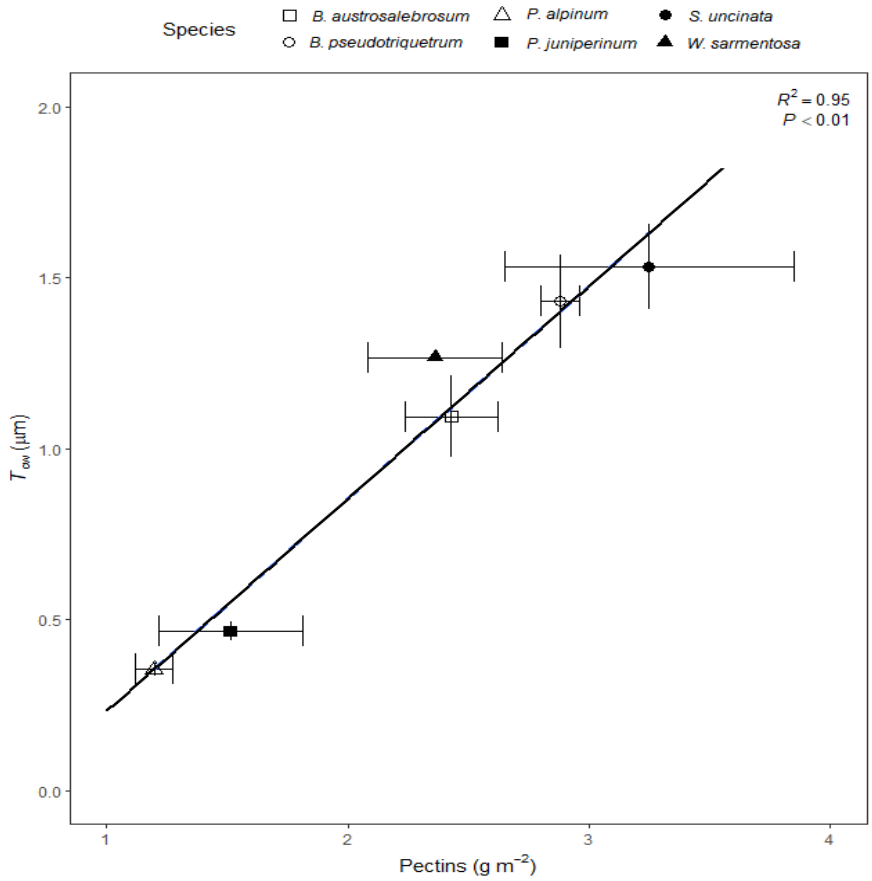

Fig. 3. Relationship between cell wall thickness (T_{CW}) and pectins content in studied moss species. n = 4–6 (means ± SE).

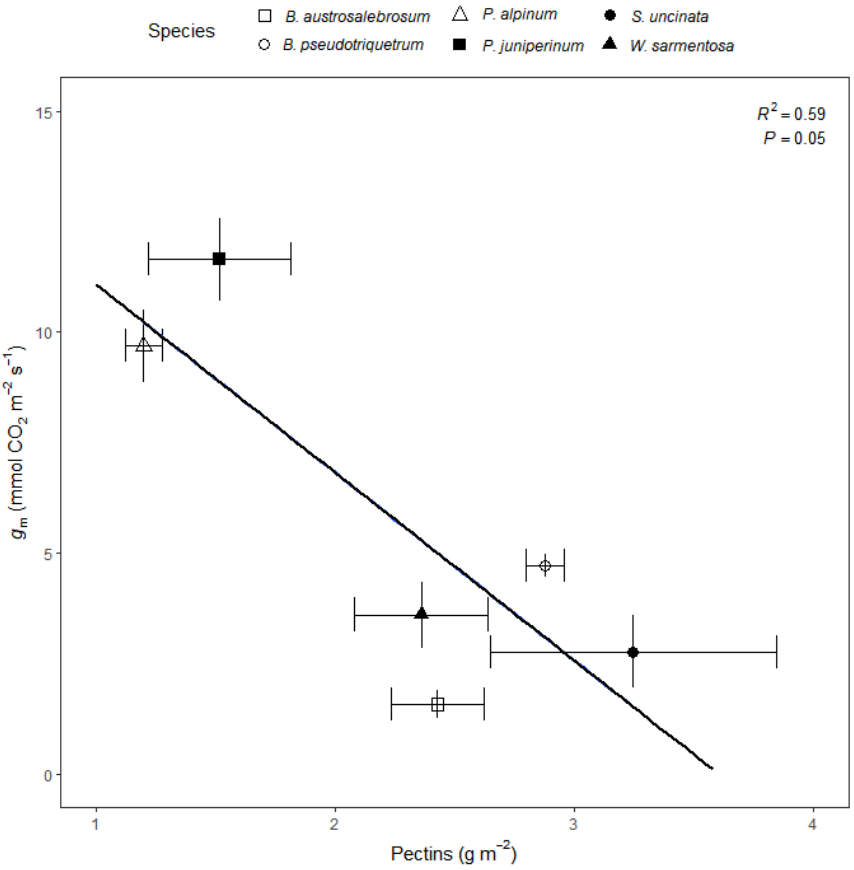

Fig. 4. Relationship between mesophyll conductance (g_m) and pectins content in studied moss species. n = 6–9 (means ± SE).

Table S1. Pearson correlation matrix of photosynthetic, cell wall and anatomical parameters measured in each moss species. Values in italics and bold indicate significant ($P < 0.05$) and highly significant ($P < 0.01$) correlation coefficients, respectively.

	A_N	g_m	*ETR*	R_{light}	*AIR*	Cel	Hemicel	Pectin	(Cel+Hemicel)/ Pectin	T_{LEAF}	T_{chl}	L_{chl}	S_m/S	S_c/S	S_c/S_m	T_{cyt}	T_{cw}
A_N		***0.98***	***0.99***	0.30	0.60	-0.58	-0.03	***-0.9***	*0.81*	***0.98***	0.78	0.66	***0.96***	***0.95***	0.43	-0.28	***-0.93***
g_m			***0.98***	0.23	0.60	-0.74	-0.11	*-0.82*	0.73	***0.96***	0.68	0.56	***0.94***	***0.93***	0.39	-0.45	***-0.86***
ETR				0.26	0.55	-0.63	-0.01	***-0.86***	0.79	***0.98***	0.74	0.68	***0.96***	***0.95***	0.49	-0.35	***-0.91***
R_{light}					-0.28	0.12	-0.42	-0.33	0.26	0.24	0.11	0.65	0.23	0.23	0.40	0.56	-0.34
AIR						-0.4	-0.02	-0.66	0.50	0.54	0.62	-0.13	0.52	0.52	-0.4	-0.3	-0.54
Cel							0.36	0.25	-0.16	-0.56	-0.11	-0.07	-0.53	-0.53	-0.13	***0.86***	0.30
Hemicel								-0.18	0.43	0.14	0.49	0.13	0.21	0.21	0.34	0.00	-0.23
Pectin									***-0.95***	***-0.9***	***-0.94***	-0.6	***-0.91***	***-0.91***	-0.31	-0.01	***0.98***
(Cel+Hemicel)/ Pectin										*0.88*	***0.98***	0.63	***0.90***	***0.91***	0.47	-0.01	***-0.96***
T_{LEAF}											***0.83***	0.68	***1.00***	***0.99***	0.53	-0.33	***-0.95***
T_{chl}												0.53	***0.86***	***0.86***	0.33	0.00	***-0.93***
L_{chl}													0.67	0.67	***0.87***	0.19	-0.73
S_m/S														***1.00***	0.53	-0.33	***-0.95***
S_c/S															0.55	-0.32	***-0.95***
S_c/S_m																-0.06	-0.5
T_{cyt}																	0.05
T_{cw}																	

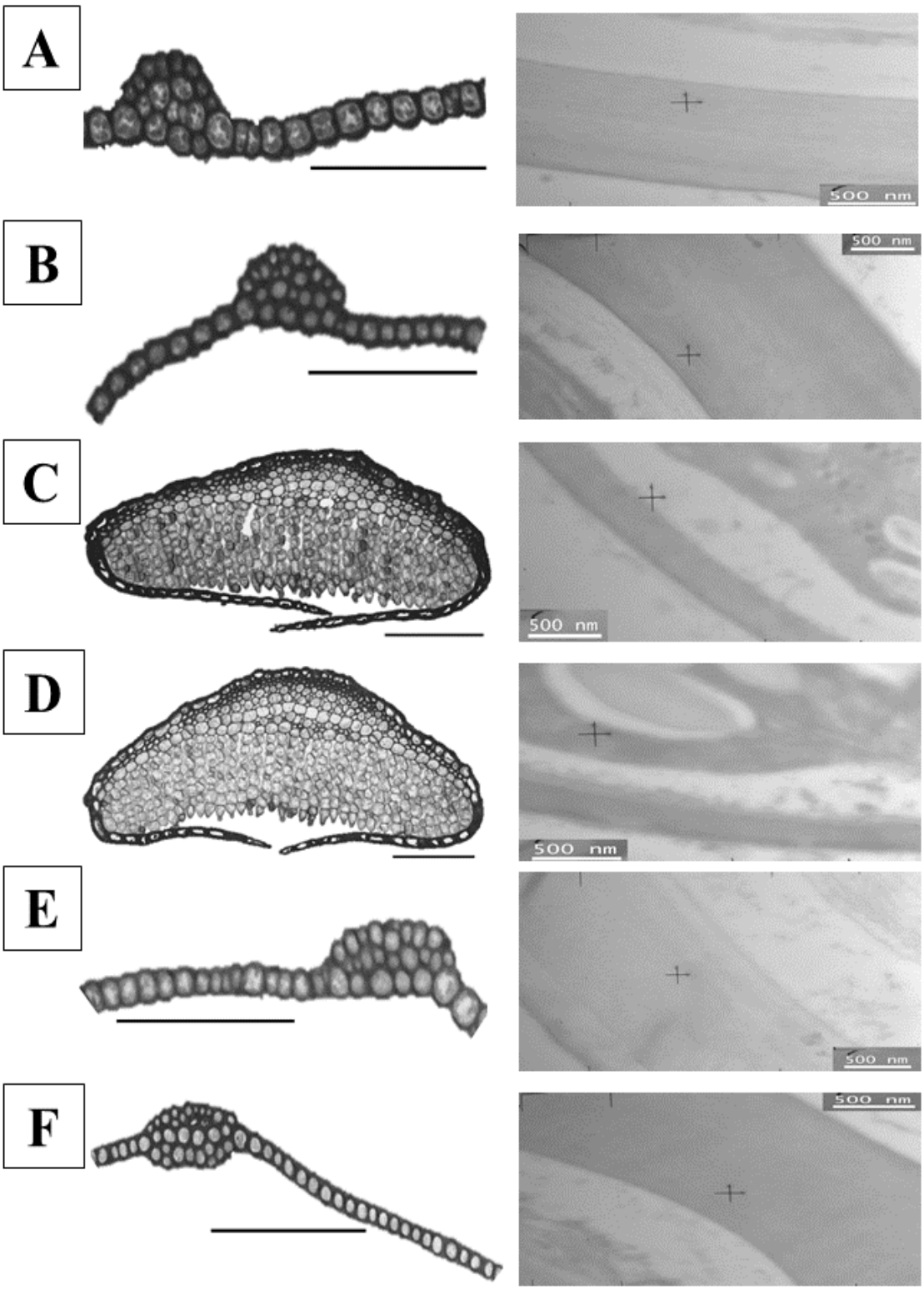

Fig. S1. Representative anatomical characteristics of all studied species from semi-fine (left) and ultra-fine (right) pictures taken at 200/500X and 30000X magnifications, respectively. Species are represented as follows: (A) *B. austrosalebrosum*, (B) *B. pseudotriquetrum*, (C) *P. alpinum*, (D) *P. juniperinum*, (E) *S. uncinata* and (F) *W. sarmentosa*. Black scale bars in light microscope pictures = 100 μm.

Chapter 7

General Discussion

The results derived from the current Thesis have been structured in four chapters – Chapters 3, 4, 5 and 6–, which include eight published or submitted publications that deal with the General and Specific Objectives (see Publications list and Chapter 2 for more detail). Since each publication comprehends a deep discussion of its most relevant findings, readers are addressed to the Discussion section of each one for proper discussion and specific answers to General and Specific Objectives. Therefore, the present chapter aims to provide a brief integrated overview of the present work contributions to the scientific knowledge regarding mesophyll conductance and photosynthesis regulation by cell wall compositional properties.

1.- Cell wall composition influences plants' functional traits

The relevance of cell wall properties affecting photosynthesis has been often neglected (Ellsworth and Reich, 1993; Niinemets, 1999; Evans *et al*., 2009). First, the cell wall only represents a tiny structure (in leaves of most land plants, it is comprised between 0.1 and 0.4 μm; Flexas and Carriquí, 2020) of the pathway that CO_2 has to follow through the leaf mesophyll, which ranges from millimetres to centimetres (Earles *et al*., 2018; Flexas and Carriquí, 2020). Additionally, the diameter of cell wall pores (30-50 Å) is sufficiently large to enable the diffusion of CO_2 molecules, only presenting 3.3 Å (Carpita *et al*., 1979). Moreover, the cell wall was thought to be a static structure from a compositional perspective (Evans *et al*., 2009), especially in mature leaves (Houston *et al*., 2016; Cosgrove, 2018). However, as explained in the General Introduction section, several studies have demonstrated dynamic changes in cell wall composition, in which plants invest many resources for its synthesis and constant remodelling (Somerville *et al*., 2004; Cosgrove, 2005, 2018; Sarkar *et al*., 2009; Keegstra, 2010; Franková and Fry, 2013; Tenhaken, 2015; De Lorenzo *et al*., 2019; Anderson and Kieber, 2020; Yokoyama, 2020). Nonetheless, just a few works proposed that cell wall composition could be a relevant trait affecting photosynthesis, and particularly, g_m (Gago *et al*., 2020; Flexas *et al*., 2021). Whilst the importance of T_{cw} regulating photosynthesis has been widely described (Flexas *et al*., 2012, 2018; Tomás *et al*., 2013; Carriquí *et al*., 2015, 2019*a*, 2020; Tosens *et al*., 2015; Peguero-Pina *et al*., 2017; Veromann-Jürgenson *et al*., 2017; Gago *et al*., 2019; Flexas and Carriquí, 2020), the role of cell wall composition has been much less studied. In this sense, only Ellsworth *et al*. (2018), Clemente-Moreno *et al*. (2019) and Carriquí *et al*. (2020) empirically demonstrated that modifications in cell wall composition correlated

with g_m in mature leaves of rice mutants, in tobacco subjected to contrasting environmental conditions and at interspecific level in non-stressed coniferous, respectively, being partially explained by anatomical characteristics.

Globally, the results derived from the current Thesis provide further evidence and novel information about the importance of cell wall composition regulating g_m and additional photosynthetic parameters (for instance, WUE_i, g_s and the g_m/g_s ratio). Furthermore, the dynamics of cell wall composition turnover in small timescales has been also demonstrated, evidencing that these fast changes affect photosynthesis at distinct levels (Publication 2). Moreover, we showed that modifications in leaf anatomical traits, specifically, in T_{cw}, are related to cell wall composition at intraspecific or even at genotype level because of acclimation to distinct environmental conditions (Publications 1 and 6) as well as at interspecific level (Publication 8).

Besides those relationships demonstrating the importance of cell wall composition modifications affecting both photosynthetic and anatomical properties, the effect of cell wall composition influencing leaf water relations was also addressed in this Thesis. In this sense, Nadal *et al*. (2018) performed a multi-species analysis covering from ferns to angiosperms and reported a trade-off between g_m and ε, suggesting that cell wall properties –specifically, thickness and composition– could strongly regulate this relationship. Given that thick cell walls limit g_m (Tomás *et al*., 2013; Carriquí *et al*., 2015, 2019*a*, 2020; Tosens *et al*., 2015; Veromann-Jürgenson *et al*., 2017; Gago *et al*., 2019; Flexas and Carriquí, 2020) and, at the same time, increase cell rigidity (Peguero-Pina *et al*., 2017), it has been proposed that cell wall compositional traits could also determine ε (Corcuera *et al*., 2002; Moore *et al*., 2008; Solecka *et al*., 2008; Álvarez-Arenas *et al*., 2018; Miranda-Apodaca *et al*., 2018). Even though the mechanistic basis by which ε is modified during plants acclimation to specific environmental stresses is still misunderstood as seems to be species- (Sobrado and Turner, 1983; Lo Gullo and Salleo, 1988; Bartlett *et al*., 2012; Scholz *et al*., 2012; Arias *et al*., 2015; Niinemets, 2016; Zhang *et al*., 2016; Nadal *et al*., 2020) or even genotype-dependent (Galmés *et al*., 2011), this Thesis evidences the species- and the genotype-specific role of cell wall composition influencing ε (Publications 1, 3, 4, 5 and 6).

2.- Inter-specific and inter-phylogenetic trait integration

In Chapter 6 it has been demonstrated that cell wall compositional characteristics determined both photosynthesis and T_{cw} in the most basal plant lineage, as similarly shown by Carriquí *et al.* (2020) in coniferous. Since these studies reported that cell wall composition influenced both g_m and T_{cw} in specific plant groups, we performed a meta-analysis from literature in which cell wall composition, photosynthesis and leaf anatomical properties were studied in a pool of species spanning from mosses to angiosperms grown under optimal conditions to explore further consequences of cell wall compositional traits determining leaf anatomy and photosynthesis from a phylogenetic perspective.

The relationship between T_{cw} and g_m that we report (Fig. 3A) shows that thinner cell walls enable for larger g_m across land plants' phylogeny, as already demonstrated by previous studies (Gago *et al*., 2019; Flexas and Carriquí, 2020). Another significant correlation emerged considering the relative abundance between cell wall compounds, in which increased pectins relative proportion allowed for larger g_m (Fig. 3B). In fact, given that pectins can bind several times their own volume of water (Schiraldi *et al*., 2012) and that CO_2 diffuses in solution, Flexas *et al*. (2021) recently proposed that modifications in pectins content could be responsible of cell wall porosity alterations since their hydrocolloid properties may affect the effective porosity to water and CO_2. Also, their physicochemical properties as well as their interactions with other cell wall compounds seem to be crucial determining g_m from a phylogenetic perspective. Consistent with this idea, the product $P/(C+H) \times 1/T_{cw}$ strongly influenced g_m (Fig. 3C), highlighting the relevance of both porosity and thickness –the first being represented by cell wall compounds relative abundance– regulating g_m across terrestrial plants phylogeny.

Interestingly, the relationships discussed above improved their significance when excluding angiosperms and, particularly, crops. This fact suggests that, whilst we detected the existence of a general trend for cell wall particularities (i.e., thickness and composition) influencing g_m across land plants' phylogeny, distinct patterns are found at smaller scale. Furthermore, it demonstrates that cell wall characteristics are more relevant determining g_m in primitive land plant lineages rather than in the most modern. In fact, mosses were the unique plant group in which g_m was co-regulated by both T_{cw} and cell wall composition (Fig. 4), maybe due to their poikilohydry (Sarkar *et al*., 2009). Thus, whilst thick cell walls could avoid water losses and decrease the CO_2 diffusion (Huttunen

et al., 2018; Carriquí *et al*., 2019*a*), simplified cell wall architecture could allow for larger g_m. In contrast, gymnosperms increased g_m due to enhanced pectins relative abundance (Fig. 4), as similarly occurred considering all land plants lineages. However, we propose that g_m regulation in angiosperms –and, specially, in crops, which have been traditionally selected to enhance their photosynthesis and productivity once subjected to specific growing conditions (Milla *et al*., 2015; Nadal and Flexas, 2019)– could be of high complexity and may be influenced by other mechanisms to a larger extent than by cell walls, for instance, aquaporins and carbonic anhydrases (Fabre *et al*., 2007; Pérez-Martín *et al*., 2014).

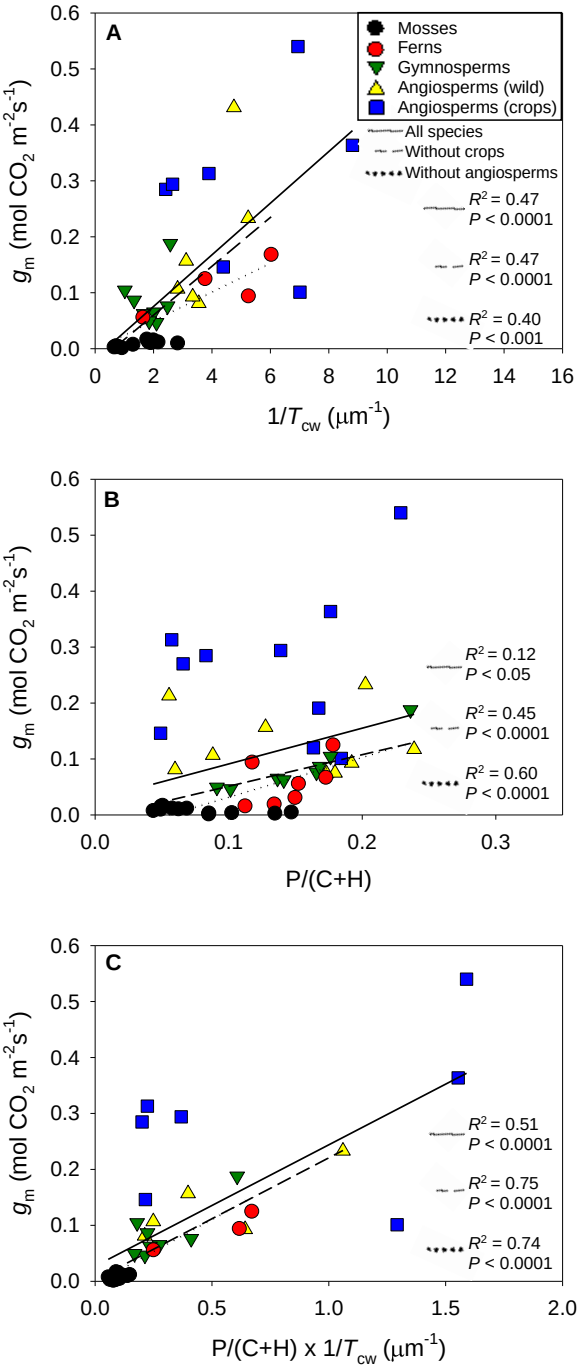

Fig. 3. Mesophyll conductance (g_m) in relation to (A) the inverse of cell wall thickness ($1/T_{cw}$), (B) the pectins to cellulose and hemicelluloses ratio (P/(C+H)), and (C) the product between the pectins to cellulose and hemicelluloses ratio and the inverse of cell wall thickness (P/(C+H) × $1/T_{cw}$) for photosynthetic organs of mosses (n=12), ferns (n=4-7), gymnosperms (n=8), wild angiosperms (n=6-9) and crop angiosperms (n=7-9). Linear regressions were fitted to data for all species, but also excluding angiosperms and crops when significant. Data was obtained from Clemente-Moreno *et al*. (2019), Carriquí *et al*. (2020), Nadal *et al*. (2020) and other unpublished works. Also, data from Publications 1, 3, 4, 5, 6 and 8 of the present Thesis was included.

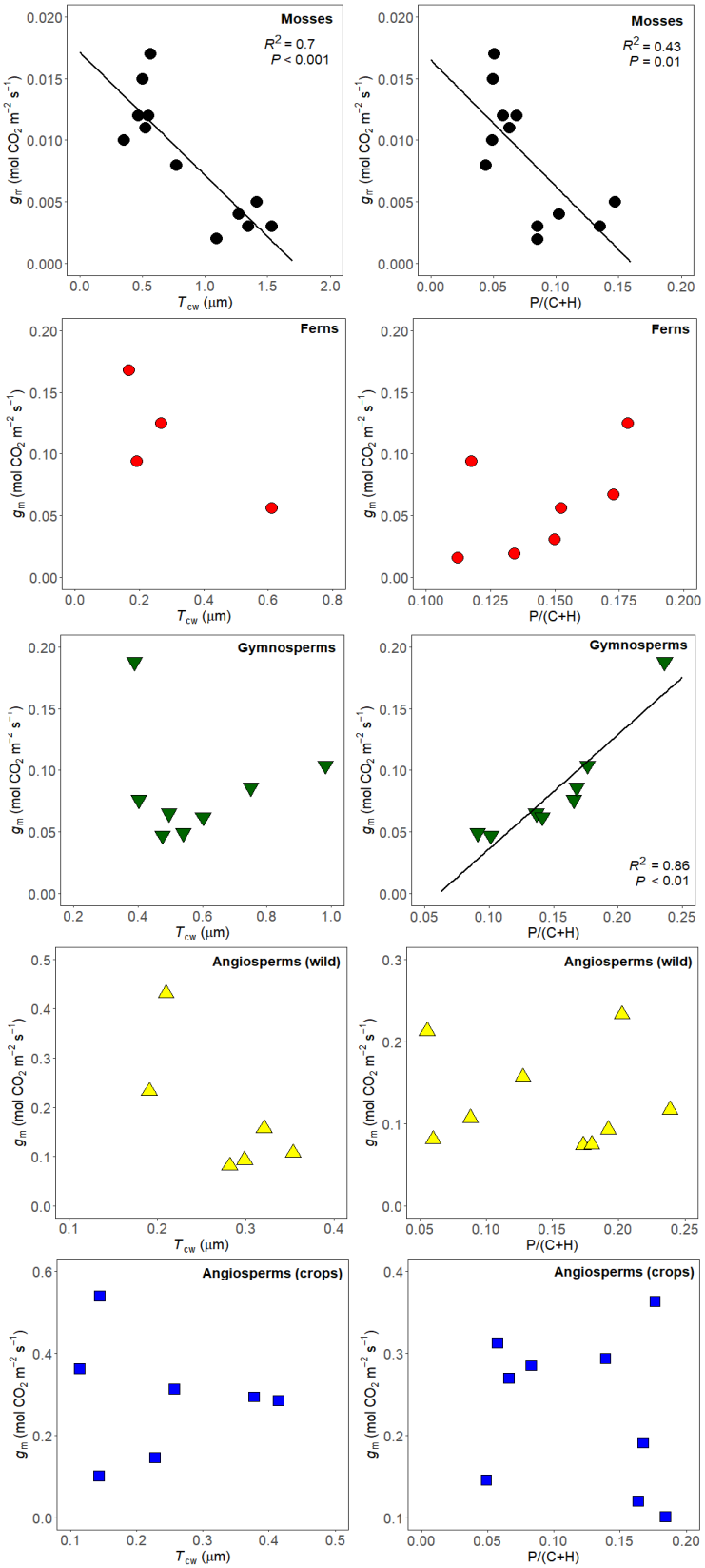

Fig. 4. Mesophyll conductance (g_m) in relation to cell wall thickness (T_{cw}) and to the pectins to cellulose and hemicelluloses ratio (P/(C+H)) for photosynthetic organs of mosses (n=12), ferns (n=4-7), gymnosperms (n=8), wild angiosperms (n=6-9) and crop angiosperms (n=7-9). Linear regressions were fitted to each group data when significant.

3.- Trait integration under abiotic stress

In Chapters 3 and 4 it was shown that cell wall composition affected photosynthesis, leaf water relations and/or anatomical characteristics. However, such correlations were species- (or even genotype-) specific and could also depend on experimental conditions. Thus, in this section we aimed to describe which are the strongest and most general g_m determinants in plants subjected to abiotic stresses analysing together all the traits studied in all tested species (i.e., those species from Publications 1-6).

When examining all analysed parameters –i.e., the ones related to photosynthesis, foliar structure, leaf water relations, anatomical properties, and cell wall composition– several correlations emerged. Based on these results and considering the relevance of g_m in this Thesis, we selected those parameters that better determined g_m regulation during abiotic stresses imposition (Table 2).

Table 2. Pearson correlation matrix containing the selected photosynthetic, foliar structure, anatomical and cell wall composition parameters analysed in those species studied in Chapters 3 and 4. Values in italics and bold indicate significant (P<0.05) and highly significant (P<0.01) correlation coefficients, respectively.

	g_m	*LMA*	*LD*	f_{ias}	AIR	Cellulose	Hemicel.	Pectins
g_m		*-0.42*	***-0.57***	0.29	*-0.43*	0.30	-0.34	***-0.48***
LMA			*0.43*	***-0.77***	0.01	*-0.53*	***0.68***	0.31
LD				0.05	0.21	-0.23	0.12	0.33
f_{ias}					0.11	0.17	*-0.71*	0.46
AIR							0.07	*0.47*
Cellulose							-0.34	-0.35
Hemicel.								-0.19
Pectins								

Further analyses of the relationships between the selected parameters showed negative correlations between g_m and AIR, pectins, *LMA* and *LD* (Fig. 5). Moreover, *LMA* was linked negatively with f_{ias} (Fig. 6A), which was also negatively related to hemicelluloses (Fig. 6B). Similarly, although a negative relationship between *LMA* and cellulose was found (Fig. 6C), *LMA* correlated positively with hemicelluloses (Fig. 6D).

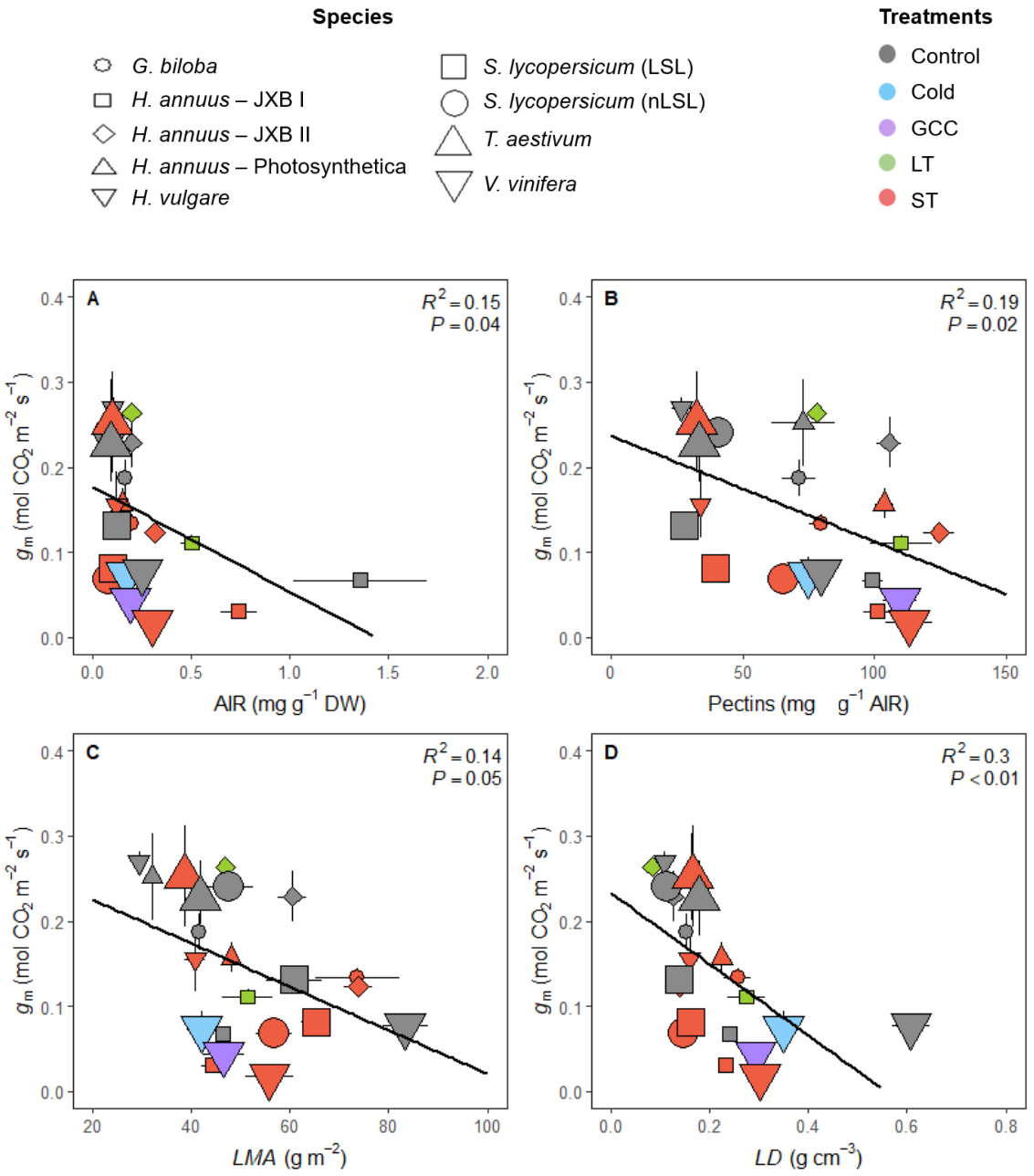

Fig. 5. Representation of the integrative relationships between the selected photosynthetic, foliar structure and cell wall composition parameters analysed in those species studied in Chapters 3 and 4. Treatments' colouring was done according to evaluated experimental conditions ("GCC": growth chamber conditions, "LT": long-term water deficit stress, "ST": short-term water deficit stress). ST and LT comprehend those experimental conditions performed under ST and ST-Rec and under LT and LT-Rec, respectively, regardless of the specific field capacity percentage. For parameters abbreviations, see "Symbols and abbreviations" section in page "iii" of this Thesis.

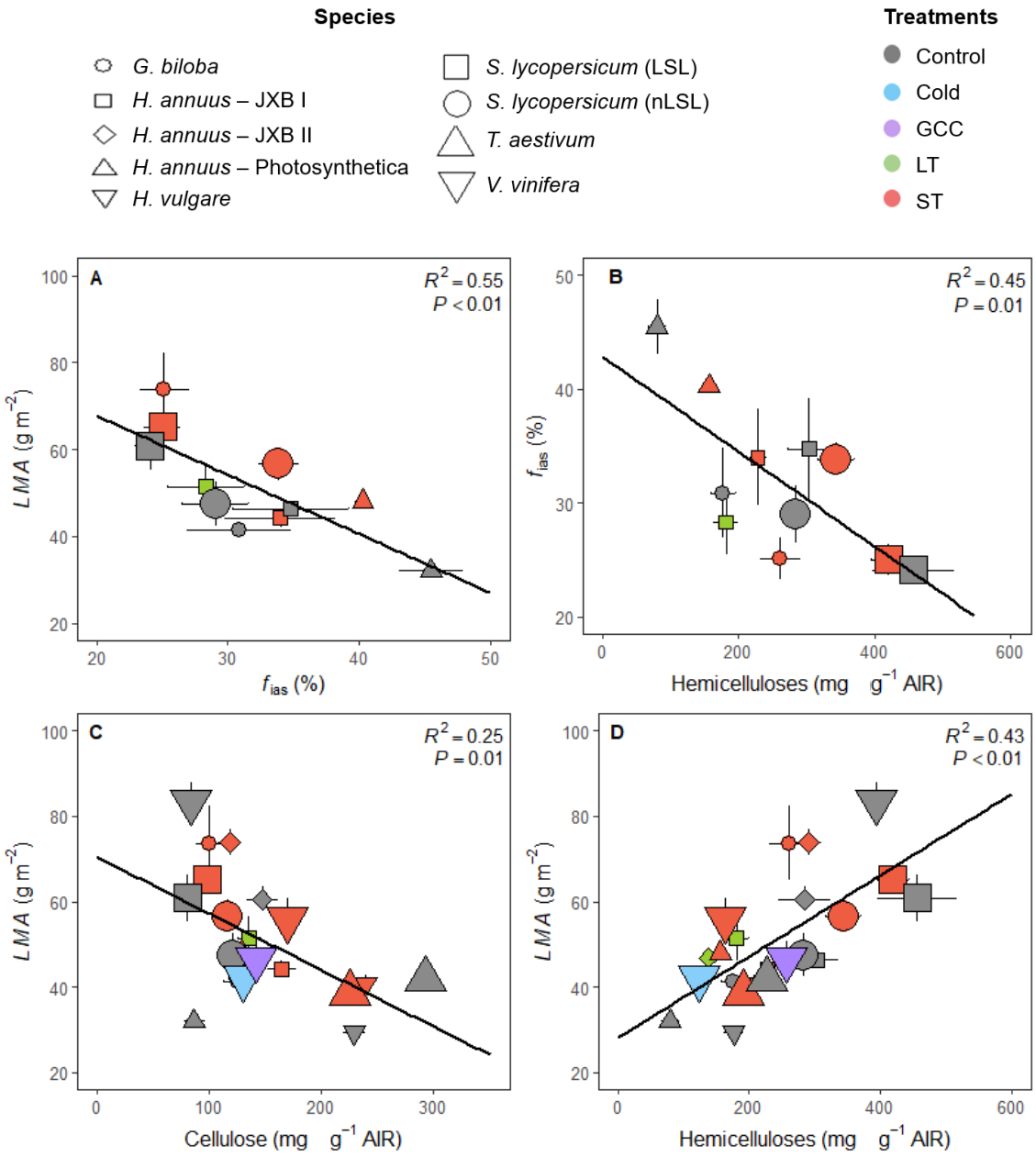

Fig. 6. Representation of the integrative relationships between the selected foliar structure, anatomical and cell wall composition parameters analysed in those species studied in Chapters 3 and 4. Treatments' colouring was done according to evaluated experimental conditions ("GCC": growth chamber conditions, "LT": long-term water deficit stress, "ST": short-term water deficit stress). ST and LT comprehend those experimental conditions performed under ST and ST-Rec and under LT and LT-Rec, respectively, regardless of the specific field capacity percentage. For parameters abbreviations, see "Symbols and abbreviations" section in page "iii" of this Thesis.

From these results, some conclusions can be reached. First, it is shown that the cell wall content per leaf (i.e., the AIR) negatively influences g_m (Fig. 5A). Additionally, whilst we reported species- and genotype-dependent cell wall modifications influencing g_m in each tested species subjected to specific environmental conditions (see publications in Chapters 3 and 4), when merging all results, we specifically demonstrate that pectins are the unique cell wall component determining g_m adjustments under abiotic stresses imposition (Fig. 5B). Thus, we propose that modifications in pectins amounts could influence several cell wall characteristics affecting the CO_2 diffusion, such as porosity, flexibility, and thickness (Carpita and Gibeaut, 1993; Carpita and McCann, 2002; Cosgrove, 2005; Leucci *et al*., 2008; Moore *et al*., 2008, 2013; Solecka *et al*., 2008; Voragen *et al*., 2009; Tenhaken, 2015; Houston *et al*., 2016; Rui and Dinneny, 2019; Yokoyama, 2020). As discussed in the previous section, we speculate that changes in pectins concentration could be related to modifications in wall porosity, but they may also lead to alterations in their enzymatic performance as well as in the overall cell wall physicochemical characteristics, modifying the interactions between cell wall compounds and, consequently, changing wall architecture and structure. Nonetheless, not only cell wall composition, but foliar structure-derived parameters (i.e., *LMA* and *LD*) also determined g_m adjustments under abiotic conditions (Figs. 5C, D), reflecting the high complexity of g_m regulation. Additionally, it has been demonstrated that cell wall composition has not an exclusive effect on g_m or photosynthetic-related parameters since it also influences leaf structure and anatomy, particularly, *LMA* and f_{ias} (Fig. 6).

Finally, it has to be considered that the potential implication of cell wall compounds others than cellulose, hemicelluloses and pectins affecting g_m remains largely unexplored. Since we revealed that cell wall minor compounds such as cell wall bound phenolics –and, particularly, coumaric acid– could also play a relevant role driving g_m adjustments during the acclimation to distinct water regimes (Publication 1), further studies evaluating their impact are required, especially, in those species presenting large amounts in their cell walls, for instance, grasses (Hartley, 1973; Harris and Hartley, 1976; Hartley and Jones, 1977; Carpita and Gibeaut, 1993; Iiyama *et al*., 1994; Carpita, 1996; Carpita and McCann, 2002; Vogel, 2009). Similarly, additional experiments testing plant groups others than angiosperms subjected to contrasting environmental conditions would be crucial to evaluate if modifications in cell wall composition are promoted and can influence g_m.

4.- Recapitulation, limitations, and perspectives

Along this Thesis, it has been evidenced that cell wall composition is related to g_m and other photosynthetic traits, leaf water relations and anatomical parameters. Besides the complexity of the hypothetical mechanism by which g_m is determined due to cell wall properties –including thickness, porosity, tortuosity, and composition– proposed by Flexas *et al*. (2021) (Fig. 7), the results provided by this Thesis demonstrate that they could be even more complex since they may depend on the tested environmental conditions as well as on the evaluated species and/or genotypes. Thus, there is a need to take advantage of the available methodologies and systems to explore in more detail how cell wall compositional characteristics affect plants' functional traits at different levels.

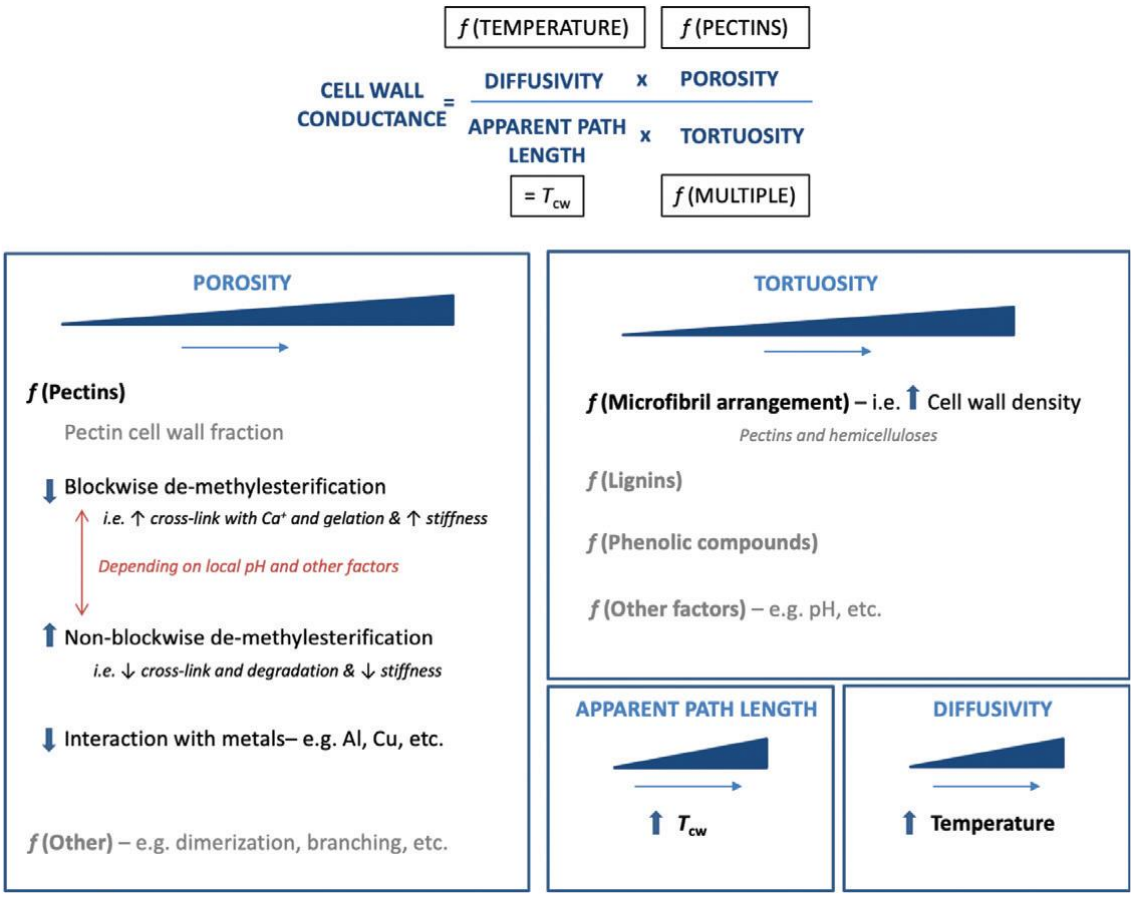

Fig. 7. Summary of the hypothetical mechanism by which cell wall properties affect cell wall conductance (Flexas *et al*., 2021). The relationship between the four properties determining cell wall conductance is displayed at the top of the diagram. Below the equation, the physicochemical factors that determine (black) or potentially determine (grey) each cell wall property are detailed. Arrows indicate the known or suggested direction of influence of each factor.

The fast development of DNA sequencing technologies has emerged as a useful tool that has increased our understanding regarding cell walls (Yokoyama, 2020). Thus, the publication of around 224 plant species genomes from algae to angiosperms (Phytozome, 2021) enables to compare the genic pool of distinct plant lineages. Hence, the generation of cell wall mutant genotypes could be useful to elucidate the functioning of a specific gene and/or enzyme (Yokoyama, 2020). However, it is still a difficult task since the biotechnological modification of a cell wall gene may promote alterations in the dynamics and/or status of other wall components (Anderson and Kieber, 2020; Yokoyama, 2020). For instance, Xiao *et al*. (2016) reported that *Arabidopsis* mutants presenting disruptions in those genes involved in xyloglucan synthesis also reduced cellulose synthesis and altered the expression of wall-integrity-sensing genes. Additionally, phenotypic effects have been observed in *Arabidopsis* mutants exhibiting cell wall modifications, ranging from embryo lethality to very specific alterations such as aberrant pollen production (Spielman *et al*., 1997; Nickle and Meinke, 1998). However, in many cases, cell wall mutations resulted in whole plant phenotypic disruptions that were accompanied by reductions in the foliar size and area (Reiter *et al*., 1993, 1997; Turner and Somerville, 1997; Nicol *et al*., 1998; Brown *et al*., 2005; Zhong *et al*., 2005; Persson *et al*., 2007; Xiao *et al*., 2016; Zhang *et al*., 2020; Chen *et al*., 2021) as well as in modified leaf anatomy (Weraduwage *et al*., 2016; Ellsworth *et al*., 2018), which could potentially secondarily affect photosynthesis performance as appreciated in Publication 7.

Given pectins' importance determining several cell wall properties, numerous studies have tested mutant genotypes presenting PRE alterations in order to elucidate the importance of their appropriated functionality (Rhee *et al*., 2003; Bosch and Hepler, 2005; Parre and Geitmann, 2005; Derbyshire *et al*., 2007; Gou *et al*., 2008, 2012; Peaucelle *et al*., 2008, 2011; Zhang *et al*., 2008; Pelletier *et al*., 2010; Müller *et al*., 2013; de Souza *et al*., 2014; Sénéchal *et al*., 2014; de Souza and Pauly, 2015; Leroux *et al*., 2015; Levesque-Tremblay *et al*., 2015; Scheler *et al*., 2015; Turbant *et al*., 2016; Wang *et al*., 2016; Weraduwage *et al*., 2016; Guénin *et al*., 2017; Hocq *et al*., 2017; Yang *et al*., 2018; Kong *et al*., 2019). Even though the biological implications of altered PRE are remaining poorly understood, the improvement of several techniques that enable to study pectins' characteristics *in muro* has demonstrated the high complexity of their regulation during different stages of cell expansion, development, growth, and in response to both biotic and abiotic stresses (De Lorenzo *et al*., 2019; Palacio-López *et al*., 2020). For

example, Dick-Pérez *et al*. (2011) used solid-state nuclear magnetic resonance (NMR) and observed interactions between pectins and cellulose microfibrils due to their close deposition in the cell wall. With the same methodology, Phyo *et al*. (2017) tested *Arabidopsis* mutant lines and showed that those mutants with altered HG molecular weight presented modifications in the interactions between HG and cellulose that affected cell expansion. Moreover, Carpita and McCann (2015) proposed that fourier-transform infrared (FTIR) microspectroscopy could be another method to differentiate cellulosic, hemicellulosic and pectic profiles from Type I and Type II primary cell walls, highlighting its potential application to detect changes in the amounts of these polysaccharides in mutant genotypes. Furthermore, the utilization of fluorescent molecules presenting specific affinity for single cell wall polysaccharides is widely recognized as a useful tool to visualize cell wall mechanical characteristics at different growth stages (Anderson *et al*., 2012; Dumont *et al*., 2016; De Lorenzo *et al*., 2019; Bidhendi *et al*., 2020; Palacio-López *et al*., 2020; Parra *et al*., 2020). In this sense, Anderson *et al*. (2012) and Dumont *et al*. (2016) used modified polysaccharides with fluorescent labelling that were metabolically incorporated into the cell wall and detected how they were progressively incorporated to RG-I and RG-II residues, respectively. More recently, Parra *et al*. (2020) utilized immunogold labelling to investigate the ultrastructural distribution of LM19, LM20, LM5 and LM6 pectin epitopes during different stages of olive ripening. Additionally, Bidhendi *et al*. (2020) performed a technical update on fluorescence procedures that enabled to visualize cellulose microfibrils orientation and pectins distribution in different tissues of *A. thaliana* and *Camellia japonica* at specific growing stages. Thus, these techniques could be used for testing specific site-location effects of specific cell wall components on the overall leaf photosynthetic performance.

Nonetheless, major challenges are remaining to elucidate pectins structure, dynamics, and interactions with other compounds because of the high structural complexity of the plant cell wall. Although the equipment that enables to study biological samples at nanometric scales is already available (super-resolution microscopy; Paës *et al*., 2018; Vangindertael *et al*., 2018) and has been employed to specifically detect lignins (Paës *et al*., 2018), higher resolution would be required to study the cell wall architecture in more detail. In the case of fluorescence labelling, further investigation is necessary to enhance the binding affinity when detecting specific cell wall structures and/or compounds (Bidhendi *et al*., 2020). Finally, a selection of the most appropriated plant

species to investigate the effects of specific cell wall alterations would be crucial since results cannot be distinctly extrapolated to all phylogenetic groups as they present characteristic genes, enzymes and/or cell wall compounds (see section 7 of the General Introduction). In this sense, whilst *A. thaliana* is the most widely utilized model plant for cell wall mutations screening to explore the functioning of a particular gene (Carpita and McCann, 2002; Somerville *et al*., 2004; Cosgrove, 2005; Anderson and Kieber, 2020), these results could just be extrapolated to dicotyledonous angiosperms, as mentioned in Publication 7. Similarly, rice and maize mutant genotypes, for example, would be much more appropriate to investigate how cell wall disruptions affect plants' functionality in grasses. The same considerations should be applied to gymnosperms, ferns, and mosses, considering that sub-classifications within each group may present specific cell wall composition. Therefore, all the appreciations mentioned in this section would be required to enhance the current knowledge about the mechanistic basis of g_m regulation due to cell wall compositional properties.

Chapter 8

Conclusions

From the results presented in Chapters 3, 4, 5 and 6 and in the General Discussion, the following conclusions have been drawn to respond to the General and Specific Objectives of this Thesis:

General Objective 1: To explore possible relationships between changes in cell wall composition and g_m during water deficit stress exposition in a model plant.

- Specific Objective 1: *To study short- and long-term water deficit stress responses in cell wall composition, leaf water relations, foliar anatomy, and photosynthesis.*
  - Conclusion 1: In *Helianthus annuus* plants submitted to short- and long-term water deficit stress followed by recovery, lignins and cell wall minor compounds –particularly, cell wall bound phenolics– were linked with photosynthetic traits. Moreover, the (Cellulose+Hemicelluloses)/Pectins ratio correlated with T_{cw}. However, changes in cell wall composition did not influence ε.
  - Conclusion 2: When compared with *H. annuus*, also in the phylogenetically distant species *Ginkgo biloba*, water deficit stress induced changes in cell wall composition that were not linked with g_m and photosynthesis, and differently modified leaf water relations parameters in both species.

- Specific Objective 2: *To determine the dynamics and the speed of those changes occurring in cell wall composition and photosynthesis after plants exposition to specific levels of water availability*.
  - Conclusion 3: During gradual short-term water deficit stress, pectins content negatively correlated with g_m in *H. annuus*. Nonetheless, the detailed monitoring of the recovery preceded by a long-term water deficit stress revealed that photosynthesis gradually increased concomitantly to significantly decreased pectins content after only 5 h of rewatering, with further recovery of photosynthesis being unrelated to cell wall composition. Remarkably, lignins content drastically increased after 24 h, being associated with g_s increments.

General Objective 2: To study the relationships between changes in cell wall composition and g_m in different crops acclimated to contrasting abiotic stresses.

- Specific Objective 3: *To investigate the effect of temperature and distinct water deficit stress regimes promoting modifications in cell wall composition that influence leaf water relations, leaf anatomy, and photosynthesis performance.*
  - Conclusion 4: In *Vitis vinifera* subjected to distinct abiotic conditions, A_N and g_m correlated with cellulose, whilst ε was linked with pectins.
  - Conclusion 5: In *Hordeum vulgare* and *Triticum aestivum* subjected to distinct water deficit stress regimes, osmotic and elastic adjustments influenced photosynthesis, being π_o, ε, and g_s key parameters. Particularly, modifications in pectins content correlated with leaf elasticity and both g_s and g_m.
  - Conclusion 6: The physiological behaviour of *Solanum lycopersicum* long shelf-life (LSL) and non-long shelf-life genotypes (nLSL) subjected to different water regimes was genotype-dependent, being influenced by distinct parameters in each case. Whilst the LSL genotype maintained g_m within a narrow range across experimental conditions due to elastic, sub-cellular anatomical and cell wall compositional adjustments, the nLSL experienced large g_m variations that were linked to changes in *LMA* as well as in supra-cellular anatomical characteristics.
  - Conclusion 7: Despite different relationships were found in the studied species, when pooling all results together, a common g_m regulation pattern emerged, involving pectins, but also other leaf traits such as *LMA*, *LD* and f_{ias}.

General Objective 3: To study genetic and phylogenetic conditionings for the relationships between photosynthesis and cell wall composition.

- Specific Objective 4: *To examine the effect of specific cell wall mutations regulating g_m in mutant plants.*
  - Conclusion 8: *Arabidopsis thaliana atpae11.1* and *atpme17.2* mutant plants, which presented specific alterations in pectin acetylesterases and pectin methylesterases, respectively, reduced photosynthesis in association with modifications in leaf chemistry.

- Specific Objective 5: *To analyse the role of cell wall composition in relation to photosynthesis and leaf anatomy in plants belonging to a single phylogenetic group distant from angiosperms.*

  - Conclusion 9: Cell wall composition influenced both T_{cw} and photosynthesis in Antarctic mosses. Low A_N and g_m were achieved due to extremely thick cell walls, which in turn, were determined by different cell wall composition, specifically, pectins.

- Specific Objective 6: *To evaluate the importance of cell wall composition in determining photosynthesis performance and leaf anatomy along land plants' phylogeny.*

  - Conclusion 10: Although cell wall composition correlated differently with g_m and T_{cw} in specific land plant lineages, both common relationships with g_m emerge when pooling all phylogenetic groups. Additionally, the relationship between g_m and the product $1/T_{cw} \times P/(C+H)$ was far better than the relationship between g_m and any of the two separate parameters. We conclude that the P/(C+H) ratio positively influences g_m at a global large scale, but the same components operate in different ways at a smaller scale (i.e., within a single species and/or phylogenetic group), likely reflecting the complex interactions between, for example, pectins and pectin remodelling enzymes with other cell wall compounds, leading to differential effects on CO_2 diffusion.

References

Anderson CT, Wallace IS, Somerville CR. (2012). Metabolic click-labeling with a fucose analog reveals pectin delivery, architecture, and dynamics in *Arabidopsis* cell walls. *Proceedings of the National Academy of Sciences* 4, 1329–1334.

Anderson CT, Kieber JJ. (2020). Dynamic construction, perception, and remodelling of plant cell walls. *Annual Review of Plant Biology* 71, 39–69.

Arabidopsis Genome Initiative. (2000). Analysis of the genome sequence of the flowering plant *Arabidopsis thaliana*. *Nature* 408, 796–815.

Arias NS, Bucci SJ, Scholz FG, Goldstein G. (2015). Freezing avoidance by supercooling in *Olea europaea* cultivars: the role of apoplastic water, solute content and cell wall rigidity. *Plant, Cell & Environment* 38, 2061–2070.

Atmodjo MA, Zhangying H, Mohnen D. (2013). Evolving views of pectin biosynthesis. *Annual Reviews of Plant Biology* 64, 747–779.

Álvarez-Arenas TEG, Sancho-Knapik D, Peguero-Pina JJ, Gómez-Arroyo A, Gil-Pelegrín E. (2018). Non-contact ultrasonic resonant spectroscopy resolves the elastic properties of layered plant tissues. *Applied Physics Letters* 113, 253704.

Baldwin L, Domon JM, Klimek JF, Fournet F, Sellier H, Gillet F, Pelloux J, Lejeune-Hénaut I, Carpita NC, Rayon C. (2014). Structural alteration of cell wall pectins accompanies pea development in response to cold. *Phytochemistry* 104, 37–47.

Barbour MM, Kaiser BN. (2016). The response of mesophyll conductance to nitrogen and water availability differs between wheat genotypes. *Plant Science* 251, 119–127.

Bartlett MK, Scoffoni C, Sack L. (2012). The determinants of leaf turgor loss point and prediction of drought tolerance of species and biomes: a global meta-analysis. *Ecology Letters* 15, 393–405.

Bálsamo RA, Bauer AM, Davis SD, Rice BM. (2003). Leaf biomechanics, morphology, and anatomy of the deciduous mesophyte *Prunus serrulate* (Rosaceae) and the evergreen sclerophyllous shrub *Heteromeles arbutifolia* (Rosaceae). *American Journal of Botany* 90, 72–77.

Bernacchi CJ, Portis AR, Nakano H, von Caemmerer S, Long SP. (2002). Temperature response of mesophyll conductance. Implications for the determination of Rubisco enzyme kinetics and for limitations to photosynthesis *in vivo*. *Plant Physiology* 130, 1992–1998.

Bernacchi C, Morgan P, Ort D, Long S. (2005). The growth of soybean under free air [CO2] enrichment (FACE) stimulates photosynthesis while decreasing *in vivo* Rubisco capacity. *Planta* 220, 434–446.

Bidhenhi AJ, Chebli Y, Geitmann A. (2020). Fluorescence visualization of cellulose and pectin in the primary cell wall. *Journal of Microscopy* 278, 164–181.

Bosch M, Hepler PK. (2005). Pectin methylesterases and pectin dynamics in pollen tubes. *Plant Cell* 17, 3219–3226.

Boyer JS, Wong SC, Farquhar GD. (1997). CO_2 and water vapor exchange across leaf cuticle (epidermis) at various water potentials. *Plant Physiology* 114, 185–191.

Bray EA. (2004). Genes commonly regulated by water-deficit stress in *Arabidopsis thaliana*. *Journal of Experimental Botany* 55, 2331–2341.

Brodribb TJ, McAdam SAM, Jordan GJ, Feild TS. (2009). Evolution of stomatal responsiveness to CO_2 and optimization of water-use efficiency among land plants. *New Phytologist* 183, 839–847.

Brodribb TJ, McAdam SAM. (2011). Passive origins of stomatal control in vascular plants. *Science* 331, 582–585.

Brown DM, Zeef LHA, Ellis J, Goodacre R, Turner SR. (2005). Identification of novel genes in *Arabidopsis* involved in secondary cell wall formation using expression profiling and reserve genetics. *The Plant Cell* 17, 2281–2295.

Bunce JA. (2009). Use of the response of photosynthesis to oxygen to estimate mesophyll conductance to carbon dioxide in water-stressed soybean leaves. *Plant, Cell & Environment* 32, 875–88.

Caffall KH, Mohnen D. (2009). The structure, function, and biosynthesis of plant cell wall pectic polysaccharides. *Carbohydrate Research* 344, 1879–1900.

Campbell MM, Sederoff R. (1996). Variation in lignin content and composition (mechanisms of control and implications for the genetic improvement of plants). *Plant Physiology* 110, 3–13.

Carpita N, Sabularse D, Montezinos D, Delmer DP. (1979). Determination of the pore size of cell walls of living plant cells. *Science* 205, 1144–1147.

Carpita NC, Gibeaut DM. (1993). Structural models of primary cell walls in flowering plants: consistency of molecular structure with the physical properties of the walls during growth. *The Plant Journal* 3, 1–30.

Carpita NC. (1996). Structure and biogenesis of the cell walls of grasses. *Annual Review of Plant Molecular Biology* 4, 445–476.

Carpita NC, McCann MC. (2002). The functions of cell wall polysaccharides in composition and architecture revealed through mutations. *Plant and Soil* 247, 71–80.

Carpita NC, McCann MC. (2015). Characterizing visible and invisible cell wall mutant phenotypes. *Journal of Experimental Botany* 66, 4145–4163.

Carriquí M, Cabrera HM, Conesa MÀ, Coopman RE, Douthe C, Gago J, Gallé A, Galmés J, Ribas-Carbó M, Tomás M, Flexas J. (2015). Diffusional limitations explain the lower

photosynthetic capacity of ferns as compared with angiosperms in a common garden study. *Plant, Cell & Environment* 38, 448–460.

Carriquí M, Roig-Oliver M, Brodribb TJ, Coopman R, Gill W, Mark K, Niinemets Ü, Perera-Castro AV, Ribas-Carbó M, Sack L, Tosens T, Waite M, Flexas J. (2019*a*). Anatomical constraints to nonstomatal diffusion conductance and photosynthesis in lycophytes and bryophytes. *New Phytologist* 222, 1256–1270.

Carriquí M, Douthe C, Molins A, Flexas J. (2019*b*). Leaf anatomy does not explain apparent short-term responses of mesophyll conductance to light and CO_2 in tobacco. *Physiologia Plantarum* 165, 604–618.

Carriquí M, Nadal M, Clemente-Moreno MJ, Gago J, Miedes E, Flexas J. (2020). Cell wall composition strongly influences mesophyll conductance in gymnosperms. *The Plant Journal* 103, 1372–1385.

Carvalho CP, Hayashi AH, Braga MR, Nievola CC. (2013). Biochemical and anatomical responses related to the in vitro survival of the tropical bromeliad *Nidularium minutum* to low temperatures. *Plant Physiology and Biochemistry* 71, 144–154.

Cavalier DM, Lerouxel O, Neumetzler L, Yamauchi K, Reinecke A, Freshour G, Zabotina OA, Hahn MG, Burgert I, Pauly M, Raikhel NV, Keegstra K. (2008). Disrupting two *Arabidopsis thaliana* xylosyltransferase genes results in plants deficient in xyloglucan, a major primary cell wall component. *The Plant Cell* 20, 1519–1537.

Chaves MM, Maroco JP, Pereira JS. (2003). Understanding plant responses to drought – from genes to the whole plant. *Functional Plant Biology* 30, 239–264.

Chaves MM, Flexas J, Pinheiro C. (2009). Photosynthesis under drought and salt stress: regulation mechanisms from whole plant to cell. *Annals of Botany* 103, 551–560.

Chen H, Fang R, Deng R, Li X. (2021). The OsmiRNA166b-OsHox32 pair regulates mechanical strength of rice plants by modulating cell wall biosynthesis. *Plant Biotechnology Journal* 19, 1468–1480.

Clemente-Moreno MJ, Gago J, Díaz-Vivancos P, Bernal A, Miedes E, Bresta P, Liakopoulos G, Fernie AR, Hernández JA, Flexas J. (2019). The apoplastic antioxidant system and altered cell wall dynamics influence mesophyll conductance and the rate of photosynthesis. *The Plant Journal* 99, 1031–1046.

Corcuera L, Camarero JJ, Gil-Pelegrín E. (2002). Functional groups in *Quercus* species derived from the analysis of pressure-volume curves. *Trees* 16, 465–472.

Cosgrove DJ. (1997). Assembly and enlargement of the primary cell wall in plants. *Annual Review of Cell Development and Biology* 13, 171–201.

Cosgrove DJ. (2005). Growth of the plant cell wall. *Nature Reviews. Molecular Cell Biology* 6, 850–861.

Cosgrove DJ. (2018). Diffusive growth of plant cell walls. *Plant Physiology* 176, 16–27.

Cowan I. (1986). Economics of carbon fixation in higher plants. In: Givnish TJ (ed.). *On the economy of plant form and function*. Cambridge University Press, Cambridge, 133–170.

Crous K, Quentin A, Lin Y, Medlyn B, Williams D, Barton C, Ellsworth D. (2013). Photosynthesis of temperate *Eucalyptus globulus* trees outside their native range has limited adjustment to elevated CO_2 and climate warming. *Global Change Biology* 19, 3790–3807.

DaMatta FM, Godoy AG, Menezes-Silva PE, Martins SCV, Sanglard LMVP, Morais LE, Torre-Neto A, Ghini R. (2016). Sustained enhancement of photosynthesis in coffee trees grown under free-air CO_2 enrichment conditions: disentangling the contributions of stomatal, mesophyll, and biochemical limitations. *Journal of Experimental Botany* 67, 341–352.

De Lorenzo G, Ferrari S, Giovannoni M, Mattei B, Cervone F. (2019). Cell wall traits that influence plant development, immunity, and bioconversion. *The Plant Journal* 97, 134–147.

de Souza AJ, Hull PA, Gille S, Pauly M. (2014). Identification and functional characterization of the distinct plant pectin esterases PAE8 and PAE9 and their deletion mutants. *Planta* 240, 1123–1138.

de Souza AJ, Pauly M. (2015). Comparative genomics of pectinacetylesterases: insight on function and biology. *Plant Signaling & Behavior* 10:e1055434.

Derbyshire P, McCann MC, Roberts K. (2007). Restricted cell elongation in *Arabidopsis* hypocotyls is associated with a reduced average pectin esterification level. *BMC Plant Biology* 7, 31.

Di Marco G, Manes F, Tricoli D, Vitale E. (1990). Fluorescence parameters measured concurrently with net photosynthesis to investigate chloroplastic CO_2 concentration in leaves of *Quercus ilex* L. *Journal of Plant Physiology* 136, 538–543.

Dick-Pérez M, Zhang Y, Hayes J, Salazar A, Zabotina OA, Hong M. (2011). Structure and interactions of plant cell-wall polysaccharides by two- and three- dimensional magic-angle-spinning solid-state NMR. *Biochemistry* 50, 989–1000.

Díaz-Espejo A, Nicolás E, Fernández JE. (2007). Seasonal evolution of diffusional limitations and photosynthetic capacity in olive under drought. *Plant, Cell & Environment* 30, 922–933.

Domon JM, Baldwin L, Acket S, Caudeville E, Arnoult S, Zub H, Gillet F, Lejeune-Hénaut I, Brancourt-Hulmel M, Pelloux J, Rayon C. (2013). Cell wall compositional modifications of *Miscanthus* ecotypes in response to cold acclimation. *Phytochemistry* 85, 51–61.

Douthe C, Dreyer E, Epron D, Warren CR. (2011). Mesophyll conductance to CO_2, assessed from online TDLAS records of $^{13}CO_2$ discrimination, displays small but significant short-term responses to CO_2 and irradiance in *Eucalyptus* seedlings. *Journal of Experimental Botany* 62, 5335–5346.

Douthe C, Dreyer E, Brendel O, Warren CR. (2012). Is mesophyll conductance to CO_2 in leaves of three *Eucalyptus* species sensitive to short-term changes of irradiance under ambient as well as low O_2? *Functional Plant Biology* 39, 435–448.

Duckett JG, Pressel S. (2018). The evolution of the stomatal apparatus: intercellular spaces and sporophyte water relations in bryophytes – two ignored dimensions. *Philosophical Transactions of the Royal Society of London Series B: Biological Sciences* 373, 20160498.

Dumont M, Lehner A, Vauzeilles B, Malassis J, Marchant A, Smyth K, Linclau B, Baron A, Mas-Pons J, Anderson CT, Schapman D, Galas L, Mollet JC, Lerouge P. (2016). Plant cell wall imaging by metabolic click-mediated labelling of rhamnogalacturonan II using azido 3-deoxy-D-manno-oct-2-ulosonic acid. *The Plant Journal* 85, 437–447.

Earles JM, Théroux-Rancourt G, Roddy AB, Gilbert ME, McElrone AJ, Brodersen CR. (2018). Beyond porosity: 3D leaf intercellular airspace traits that impact mesophyll conductance. *Plant Physiology* 178, 148–162.

Earles JM, Buckley TN, Brodersen CR, Busch FA, Cano FJ, Choat B, Evans JR, Farquhar GD, Harwood R, Huynh M, John GP, Miller ML, Rockwell FE, Sack L, Scoffoni C, Struik PC, Wu A, Yin X, Barbour MM. (2019). Embracing 3D complexity in leaf carbon-water exchange. *Trends in Plant Science* 24, 15–24.

Ellsworth D, Reich P. (1993). Canopy structure and vertical patterns of photosynthesis and related leaf traits in a deciduous forest. *Oecologia* 96, 169–178.

Ellsworth PV, Ellsworth PZ, Koteyeva NK, Cousins AB. (2018). Cell wall properties in *Oryza sativa* influence mesophyll CO_2 conductance. *New Phytologist* 219, 66–76.

Epron D, Godard D, Cornic G, Genty B. (1995). Limitation of net CO_2 assimilation rate by internal resistances to CO_2 transfer in the leaves of two tree species (*Fagus sylvatica* L. and *Castanea sativa* Mill.). *Plant, Cell & Environment* 18, 43–51.

Ethier GJ, Livingston NJ. (2004). On the need to incorporate sensitivity to CO_2 transfer conductance into the Farquhar-von Caemmerer-Berry leaf photosynthesis model. *Plant, Cell & Environment* 27, 137–153.

Evans JR, Sharkey TD, Berry JA, Farquhar GD. (1986). Carbon isotope discrimination measured concurrently with gas exchange to investigate CO_2 diffusion in leaves of higher plants. *Australian Journal of Plant Physiology* 13, 281–292.

Evans JR. (1989). Photosynthesis and nitrogen relationships in leaves of C_3 plants. *Oecologia* 78, 9–19.

Evans JR, von Caemmerer S, Setchell BA, Hudson GS. (1994). The relationship between CO_2 transfer conductance and leaf anatomy in transgenic tobacco with a reduced content of Rubisco. *Australian Journal of Plant Physiology* 21, 475–495.

Evans JR, Kaldenhoff R, Genty B, Terashima I. (2009). Resistances along the CO_2 diffusion pathway inside leaves. *Journal of Experimental Botany* 60, 2235–2248.

Evans JR, Von Caemmerer S. (2013). Temperature response of carbon isotope discrimination and mesophyll conductance in tobacco. *Plant, Cell & Environment* 36, 745–756.

Fabre N, Reiter IM, Becuwe-Linka N, Genty B, Rumeau D. (2007). Characterization and expression analysis of genes encoding alpha and beta carbonic anhydrases in *Arabidopsis*. *Plant, Cell & Environment* 30, 617–629.

Fan L, Linker R, Gepstein S, Tanimoto E, Yamamoto R, Neumann PM. (2006). Progressive inhibition by water deficit of cell wall extensibility and growth along the elongation zone of maize roots is related to increased lignin metabolism and progressive stelar accumulation of wall phenolics. *Plant Physiology* 140, 603–612.

Farquhar GD, Caemmerer SV, Berry JA. (1980). A biochemical model of photosynthetic CO_2 assimilation in leaves of C_3 species. *Planta* 149, 78–90.

Farquhar GD, Sharkey TD. (1982). Stomatal conductance and photosynthesis. *Annual Review of Plant Physiology* 33, 317–345.

Flexas J, Bota J, Escalona JM, Sampol B, Medrano H. (2002). Effects of drought on photosynthesis in grapevines under field conditions: an evaluation of stomatal and mesophyll limitations. *Functional Plant Biology* 29, 461–471.

Flexas J, Bota J, Loreto F, Cornic G, Sharkey TD. (2004). Diffusive and metabolic limitations to photosynthesis under drought and salinity in C_3 plants. *Plant Biology* 6, 269–279.

Flexas J, Ribas-Carbó M, Hanson DT, Bota J, Otto B, Cifre J, McDowell N, Medrano H, Kaldenhoff R. (2006*a*). Tobacco aquaporin *NtAQP1* is involved in mesophyll conductance to CO_2 *in vivo*. *The Plant Journal* 48, 427–439.

Flexas J, Ribas-Carbó M, Bota J, Galmés J, Henkle M, Martínez-Cañellas S, Medrano H. (2006*b*). Decreased Rubisco activity during water stress is not induced by decreased relative water content but related to conditions of low stomatal conductance and chloroplast CO_2 concentration. *New Phytologist* 172, 73–82.

Flexas J, Díaz-Espejo A, Galmés J, Kaldenhoff R, Medrano H, Ribas-Carbó M. (2007). Rapid variations of mesophyll conductance in response to changes in CO_2 concentration around leaves. *Plant, Cell & Environment* 30, 1284–1298.

Flexas J, Ribas-Carbó M, Díaz-Espejo A, Galmés J, Medrano H. (2008). Mesophyll conductance to CO_2: current knowledge and future prospects. *Plant, Cell & Environment* 31, 602–621.

Flexas J, Barón M, Bota J, Ducruet JM, Gallé A, Galmés J, Jiménez M, Pou A, Ribas-Carbó M, Sajnani C, Tomás M, Medrano H. (2009). Photosynthesis limitations during water stress acclimation and recovery in the drought-adapted *Vitis* hybrid *Richter*-110 (*V. berlandieri* x *V. rupestris*). *Journal of Experimental Botany* 60, 2361–2377.

Flexas J, Barbour MM, Brendel O, Cabrera HM, Carriquí M, Díaz-Espejo A, Douthe C, Dreyer E, Ferrio JP, Gago J, Gallé A, Galmés J, Kodama N, Medrano H, Niinemets Ü, Peguero-Pina JJ, Pou A, Ribas-Carbó M, Tomás M, Tosens T, Warren CR. (2012). Mesophyll diffusion conductance to CO_2: an unappreciated central player in photosynthesis. *Plant Science* 193, 70–84.

Flexas J, Niinemets Ü, Gallé A, Barbour MM, Centritto M, Díaz-Espejo A, Douthe C, Galmés J, Ribas-Carbó M, Rodríguez PL, Rosselló F, Soolanayakanahally R, Tomás M, Wright IJ, Farquhar GD, Medrano H. (2013*a*). Diffusional conductances to CO_2 as a target for increasing photosynthesis and photosynthetic water-use efficiency. *Photosynthesis Research* 117, 45–59.

Flexas J, Scoffoni C, Gago J, Sack L. (2013*b*). Leaf mesophyll conductance and leaf hydraulic conductance: an introduction to their measurement and coordination. *Journal of Experimental Botany* 64, 3965–3981.

Flexas J, Díaz-Espejo A, Conesa MÀ, Coopman RE, Douthe C, Gago J, Gallé A, Galmés J, Medrano H, Ribas-Carbó M, Tomás M, Niinemets Ü. (2015). Mesophyll conductance to CO_2 and Rubisco as targets for improving intrinsic water use efficiency in C_3 plants. *Plant, Cell & Environment* 39, 965–982.

Flexas J, Cano FJ, Carriquí M, Coopman RE, Mizokami Y, Tholen D, Xiong D. (2018). CO_2 diffusion inside photosynthetic organs. In: Adams III W, Terashima I (eds.). *The leaf: a platform for performing photosynthesis. Advances in Photosynthesis and Respiration (Including bioenergy and related processes).* Springer, Cham, vol. 44, 163–208.

Flexas J, Carriquí M. (2020). Photosynthesis and photosynthetic efficiencies along the terrestrial plant's phylogeny: lessons for improving crop photosynthesis. *The Plant Journal* 101, 964–978.

Flexas J, Clemente-Moreno MJ, Bota J, Brodribb TJ, Gago J, Mizokami Y, Nadal M, Perera-Castro AV, Roig-Oliver M, Sugiura D, Xiong D, Carriquí, M. (2021). Cell wall

thickness and composition are involved in photosynthetic limitation. *Journal of Experimental Botany* 72, 3971–3986.

Franková L, Fry SC. (2013). Biochemistry and physiological roles of enzymes that 'cut and paste' plant cell-wall polysaccharides. *Journal of Experimental Botany* 64, 3519–3550.

Franks PJ, Farquhar GD. (2007). The mechanical diversity of stomata and its significance in gas exchange control. *Plant Physiology* 143, 78–87.

Fry SC. (1979). Phenolic components of the primary cell wall and their possible role in the hormonal regulation of growth. *Planta* 146, 343–351.

Fry SC. (2004). Primary cell wall metabolism: tracking the careers of wall polymers in living plant cells. *New Phytologist* 161, 641–675.

Gaastra P. (1959). Photosynthesis of crop plants as influenced by light, carbon dioxide, temperature, and stomatal diffusion resistance. *Mededelingen van de Landbouwhogeschool te Wageningen* 59, 1–69.

Gago J, Coopman RE, Cabrera HM, Hermida C, Molins A, Conesa MÀ, Galmés J, Ribas-Carbó M, Flexas J. (2013). Photosynthesis limitations in three fern species. *Physiologia Plantarum* 149, 599–611.

Gago J, Carriquí M, Nadal M, Clemente-Moreno MJ, Coopman, RE, Fernie AR, Flexas J. (2019). Photosynthesis optimized across land plant phylogeny. *Trends in Plant Science* 24, 947– 958.

Gago J, Daloso DM, Carriquí M, Nadal M, Morales M, Araújo WL, Nunes-Nesi A, Flexas J. (2020). Mesophyll conductance: the leaf corridors for photosynthesis. *Biochemical Society Transactions* 48, 429–439.

Gallé A, Florez-Sarasa I, Tomás M, Pou A, Medrano H, Ribas-Carbó M, Flexas J. (2009). The role of mesophyll conductance during water stress and recovery in tobacco

(*Nicotiana sylvestris*): acclimation or limitation? *Journal of Experimental Botany* 60, 2379–2390.

Gallé A, Florez-Sarasa I, El Aououad H, Flexas J. (2011). The Mediterranean evergreen *Quercus ilex* and the semi-deciduous *Cistus albidus* differ in their lead gas exchange regulation and acclimation to repeated drought and re-watering cycles. *Journal of Experimental Botany* 62, 5207–5216.

Galmés J, Medrano H, Flexas J. (2007). Photosynthetic limitations in response to water stress and recovery in Mediterranean plants with different growth forms. *New Phytologist* 175, 81–93.

Galmés J, Conesa MÀ, Ochogavía JM, Perdomo JA, Francis DM, Ribas-Carbó M, Savé R, Flexas J, Medrano H, Cifre J. (2011). Physiological and morphological adaptations in relation to water use efficiency in Mediterranean accessions of *Solanum lycopersicum*. *Plant, Cell & Environment* 34, 245–260.

Galmés J, Ochogavía JM, Gago J, Roldán EJ, Cifre J, Conesa MÀ. (2013). Leaf responses to drought stress in Mediterranean accessions of *Solanum lycopersicum*: anatomical adaptations in relation to gas exchange parameters. *Plant, Cell & Environment* 36, 920–935.

Gardiner W. (1900). The genesis and development of the cell wall and connecting threads in the plant cell. Preliminary communication. *Proceedings of the Royal Society of London* 66, 186–188.

Gillon JS, Yakir D. (2000). Internal conductance to CO_2 diffusion and $C^{18}OO$ discrimination in C_3 leaves. *Plant Physiology* 123, 201–213.

Gou JY, Park S, Yu XH, Miller LM, Liu CJ. (2008). Compositional characterization and imaging of “wall-bound” acylesters of *Populus trichocarpa* reveal differential accumulation of acyl molecules in normal and reactive woods. *Planta* 229, 15–24.

Gou JY, Miller LM, Hou G, Yu XH, Chen XY, Liu CJ. (2012). Acetylesterase-mediated deacetylation of pectin impairs cell elongation, pollen germination, and plant reproduction. *Plant Cell* 24, 50–65.

Grassi G, Magnani F. (2005). Stomatal, mesophyll conductance and biochemical limitations to photosynthesis as affected by drought and leaf ontogeny in ash and oak trees. *Plant, Cell & Environment* 28, 834–849.

Groszmann M, Osborn HL, Evans JR. (2017). Carbon dioxide and water transport through plant aquaporins. *Plant, Cell & Environment* 40, 938–961.

Guénin S, Hardouin J, Paynel F, Müller K, Mongelard G, Driouich A, Lerouge P, Kermode AR, Lehner A, Mollet JC, Pelloux J, Gutiérrez L, Mareck A. (2017). AtPME3, a ubiquitous cell wall pectin methylesterase of *Arabidopsis thaliana*, alters the metabolism of cruciferin seed storage proteins during post-germinative growth of seedlings. *Journal of Experimental Botany* 68, 1083–1095.

Haas KT, Wightman R, Meyerowitz EM, Peaucelle A. (2020). Pectin homogalacturonan nanofilament expansion drives morphogenesis in plant epidermal cells. *Plant Science* 367, 1003–1007.

Hanba Y, Kogami H, Terashima I. (2002). The effect of growth irradiance on leaf anatomy and photosynthesis in *Acer* species differing in light demand. *Plant, Cell & Environment* 25, 1021–1030.

Hanba YT, Shibasaka M, Hayashi Y, Hayakawa T, Kasamo K, Terashima I, Katsuhara M. (2004). Overexpression of the barley aquaporin *HvPIP2;1* increases internal CO_2 conductance and CO_2 assimilation in the leaves of transgenic rice plants. *Plant and Cell Physiology* 45, 521–529.

Hanson DT, Renzaglia K, Villarreal JC. (2014). Diffusional limitations to CO_2 concentrating mechanisms in bryophytes. *In: Hanson DT, Rice SK (eds.). Photosynthesis in Bryophytes and Early Land Plants*. Berlin, *Heidelberg: Springer, Berlin Heidelberd*, 95–111.

Harley PC, Loreto F, Di Marco G, Sharkey TD. (1992). Theoretical considerations when estimating the mesophyll conductance to CO_2 flux by the analysis of the response of photosynthesis to CO_2. *Plant Physiology* 98, 1429–1436.

Harris PJ, Hartley RD. (1976). Detection of bound ferulic acid in cell walls of the Gramineae by ultraviolet fluorescence microscopy. *Nature* 259, 508–510.

Hartley RD. (1973). Carbohydrate esters of ferulic acid as components of cell-walls of *Lolium multiflorum*. *Phytochemistry* 12, 661–665.

Hartley RD, Jones EC. (1977). Phenolic components and degradability of cell walls of grass and legume species. *Phytochemistry* 16, 1531–1534.

Haworth WN, Hirst EL, Oliver E. (1934). Polysaccharides. Part XVIII. The constitution of xylan. *Journal of the Chemical Society*, 1917–1923.

Haworth WN. (1946). Bakerian lecture – The structure, function and synthesis of polysaccharides. *Proceedings of the Royal Society of London* 186, 1–19.

Heckwolf M, Pater D, Hanson DT, Kaldenhoff R. (2011). The *Arabidopsis thaliana* aquaporin *AtPIP1;2* is a physiologically relevant CO_2 transport facilitator. *The Plant Journal* 67, 795–804.

Hirst EL, Jones JKN. (1938). Pectic substances. Part I. The araban and pectic acid of the peanut. *Journal of the Chemical Society*, 496–505.

Hirst EL, Jones JKN. (1939). Pectic substances. Part II. Isolation of an araban from the carbohydrate constituents of the peanut. *Journal of the Chemical Society*, 452–453.

Ho QT, Berghuijs HN, Watté R, Verboven P, Herremans E, Yin X, Helfen L. (2016). Three-dimensional microscale modelling of CO_2 transport and light propagation in tomato leaves enlightens photosynthesis. *Plant, Cell & Environment* 39, 50–61.

Hocq L, Sénéchal F, Lefebvre V, Lehner A, Domon JM, Mollet JC, Dehors J, Pageau K, Marcelo P, Guérineau F, Kolšek K, Mercadante D, Pelloux J. (2017). Combined experimental and computational approaches reveal distinct pH dependence of pectin methylesterase inhibitors. *Plant Physiology* 173, 1075–1093.

Houston K, Tucker MR, Chowdhury J, Shirley N, Little A. (2016). The plant cell wall: a complex and dynamic structure as revealed by the responses of genes under stress conditions. *Frontiers in Plant Science* 7:984.

Hura T, Hura K, Grzesiak S. (2009). Possible contribution of cell-wall bound ferulic acid in drought resistance and recovery in triticale seedlings. *Journal of Plant Physiology* 166, 1720–1733.

Hura T, Hura K, Dziurka K, Ostrowska A, Bączek-Kwinta R, Grzesiak M. (2012). An increase in the content of cell wall-bound phenolics correlates with the productivity of triticale under soil drought. *Journal of Plant Physiology* 169, 1728–1736.

Huttunen S, Bell N, Hedenäs L. (2018). The evolutionary diversity of mosses – taxonomic heterogeneity and its ecological drivers. *Critical Reviews in Plant Sciences* 37, 128–174.

Iiyama K, Lam T, Stone BA. (1994). Covalent cross-links in the cell wall. *Plant Physiology* 104, 315–320.

Jones DIH. (1970). Cell-wall constituents of some grass species and varieties. *Science of Food and Agriculture* 21, 559–562.

Keegstra K, Talmadge KW, Bauer WD, Albersheim P. (1973). The structure of plant cell walls. III. A model of the walls of suspension-cultured sycamore cells based on the interconnections of the macromolecular components. *Plant Physiology* 51, 188–197.

Keegstra K. (2010). Plant cell walls. *Future Perspective in Plant Biology* 154, 483–486.

Kong G, Wan L, Deng YZ, Yang W, Li W, Jiang L, Situ J, Xi P, Li M, Jiang Z. (2019). Pectin acetylesterase PAE5 is associated with the virulence of plant pathogenic oomycete *Peronophythora litchii*. *Physiological and Molecular Plant Pathology* 106, 16–22.

Kubacka-Zębalska M, Kacperska A. (1999). Low temperature-induced modifications of cell wall content and polysaccharide composition in leaves of winter oilseed rape (*Brassica napus* L. var. *oleifera* L.). *Plant Science* 148, 59–67.

Le Gall H, Philippe F, Domon JM, Gillet F, Pelloux J, Rayon C. (2015). Cell wall metabolism in response to abiotic stress. *Plants* 4, 112–166.

Leroux C, Bouton S, Kiefer-Meyer MC, Fabrice TN, Mareck A, Guénin S, Fournet F, Ringli C, Pelloux J, Drioich A, Lerouge P, Lehner MJC. (2015). Pectin methylesterase48 is involved in *Arabidopsis* pollen grain germination. *Plant Physiology* 167, 367–380.

Leucci MR, Lenucci MS, Piro G, Dalessandro G. (2008). Water stress and cell wall polysaccharides in the apical root zone of wheat cultivars varying in drought tolerance. *Journal of Plant Physiology* 165, 1168–1180.

Levesque-Tremblay G, Pelloux J, Braybrook SA, Müller K. (2015). Tuning of pectin methylesterification: consequences for cell wall biomechanics and development. *Planta* 242, 791–811.

Li G, Santoni V, Maurel C. (2014). Plant aquaporins: roles in plant physiology. *Biochimica et Biophysica Acta* 1840, 1574–1582.

Ligrone R, Carafa A, Duckett JG, Renzaglia KS, Ruel K. (2008). Immunocytochemical detection of lignin-related epitopes in cell walls in bryophytes and the charalean alga *Nitella*. *Plant Systematics and Evolution* 270, 257–272.

Lima RB, dos Santos TB, Vieira LGE, de Lourdes L, Ferrarese M, Ferrarese-Filho O, Donatti L, Boeger MRT, de Oliveira Petkowicz CL. (2013). Heat stress causes alterations in the cell-wall polymers and anatomy of coffee leaves (*Coffea arabica* L.). *Carbohydrate Polymers* 93, 135–143.

Lipiec J, Doussan C, Nosalewicz A, Kondracka K. (2013). Effect of drought and heat stresses on plant growth and yield: a review. *Integrated Agrophysics* 27, 463–477.

Lo Gullo MA, Salleo S. (1988). Different strategies of drought resistance in three Mediterranean sclerophyllous trees growing in the same environmental conditions. *New Phytologist* 108, 267–276.

Loreto F, Harley PC, Di Marco G, Sharkey TD. (1992). Estimation of mesophyll conductance to CO_2 flux by 3 different methods. *Plant Physiology* 98, 1437–1443.

Lundgren MR, Fleming AJ. (2020). Cellular perspectives for improving mesophyll conductance. *The Plant Journal* 101, 845–847.

Matsunaga T, Ishii T, Matsumoto S, Higuchi M, Darvill A, Albersheim P, O'Neill MA. (2004). Occurrence of the primary cell wall polysaccharide rhamnogalacturonan II in pteridophytes, lycophytes, and bryophytes. Implications for the evolution of vascular plants. *Plant Physiology* 134, 339–351.

McCann MC, Roberts K. (1992). Architecture of the primary cell wall. In: Lloyd CW (ed.). *The Cytoskeletal Basis of Plant Growth and Form*. London: Academic, 109–129.

Meyer M, Seibt U, Griffiths H. (2008). To concentrate or ventilate? Carbon acquisition, isotope discrimination and physiological ecology of early land plant life. *Philosophical Transactions of the Royal Society B* 363, 2767–2778.

Milla R, Osborne CR, Turcotte MM, Violle C. (2015). Plant domestication through an ecological lens. *Trends in Ecology & Evolution* 30, 463–469.

Miranda-Apodaca J, Pérez-López U, Lacuesta M, Mena-Petite A, Muñoz-Rueda A. (2018). The interaction between drought and elevated CO_2 in water relations in two grassland species is species-specific. *Journal of Plant Physiology* 220, 193–202.

Momayyezi M, Guy RD. (2017). Substantial role for carbonic anhydrase in latitudinal variation in mesophyll conductance of *Populus trichocarpa* Torr. & Gray. *Plant, Cell & Environment* 40, 138–149.

Moore JP, Nguema-Ona E, Chevalier L, Lindsey GG, Brandt WF, Lerouge P, Farrant JM, Driouich A. (2006). Response of the leaf cell wall to desiccation in the resurrection plant *Myrothamnus flabellifolius*. *Plant Physiology* 141, 651–662.

Moore JP, Farrant JM, Driouich A. (2008). A role for pectin-associated arabinans in maintaining the flexibility of the plant cell wall during water deficit stress. *Plant Signaling & Behavior* 3, 102–104.

Moore JP, Nguema-Ona EE, Vicré-Gibouin M, Sørensen I, Willats WGT, Driouich A, Farrant JM. (2013). Arabinose-rich polymers as an evolutionary strategy to plasticize resurrection plant cell walls against desiccation. *Planta* 237, 739–754.

Müller K, Levesque-Tremblay G, Bartels S, Weitbrecht K, Wormit A, Usadel B, Haughn G, Kermode AR. (2013). Demethylesterification of cell wall pectins in *Arabidopsis* plays a role in seed germination. *Plant Physiology* 161, 305–316.

Nadal M, Flexas J, Gulías J. (2018). Possible link between photosynthesis and leaf modulus of elasticity among vascular plants: a new player in leaf traits relationships? *Ecology Letters* 21, 1372–1379.

Nadal M, Flexas J. (2019). Variation in photosynthetic characteristics with growth form in a water-limited scenario: implications for assimilation rated and water use efficiency in crops. *Agricultural Water Management* 216, 457–472.

Nadal M, Roig-Oliver M, Bota J, Flexas J. (2020). Leaf age-dependent elastic adjustment and photosynthetic performance under drought stress in *Arbutus unedo* seedlings. *Flora* 271, 151662.

Nevins DJ, English PD, Albersheim P. (1967). The specific nature of plant cell wall polysaccharides. *Plant Physiology* 42, 900–906.

Nickle TC, Meinke DW. (1998). A cytokinesis-defective mutant of *Arabidopsis* (*cyt1)* characterized by embryonic lethality, incomplete cell walls, and excessive callose accumulation. *The Plant Journal* 15, 321–332.

Nicol F, His I, Jauneau A, Vernhettes S, Canut H, Höfte H. (1998). A plasma membrane-bound putative endo-1,4-β-D-glucanase is required for normal wall assembly and cell elongation in *Arabidopsis*. *The EMBO Journal* 17, 5563–5576.

Niinemets Ü. (1999). Components of leaf dry mass per area - thickness and density - alter leaf photosynthetic capacity in reverse directions in woody plants. *New Phytologist* 144, 35–47.

Niinemets Ü. (2001). Global-scale climatic controls of leaf dry mass per area, density, and thickness in trees and shrubs. *Ecology* 82, 453–469.

Niinemets Ü, Reichstein M. (2003). Controls on the emission of plant volatiles through stomata: a sensitivity analysis. *Journal of Geophysical Research-Atmospheres* 108, 4211.

Niinemets Ü, Díaz-Espejo A, Flexas J, Galmés J, Warren CR. (2009). Role of mesophyll diffusion conductance in constraining potential photosynthetic productivity in the field. *Journal of Experimental Botany* 60, 2249–2270.

Niinemets Ü. (2016). Does the touch of cold make evergreen leaves tougher? *Tree Physiology* 36, 267–272.

Niklas KJ. (2004). The cell walls that bind the tree of life. *BioScience* 54, 831–841.

Novaković L, Guo T, Bacic A, Sampathkumar A, Johnson K. (2018). Hitting the wall – Sensing and signaling pathways involved in plant cell wall remodeling in response to abiotic stress. *Plants* 7:89.

Ochoa-Villarreal M, Aispuro-Hernández E, Vargas-Arispuro I, Martínez-Téllez MA. (2012). In: De Souza Gomes A (ed.). *Plant cell wall polymers: function, structure and biological activity of their derivatives*. Polymerization. InTechOpen. doi: 10.5772/2750.

Paës G, Habrant A, Terryn C. (2018). Fluorescent nano-probes to image plant cell walls by super-resolution STED microscopy. *Plants (Basel)* 7:11, doi: 10.3390/plants7010011.

Palacio-López K, Sun L, Reed R, Kang E, Sørensen I, Rose JKC, Domozych DS. (2020). Experimental manipulation of pectin architecture in the cell wall of the unicellular charophyte, *Penium margaritaceum*. *Frontiers in Plant Science* 11:1032.

Park YB, Cosgrove DJ. (2012). Changes in cell wall biomechanical properties in the xyloglucan-deficient *xxt1*/*xxt2* mutant of *Arabidopsis*. *Plant Physiology* 158, 465–475.

Parra R, Paredes MA, Labrador J, Nunes C, Coimbra MA, Fernández-García N, Olmos E, Gallardo M, Gómez-Jiménez MC. (2020). Cell wall composition and ultrastructural immunolocalization of pectin and arabinogalactan protein during *Olea europaea* L. fruit abscission. *Plant and Cell Physiology* 61, 814–825.

Parre E, Geitmann A. (2005). Pectin and the role of the physical properties of the cell wall in pollen tube growth of *Solanum chacoense*. *Planta* 220, 582–592.

Peaucelle A, Louvet R, Johansen JN, Höfte H, Laufs P, Pelloux J, Mouille G. (2008). *Arabidopsis* phyllotaxis is controlled by the methylesterification status of cell-wall pectins. *Current Biology* 18, 1943–1948.

Peaucelle A, Braybrook SA, Le Guillou L, Bron E, Kuhlemeier C, Höfte H. (2011). Pectin-induced changes in cell wall mechanics underlie organ initiation in *Arabidopsis*. *Current Biology* 21, 1720–1726.

Peguero-Pina JJ, Sisó S, Flexas J, Galmés J, García-Nogales A, Niinemets Ü, Sancho-Knapik D, Saz MÁ, Gil-Pelegrín E. (2017). Cell-level anatomical characteristics explain high mesophyll conductance and photosynthetic capacity in sclerophyllous Mediterranean oaks. *New Phytologist* 214, 585–596.

Pelletier S, Van Orden J, Wolf S, Vissenberg K, Delacourt J, Ndong YA, Pelloux J, Bischoff V, Urbain A, Mouille G, Lemonnier G, Renou JP, Höfte H. (2010). A role for

pectin de-methylesterification in a developmentally regulated growth acceleration in dark-grown *Arabidopsis* hypocotyls. *New Phytologist* 188, 726–739.

Pelloux J, Rustérucci C, Mellerowicz EJ. (2007). New insights into pectin methylesterase structure and function. *Trends in Plant Science* 12, 267–277.

Peña MJ, Darvill AG, Eberhard S, York WS, O'Neill MA. (2008). Moss and liverwort xyloglucans contain galacturonic acid and are structurally distinct from the xyloglucans synthesized by hornworts and vascular plants. *Glycobiology* 18, 891–904.

Perera-Castro AV, Nadal M, Flexas J. (2020*a*). What drives photosynthesis during desiccation? Mosses and other outliers from the photosynthesis-elasticity trade-off. *Journal of Experimental Botany* 71, 6460–6470.

Perera-Castro AV, Waterman MJ, Turnbull JD, Aschcroft MB, McKinley E, Watling JR, Bramley-Alves J, Casanova-Katny A, Zuniga G, Flexas J, Robinson SA. (2020*b*). It is hot in the sun: Antarctic mosses have high temperature optima for photosynthesis despite cold climate. *Frontiers in Plant Science* 11:1178.

Persson S, Caffall KH, Freshour G, Hilley MT, Bauer S, Pondexter P, Hahn MG, Mohnen D, Somerville C. (2007). The *Arabidopsis irregular xylem8* mutant is deficient in glucuronoxylan and homogalacturonan, which are essential for secondary cell wall integrity. *The Plant Cell* 19, 237–255.

Pérez-Martín A, Michelazzo C, Torres-Ruiz JM, Flexas J, Fernández JE, Sebastiani L, Díaz-Espejo A. (2014). Regulation of photosynthesis and stomatal and mesophyll conductance under water stress and recovery in olive trees: correlation with gene expression of carbonic anhydrase and aquaporins. *Journal of Experimental Botany* 65, 3143–3156.

Phyo P, Wang T, Xiao C, Anderson CT, Hong M. (2017). Effects of pectin molecular weight changes on the structure, dynamics, and polysaccharide interactions of primary cell walls of *Arabidopsis thaliana*: insights from solid-state NMR. *Biomacromolecules* 18, 2937–2950.

Phytozome. The Plant Genomics Resource. (2021). Available at: https://phytozome-next.jgi.doe.gov/. Accessed on 9th March 2021.

Pons TL, Welschen RAM. (2003). Midday depression of net photosynthesis in the tropical rainforest tree *Eperua grandiflora*: contributions of stomatal and internal conductances, respiration and Rubisco functioning. *Tree Physiology* 23, 937–947.

Pons TL, Flexas J, von Caemmerer S, Evans JR, Genty B, Ribas-Carbó M, Brugnoli E. (2009). Estimating mesophyll conductance to CO_2: methodology, potential errors, and recommendations. *Journal of Experimental Botany* 60, 2217–2234.

Poorter H, Niinemets Ü, Poorter L, Wright IJ, Villar R. (2009). Causes and consequences of variation in leaf mass per area (LMA): a meta-analysis. *New Phytologist* 182, 565–588.

Popper ZA, Fry SC. (2003). Primary cell wall composition of Bryophytes and Charophytes. *Annals of Botany* 91, 1–12.

Popper ZA, Fry SC. (2004). Primary cell wall composition of pteridophytes and spermatophytes. *New Phytologist* 164, 165–174.

Popper ZA. (2006). The cell walls of Pteridophytes and other green plants – A review. *Fern Gazette* 17, 247–257.

Popper ZA. (2008). Evolution and diversity of green plant cell walls. *Current Opinion in Plant Biology* 11, 286–292.

Popper ZA, Tuohy MG. (2010). Beyond the green: understanding the evolutionary puzzle of plant and algal cell walls. *Plant Physiology* 153, 373–383.

Popper ZA, Michel G, Hervé C, Domozych DS, Willats WGT, Tuohy MG, Kloareg B, Stengel DB. (2011). Evolution and diversity of plant cell walls: from algae to flowering plants. *Annual Review of Plant Biology* 62, 567–590.

Price GD, von Caemmerer S, Evans JR, Yu JW, Lloyd J, Oja V, Kell P, Harrison K, Gallagher A, Badger MR. (1994). Specific reduction of chloroplast carbonic-anhydrase activity by antisense RNA in transgenic tobacco plants has a minor effect on photosynthetic CO_2 assimilation. *Planta* 193, 331–340.

Reiter WD, Chapple CCS, Somerville CR. (1993). Altered growth and cell walls in a fucose-deficient mutant of *Arabidopsis*. *Science* 261, 1032–1035.

Reiter WD, Chapple CCS, Somerville CR. (1997). Mutants of *Arabidopsis thaliana* with altered cell wall polysaccharide composition. *The Plant Journal* 12, 335–345.

Ren T, Weraduwage SM, Sharkey TD. (2019). Prospects for enhancing leaf photosynthetic capacity by manipulating mesophyll cell morphology. *Journal of Experimental Botany* 70, 1153–1165.

Rhee S Y, Osborne E, Poindexter PD, Somerville CR. (2003). Microspore separation in the quartet 3 mutants of *Arabidopsis* is impaired by a defect in a developmentally regulated polygalacturonase required for pollen mother cell wall degradation. *Plant Physiology* 133, 1170–1180.

Rho H, Yu DJ, Kim SJ, Lee HJ. (2012). Limitation factors for photosynthesis in '*Bluecrop*' highbush blueberry (*Vaccinium corymbosum*) leaves in response to moderate water stress. *Journal of Plant Biology* 55, 450–457.

Roberts AW, Roberts EM, Haigler CH. (2012). Moss cell walls: structure and biosynthesis. *Frontiers in Plant Science* 3:166.

Rui Y, Dinneny JR. (2019). A wall with integrity: surveillance and maintenance of the plant cell wall under stress. *New Phytologist* 225, 1428–1439.

Ruiz-Vera UM, De Souza AP, Long SP, Ort DR. (2017). The role of sink strength and nitrogen availability in the down-regulation of photosynthetic capacity in field-grown *Nicotiana tabacum* L. at elevated CO_2 concentration. *Frontiers in Plant Science* 8, 998.

Sade N, Shatil-Cohen A, Attia Z, Maurel C, Boursiac Y, Kelly G, Granot D, Yaaran A, Lerner S, Moshelion M. (2014). The role of plasma membrane aquaporins in regulating the bundle sheath-mesophyll continuum and leaf hydraulics. *Plant Physiology* 166, 1609–1620.

Sage RF, Kubien DS. (2007). The temperature response of C_3 and C_4 photosynthesis. *Plant, Cell & Environment* 30, 1086–1106.

Sarkar P, Bosneaga E, Auer M. (2009). Plant cell walls throughout evolution: towards a molecular understanding of their design principles. *Journal of Experimental Botany* 60, 3615–3635.

Scafaro AP, von Caemmerer S, Evans JR, Atwell BJ. (2011). Temperature response of mesophyll conductance in cultivated and wild *Oryza* species with contrasting mesophyll cell wall thickness. *Plant, Cell & Environment* 34, 1999–2008.

Scheler C, Weitbrecht K, Pearce SP, Hampstead A, Büttner-Mainik A, Lee KJD, Voegele A, Oracz K, Dekkers BJW, Wang X, Wood ATA, Bentsink L, King JR, Knox JP, Holdsworth MJ, Müller K, Leubner-Metzger G. (2015). Promotion of testa rupture during garden cress germination involves seed compartment-specific expression and activity of pectin methylesterases. *Plant Physiology* 167, 200–215.

Schiraldi A, Fessas D, Signorelli M. (2012). Water activity in biological systems—a review. *Polish Journal of Food and Nutrition Sciences* 62, 5–13.

Scholz FG, Bucci SJ, Arias N, Meinzer FC, Goldstein G. (2012). Osmotic and elastic adjustments in cold desert shrubs differing in rooting depth: coping with drought and subzero temperatures. *Oecologia* 170, 885–897.

Sestak Z, Catsky J, Jarvis PG. (1971). Plant photosynthetic production. Manual of methods. *The Quarterly Review of Biology* 47, 235.

Sénéchal F, Graff L, Surcouf O, Marcelo P, Rayon C, Bouton S, MAreck A, Mouille G, Stintzi A, Höfte H, Lerouge P, Schaller A, Pelloux J. (2014). *Arabidopsis* PECTIN

METHYLESTERASE17 is co-expressed with and processed by SBT3.5, a subtilisin-line serine protease. *Annals of Botany* 114, 1161–1175.

Sharkey TD, Bernacchi CJ, Farquhar GD, Singsaas EL. (2007). Fitting photosynthetic carbon dioxide response curves for C_3 leaves. *Plant, Cell & Environment* 30, 1035–1040.

Shrestha A, Buckley TN, Lockhart EL, Barbour MM. (2018). The response of mesophyll conductance to short- and long-term environmental conditions in chickpea genotypes. *Annals of Botany Plants* 11, ply073.

Silva GB, Ionashiro M, Carrara TB, Crivellari AC, Tiné MAS, Prado J, Carpita NC, Buckeridge MS. (2011). Cell wall polysaccharides from fern leaves: evidence for mannan-rich Type III cell wall in *Adiantum raddianum*. *Phytochemistry* 72, 2352–2360.

Singh SK, Badgujar G, Reddy VR, Fleisher DH, Bunce JA. (2013). Carbon dioxide diffusion across stomata and mesophyll and photo-biochemical processes as affected by growth CO_2 and phosphorus nutrition in cotton. *Journal of Plant Physiology* 170, 801–813.

Singh SK, Reddy VR. (2018). Co-regulation of photosynthetic processes under potassium deficiency across CO_2 levels in soybean: mechanisms of limitations and adaptations. *Photosynthesis Research* 137, 183–200.

Sobrado MA, Turner NC. (1983). A comparison of the water relations characteristics of *Helianthus annuus* and *Helianthus petiolaris* when subjected to water deficits. *Oecologia* 58, 309–313.

Solecka D, Zebrowski J, Kacperska A. (2008). Are pectins involved in cold acclimation and de-acclimation of winter oil-seed rape plants? *Annals of Botany* 101, 521–530.

Somerville C, Bauer S, Brinistool G, Facette M, Hamann T, Milne J, Osborne E, Paredez A, Persson S, Raab T, Vorwerk S, Youngs H. (2004). Toward a systems approach to understanding plant cell walls. *Science* 306, 2206–2211.

Sørensen I, Domozych D, Williats WGT. (2010). How have plant cell walls evolved? *Plant Physiology* 153, 366–372.

Spielman M, Preuss D, Li FL, Browne WE, Scott RJ, Dickinson HG. (1997). TETRASPORE is required for male meiotic cytokinesis in *Arabidopsis thaliana*. *Development* 124, 2645–2657.

Suwa R, Hakata H, Hara H, El-Shemy HA, Adu-Gyamfi JJ, Nguyen NT, Kanai S, Lightfoot DA, Mohapatra PK, Fujita K. (2010). High temperature effects on photosynthate partitioning and sugar metabolism during ear expansion in maize (*Zea mays* L.) genotypes. *Plant Physiology and Biochemistry* 48, 124–130.

Sweet WJ, Morrison JC, Labavitch J, Matthews MA. (1990). Altered synthesis and composition of cell wall of grape (*Vitis vinifera* L.) leaves during expansion and growth-inhibiting water deficits. *Plant and Cell Physiology* 31, 407–414.

Tazoe Y, von Caemmerer S, Estavillo GM, Evans JR. (2011). Using tunable diode laser spectroscopy to measure carbon isotope discrimination and mesophyll conductance to CO_2 diffusion dynamically at different CO_2 concentrations. *Plant, Cell & Environment* 34, 580–591.

Tenhaken R. (2015). Cell wall remodeling under abiotic stress. *Frontiers in Plant Science* 5, 771.

Terashima I, Miyazawa SI, Hanba YT. (2001). Why are sun leaves thicker than shade leaves? Consideration based on analyses of CO_2 diffusion in the leaf. *Journal of Plant Research* 114, 93–105.

Terashima I, Ono K. (2002). Effects of $HgCl_2$ on CO_2 dependence of leaf photosynthesis: evidence indicating involvement of aquaporins in CO_2 diffusion across the plasma membrane. *Plant and Cell Physiology* 43, 70–78.

Terashima I, Hanba YT, Tazoe Y, Vyas P, Yano S. (2006). Irradiance and phenotype: comparative eco-development of sun and shade leaves in relation to photosynthetic CO_2 diffusion. *Journal of Experimental Botany* 57, 343–354.

Terashima I, Hanba YT, Tholen D, Niinemets Ü. (2011). Leaf functional anatomy in relation to photosynthesis. *Plant Physiology* 155, 108–116.

Terrett OM, Dupree P. (2019). Covalent interactions between lignin and hemicelluloses in plant secondary cell walls. *Current Opinion in Biotechnology* 56, 97–104.

Tholen D, Boom C, Noguchi K, Ueda S, Katase T, Terashima I. (2008). The chloroplast avoidance response decreases internal conductance to CO_2 diffusion in *Arabidopsis thaliana* leaves. *Plant, Cell & Environment* 31, 1688–1700.

Tomás M, Flexas J, Copolovici L, Galmés J, Hallik L, Medrano H, Ribas-Carbó M, Tosens T, Vislap V, Niinemets Ü. (2013). Importance of leaf anatomy in determining mesophyll diffusion conductance to CO_2 across species: quantitative limitations and scaling up by models. *Journal of Experimental Botany* 64, 2269–2281.

Tomás M, Medrano H, Brugnoli E, Escalona JM, Martorell S, Pou A, Ribas-Carbó M, Flexas J. (2014). Variability of mesophyll conductance in grapevine cultivars under water stress conditions in relation to leaf anatomy and water use efficiency. *Australian Journal of Grape and Wine Research* 20, 272–280.

Tosens T, Niinemets Ü, Westoby M, Wright IJ. (2012*a*). Anatomical basis of variation in mesophyll resistance in eastern Australian sclerophylls: news of a long and winding path. *Journal of Experimental Botany* 63, 5105–5119.

Tosens T, Niinemets Ü, Vislap V, Eichelmann H, Castro-Díez P. (2012*b*). Developmental changes in mesophyll diffusion conductance and photosynthetic capacity under different light and water availabilities in *Populus tremula*: how structure constrains function. *Plant, Cell & Environment* 35, 839–856.

Tosens T, Nishida K, Gago J, Coopman RE, Cabrera HM, Carriquí M, Laanisto L, Morales L, Nadal M, Rojas R, Talts E, Tomás M, Hanba Y, Niinemets Ü, Flexas J. (2015). The photosynthetic capacity in 35 ferns and fern allies: mesophyll CO_2 diffusion as a key trait. *New Phytologist* 209, 1576–1590.

Tucker MR, Lou H, Aubert MK, Wilkinson LG, Little A, Houston K, Pinto SC, Shirley NJ. (2018). Exploring the role of cell wall-related genes and polysaccharides during plant development. *Plants* 7:42.

Turbant A, Fournet F, Lequart M, Zabijak L, Pageau K, Bouton S, Wuytswinkel V. (2016). PME58 plays a role in pectin distribution during seed coat mucilage extrusion through homogalacturonan modification. *Journal of Experimental Botany* 67, 2177–2190.

Turner SR, Somerville CR. (1997). Collapsed xylem phenotype of *Arabidopsis* identifies mutants deficient in cellulose deposition in the secondary cell wall. *The Plant Cell* 9l, 689–701.

Uehlein N, Lovisolo C, Siefritz F, Kaldenhoff R. (2003). The tobacco aquaporin NtAQP1 is a membrane CO_2 pore with physiological functions. *Nature* 425, 734–737.

Uehlein N, Otto B, Hanson DT, Fischer M, McDowell N, Kaldenhoff R. (2008). Function of *Nicotiana tabacum* aquaporins as chloroplast gas pores challenges the concept of membrane CO_2 permeability. *Plant Cell* 20, 648–657.

Valentini R, Epron D, Angelis P, Matteucci G, Dreyer E. (1995). *In situ* estimation of net CO_2 assimilation, photosynthetic electron flow and photorespiration in Turkey oak (*Q. cerris* L.) leaves: diurnal cycles under different levels of water supply. *Plant, Cell & Environment* 18, 631–640.

Vangindertael J, Camacho R, Sempels W, Mizuno H, Dedecker P, Janssen KPF. (2018). An introduction to optical super-resolution microscopy for the adventurous biologist. *Methods and Applications in Fluorescence* 6, 022003.

Veromann-Jürgenson LL, Tosens T, Laanisto L, Niinemets Ü. (2017). Extremely thick cell walls and low mesophyll conductance: welcome to the world of ancient living! *Journal of Experimental Botany* 68, 1639–1653.

Vicré M, Sherwin HW, Driouich A, Jaffer MA, Farrant JM. (1999). Cell wall characteristics and structure of hydrated and dry leaves of the resurrection plant *Craterostigma wilmsii*, a microscopical study. *Journal of Plant Physiology* 155, 719–726.

Vicré M, Lerouxel O, Farrant J, Lerouge P, Driouich A. (2004). Composition and desiccation-induced alterations of the cell wall in the resurrection plant *Craterostigma wilmsii*. *Physiologia Plantarum* 120, 229–239.

Vogel J. (2009). Unique aspects of the grass cell wall. *Current Opinion in Plant Biology* 11, 301–307.

Volkova L, Bennett LT, Tausz M. (2009). Effects of sudden exposure to high light levels on two tree fern species *Dicksonia antarctica* (Dicksoniaceae) and *Cyathea australis* (Cyatheaceae) acclimated to different light intensities. *Australian Journal of Botany* 57, 562–571.

von Caemmerer S, Farquhar G, Berry J. (2009). Biochemical model of C_3 photosynthesis. In: Laisk A, Nedbal L, Govindjee (eds.). *Photosynthesis in Silico: Understanding Complexity from Molecules to Ecosystems.* Springer Science + Business Media B.V., 209–230.

von Caemmerer S, Evans JR. (2015). Temperature responses of mesophyll conductance differ greatly between species. *Plant, Cell & Environment* 38, 629–637.

Voragen AGJ, Coenen GJ, Verhoef RP, Schols HA. (2009). Pectin, a versatile polysaccharide present in plant cell walls. *Structural Chemistry* 20, 263–275.

Vrabl D, Vaskova M, Hronkova M, Flexas J, Santrucek J. (2009). Mesophyll conductance to CO_2 transport estimated by two independent methods: effect of variable CO_2 concentration and abscisic acid. *Journal of Experimental Botany* 60, 2315–2323.

Wallace G, Fry SC. (1994). Phenolic components of the plant cell wall. *International Review of Cytology* 151, 229–267.

Wang F, Sun X, Shi X, Zhai H, Tian C, Kong F, Liu B, Yuan X. (2016). A global analysis of the polygalacturonase gene family in soybean (*Glycine max*). PLoS One 11:e0163012.

Wardrop AB. (1962). Cell wall organisation in higher plants. *The Botanical Review* 28, 241–285.

Weraduwage SM, Kim SJ, Renna L, Anozie FC, Sharkey TD, Brandizzi F. (2016). Pectin methylesterification impacts the relationship between photosynthesis and plant growth in *Arabidopsis thaliana*. *Plant Physiology* 171, 833–848.

Williams TG, Flanagan LB, Coleman JR. (1996). Photosynthetic gas exchange and discrimination against $^{13}CO_2$ and $C^{18}O^{16}O$ in tobacco plants modified by an antisense construct to have low chloroplastic carbonic anhydrase. *Plant Physiology* 112, 319–326.

Williams TG, Flanagan LB. (1998). Measuring and modelling environmental influences on photosynthetic gas exchange in *Sphagnum* and *Pleurozium*. *Plant, Cell & Environment* 21, 555–564.

Xiao C, Zhang T, Zheng Y, Cosgrove DJ, Anderson CT. (2016). Xyloglucan deficiency disrupts microtubule stability and cellulose biosynthesis in *Arabidopsis*, altering cell growth and morphogenesis. *Plant Physiology* 170, 234–249.

Xiao Y, Zhu XG. (2017). Components of mesophyll resistance and their environmental responses: A theoretical modelling analysis. *Plant, Cell & Environment* 40, 2729–2742.

Xiong D, Liu X, Liu L, Douthe C, Li Y, Peng S, Huang J. (2015). Rapid responses of mesophyll conductance to changes of CO_2 concentration, temperature and irradiance are affected by N supplements in rice. *Plant, Cell & Environment* 38, 2541–2550.

Xiong D, Wang D, Liu X, Peng S, Huang J, Li Y. (2016). Leaf density explains variation in leaf mass per area in rice between cultivars and nitrogen treatments. *Annals of Botany* 117, 963–971.

Xu J, Belanger F, Huang B. (2008). Differential gene expression in shoots and roots under heat stress for a geothermal and non-thermal *Agrostis* grass species contrasting in heat tolerance. *Environmental and Experimental Botany* 63, 240–247.

Xu Z, Zhang D, Hu J, Zhou X, Ye X, Reichel KL, Stewart NR, Syrenne RD, Yang X, Gao P, Shi W, Doeppke C, Sykes RW, Burris JN, Bozell JJ, Cheng MZM, Hayes DG, Labbe N, Davis M, Stewart Jr CN, Yuan JS. (2009). Comparative genome analysis of lignin biosynthesis gene families across the plant kingdom. *BMC Bioinformatics* 10, S3.

Yamori W, Noguchi K, Hanba YT, Terashima I. (2006). Effects of internal conductance on the temperature dependence of the photosynthetic rate in spinach leaves from contrasting growth temperatures. *Plant and Cell Physiology* 47, 1069–1080.

Yamori W, Hikosaka K, Way DA. (2014). Temperature response of photosynthesis in C_3, C_4 and CAM plants: temperature acclimation and temperature adaptation. *Photosynthesis Research* 119, 101–117.

Yang KA, Lim CJ, Hong JK, Park CY, Cheong YH, Chung WS, Lee KO, Lee SY, Cho MJ, Lim CO. (2006). Identification of cell wall genes modified by a permissive high temperature in Chinese cabbage. *Plant Science* 171, 175–182.

Yang Y, Yu Y, Liang Y, Anderson CT, Cao J. (2018). A profusion of molecular scissors for pectins: classification, expression, and functions of plant polygalacturonase. *Frontiers in Plant Science* 9:1208.

Yokoyama R. (2020). A genomic perspective on the evolutionary diversity of the plant cell wall. *Plants* 9, 1195.

Zhang Q, Huang L, Liu T, Yu X, Cao J. (2008). Functional analysis of a pollen-expressed polygalacturonase gene BcMF6 in Chinese cabbage (*Brassica campestris* L. ssp. *chinensis* Makino). *Plant and Cell Reports* 27, 1207–1215.

Zhang Y, Bucci SJ, Arias NS. (2016). Freezing resistance in Patagonian woody shrubs: the role of cell wall elasticity and stem vessel size. *Tree Physiology* 36, 1007–1018.

Zhang R, Hu H, Wang Y, Hu Z, Ren S, Li J, He B, Wang Y, Xia T, Chen P, Xie G, Peng L. (2020). A novel rice *fragile culm* 24 mutant encodes a UDP-glucose epimerase that affects cell wall property and photosynthesis. *Journal of Experimental Botany* 71, 2956–2969.

Zheng M, Meng Y, Yang C, Zhou Z, Wang Y, Chen B. (2014). Protein expression changes during cotton fibre elongation in response to drought stress and recovery. *Proteomics* 14, 1776–1795.

Zhong R, Peña MJ, Zhou GK, Nairn J, Wood-Jones A, Richardson EA, Morrison III WH, Darvill AG, York WS, Ye ZH. (2005). *Arabidopsis fragile fiber8*, which encodes a putative glucuronyltransferase, is essential for normal secondary wall synthesis. *The Plant Cell* 17, 3390–3408.